ABSTRACT

Title of dissertation: MODELING OF SEASONAL TRACE GAS AND PARTICULATE EMISSIONS FROM VEGETATION FIRES IN SOUTHERN AFRICA

Stefania Korontzi, Doctor of Philosophy, 2004

Dissertation directed by: Professor Christopher O. Justice
Department of Geography

Fire is widespread in southern African savannas with important implications for tropical and global atmospheric chemistry. However, previous regional emission studies have not fully accounted for the variability of the emissions throughout the burning season and the associated impacts on emissions quantification. The main aim of this study is to address this gap. The complexity of the emissions process is described using a spatially and temporally explicit modeling approach that integrates recently published satellite-driven fuel load amounts, satellite burned area products, and empirically derived parameterizations of combustion completeness and emission factors. To represent fire behavior characteristics, land cover is classified into grasslands and woodlands, using a satellite-derived percent tree cover product. The combustion completeness is modeled as a function of grass fuel moisture and the emission factors as a function of grass fuel moisture in grasslands and fuel mixture in woodlands. Fuel moisture is derived from a fuel load model and by using satellite vegetation index time series. A sensitivity analysis

with respect to three satellite burned area products reveals large differences in emissions due to differences in their amounts and spatial distribution. The analysis at the regional scale shows, that early burning in grasslands may lead to higher amounts of products of incomplete combustion despite the lower amounts of fuel consumed, compared with late dry season burning. In contrast, early burning in woodlands results in lower emissions because less fuel gets consumed. These seasonal emissions trends become more pronounced when the fuels are wetter. Burning in woodlands dominates the regional emissions budgets. Emissions estimates for various atmospheric species, many of which are modeled for the first time, are reported and compared with other regional sources of pyrogenic emissions and global biomass burning and fossil fuel emissions. The modeled estimates for 2000 are (in Tg): 537 CO_2, 23.2 CO, 0.726 CH_4, 0.661 NMHC, 2.4 particulates (< 2.5 μm), 1.0 NO_x and account for significant fractions of regional emissions from all pyrogenic sources. Especially high is the previously undetermined contribution of Oxygenated Volatile Organic Compounds (1.8 Tg). The methodology and results have direct implications for national reporting of savanna fire emissions.

MODELING OF SEASONAL TRACE GAS AND PARTICULATE EMISSIONS FROM VEGETATION FIRES IN SOUTHERN AFRICA

by

Stefania Korontzi

Thesis submitted to the Faculty of the Graduate School of the
University of Maryland, College Park, in partial fulfillment
of the requirements for the degree of
Doctor of Philosophy
2004

Advisory Committee:

Professor Christopher O. Justice, Chair
Dr. Ivan Csiszar
Professor Ruth S. DeFries
Professor Peter Kofinas
Professor John R.G. Townshend

© Copyright by

Stefania Korontzi

2004

To my parents,
Yanni and Georgia

Acknowledgements

I am particularly grateful to my major advisor, Professor Chris Justice, for his ideal mentoring and support during the course of this research. His advice and encouragement proved to be invaluable on several occasions. Dr. David Roy has also been very generous with his time and assistance during the preparation of this dissertation. I would also like to thank the other members of my committee, Dr. John Townshend, Dr. Ruth DeFries, Dr. Ivan Csiszar and Dr. Peter Kofinas for their help and guidance.

This study was part of the Southern African Regional Science Initiative (SAFARI 2000). I have tremendously benefited from collaborations developed during and after SAFARI 2000 with a number of researchers, including, Dr. Darold Ward, Dr. Peter Hobbs, Dr. Bob Yokelson, Dr. Wei Min Hao, Dr. Bob Scholes, Dr. Compton Tucker, Dr. Assaf Anyamba and Louis Giglio. Funding for this research was provided by the NASA MODIS grant and NASA's Earth System Science Fellowship.

My deepest thanks go to my mother and my sisters for their love and support throughout this endeavor.

Table of Contents

List of Tables

Chapter 4:

List of Figures

Chapter 3:

Chapter 4:

burned, (c) combustion completeness, (d) CO_2 emission factors, (e) CO_2 emissions, (f) CO emission factors, and (g) CO emissions. The grassland (0% <= PTC <= 10%) statistics are shown at PTC = 5%. The woodland (PTC > 10%) statistics are defined over 5% PTC intervals.

Figure 9. Mean (symbol) and one standard deviation statistics computed from the southern Africa, September 2000, GBA-2000 burned pixels of (a) fuel load, (b) biomass burned, (c) combustion completeness, (d) CO_2 emission factors, (e) CO_2 emissions, (f) CO emission factors, and (g) CO emissions. The grassland (0% <= PTC <= 10%) statistics are shown at PTC = 5%. The woodland (PTC > 10%) statistics are defined over 5% PTC intervals.

Figure 10. Mean (symbol) and one standard deviation statistics computed from the southern Africa, September 2000, GLOBSCAR burned pixels of (a) fuel load, (b) biomass burned, (c) combustion completeness, (d) CO_2 emission factors, (e) CO_2 emissions, (f) CO emission factors, and (g) CO emissions. The grassland (0% <= PTC <= 10%) statistics are shown at PTC = 5%. The woodland (PTC > 10%) statistics are defined over 5% PTC intervals.

Figure 11. Mean (symbol) and one standard deviation (error bar) statistics computed from the southern Africa, September 2000, MODIS, GBA-2000 and GLOBSCAR burned area products for (a) fuel load, (b) combustion completeness, (c) CO_2 emission factors, and (d) CO emissions factors.

Figure 12. MODIS, GBA-2000 and GLOBSCAR woodland over grasslands ratios for burned area, and selected trace gas and particulate emissions for September 2000. Only those southern African countries situated completely south of the Equator are reported.

Chapter 5:

Figure 1. Overview of monthly regional spatially-explicit emissions model for grassland (G) and woodland (W) fires. Emissions variables are denoted by colored rectangles. Important input data used to derive various emissions variables are denoted by ovals. Thresholds applied to the MODIS Percent Tree Cover (PTC) and the percentage of green grass relative to the total grass (PGREEN) are shown in italics (LT = less than, GE = greater than or equal, GT = greater than, LE = less than or equal). CC is the combustion completeness, MCE the modified combustion efficiency and EF the emission factors.

Figure 2. Contribution of seasonal burned area to total burned area in a) grasslands and b) woodlands using GBA-2000.

Chapter 1: Introduction

1.1 Background

The high incidence, extent and severity of wildfires worldwide, have raised global awareness of biomass burning from the general public to the international policy arena. Examples of such severe fire events include the 1997-1998 Indonesia/Southeast Asia fire/smog problem, the 2000 fire season in the United States and the 2003 severe wildfires in Australia and the south of the Russian Federation, with adverse impacts on human health, livelihoods and economies. There is a need to accurately assess the spatial and temporal distribution and patterns of biomass burning emissions from a scientific, as well as a policy making point of view at the country and regional level (Hicks *et al.*, 2001). Atmospheric chemistry and transport models require information on the seasonal and inter-annual distribution of gaseous and particulate emissions from biomass burning (Chatfield *et al.*, 1996; Bergamaschi *et al.*, 2000; Duncan *et al.*, 2003). Within the context of the International Panel on Climate Change (IPCC), party countries, are to provide a national inventory of their anthropogenic greenhouse gas emissions, including those resulting from vegetation fires (IPCC, 1997a).

Vegetation fires have significant implications for atmospheric chemistry, hydrological processes and biogeochemical cycling (Justice and Korontzi, 2001). There is a consensus in the global climate change research community, that biomass burning largely contributes to emissions of greenhouse gases and tropospheric ozone (O_3) precursors, including carbon monoxide (CO), methane (CH_4), non-methane hydrocarbons (NMHC), nitrogen oxides (NO_X) and nitrous oxide (N_2O) (Crutzen and Andreae, 1990; Lobert *et al.*, 1990; Helas and Pienaar, 1996: Crutzen and Lelieveld, 2001). CH_4 and N_2O

are gases with high global warming potentials. CO is only a very weak direct greenhouse gas, but has important indirect effects on global warming. It reacts with hydroxyl radicals (OH) in the atmosphere, thus reducing the main sink for CH_4 and lengthening its lifetime. The photochemical oxidation of CO and hydrocarbons in the presence of NO_x in smoke produces ozone (O_3) (*e.g.*, Radke *et al.*, 1978; Hobbs *et al.*, 2003). Methyl chloride (CH_3Cl), methyl bromide (CH_3Br), methyl iodide (CH_3I) and other halocarbons released by biomass burning may contribute to stratospheric ozone depletion (McKenzie *et al.*, 1996; Lobert *et al.*, 1999). Acids in smoke from biomass burning, such as acetic acid (CH_3COOH), formic acid (HCOOC), nitric acid (HNO_3) and sulfuric acid (H_2SO_4), can acidify precipitation (Lacaux *et al.*, 1991; Yokelson *et al.*, 1996).

In addition, pyrogenically produced aerosols influence climate directly by reflecting incoming solar radiation, and indirectly by modifying cloud microphysics because they act as cloud condensation nuclei (Kaufman and Nakajima, 1993; Kaufman and Fraser, 1997). In general, biomass burning aerosols are considered to have a cooling effect. The inorganic and organic aerosols scatter solar radiation, reducing the downwelling flux available for photochemistry and warming of the Earth's surface (Sinha *et al.*, 2003). On the other hand, black carbon in aerosols absorbs solar radiation, creating vertical stability below them that can trap pollutants near the surface. The black carbon produced globally may have a warming effect equivalent to the cooling effect of sulfate aerosols (Jacobson, 2001).

Biomass burning has been shown to affect precipitation patterns in the tropics (Rosenfeld, 1999), and contribute to increased stratospheric water vapor (Sherwood, 2002) and enhanced carbonyl sulfide levels in the upper tropical troposphere (Notholt *et*

al., 2003). Fires may modify ecosystem composition and functioning, and may perturb biogeochemical nutrient cycling both directly, *e.g.*, due to the effects of fire on soil nutrient cycling where burning takes place (Levine *et al.*, 1996), and indirectly, *e.g.*, through the long-range transport and deposition of aerosols and trace gases produced during biomass burning (Garstang *et al.*, 1998).

The largest number of vegetation fires globally occurs in the fire-dependent savannas of Africa, estimated to contribute up to 49% of the carbon lost from global biomass burning (Dwyer *et al.*, 2000; van der Werf *et al.*, 2003). Two thirds of tropical savannas are located in Africa, 60% of which lie south of the equator. Most of the savanna fires occurring today are anthropogenic. Only about 10% of savanna fires are due to lightning (Frost, 1996). The distinct seasonality of the rainfall in southern Africa, which is generally concentrated into one rainy season, allows enough fuel to accumulate during the growing season and become dry and prone to burning during the subsequent dry season. Typically, the dry season in southern Africa lasts from April to October (Scholes *et al.*, 1996a). Herbaceous vegetation and litter from leaf fall and twigs make up most of the fuel for savanna fires, which tend to be surface fires (Frost, 1996; Trollope and Trollope, 2002). Savanna fires have been linked to the elevated tropical ozone anomaly spanning from the western coast of southern Africa to South America during the southern hemisphere dry season (Fishman *et al.*, 1991; Thompson *et al.*, 1996; 2001).

A comparison of different estimates of burned area, burned biomass and CO_2 emissions in southern Africa, is shown in Table 1. Annual emissions estimates have often relied on crude inventory-based aboveground mean fuel estimates by vegetation type, average, late dry season emission factors and anecdotal estimates of the proportion of fuel

consumed and the area burned (Crutzen and Andreae, 1990; Hao *et al.*, 1990; Andreae, 1993, Hao and Liu, 1994; Hao *et al.*, 1996; Andreae 1997; Scholes and Andreae, 2000; Andreae and Merlet, 2001). Substantial uncertainties in these classification methods arise from assumptions of broadly defined homogenous areas with respect to these variables, which moreover have varying degrees of uncertainty themselves. Furthermore, inter-annual variations in fuel loadings in response to different rainfall conditions and seasonal variations in emissions factors and the proportion of fuel consumed are not accounted for in these inventories.

Current modeling methodologies for emissions quantification can be classified into top-down (land-based) and bottom-up (atmospheric-based) approaches. In top-down modeling approaches, global atmospheric chemical transport models are applied to study the distribution, budgets and seasonal and inter-annual variability of gas tracers (e.g., CO) or particulates. These methods however, rely on highly uncertain static biomass burning inventories (usually Hao and Liu, 1994; later updated by Liousee *et al.*, 1996; and the Global Emissions Inventory Activity (GEIA) inventory by Logan and Yevich described in Lobert *et al.*, 1999) and average emission factors for broadly defined vegetation cover classes. Further uncertainties arise from the quantification of contributing sources other than biomass burning that control the chemistry of the atmosphere, such as biogenic, and biofuel emissions. These models constrain emissions using inverse numerical modeling techniques, local observations and satellite data (Liousse *et al.*, 1996; Cooke *et al.*, 1996; Bergamaschi *et al.*, 2000; Schultz, 2002; Duncan *et al.*, 2003; Generoso *et al.*, 2003).

Table 1. Comparison of previous estimates of annual burned area, biomass burned and emissions for southern Africa.

Study	*Burned area (10^6 km^2/yr)*	*Biomass burned (Tg/yr)*	*CO_2 (Tg/yr)*	*CO (Tg/yr)*
Hao *et al.* (1990)	-	1200	1560	99 [a]
Hao and Liu (1994)	-	827	-	68[b]
Hao *et al.* (1996)	-	1000[c]	-	75
Scholes *et al.* (1996a) (year 1989)	1.68	177	324	14.9
Scholes *et al.* (1996b) classification method	3.99	1152	-	-
Barbosa *et al.* (1999) (year 1989)	1.54	456	748	31.0
van der Werf *et al.* (2003) (years 1998-2001)	1.16	1147	1848[d]	76.8[d]
van der Werf *et al.* (2004) (years 1997-2001)	-	2040	3286	136.7

[a] Assuming molar ratio of CO to CO_2 is 0.1 from Hao *et al.* (1990). The calculations assume 50% carbon content

[b] Based on extrapolation from Hao *et al.* (1990)

[c] Calculated based on the contribution of southern Africa to continental Africa from Hao *et al.* (1990)

[d] Using the emissions factors from van der Werf *et al.* (2004)

Bottom-up emissions modeling studies, attempt to explicitly capture critical aspects of the biomass burning process that occur in specific regions and have generally used satellite data to assess the burned area. The first such model for southern Africa was developed as part of SAFARI-92 by Scholes *et al.* (1996a; 1996b). Scholes *et al.* (1996a; 1996b), used a calibration approach of Advanced Very High Resolution Radiometer (AVHRR) active fires with high resolution Landsat Multi-Spectral Scanner (MSS) and Normalized Difference Vegetation Index (NDVI) to derive burned area. They constrained fuel production by rainfall and considered fuel removal by herbivory and decay and

applied field measurements of emission factors to derive pyrogenic emissions of trace gases and particulates for an average rainfall year in southern Africa. One of the main findings of Scholes *et al.* (1996b) was that the inventory-based methods, termed "classification method", tend to overestimate burned areas because fire return times of frequently burned parts of the savanna landscape are assumed to represent larger regions (Table 1). Furthermore, the fuel load estimates that were previously applied to savannas in the inventory methods tended to overestimate fuel loads because they were derived from a handful of measurements, generally in places on the wetter end of the savanna gradient and that are lightly grazed. The research conducted by Scholes *et al.* (1996a; 1996b) greatly improved the state-of-knowledge of the magnitude of biomass burning emissions. Their emissions model though, was limited by direct estimates of burned area, and modeling of potential fuel load of broad vegetation classes. Both of these model parameters have been recognized as the main sources of errors in emissions modeling (Andreae, 1997; Andreae and Merlet, 2001).

Barbosa *et al.* (1999) assessed the inter-annual variability of emissions in southern Africa using AVHRR Global Area Coverage (GAC) 5 km data to estimate burned area, annual biomass density maps constructed from NDVI and reported field values, fixed emission factors from the literature and variable combustion completeness also based on GAC NDVI. It was found that significant inter-annual variations may result in response to rainfall patterns during the growing season. Emissions during an El Niño year were estimated to be approximately half those in an average rainfall year due to the diminished vegetation production in the drought year, resulting in less burning. Limitations in the work by Barbosa *et al.* (1999) include the low spatial resolution of the GAC data, the

very small number of sites used to derive biomass density, not accounting for fuel removal processes such as herbivory and fuel decay and using constant emission factors for different vegetation classes.

Recently, van der Werf *et al.* (2003) used a percent tree cover dataset to convert TRMM active fire counts to burned area. This approach yielded lower amounts of burned area than the previous satellite-based studies by Scholes *et al.* (1996a) and Barbosa *et al.* (1999). However, van der Werf *et al.* (2003) introduced coarse wood fuels in the estimates of fuel load available to burn in woodlands, which is one of the main causes for the larger biomass burned estimates compared with Scholes *et al.* (1996b) and Barbosa *et al.* (1999). In their later study, van der Werf *et al.* (2004) also significantly increased the amount of area burned in southern Africa. The atmospheric modeling studies have identified southern Africa as a region with large discrepancies between bottom-up estimations and atmospheric observations of CO (Chatfield *et al.*, 1996; 1997). This unresolved controversy highlights the need for improved estimates.

Moreover, the seasonal variations of biomass burning emissions in southern Africa are largely unknown. Only one field study has been conducted in southern Africa during the early dry season (typically April through the end of July) (Hoffa *et al.*, 1999). Hoffa *et al.*, (1999) showed that the higher fuel moisture content during the early dry season burning affects fire behavior so that significant seasonal trends may occur in the resulting emissions for products, in particular for products of incomplete combustion, such as CO, CH_4 and particulates with diameter less than 2.5μm (PM2.5). At the regional scale there are no specific studies aimed at explicitly quantifying the seasonal variability of burning and the contribution of the different amounts of seasonal emissions to the

regional and global atmospheric budgets. The previously mentioned bottom-up studies focused mainly in the late dry season. In top-down approaches, the seasonality of biomass burning emissions has commonly been inferred from the seasonal distribution of active fire counts. Uncertainties in these methodologies are not just limited to the unsuitability of active fires to represent the amounts of burned area (Robinson, 1991; Justice *et al.*, 1993). Recent comparisons of different South African active fire and spatially explicit burned area data sets indicate differences in the seasonal cycles as well (Generoso *et al.*, 2003). A shortcoming in these studies is that they assume that seasonal emissions are proportional to the active fire distribution. However, there is some evidence that the same size of fire emits different types and amounts of emission products early in the dry season compared with the late dry season (Hoffa *et al.*, 1999).

1.2 Research Objectives

The fundamental goal of this research is to develop and evaluate a spatially and temporally explicit model of biomass burning emissions for southern African, in order to improve the reliability and accuracy of emissions estimates from vegetation fires in the region. Recently developed satellite-driven fuel load model outputs and satellite-derived burned area and percent tree cover products are used as inputs to the model in this study. The region is classified into woodlands and grasslands, to account for the different fire behavior in these two land cover types. Particular attention is given to elucidating the seasonal cycle of biomass burning emissions by adapting a dynamic modeling approach that accounts for differences in the type of combustion. Specifically, the following research objectives are addressed by this work:

1. Develop algorithms to estimate the seasonal emission factors for selected trace gases and aerosols for woodland and grassland fires in southern Africa.

2. Develop a regional spatio-temporal model of pyrogenic emissions from southern African savannas for the 2000 dry season to identify source regions and quantities of biomass burning emissions.

3. Conduct sensitivity analyses to study the impact of selected model inputs/variables (burned area, percent tree cover, fuel greenness) on emissions estimation.

4. Evaluate the contribution of early dry season emissions to annual pyrogenic emissions budgets and examine seasonal emissions trends at landscape and regional scales.

5. Compare vegetation fires with other regional sources of greenhouse gases and particulates, namely industrial, biogenic and biofuel emissions.

6. Compare selected national fire emissions estimated in this study with the latest national reports presented by the Intergovernmental Panel on Climate Change (IPCC).

This study also contributes to meeting one of the main Southern Africa Fire and Atmospheric Research Initiative-2000 (SAFARI-2000) project research objectives: quantifying the spatio-temporal distribution of savanna burning trace gas and aerosol emissions. SAFARI 2000 was an international research initiative with the goal of better understanding land-atmosphere interactions (Swap *et al.*, 2003).

1.3 Outline of the Dissertation

The organization of this dissertation consists of seven chapters, including four self-contained chapters, presenting research on biomass burning emissions in southern Africa and one chapter on the potential applications of this research. An overview of the research and the chapter progression is illustrated in Figure 1. Chapter 1 introduces

biomass burning impacts on atmospheric chemistry and the current state of biomass burning emissions studies in southern Africa. In Chapter 2, the importance of seasonal variations of emissions from grassland fires is investigated at the landscape level and within a sensitivity analysis framework. This chapter also examines the spatial characteristics of burned area in representative semi-arid and humid locations and dry and average rainfall years, in support of regional satellite burned area product development. Chapter 2 provided preliminary evidence for the importance of seasonal trends on annual vegetation fire emissions estimation and served as an impetus to study seasonal emissions variations at the regional scale. There have been no previous studies addressing the seasonal patterns of emissions factors in southern Africa, and this gap in our knowledge led to the research described in Chapter 3.

Chapter 3 reports the first seasonal emission factor measurements of selected carbon-containing trace gases and particulate matter made for prescribed grassland and woodland burns in southern Africa. These datasets were collected in Western Province, Zambia, in 1996, by Dr. Darold Ward and Dr. Erica Smithwick. To the knowledge of this author, these are the only seasonal measurements of emission factors globally. The main aim of this chapter is to derive models to predict the seasonal variations of emission factors associated with changes in fuel moisture condition and to evaluate differences in emission factors between grassland and woodland fires. By making use of the modified combustion efficiency, the ecosystem-specific correlations described in this chapter can be applied in spatially and temporally explicit fire emissions models. The emission factor models developed here are integrated in the regional emissions modeling framework described in Chapters 4 and 5.

Chapter 4 describes the spatially explicit regional emissions modeling methodology developed in this dissertation for grasslands and woodlands and assesses the model sensitivity to selected satellite product inputs. In this chapter, spatially-explicit regional emissions estimates are compared using three recently developed, moderate resolution satellite-derived burned area products, for a month during the SAFARI 2000 dry season field campaign. This study quantifies uncertainties in emissions resulting from differences in the amounts and spatial distribution among the three burned area products. This chapter provides an evaluation of the emissions model behavior in response to various burned area inputs. Furthermore, it highlights the need for spatially explicit burned area uncertainty information to characterize the errors in emission models estimates. In addition, the sensitivity of the emissions model to the application of percent tree cover thresholds used to stratify the region into grasslands and woodlands, is assessed.

Chapter 5 applies an improved version of the spatially explicit emissions model of Chapter 4, for the entire 2000 dry season, to investigate the seasonal dynamics of woodland and grassland fire emissions. The effect of the seasonally changing fuel moisture content on emissions is investigated. Emissions results for a number of atmospheric species (30+), many of which are modeled for the first time regionally, are presented. The importance of southern African vegetation fires as a source of trace gases and particulates is placed within the regional and global context. An approximation of the error propagation in the emissions models with respect to the uncertainties in the input variables is performed and priority needs to reduce uncertainties are discussed.

Chapter 6 is a discussion of several potential applications of the research, specifically as it relates to IPCC national reporting, air quality monitoring and fire management policy making. Country-level emission results from Chapter 5 are compared with published national IPCC reports and large differences are found. Chapter 7 provides a synthesis summary of this dissertation and recommendations for further research.

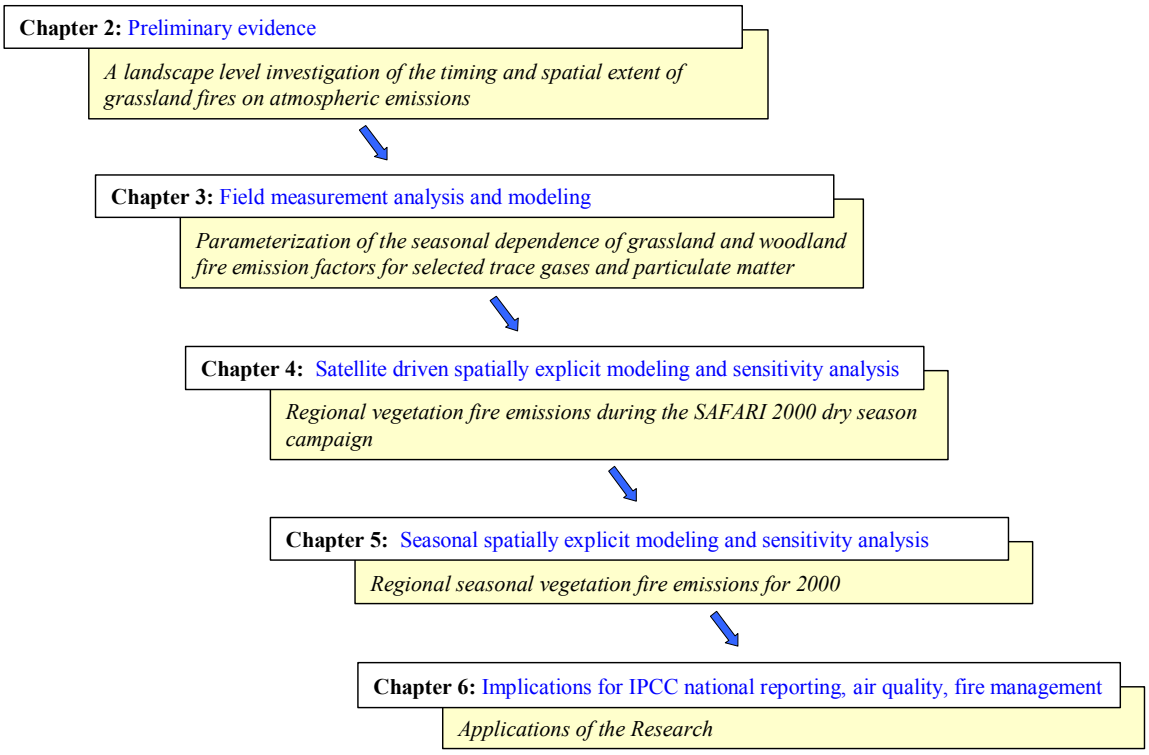

Figure 1. Research overview and progression (chapter titles in italics).

Chapter 2: A landscape level investigation of the timing and spatial extent of grassland fires on atmospheric emissions

2.1 Introduction

Emission estimates relying on remote sensing for area burned are much lower than those based on anecdotal estimates of fire return times for broad vegetation classes (Scholes *et al.*, 1996a; Barbosa *et al.*, 1999; Hao *et al.*, 1990; Hao and Liu, 1994). Current efforts are focused on developing and evaluating regional burned area satellite products (Roy *et al.*, 2002a; Grégoire *et al.*, 2003; Simon *et al.*, in press). The temporal and spatial resolution requirements for burned area information in tropical savannas driven by the need for accurate pyrogenic emissions quantification are not well known.

In this chapter, burned area characteristics are studied for average and dry rainfall years along a rainfall gradient, representative of a strong climatic gradient, from the arid south to the humid north, that exists in southern Africa, using representative Landsat imagery. Furthermore, seasonal emissions from grassland fires are estimated at the landscape scale. Hoffa *et al*. (1999) found that early dry season burning in grassland savannas releases higher amounts of products of incomplete combustion per unit area, compared with late dry season burning. However, Hoffa *et al*. (1999) did not investigate the combined effects of the timing and spatial extent of fires on emissions. In addition, an emissions sensitivity analysis is conducted by simulating different amounts of burned area.

2.2 Methodology

2.2.1 Burned Area Mapping

In this study, Landsat data were used to estimate the burned area for 12 Landsat path-row scene locations in 1989 and six scene locations in 1992, distributed over semi-arid and humid areas in southern Africa (Figure 1). Humid areas receive more than 1100 mm of rain annually (Chidumayo, 1987). Burn scars were visually mapped on 1:250,000 Landsat multispectral scanner (MSS) false color composite prints (Red = band 4, Green = band 3, Blue = band 2) and digitized. The minimum mapping unit was 180 m. For each Landsat scene, a difference image was derived from two images from the beginning and the end of the burning season. This difference image has been assumed to represent the actual annual area burned (Scholes *et al.*, 1996b). This method will be referred to as the start/end method.

To test the accuracy of the start/end method, a time-series analysis was performed for three scenes located in humid areas (Figure 1), where burn scars were expected to be the most transient due to the flush of green vegetation following burning. The new area burned between each image and its preceding image was mapped on five Landsat images per path-row scene location, covering the dry season, spaced about a month apart. This is termed the time-series method. The start/end method slightly underestimated (8-12%) the total area burned compared with the time-series method. The difference was attributed to rapid post-burn regrowth. Because most of the fire scars remained visible throughout the fire season, the start/end method was used for the total burned area analysis.

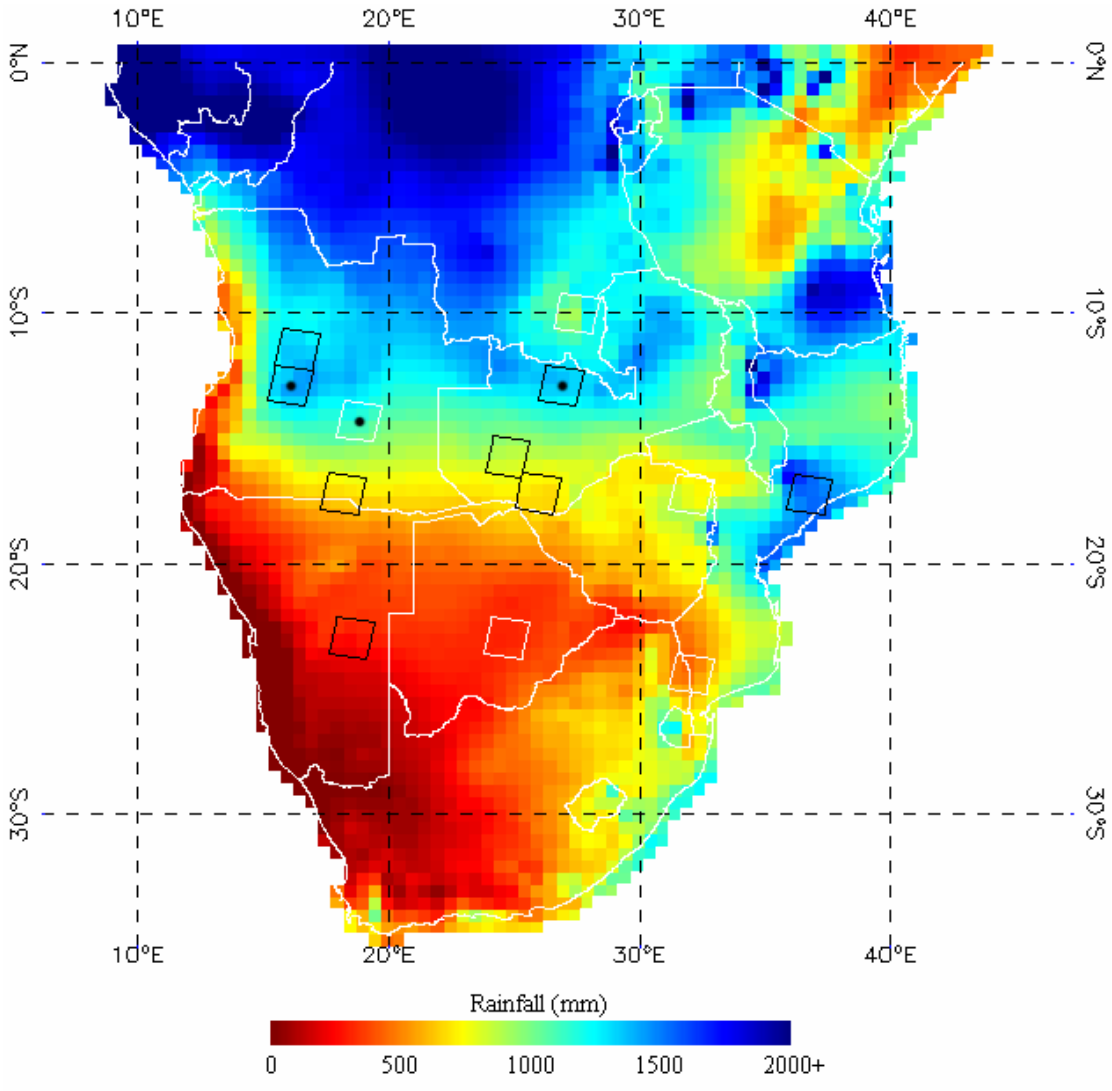

Figure 1. Location of study sites overlayed on a long-term mean annual rainfall map derived from data by New *et al.* (1999). Polygons outlined with white, show sites for which both 1989 and 1992 data were analyzed. Polygons marked with a black dot, show sites for which Landsat time series were analyzed.

2.2.2 Emissions Estimation

Total emissions are estimated at the landscape scale using Equation (2.1), based on the Seiler and Crutzen (1980) model. The spatially-explicit form of Equation (2.1) is Equation (4.1).

$$E_x = A \times F \times CC \times EF_x \quad (2.1)$$

where,

E_x pyrogenic emissions for atmospheric species x (g)

A burned area (km^2)

F fuel load ($kg\ km^{-2}$)

CC combustion completeness ($g\ g^{-1}$)

EF_x emission factor for atmospheric species x ($g\ kg^{-1}$)

To compare emissions calculated from the two methods used to derive burned area, time-series images were analyzed for 1989 (a normal precipitation year) for a scene comprised largely of grassland in Central Zambia (WRS #173069), using Equation (2.1). The seasonal fuel load and combustion completeness values were retrieved from the Hoffa *et al.* (1999) empirical study. These measurements were sampled at prescribed burning plots that were successively burned weekly or biweekly between June and August, 1996. The biomass amounts reported by Hoffa *et al.* (1999) fall within the normal range of fuel loadings for a grassland in an average rainfall year at an annually or biannually burned site (Shea *et al.*, 1996; Stocks *et al.*, 1996). Therefore, the seasonal values of fuel load and combustion completeness were deemed as representative for the 1989 grassland location studied here. Seasonal emission factor algorithms were derived

from late dry season raw emission factor data by Ward *et al.* (1996) and seasonal modified combustion efficiency (MCE, the molar ratio of carbon emitted as CO_2 to carbon emitted as CO_2 + CO) data from Hoffa *et al.* (1999) for carbon dioxide (CO_2), carbon monoxide (CO), methane (CH_4), non-methane hydrocarbons (NMHC), and fire particulate matter with diameter less than 2.5 μm (PM2.5) (Table 1). To obtain estimates of the total and seasonal amounts of the above atmospheric species with the time-series method, the calculated emission factors of Table 1 were applied to the biomass burned. To quantify emissions with the start/end method, the average values of fuel load, and late dry season combustion completeness and emission factor values were applied to Equation (2.1), which is the methodology used to estimate emissions in classification approaches (*e.g.*, Hao and Liu, 1994; Ward *et al.*, 1996; Hao *et al.*, 1996; Andreae, 1997; Andreae and Merlet, 2001).

Table 1. Calculated seasonal emission factors (EF) (in gkg^{-1}) for the grassland fires.

Emission Factors	*June*	*July*	*August*	*September*
$EFCO_2$	1586	1650	1734	1755
EFCO	138	104	58	46
$EFCH_4$	5.8	4.0	1.5	0.8
EFNMHC	5.2	3.8	2.0	1.5
EFPM2.5	9.7	7.1	3.6	2.7

Furthermore, a simulation analysis was performed for the same grassland scene to assess the possible contributions of early and late dry season burning to the total emissions. This is an important question from a fire management perspective since controlled early burning is a major natural resources management tool in the African region, used to prevent degrading effects in the various ecosystems that are caused by high intensity late season fires (Chidumayo, 1987; Frost, 1996). The simulation was done

by varying the area burned for different scenarios of early and late dry season burning and calculating the resulting total emissions. For this particular simulation study, the early and late dry season pyrogenic emissions were calculated using the emission factor, fuel load, and combustion completeness values by Hoffa *et al.* (1999) for June and September, respectively.

2.3 Results and Discussions

2.3.1 Burned Area

Differences in the total area burned and the scar size distribution were found between semi-arid and humid scenes in 1989. A slightly larger percentage of the total scene area was burned in semi-arid (12%) than in humid savannas (9%). In semi-arid areas there was a greater number of fire scars larger than 1 km^2, whereas in the more humid areas smaller fire scars (<1 km^2) were predominant (Figure 2). An example of the appearance of the fire scars in the semi-arid and humid scenes is presented in Figures 3a and 3b. In the semi-arid areas a few very large fires (> 100 km^2) accounted for about 60% of the total burned area (Figure 4a). In the humid areas, even though about 70% of the scars were smaller than 1km^2, they comprised only 12% of the total area burned (Figure 4b). It should be noted, that the size range categories shown in the graphs were deliberately chosen to correspond to the spatial resolution of the 250 m, 500 m and 1 km MODIS channels, which are candidate spatial resolutions for the Moderate Resolution Imaging Spectroradiometer (MODIS) standard burned area products. These findings indicate that a satellite burned area product that can detect fire scars with a size of 1 km^2 would satisfy regional information requirements for burned area assessment.

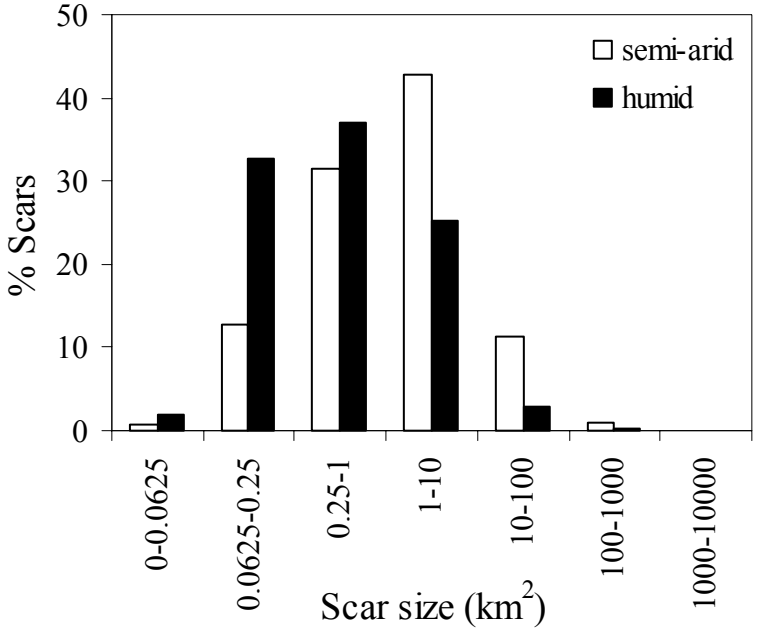

Figure 2. Scar size distribution for the 1989 burned areas.

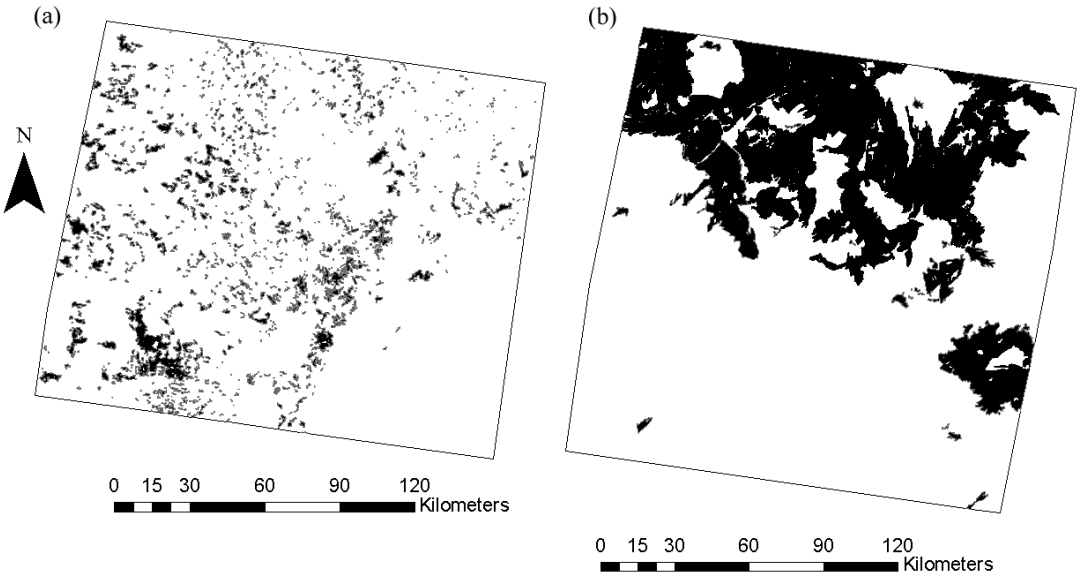

Figure 3. Fire scars in two areas with different climatic conditions in 1989: (a) humid site in Mozambique, (b) semi-arid site in Botswana.

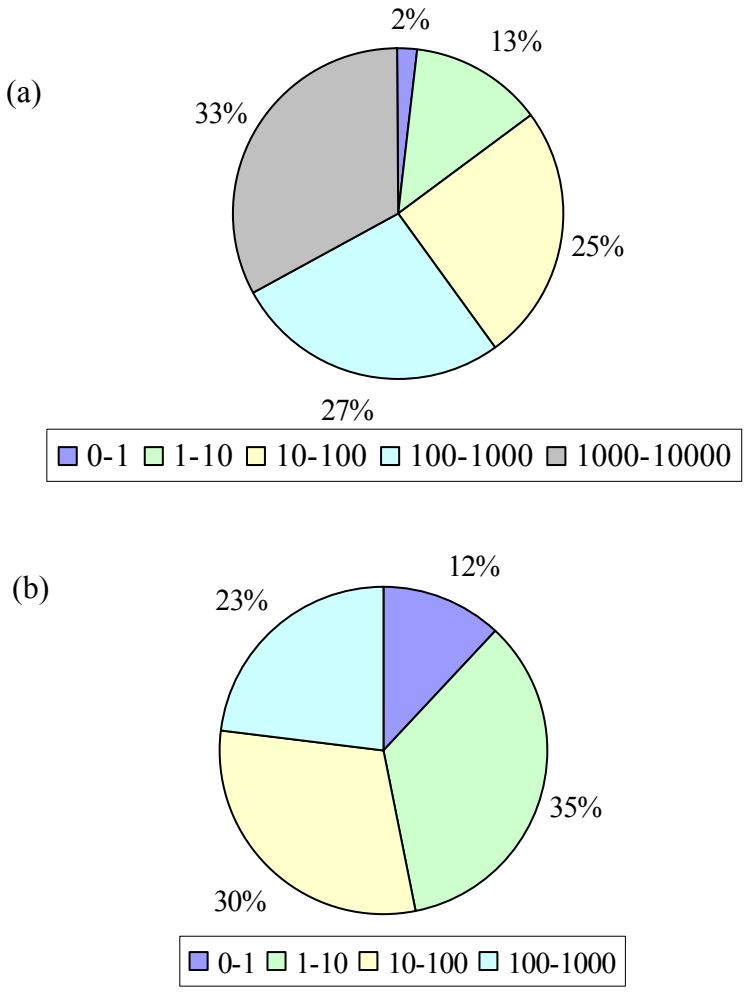

Figure 4. Percentage of the total area burned in each scar size category (km^2) for the 1989 scenes: (a) semi-arid, (b) humid.

The 1992 fire season (April to October) followed an exceptionally dry summer throughout southern Africa. Differences in the total area burned, the scar size distribution and the area burned in each fire size range were observed between 1992 and an average rainfall year (1989). Comparison of three semi-arid scenes from the two years showed that in 1992 the regional drought resulted in a decrease in the burned area by a factor of

10. In992, a decline in the number of larger size burn scars was observed with an 11% increase in scars smaller than 1 km^2 (Figure 5a). In 1989, a small number of very large fires greater than 1000 km^2 accounted for the majority of the burned area, whereas in 1992 there was an absence of fires greater than 1000 km^2 and the burning was more evenly distributed among the three smaller scar size ranges between 1-1000 km^2 (Figure 5b). These results support the previously formulated hypothesis that drought reduces fuel load abundance and the extent of burning in semi-arid regions (Justice *et al.*, 1996; Anyamba *et al*., 2003). In 1992, there was a shift to larger size scars in humid areas compared with 1989 (Figures 2 and 6). This could be attributed to the drying out and increased flammability of the fuel because of the reduced rainfall in the normally humid areas.

2.3.2 Vegetation Fire Emissions

The time-series method was used as the reference for the actual biomass burned and emission estimates. For the particular grassland scene, the start/end method underestimated the true area burned by 12%. Serendipitously, this underestimate of the area burned gave an overestimate of the biomass burned (12%) as compared to the time-series analysis. This overestimation was attributed to an almost even temporal distribution of burning (20% June, 24% July, 24% August, 32% September) and the seasonally increasing combustion completeness. A simulation, done by varying the amounts of burning, showed that the start/end method representing 100% of the area burned, would overestimate the biomass burned by 22%. To get equal amounts of biomass burned by the two methods, the start/end method would have to underestimate the true area burned by 21%.

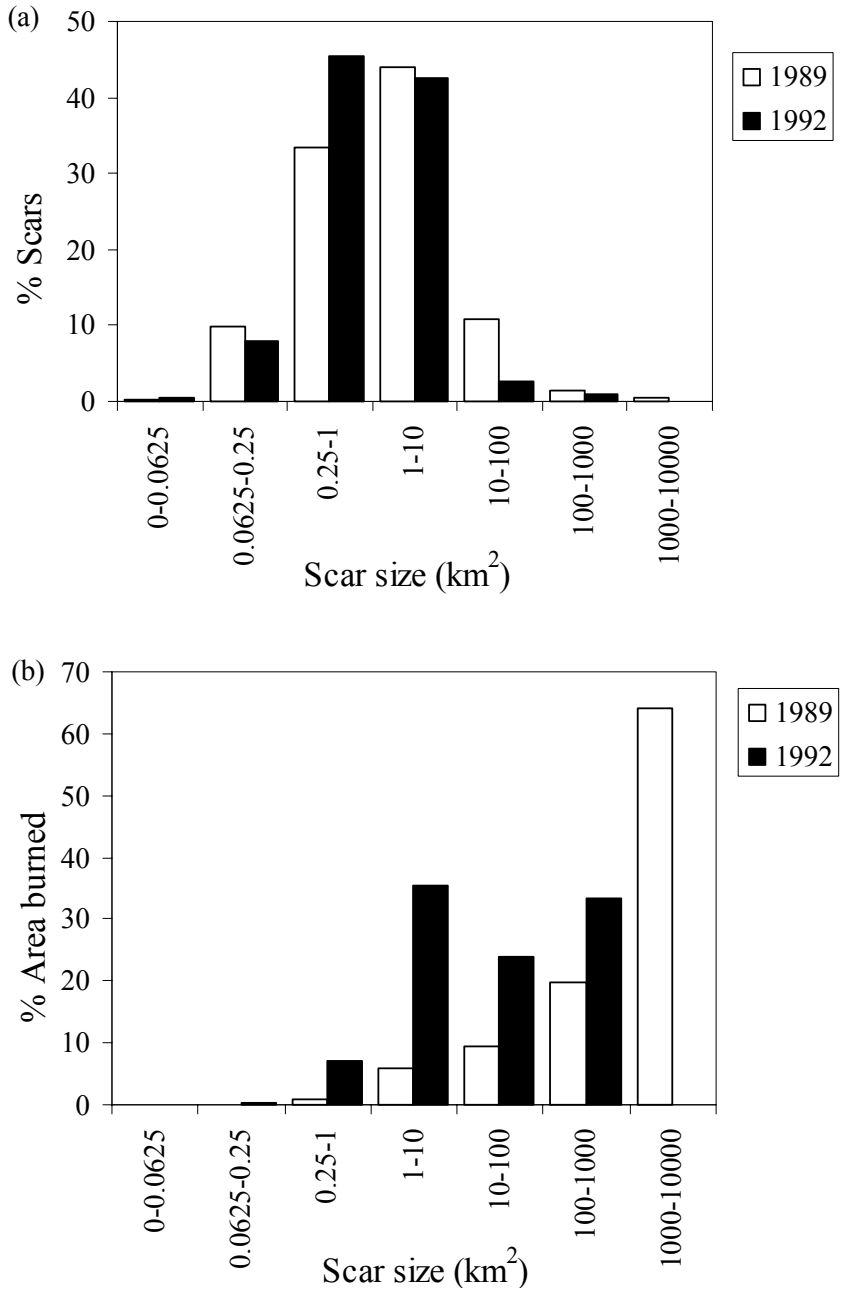

Figure 5. Comparison of the same three semi-arid scenes for 1989 and 1992: (a) scar size distribution, (b) percentage area burned in each scar size category.

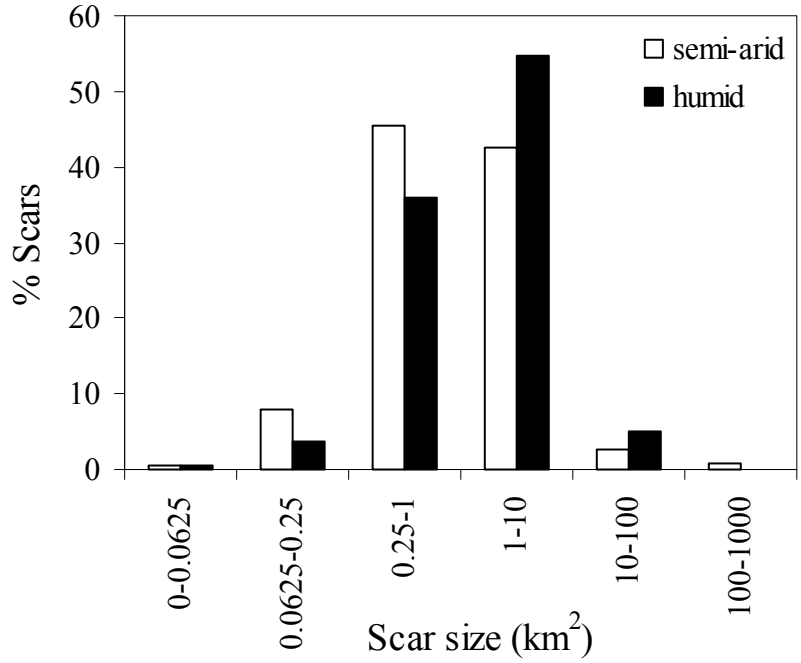

Figure 6. Scar size distribution for the 1992 burned areas.

Distinct differences in the calculated total emissions were also found between the two methods. The start/end method underestimated emissions of products of incomplete combustion relative to the time series method (Table 2). Considering that the start/end method also overestimates the biomass burned, the underestimation error in the emissions is likely even larger than presented here. In the case of CO_2, a slight overestimation occurs with the start/end method which though at the regional level is not deemed important. This is a result of the smaller seasonal variability of the emission factors for CO_2 compared with those for products of incomplete combustion (Table 1). It should also be noted, that in this region of the world, the existing emission factors algorithms for the different pyrogenically produced atmospheric species are derived from late dry season measurements. Therefore, the validity of extrapolating to early dry season burning emission factors is not known. Obviously, seasonal measurements of emission factors are

necessary to test this. These results, at the landscape level, support the hypothesis by Hoffa *et al*. (1999) that incorporation of seasonal dynamics of vegetation fire emissions will tend to increase estimates of products incomplete combustion. However caution should be used in extrapolating this study to regional scales, since the seasonal trends found here for grassland fires at the landscape scale may not be representative for grassland fires at the regional scale. Furthermore, seasonal emission trends for woodland fires are largely unexplored.

Table 2. Total pyrogenic emissions (Gg) for the grassland scene using the time-series and start/end methods.

Emissions	*Time-series method*	*Start/end method*	*% Difference*
CO	257.56	167.68	-54
CH_4	8.61	3.09	-179
NMHC	9.30	5.62	-65
PM2.5	16.95	9.72	-74
CO_2	5493.6	6400.6	14

Figure 7 illustrates the seasonal CO_2 emissions for the grassland scene in Central Zambia. There was more than a doubling in CO_2 emissions from June to July. After this time, CO_2 emissions reached a plateau. This increase in CO_2 as the dry season progressed was primarily due to the higher combustion completeness as the season progresses and the grass fuel dries out, and to a lesser extent due to the increase in area burned in July compared with June. At the same time, emission factors for CO_2 did not vary significantly from July to September (Table 1), which in combination with the almost even distribution of area burned could explain the similarity in CO_2 emissions from July through September.

On the other hand, emissions of products of incomplete combustion exhibited an almost opposite trend to CO_2 (Figure 8). This was somewhat anticipated, as the moister

vegetation burning at the beginning of the dry season produces more products of incomplete combustion relative to later in the season (Hoffa *et al*., 1999). Emissions for products of incomplete combustion reached a peak in July and then dropped substantially at the latter part of the fire season. This was attributed to the fact that fuel consumption was much higher in July than in June. It could be explained if one considers that the fuel is wetter at the beginning of the season, and as it dries out, more burns. At the same time the fuel remains wet enough in July to burn by smoldering. Therefore, the emission factors for products of incomplete combustion in July, even though smaller than in June, were still high enough to drive up emissions. What is interesting to note, though, is the fact that the emissions for products of incomplete combustion were similar to or slightly higher than those in the late dry season, despite the smaller area burned in June compared with August and September. Towards the end of the season, even though fuel consumption was higher, the emission factors for products of incomplete combustion (Table 1) were much lower and resulted therefore in lower emissions.

Using the start/end method to estimate emissions resulted in an underestimation of products of incomplete combustion, as noted above. For example, CH_4 emissions were underestimated by a factor of 2.8. These results suggest that assessment of the intra-seasonal variability of the burning activity parameters, such as burned area, biomass burned, and emission factors, is required to calculate emissions and account for the complexity of fire patterns and their controlling variables at different times of the fire season in savanna ecosystems. This study indicates the requirement for at least a monthly estimation of burned area from satellites in savanna systems.

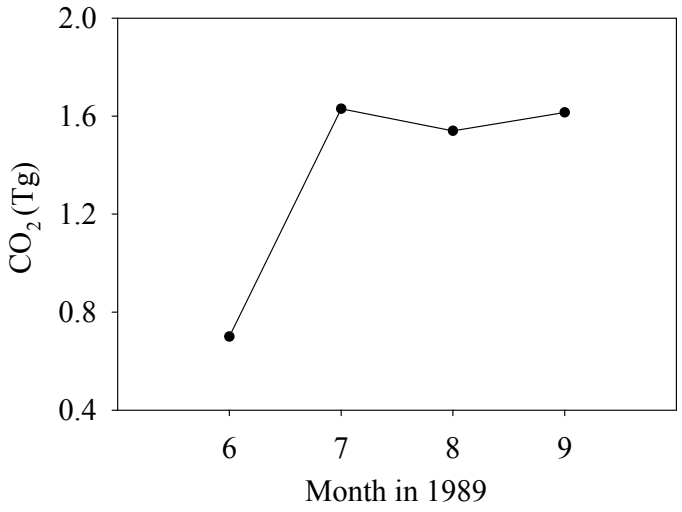

Figure 7. Seasonal CO_2 emissions from the grassland fires.

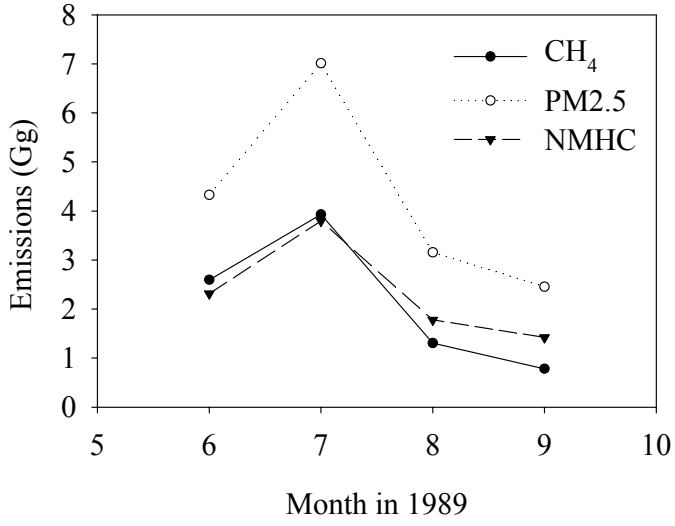

Figure 8. Seasonal emissions of CH_4, PM2.5 and NMHC from the grassland fires.

To facilitate the determination of satellite-derived burned area spatial requirements for accurate pyrogenic emissions modeling in savanna ecosystems, the same grassland scene was used to assess whether a burned area product that detects 1 km^2 scars, is satisfactory or whether a higher resolution would be more desirable. As seen in Figure 9, scars smaller than 1 km^2 contributed 16–19% of the monthly CH_4 emissions. These

numbers, though, could be slightly larger considering that there are additional cases in which scars smaller than 1 km^2 might go undetected using Landsat due to vegetation regrowth between dates or removal of the char by wind.

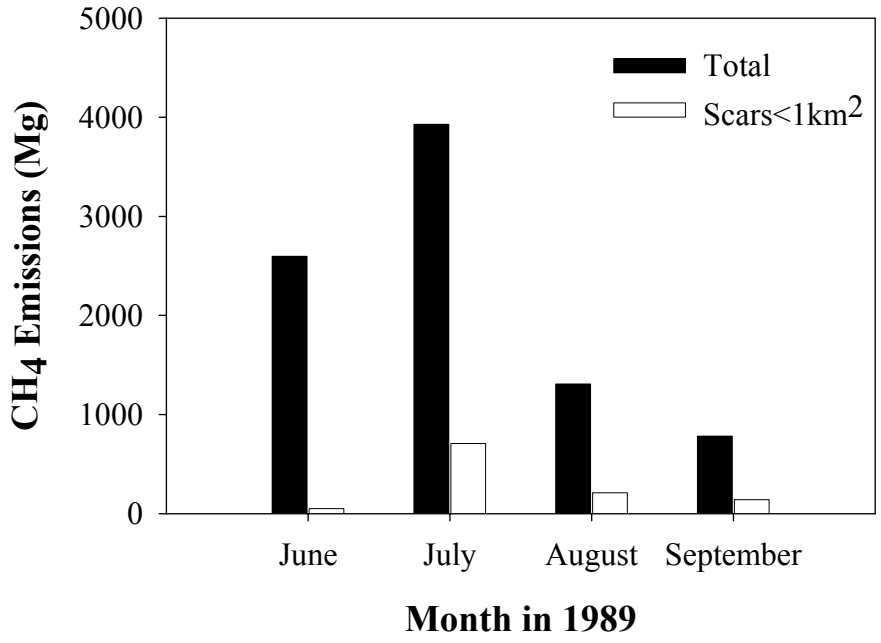

Figure 9. Contribution of fire scars smaller than 1 km^2 to total CH_4 emissions from the grassland fires.

It should also be noted that the July CH_4 emissions from scars smaller than 1 km^2 were almost equal to the total CH_4 emissions in September. This study was for one location and additional studies are needed to evaluate the contribution of smaller scars (< 1 km^2) to regional emissions budgets, but it appears that they might be important, and that a regional burned area products that can map scars smaller than 1 km^2 is more desirable. The limited results of this study also indicate that the spatial resolution requirements for emissions modeling might be higher than those for regional burned area mapping. A 500 m MODIS burned area product has been developed now (Roy *et al.*, 2002a) and offers unprecedented capabilities in regional burned area mapping.

2.3.3 Emissions Sensitivity Analysis

To explore further the potential implications of early dry season burning on annual emissions budgets, a sensitivity analysis was performed for the same grassland scene in Central Zambia, by varying the amount of burning for different scenarios of early and late dry season burning and calculating the resulting total emissions (Table 3). If most of the burning (95%) occurred at the beginning of the season, this would significantly increase the total amounts of incomplete combustion products emitted (CO by a factor of 2, the total CH_4 by a factor of 4, the total NMHC by a factor of 2.4, and the total PM2.5 by a factor of 2.5). Despite the lower fuel consumption, the same amount of burning in the early dry season produces more products of incomplete combustion compared with the late dry season. In general, for annual emissions of products of incomplete combustion, there is a trade off effect between the lower fuel consumption and higher emissions factors in the early dry season, and the higher fuel consumption and lower emission factors in the late dry season. This trade off effect still needs to be explored at the regional level.

Analysis of the 1992 AVHRR active fire product (Giglio *et al.*, 1999) showed that approximately 30% of all fires occurred in the early dry season (May - June). The time-series analysis of another grassland scene showed again that the burning in the early dry season was significant (70% June-July, 30% August-September), whereas in a miombo woodland scene most of the burning occurred at the end of the dry season (6% June-July, 94% August-September). This indicates that early dry season fires could account for a significant portion of the annual emissions for products of incomplete combustion, at least in grassland ecosystems (Table 3). In the case of CO_2, where seasonal emission

factors are less variable, early versus late burning does not have a large effect on the total emissions.

Table 3. Sensitivity analysis of seasonal emissions for the grassland scene.

	Percentage of early/late dry season burning					
Emissions	95/5	75/25	50/50	35/65	15/85	5/95
Total CO (Gg)	298	267	220	188	157	141
% early CO	97.8	87.4	69.8	55.4	28.9	10.8
% late CO	2.2	12.6	30.2	44.6	71.1	89.2
Total CH_4 (Gg)	12.4	11.6	9.6	8.0	5.2	2.8
% early CH_4	99.1	95	87.9	81.1	62.1	22.7
% late CH_4	0.9	5	12.1	18.9	37.9	77.3
Total NMHC (Gg)	11.3	9.8	8.0	6.9	5.5	4.7
% early NMHC	98.1	88.9	72.7	58.9	32	12.3
% late NMHC	1.9	11.1	27.3	41.1	68	87.7
Total PM2.5 (Gg)	20.4	18.9	14.8	12.7	9.9	8.5
% early PM2.5	98.1	89.2	73.4	59.8	32.8	12.7
% late PM2.5	1.9	10.8	26.6	40.2	67.2	87.3
Total CO_2 (Gg)	3617	3932	4246	4561	4875	5033
% early CO_2	93	67.6	41	27.2	10.9	3.5
% late CO_2	7	20.3	43.7	59	89.1	96.5

It is also important to bear in mind that the values of the input parameters to the emissions calculations used in this study fall within their normal ranges in an average precipitation year. Extrapolating the results to years with above or below average precipitation requires a dynamic modeling approach that can simulate the effects of inter-annual climate variability, altered fire regimes and grazing pressure on these input variables. This further supports the need to move from a static emissions estimation approach, to the development of spatially and temporally explicit regional emissions data sets.

2.4 Conclusions

In summary, the results in this chapter demonstrate that incorporation of the temporal patterns of biomass burning in emissions modeling is important when assessing seasonal fluxes of trace gases and aerosols from savanna landscapes. Despite the slight underestimation of the total burned area with the start/end method as compared to a time series approach, at the regional level the results are acceptably close. Similarly, the start/end method produces credible estimates of total CO_2 emissions as compared to the time-series method. In contrast, the intrinsic limitation of the start/end method to account for the temporal variations of fuel consumption and emission factors has a marked effect on the accurate quantification of pyrogenic emissions of products of incomplete combustion. The temporal distribution and amount of the burning will determine the type (*i.e.*, products of complete versus incomplete combustion) and quantities of biomass burning products emitted during the fire season. Time-series rather than annual burned area products are needed to drive increasingly sophisticated emissions models. The availability of fire information at suitable space and time scales will enable the improved understanding and prediction of the environmental impacts of pyrogenic emissions and strengthen natural resources management in the region.

Chapter 3: Parameterization of the seasonal dependence of grassland and woodland fire emission factors for selected trace gases and particulate matter

3.1 Introduction

Emission factors for pyrogenically produced atmospheric species are among the information required for emissions modeling. Thus far, regional fire emissions calculations in southern Africa have been mainly based on late dry season (August to October) ground-based and airborne measurements of emission factors (Ward *et al.*, 1996; Hao *et al.*, 1996; Cofer *et al.*, 1996; Scholes *et al.*, 1996a; Yokelson *et al.*, 2003; Sinha *et al.*, 2003) and/or average values for a particular ecosystem type (Andreae and Merlet, 2001). During the early dry season, from May to late July, fires transition from a condition where they will barely burn to one where they burn with higher intensity. There is a need to determine the effects of this transition on emissions.

In the early part of the fire season the ground fuels typically have higher moisture content, which in addition to other important factors such as fuel loading variations, leaf fall, and weather conditions, may affect the type and the amount of the combustion products and play an important role in the overall budgets of pyrogenically-produced trace gases and aerosols (Hoffa *et al.*, 1999; Chapter 2). Prescribed burning in the early part of the dry season is commonly advocated as a land management tool in tropical savannas (Frost, 1996; Williams *et al.*, 1998). Wetter burns produce lower fire intensities and result in less vegetation consumed and damage to the soil. Pastoralists burn extensively in the early dry season to stimulate regrowth of palatable grasses for their cattle; fire is used for rapid nutrient release prior to the new growing season by farmers; and early burning is used in national parks as a preventive measure against late dry

season fires which tend to have higher intensities and be presumably more destructive. Fire is also used to maintain the competitive balance between trees and grasses.

Currently, the majority of the fires occurring in southern Africa are of anthropogenic origin. Fire regimes are likely to change with changing human population and land use practices, making early burning more widespread (Russell-Smith *et al.*, 1997; Bucini and Lambin, 2002). Figure 1 illustrates four years of Tropical Rainfall Mapping Mission (TRMM) active fire distribution in southern Africa in the main dry season (Giglio *et al.*, 2000). Despite the limitations of using active fire as a surrogate for burned area, these satellite data provide evidence for the seasonal variability of fires and the important contribution of early dry season burning (Justice and Korontzi, 2001).

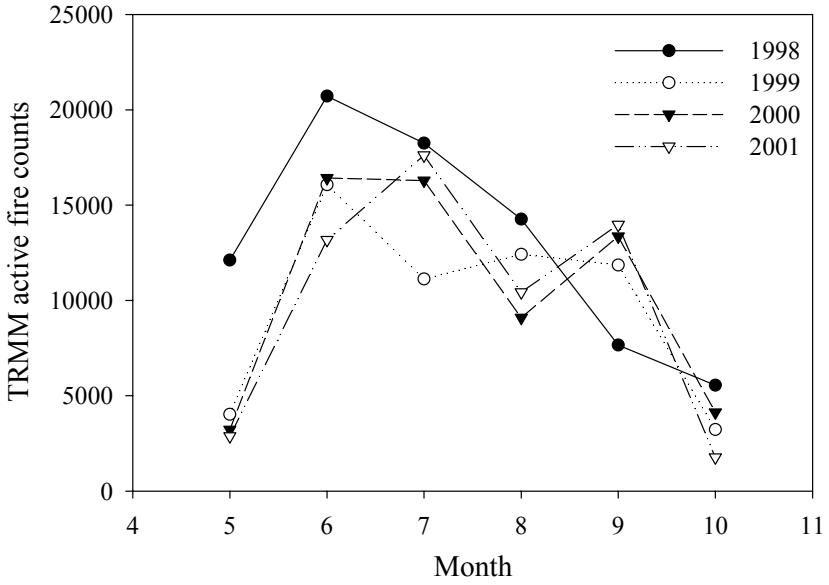

Figure 1. Seasonal and inter-annual TRMM active fire distribution in southern Africa in the dry season (May to October).

In this chapter, explicit early dry season measurements of emission factors for selected carbonaceous (*i.e.*, carbon-containing) trace gases and aerosols in southern African savanna fires made by Dr. Darold Ward and Dr. Erica Smithwick from early June

to early August, 1996, are presented. In addition, the dependency of emission factors on ecosystems with distinct fuel types, grasslands or woodlands, is explored. More specifically, the following questions are posed: 1) What are the seasonal trends in emission factors and how do they relate to the fuel moisture condition? 2) Is the relationship between modified combustion efficiency (an index of the completeness of emission oxidation) and emission factors for each of the atmospheric species analyzed here different for grasslands and woodlands, or can a single model be used to describe the data? 3) How well do results from the early dry season of 1996 compare with results from the late dry season SAFARI-92 (Lindesay *et al.*, 1996) and SAFARI-2000 (Swap *et al.*, 2002) campaigns in southern Africa?

3.2 Methods

3.2.1 Site Description

The field site and fires used for the 1996 study of early dry season fire emission measurements are reported in detail by Hoffa *et al.* (1999). The field site was located about 7.5 km southeast of Kaoma, Western Province, Zambia in the Kaoma Local Forest 310 ($14^{o}52$'S, $24^{o}49$'E at approximately 1170m). Thirteen two-hectare plots (100m x 200m) were burned by Dr. Darold Ward and Dr. Erica Smithwick between June 5 and August 6, 1996. Six plots were in a semi-deciduous, open canopy, semi-arid woodland (miombo) and seven in a seasonally flooded grassland (dambo). The ecosystem sites were separated by approximately 500 m and a dirt road. Three distinct sampling clusters were equally spaced along the long axis of each two hectare plot, as described by Hoffa *et al.* (1999).

Miombo is used to describe the central, southern and eastern African woodlands, dominated by the genera *Brachystegia*, *Julbernardia* and/or *Isoberlinia* (Frost, 1996). It

covers more than 2.7 million km^2 of Africa and 80% of Zambia. Miombo woodlands receiving less than 1100 mm rain annually are considered semi-arid (Chidumayo, 1987). Fire spread in the miombo ecosystem is largely dependent on the amount of grass cover, coupled with meteorological parameters (*i.e.*, wind speed, relative humidity and temperature). Grass production is high in areas of low woodland cover or where the land cover has been disturbed by, for example, gardening or charcoal making. Leaf litter and downed wood are likely the major components of the fuel in the undisturbed miombo. Fires in the humid miombo ecosystem tend to be more frequent and burn with higher fire intensities, presumably due to higher fuel loads (Frost, 1996). Dambos are distinctive areas of African grassland produced by seasonal flooding; they occupy about 10% of Zambia (Hoffa *et al.*, 1999). Dambos play an important role in traditional land use systems in Africa. They are mainly used for grazing, cultivation of food and cash crops, and as a water supply for domestic use and livestock (Acres *et al.*, 1985).

3.2.2 Measurement of Emissions

SAFARI-2000 results showed that the composition of smoke from savanna fires changes rapidly as the smoke ages (Hobbs *et al.*, 2003). In the 1996 study the initial emissions from grassland savanna and miombo woodland fires for carbon dioxide (CO_2), carbon monoxide (CO), methane (CH_4), non-methane hydrocarbons (NMHC) and particulate matter with diameter less than 2.5 μm (PM2.5) were measured. The sampling design at each plot and the emissions analyses are described by Shea *et al.* (1996), Ward *et al.* (1996) and Hao *et al.* (1996). A Fire-Atmosphere Sampling System (FASS) tower was placed at the center of each cluster (three towers per plot) to collect smoke samples for emissions measurements. Each FASS system collected a background sample before

the fire was ignited and two canisters from each burn approximately timed to sample separately the flaming and smoldering combustion. The plots were successively burned at approximately 1-2 week intervals throughout the study period. Hoffa *et al.* (1999) give descriptions of the vegetation fuel types, loads, environmental conditions and fire behavior at these plots. CO_2, CO, CH_4, and NMHC (C_2-C_3 aliphatic compounds and some aromatic compounds) were analyzed with gas chromatography (GC) as described by Hao *et al.* (1996). The PM2.5 concentration was determined from the increase in weight of Teflon filters exposed to the smoke divided by the volume of air sampled (Ward *et al.*, 1996).

The quantification of different compounds emitted from fires is commonly expressed using the emission factor (EF). The EF is the mass of a specific gas or particulate matter emitted by the combustion per unit mass of dry fuel consumed (g kg^{-1}). Table 1 (Appendix A) provides the net concentrations of emitted CO_2, CO, CH_4, NMHC and PM2.5 and the proportion of fuel consumed during the flaming and smoldering combustion in the fire at each plot. EFs are calculated from the net concentrations using the carbon mass balance technique described by Ward *et al.* (1982). The underlying premise of this method is that all of the carbon combusted in a fire and released to the atmosphere is emitted into the smoke plume as CO_2, CO, CH_4, non-methane hydrocarbons (NMHC) and particulate matter (PM2.5). The EF of a species x is defined here as the ratio of the net mass concentration [Δx] of x emitted by a fire to the net mass concentration of total carbon, [ΔC], emitted by the fire:

$$EF_x = \frac{[\Delta x]}{[\Delta C]_{CO_2} + [\Delta C]_{CO} + [\Delta C]_{CH_4} + [\Delta C]_{NMHC} + [\Delta C]_{PM2.5}} \qquad (3.1)$$

The EF is expressed in units of grams of x emitted per kilogram of carbon burned. To convert this emissions factor to units of grams of x per kilogram of fuel burned, EF is multiplied by the mass fraction of carbon in the fuel. To make the results of this research comparable with those from previous studies a standard carbon fuel content of 50% is used (Ward *et al*, 1996; Yokelson *et al.,* 2003*;* Sinha *et al.,* 2003).

The fuel consumption ratios are determined using the FASS carbon flux technique and they are used in calculating the fire-weighted emissions factors. The measured background range for CO_2 was 340 ppm to 360 ppm. Many of the smoldering samples and two flaming samples in the grassland fires were close to natural background with very low net concentrations and within the error range of the canister analysis. While background might change with season, there should not be much change across the plot on the same day. EFs for non-CO_2 compounds cannot be calculated without the CO_2, in the carbon mass balance method used. Therefore, all samples that had net CO_2 concentrations less than 20 ppm difference from background were rendered as highly uncertain and are not included in the calculations of the MCE or the EFs for all atmospheric species in the grassland fires. The low concentration non-CO_2 EFs are excluded since MCE is a linear function of the CO_2 and any uncertainty in MCE will propagate in the regressions of EFs versus MCE. The July 26 PM2.5 collections were also below our limit for accurate emission factor data.

The EFs for carbon-containing species are often linearly correlated to the modified combustion efficiency (MCE), which is the molar ratio of carbon emitted as CO_2 to the sum of carbon emitted as CO and CO_2 (Ward *et al.*, 1996; Sinha *et al.*, 2003; Yokelson *et al.*, 2003).

$$MCE = \frac{[\Delta C]_{CO_2}}{[\Delta C]_{CO_2} + [\Delta C]_{CO}} \quad (3.2)$$

The MCE is an indicator of the relative contribution of flaming and smoldering combustion in a fire. Laboratory fire experiments have shown that MCE ranges from 0.98±0.01 for flaming combustion to near 0.80±0.08 for smoldering combustion (Yokelson *et al.*, 1996). An MCE < 0.9 suggests > 50% smoldering combustion, and an MCE > 0.9 suggests > 50% flaming combustion (Sinha *et al*., 2003).

In the case of the miombo woodland samples, due to the unavailability of reliable FASS fuel consumption data, EFs are weighted by assuming a 85/15 ratio for flaming and smoldering, respectively (Ward *et al.*, 1996; Hoffa *et al.*, 1999). Hoffa *et al.* (1999) weighted the MCEs by assuming the 85/15 ratio in both dambo grasslands and miombo woodlands. Since a different weighting procedure is applied for the grassland fires in this study, the grassland MCEs presented here are slightly different than those reported by Hoffa *et al.* (1999). A single MCE and EF value is calculated for each FASS tower. The MCE and EF values from the FASS towers at each plot are then averaged to obtain a plot value used in the analysis (Table 2).

3.2.3 Statistical Analyses

The EF data versus MCE are analyzed using simple linear regression. Models are developed for each set of woodland and grassland EF data using a linear least squares residual fitting technique. The separate regression lines are then compared to a single regression model, derived from the combined grassland and woodland data. The purpose of this analysis is to determine possible statistically significant differences (hereafter, referred to as significant) in EFs between ecosystems in the unique, but limited amount of

Table 2. Early dry season modified combustion efficiency (MCE) and weighted average emission factors (EF) for CO_2, CO, CH_4, NMHC and PM2.5 for grassland (G) and woodland (W) fires.

Site	*Date*	*MCE*	*$EFCO_2$ (g kg^{-1})*	*EFCO (g kg^{-1})*	*$EFCH_4$ (g kg^{-1})*	*EFNMHC (g kg^{-1})*	*EFPM2.5 (g kg^{-1})*
G1	6/5/96	0.912	1637.4	101.12	3.132	4.734	6.461
G2	6/14/96	0.913	1638.5	100.35	3.045	5.036	6.293
G3	6/26/96	0.955	1735.3	52.27	1.181	2.142	2.842
G4	7/9/96	0.963	1754.4	42.98	0.940	1.449	2.042
G5	7/18/96	0.972	1772.3	32.56	0.584	1.074	2.288
G6	7/26/96	0.953	1706.8	54.16	1.011	1.554	---
G7	8/6/96	0.944	1707.8	64.31	2.282	2.747	4.514
W1	6/6/96	0.940	1700.0	68.99	1.754	2.363	5.889
W2	6/18/96	0.941	1704.4	68.03	1.971	1.861	4.997
W3	7/5/96	0.952	1722.9	55.44	1.374	1.737	6.493
W4	7/16/96	0.932	1685.8	78.19	2.529	2.014	5.310
W5	7/24/96	0.937	1692.9	72.60	2.185	2.053	6.436
W6	7/29/96	0.907	1614.6	105.79	3.921	2.786	15.145

the 1996 data. However, interpretation of the results, does not rely solely on the accept/reject logic of statistical hypothesis testing because, in some cases, small statistical differences are meaningless to prospective fire information users (*e.g.*, in regional and global emissions modeling).

To measure the overall variability around the regression lines, the pooled estimate of the variance about the two regression lines, $s^2_{EF.MCE_p}$ is computed as:

$$s^2_{EF.MCE_p} = ((n_g-2)*s^2_{EF.MCE_g} + (n_w-2)\, s^2_{EF.MCE_w})/ (n_g+n_w-4) \qquad (3.3)$$

where $s^2_{EF.MCE}$ is the standard error of the estimate, and $n_g+n_w-4 = \nu$ are the degrees of freedom (Glantz, 1997). Subscripts 'g' and 'w' refer to the grassland and woodland data, respectively. The improvement in the fit obtained by fitting the data sets with separate regression lines, compared to a single regression line is computed using:

$$s^2_{EF.MCE_{imp}} = (SS_{res_c} - SS_{res_p}) / 2 \qquad (3.4)$$

where, SS_{res_c} is the sum of squared residuals around the common regression line and SS_{res_p} is the sum of squared residuals about the separate regression lines.

The relative improvement in the fit obtained by fitting the two data sets separately is quantified using the *F*-test statistics. This value is then compared with the critical value of the *F*-test statistic for $v_n = 2$ numerator degrees of freedom and $v_d = n_g+n_w-4$ denominator degrees of freedom. The *F*-test statistic is defined as:

$$F = s^2_{EF.MCE_{imp}} / s^2_{EF.MCE_p} \quad (3.5)$$

If the observed value of *F* exceeds the critical value of *Fcrit*, it indicates that a significantly better fit to the data (measured by the residual variation about the regression line) is obtained by fitting the two datasets with separate regression lines than by fitting all of the data to a single line.

Finally, all of the EFs from this study are combined with results from the SAFARI-92 and SAFARI-2000 late dry season field campaigns to derive a synthetic regression predictive model for regional EFs from MCEs. The conventional significance level of 95% ($P \leq 0.05$) is used for all hypotheses tested. Throughout the analyses, checks are performed to test for the assumptions of normality of the residuals and homogeneity of the variances. In some cases, violation of one or both of the assumptions may occur, mostly when all the data are fitted with the common regression line. Other investigators encountered similar problems (*e.g.*, Ward *et al.*, 1996, Hao *et al.*, 1996; Yokelson *et al.*, 2003). Despite these statistical problems, the empirically derived regression models combined with conceptual models provide a useful tool to estimate the natural variation of the data and for comparison with previous results.

3.3 Results and Discussion

3.3.1 Seasonal Trends

3.3.1.1 Modified Combustion Efficiency

In the 1996 data there is a lower limit for MCE of 0.907 and 0.912 and an upper limit of 0.952 and 0.972 for the woodland and the grassland fires, respectively (Table 2). There is a more pronounced seasonal change in the grassland MCE than in the woodland MCE (Figure 2). In grasslands, it appears that MCE varies inversely to the moisture content of the grass fuel (Hoffa *et al.*, 1999; Saarnak, 1999). Generally, for this region, as the season progresses and the grasses achieve lower moisture content, the combustion process becomes more efficient and the MCE increases.

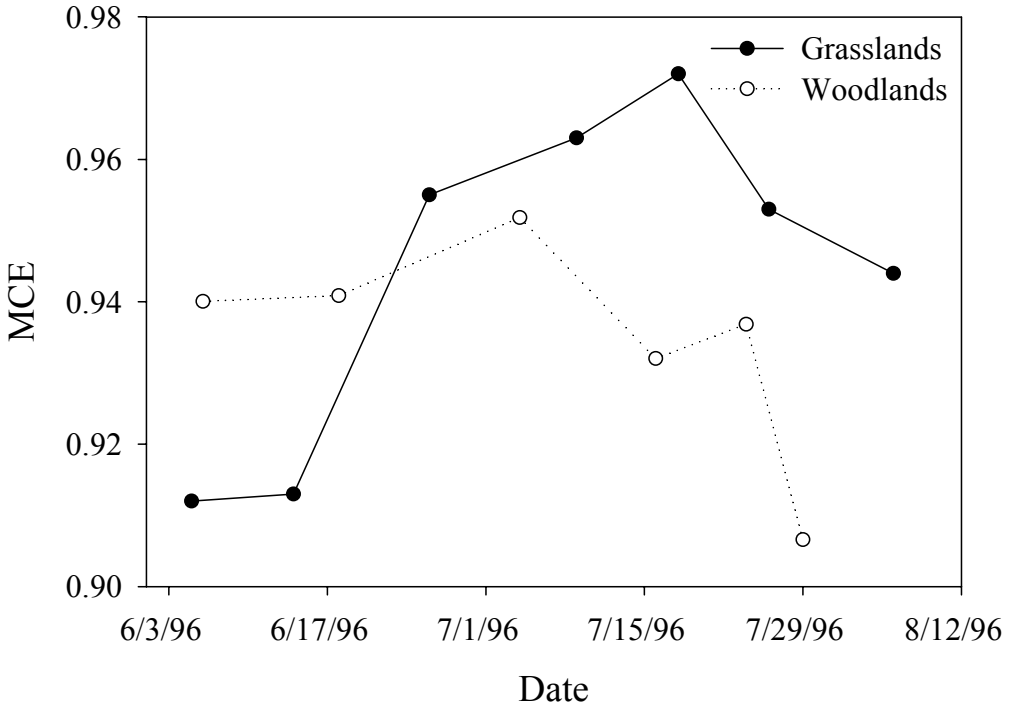

Figure 2. Seasonal progression of the modified combustion efficiency (MCE) for grassland and woodland fires.

Hoffa *et al.* (1999) found that the MCE of the 1996 grassland fires was correlated with the proportion of green grass (PGREEN) in the fuel, with higher moisture content than dead grass. The correlation between MCE and PGREEN (Figure 3) is recalculated here since a different weighting procedure is used to derive the grassland MCEs than Hoffa *et al.*:

$$MCE = 1.010\text{-}0.217(PGREEN), \quad R^2 = 0.73 \tag{3.6}$$

It should be pointed out, that despite the different weighting factors used for flaming and smoldering in the 1996 study for the grassland fires compared with Hoffa *et al.* (1999) the seasonal trends in MCE are similar for both methods of data analysis.

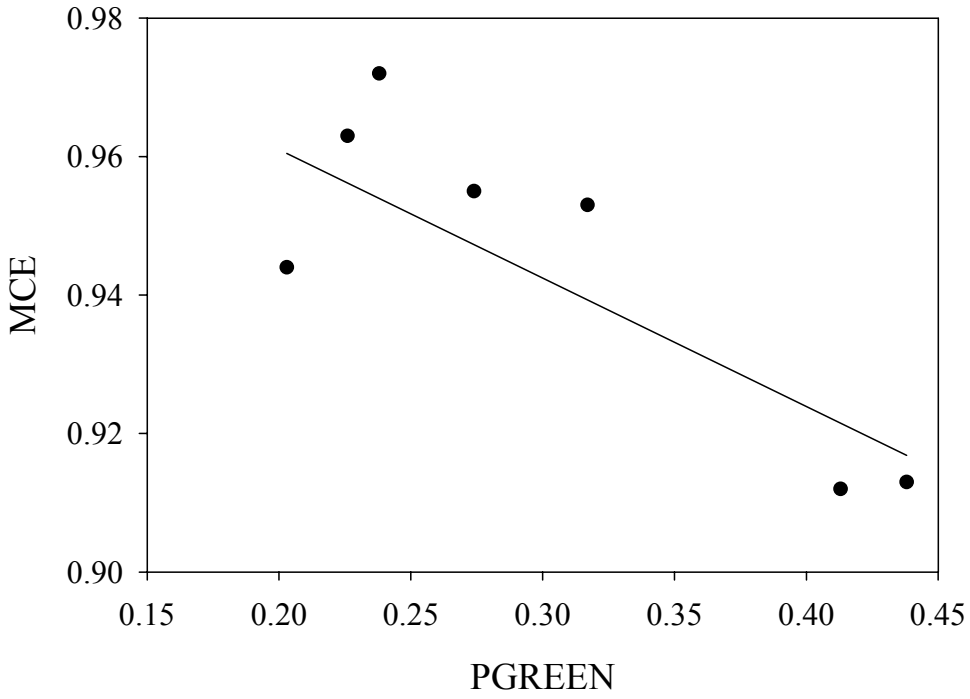

Figure 3. Modified combustion efficiency (MCE) versus proportion of green grass (PGREEN) for grassland fires.

Ward *et al.* (1996) found, that in woodlands, where grass was a larger fraction of the fuel, the MCE relates to the proportion of the grass in the fuel. In other woodlands, where the grass fuel component is minor, as was the case for the specific 1996 Zambian site (between 7% and 14%), it appears that other fuel types than grass, that increasingly contribute to burning as the dry season progresses, control the MCE. Litter fall occurs as the dry season progresses, so that the amount of leaf litter increases seasonally (Hoffa *et al.*, 1999). The litter and woody fuels dry slower than the grasses and tend to burn by smoldering, which can lower MCE (Bertschi *et al.*, 2003). Each fuel type makes a different contribution to the MCE, with litter and woody fuels having the opposite effect compared to the grasses. The combustion factors (the percentage of fuel consumed by the fire) for the burning of all fuel types and the fire intensity generally increase as the dry season progresses (Hoffa *et al.*, 1999). Whereas though, the grasses tend to involve more flaming combustion which seems to increase the MCE, the litter and woody fuels tend to involve more smoldering combustion and may decrease the MCE. This might explain the lower MCE in the July 29, 1996 woodland burn. Given the vast area and diversity of African woodlands there could be seasonal trends in miombo woodlands, which are not apparent from the limited measurements made in this 1996 study.

3.3.1.2 Emission Factors

A distinct seasonal trend is observed in the EFs for all measured species in smoke from the dambo grassland fires. The $EFCO_2$ increase as the season progresses due to the higher degree of oxidation from the combustion of the drier fuels, but the variability is small with a maximum difference of about 8.2% (Figure 4a). On the other hand, the EFs of the products of incomplete combustion vary substantially during the fire season

(Figures 4b, 5a-c). On average, they are highest in the first part of the early dry season relative to later in the early dry season by maximum factors of 3.1 for CO, 5.4 for CH_4, 4.7 for NMHC and 3.2 for PM2.5.

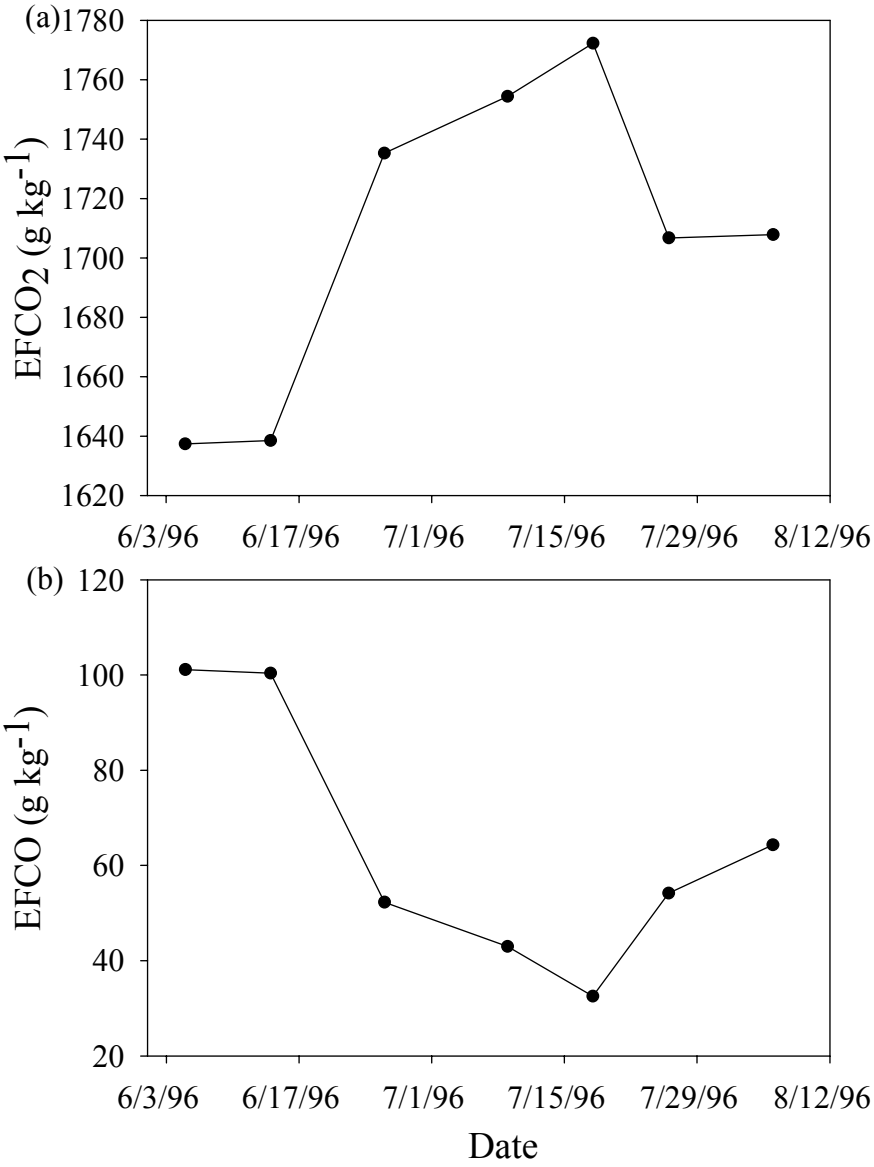

Figure 4. Seasonal emission factors for (a) CO_2 and (b) CO for grassland fires.

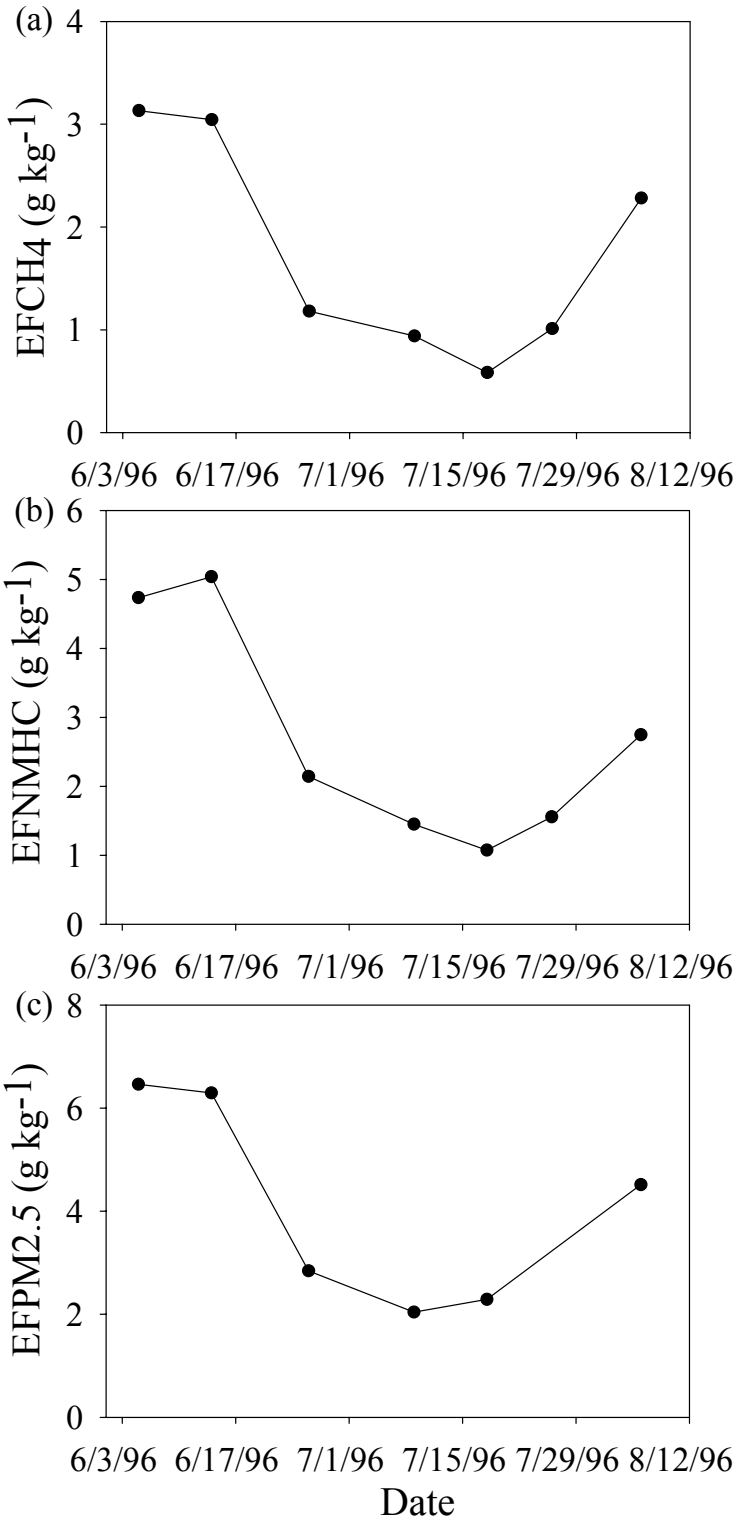

Figure 5. Seasonal emission factors for (a) CH_4, (b) NMHC and (c) PM2.5 for grassland fires.

EFs are directly related to PGREEN in grasslands, supporting the hypothesis that as the fuels dry out a higher degree of oxidation is achieved, resulting in more CO_2 and less products of incomplete combustion compared with earlier in the dry season when the grasses have a higher moisture content. The regression models of EFs versus PGREEN in grasslands (Figures 6a-b, 7a-c) are:

$$EFCO_2 = 1857.8 - 499.0(PGREEN), \quad R^2 = 0.76 \tag{3.7}$$

$$EFCO = -11.06 + 249.02(PGREEN), \quad R^2 = 0.73 \tag{3.8}$$

$$EFCH_4 = -0.705 + 8.114(PGREEN), \quad R^2 = 0.50 \tag{3.9}$$

$$EFNMHC = -1.631 + 14.298(PGREEN), \quad R^2 = 0.68 \tag{3.10}$$

$$EFPM2.5 = -0.747 + 16.138(PGREEN), \quad R^2 = 0.68 \tag{3.11}$$

Linking PGREEN to a remotely-sensed vegetation condition index, such as the Normalized Difference Vegetation Index (NDVI), which is sensitive to the presence of green vegetation, may be useful for regional applications of the above relationships to estimate emissions from grassland fires.

In the woodland site, the lower $EFCO_2$ (Figure 8a) and the higher EFs for products of incomplete combustion (Figures 8b, 9a-c) on the last day of burning suggest a higher contribution of smoldering combustion. This could be due to drier litter and woody fuels becoming more involved in the combustion and lowering the MCE. Additional early dry season studies are needed to evaluate seasonal emissions from diverse types of miombo woodlands, with different canopy covers, fuel loadings, land uses, vegetation structure and moisture conditions.

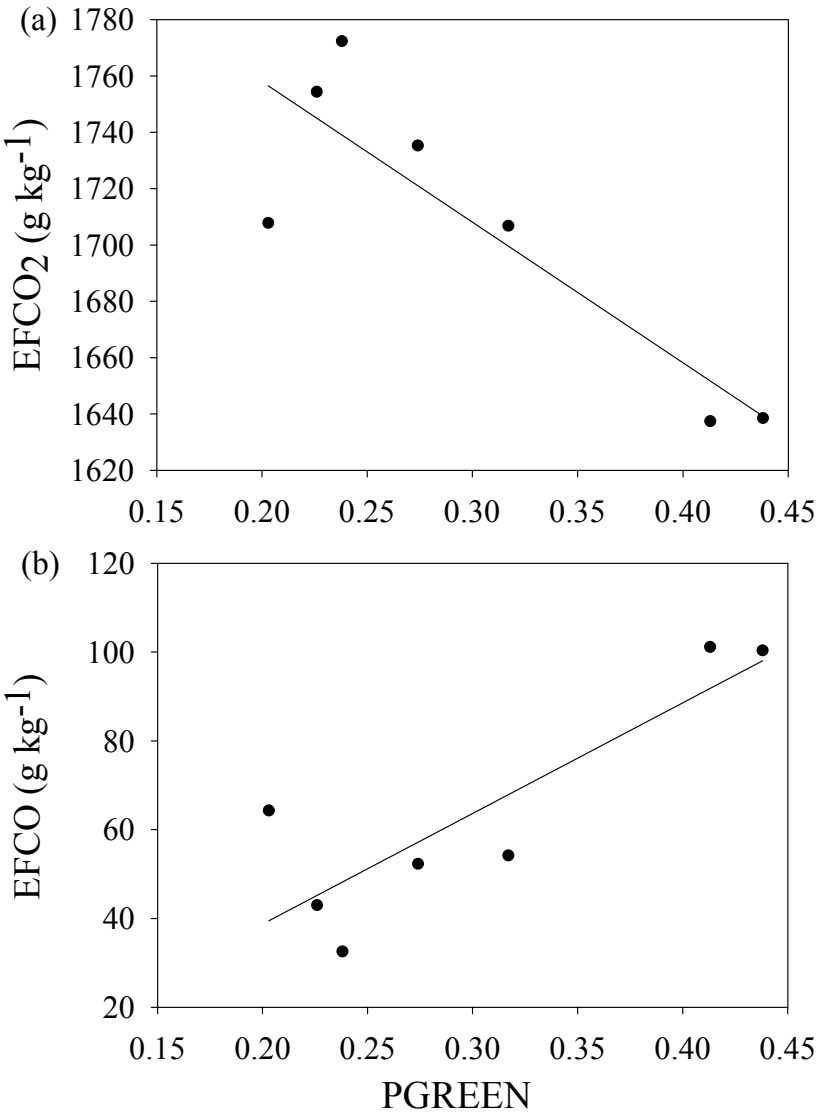

Figure 6. Emission factors for (a) CO_2 and (b) CO versus proportion of green grass (PGREEN) for grassland fires.

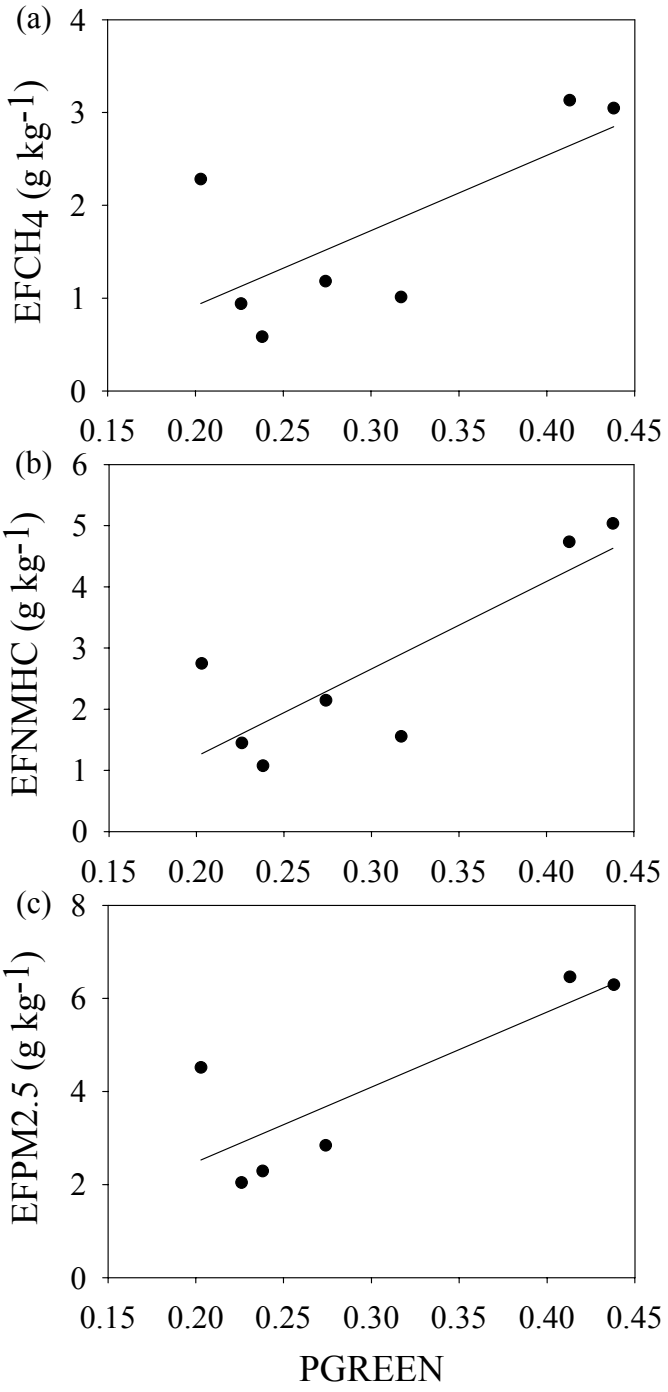

Figure 7. Emission factors for (a) CH_4, (b) NMHC and (c) PM2.5 versus proportion of green grass (PGREEN) for grassland fires.

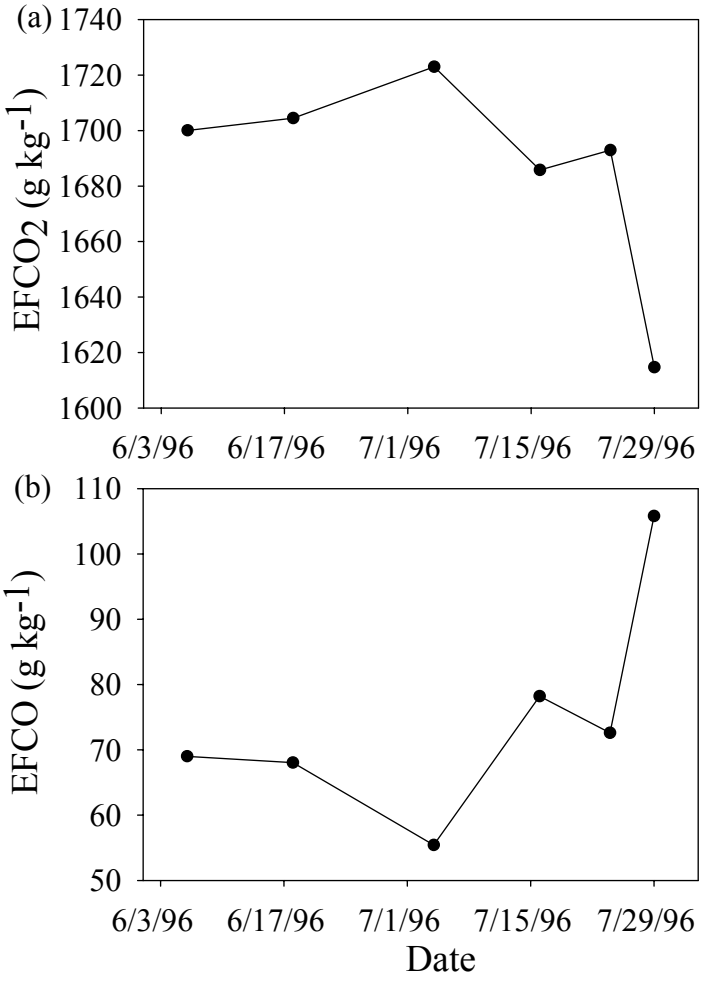

Figure 8. Seasonal emission factors for (a) CO_2 and (b) CO for woodland fires.

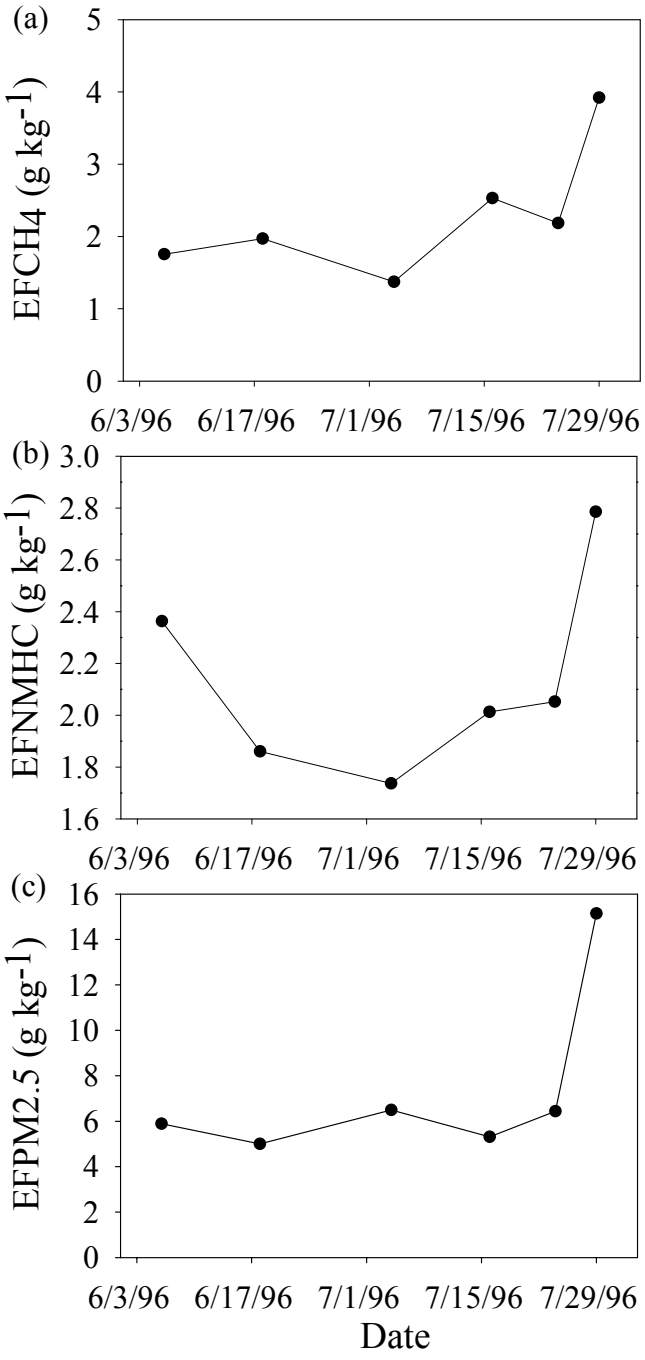

Figure 9. Seasonal emission factors for (a) CH_4, (b) NMHC and (c) PM2.5 for woodland fires.

3.3.2 Ecosystem Differences

3.3.2.1 Methane

Table 3 shows the regression lines and coefficients of EFs versus MCE using the ecosystem-specific data and those using the combined grassland and woodland data set. A comparison of the $EFCH_4$ versus MCE regression models for the woodland and grassland ecosystems (Figure 10a) shows that the mean residual variation for the two separate models is not significantly different from the mean residual variation about a single regression model (*i.e.*, for grassland and woodland EFs taken together) ($F = 1.90 < Fcrit = 4.26$). This indicates that for the 1996 data the EFs for CH_4 are essentially the same for grassland and woodland savanna fires. No ecosystem difference was found in the $EFCH_4$ for controlled burns conducted in different southern African savanna ecosystems during SAFARI-92, as well (Hao *et al.*, 1996).

3.3.2.2 Non-Methane Hydrocarbons

For NMHC, the mean residual variation about the two ecosystem-specific regression lines is significantly different from that of the common regression line ($F = 36.77 > Fcrit = 4.26$), indicating an ecosystem dependence for the EFNMHC in the 1996 data (Table 3). Figure 10b illustrates the relationship between EFs and MCE for the two ecosystem types. There is a much greater increase in NMHC emissions with decreasing MCE in grassland than in woodland savannas. At the lowest MCE (0.907) found in this 1996 study, the predicted grassland EFNMHC is 86% higher than the measured woodland EFNMHC at this MCE. Thus, it appears that using an ecosystem-specific model improves the fit for the 1996 NMHC data. This is in contrast with Hao *et al.* (1996) who found that the emission ratios of NMHC over CH_4 were independent of savanna type and fuel amount in the SAFARI-92 measurements.

Table 3. Average values of regression slopes, intercepts and correlation coefficients (R^2) for emission factors (EF) for CO_2, CO, CH_4, NMHC and PM2.5 versus the modified combustion efficiency (MCE). All hypotheses were tested at $P \leq 0.05$.

	Grasslands	*Woodlands*	*Combined*	*Regional*
$EFCO_2$				
Intercept	-388.1	-613.6	-436.9	-288.4
Slope	2218.6	2460.7	2270.9	2118.1
R^2	0.97	0.99	0.98	0.90
EFCO				
Intercept	1145.30	1119.07	1137.23	1158.08
Slope	-1144.79	-1117.02	-1136.34	-1157.63
R^2	0.99	0.99	0.99	0.98
$EFCH_4$				
Intercept	42.951	56.710	47.068	46.929
Slope	-43.630	-58.214	-47.948	-47.737
R^2	0.94	0.98	0.94	0.81
EFNMHC				
Intercept	65.982	22.757	47.916	36.367
Slope	-67.021	-22.059	-48.389	-35.885
R^2	0.97	0.76	0.65	0.44
EFPM2.5				
Intercept	75.924	211.108	124.050	95.762
Slope	-76.180	-217.932	-126.011	-95.488
R^2	0.96	0.73	0.58	0.32

3.3.2.3 Particulate Matter

An ecosystem dependence exists also for PM2.5 ($F = 6.44 > Fcrit = 4.46$) (Table 3). There is approximately a difference of a factor of two between the two ecosystems at the lowest MCE in EFPM2.5 (Figure 10c). The emissions are higher from woodland savanna than from grassland savanna fires, which is the opposite of what was observed for the NMHC emissions.

The NMHC and PM2.5 data indicate that there may be more of an ecosystem dependence early in the dry season than later in the dry season. The ecosystem-specific models for EF versus MCE hinge on a small number of low MCE samples (especially for woodlands) and they need to be verified by more study. However, if the trends suggested from this unique set of early dry season measurements are valid, this has important implications for estimates of smoke emissions from southern African savanna fires.

3.3.3 Regional Synthesis of Emission Factors

Figures 11a-c and Table 3 integrate the EFs from the 1996 study with those from the SAFARI-92 and SAFARI-2000 dry season field campaigns (Ward *et al.*, 1996; Hobbs *et al.*, 2003; Yokelson *et al.*, 2003) to develop regional-average models of EFs versus MCE. Specifically, the woodland and grassland ecosystem-specific regression models from 1996 (Figures 10a-c) are compared with the regional-average EF models to determine their maximum differences over the corresponding range of MCE values measured in this 1996 study. The regional-average models described in this section are considered to be more robust because they are based on measurements that were conducted in a variety of savanna regions, including humid woodland, semiarid woodland and moist grassland sites, and combine both late and early dry season measurements. In the case of NMHC and PM2.5 (Figures 10b-c and 11b-c, respectively), the integration of the data sets significantly decreases the regression coefficients (Table 3).

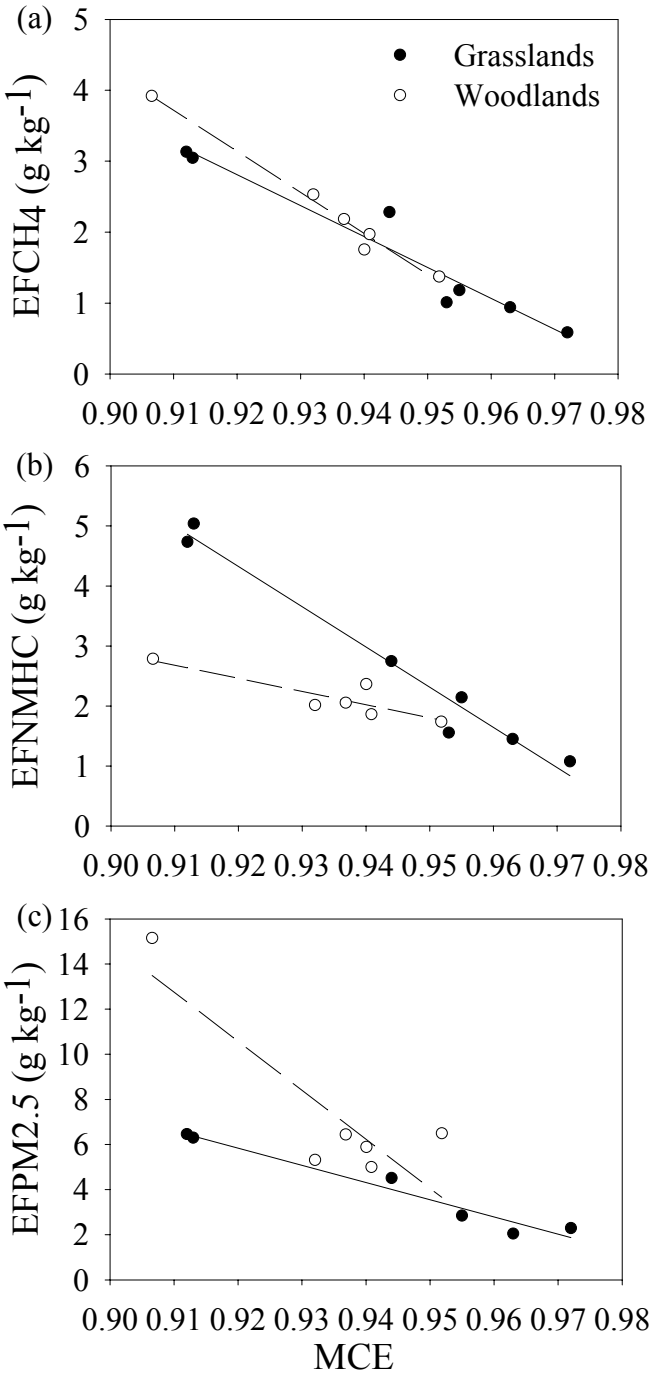

Figure 10. Emission factors for (a) CH_4, (b) NMHC and (c) PM2.5 versus modified combustion efficiency (MCE) for grassland and woodland fires.

For woodlands, the regional average model predicts an EFNMHC that is 39% larger at the lowest MCE of 0.907. The difference decreases with increasing MCE and becomes zero at an MCE value of 0.984. At the mean of all woodland MCE values observed here (0.935) the regional-average approach predicts an EFNMHC that is 32% larger compared with the woodland model. On the other hand, the regional-average model predicts an EFNMHC that is lower by 25% at the lowest grassland MCE of 0.912 and by 7% at the average grassland MCE of 0.945 compared with the grassland model. There is no difference in the grassland EFNMHC when using the two models at the MCE of 0.951 (where the regression lines cross). For MCE values greater than this, the regional average model predicts EFNMHC that are higher than the grassland model. For example, at the highest grassland MCE of 0.972, measured in this 1996 study, the regional average model predicts an EFNMHC that is higher by 78% compared with the grassland model.

In the case of EFPM2.5, the maximum difference between the regional-average and the grassland models of 57% occurs at the highest grassland MCE value of 0.972. As the MCE decreases, the difference between the two models decreases but the two models never coincide over the entire range of grassland MCE values measured here. At the lowest grassland MCE of 0.912 the regional-average model predicts an EFPM2.5 that is higher by 35% compared with the grassland model. Theoretically, the regional-average model will always over predict the grassland MCE values compared with the grassland model, since the calculated concurrence between the two models occurs at an MCE value of greater than 1.000. The regional-average model predicts an EFPM2.5 woodland fires that is higher by 34% at the highest woodland MCE value of 0.952, smaller by 32% at the

lowest woodland MCE value of 0.907, and smaller by 12% at the average woodland MCE of 0.935, compared with the woodland model. More measurements are needed in the early dry season to determine if the 1996 data are outliers, or if an ecosystem dependence can be documented more strongly. In the case of CH_4 (Figures 10a and 11a), the integration of the datasets produces a small decrease in the correlation coefficient (Table 3) and little difference compared with the ecosystem-specific algorithms.

Considering that the data used here were collected in different rainfall years (1992 was dry, 1996 was average, and 2000 was wet), in different locations, and were collected (ground and airborne) and analyzed using different methods (GC and airborne Fourier transform infrared spectroscopy), it is not surprising to find these variations between regional-average and ecosystem-specific EFs. It should be noted, that these differences have different meanings for various users of fire information. For regional and global emissions estimation, the differences in these EFs are likely of lesser importance relative to the larger uncertainties in some of the other modeling variables, such as fuel load and burned area, which may result in emission estimates that vary substantially (compare Scholes *et al.* (1996a) with Hao *et al.* (1990)).

At the same time, it is important to know and consider the differences in EFs discussed here when reporting the overall error of a regional emissions model. For example, Scholes *et al.* (1996a, 1996b) estimated that their emissions model was accurate to within ± 60%. Compared to that level of claimed accuracy, the differences between regional-average and ecosystem-specific EFs presented here appear significant and

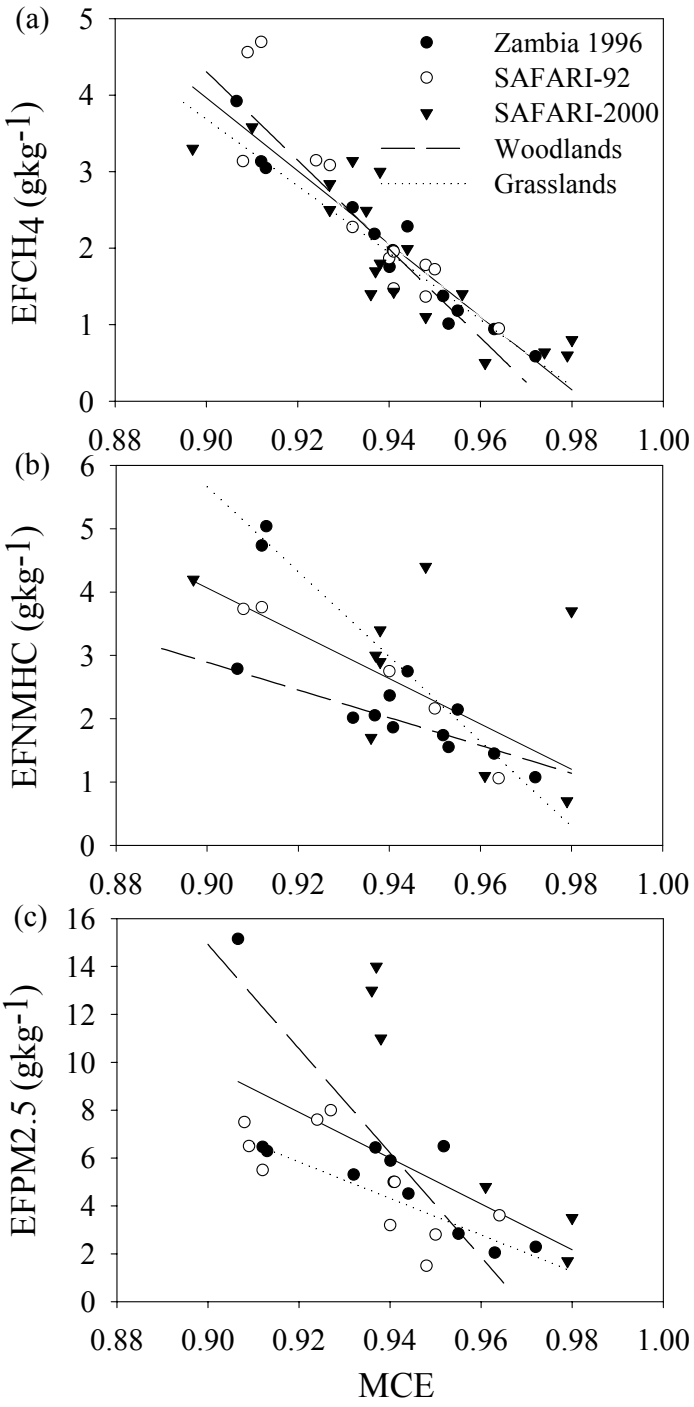

Figure 11. Regional integration of emission factors from this study, SAFARI-92 and SAFARI-2000 for (a) CH_4, (b) NMHC and (c) PM2.5 versus modified combustion efficiency (MCE). The corresponding grassland and woodland models are also shown.

suggest that an ecosystem-specific approach could be more appropriate. The mixture of grassland and woodland fires, which likely changes seasonally and from year to year, will determine the importance of these differences and the resulting implications for regional emissions estimation.

On the other hand, for landscape-level emission studies, for which accurate fuel loading databases are in place (*e.g.*, national parks), EFs might prove to be a larger source of uncertainty than burned area and fuel consumption. Comprehensive ground-based measurements of burned area and fuel consumption are possible at this scale and the availability of high-resolution satellite information (*e.g.*, Landsat, SPOT) permits a reasonably accurate estimation of area burned (*e.g.*, Chapter 2). Field data combined with satellite information can also provide reliable modeling of fuel consumption (Landmann, unpublished results, 2000). Unless there are explicit EF measurements over a specific fire event, EFs have to be modeled (Ward *et al.*, 1996; Hoffa *et al.*, 1999). Depending on whether an ecosystem-specific model is used or not, the resulting emissions quantification outcome may differ significantly.

3.3.4 Prediction of Early Dry Season Emission Factors from the SAFARI-92 Models

The objective of this section is to test the validity of applying the SAFARI-92 late dry season EFs versus MCE models to predict the range of early dry season EF values measured here. In Chapter 2, seasonal emissions of products of incomplete combustion, using Landsat-derived monthly time-series of burned area and calculated seasonal EFs, were compared with emissions using the annual area burned and late dry season values of EFs. The SAFARI-92 late dry season modeled relationships (Ward *et al.*, 1996) and the early dry season MCE values from Hoffa *et al.* (1999) were applied to derive the seasonal

EF values. Chapter 2 showed that considerable underestimation of products of incomplete combustion may occur in grasslands at the landscape level when average late dry season EF values are used as representative of early dry season burning.

Here, the EF values predicted from the SAFARI-92 late dry season models are compared with the EF values predicted from the combined grassland-woodland models, over the range of grassland and woodland MCE values measured in this early dry season 1996 study. The lowest MCE value (0.907) was measured in a woodland burn, whereas the highest MCE value (0.972) was measured in a grassland fire (Table 2). In the comparison, the combined (Table 3) rather than the ecosystem-specific grassland and woodland models are used, since the SAFARI-92 models were developed from a number of measurements at sites with variable fuel composition. The comparison indicates that the EF differences between the SAFARI-92 models and the combined models from this study are highest either at the low or the high end of MCE values, depending on the atmospheric species, and that the level of agreement improves for values of MCE that are in between (Table 4). The large difference, by a factor of 4.7, in late dry season $EFCH_4$ raises some questions about using the SAFARI-92 model to estimate CH_4 emissions at higher MCEs, such as the ones of grassland fires in the late dry season. The highest grassland MCE measured here (0.972) is greater than any of the MCEs measured during the SAFARI-92 campaign. This might be explained by the fact that only one pure grassland fire was studied in SAFARI-92.

Table 4. Comparison of seasonal emission factors (EF) for CH_4, NMHC and PM2.5 predicted from the combined grassland-woodland models of this 1996 study with the corresponding seasonal emission factors calculated using the SAFARI-92 models over the range of modified combustion efficiency (MCE) values measured in this study.

MCE	*% Difference in $EFCH_4$*	*% Difference in EFNMHC*	*% Difference in EFPM2.5*
0.907	-13.9	1.6	32.6
0.912	-13.2	1.3	32.0
0.952	5.5	-2.9	30.0
0.972	369.0	-10.7	-2.7

3.3.5 Seasonal Emission Factors for Oxygenated Volatile Organic Compounds

One of the major gaps in our knowledge of the chemistry of the emissions from African savanna fires has been addressed recently by the first quantitative measurements of the EFs for oxygenated volatile organic compounds (OVOCs) during the SAFARI-2000 dry season field campaign (Yokelson *et al.*, 2003). The OVOC are about five times more abundant than NMHC in the southern hemisphere and they are more reactive (*e.g.*, acetic acid (CH_3COOH), formic acid (HCOOH), and formaldehyde (HCHO), reported here) (Singh *et al.*, 2001). Methanol (CH_3OH), which is fairly long lived, is the second most abundant organic compound in the atmosphere after methane. Here, the seasonal grassland MCE values are combined with the relationship of MCE versus PGREEN with the relationships of EFOVOCs vs. MCE reported by Yokelson *et al.* (2003) to calculate the first seasonal trends in EF of these compounds for southern African grassland fires (Figure 12) and relate them to PGREEN. In the absence of early dry season EFOVOCs versus MCE models, the late dry season relationships are applied to predict the early dry season EFOVOCs.

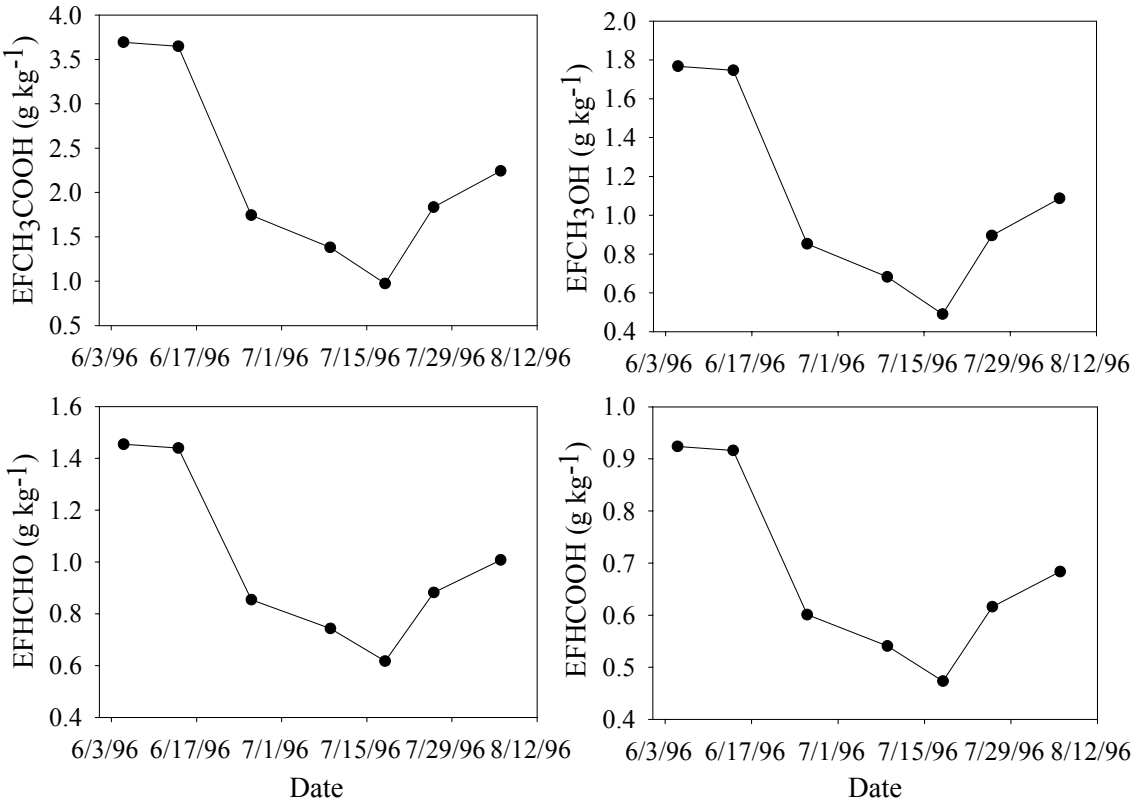

Figure 12. Calculated seasonal emission factors for selected oxygenated volatile organic compounds for grassland fires.

The calculated values of the EFOVOCs in the early dry season are a maximum of 3.8, 2.4, 3.6, and 2.0 times higher for CH_3COOH, HCHO, CH_3OH and HCOOH, respectively, than the corresponding values in the late dry season. The OVOCs emissions are related to PGREEN as following:

$$EFCH_3COOH = 9.836(PGREEN) - 0.749 \quad (3.12)$$

$$EFHCHO = 3.025(PGREEN) + 0.088 \quad (3.13)$$

$$EFCH_3OH = 4.618(PGREEN) - 0.318 \quad (3.14)$$

$$EFHCOOH = 1.630(PGREEN) + 0.188 \quad (3.15)$$

Note that the sum of the EFOVOCs for the four OVOCs that were most abundant in the SAFARI-2000 measurements is greater than the EFNMHC.

3.4 Conclusions

Savanna fires are believed to produce zero net emissions of CO_2 due to its sequestration by subsequent vegetation growth (Scholes *et al.*, 1996a). At the same time products of incomplete combustion may exhibit significant seasonal variations in their emissions (Hoffa *et al.*, 1999; Chapter 2). The seasonal budgets of these non-CO_2 trace gases and aerosols, and the implications for regional and global atmospheric chemistry, are largely unknown. The contribution of the early dry season emissions to the total annual emissions needs to be quantified.

Information on EFs is required to improve the accuracy of emissions models. The first early dry season EF measurements in southern African are presented here and they indicate some important and interesting seasonal trends in fire emissions and correlations to fuel characteristics. Furthermore, the first seasonal EFOVOCs for grassland fires and their relation to the proportion of green grass are derived, which due to the importance of OVOCs in tropospheric chemistry need to be included in future emissions modeling studies. The results from the integration of the different EF datasets enables estimates of the effects of using regional-average rather than ecosystem-specific EF models. The results presented here indicate that the seasonal trends of fire emissions require further attention. Clearly, a more intensive sampling is required to create a larger database that will allow the development of more robust seasonal EF models as a function of fuel condition. Fires exhibit high variability and the degree to which the seasonal measurements in this chapter are representative of African savanna fires should not be

overestimated. Through the development of seasonally sensitive emission estimates, it should be possible though, to do a better job of assessing emissions for Intergovernmental Panel on Climate Change (IPCC) national reporting.

Chapter 4: Regional vegetation fire emissions during the SAFARI 2000 dry season campaign

4.1 Introduction

Reliable burned area information is required by a number of users, including global change scientists modeling the source strength, transport, fate and impacts of trace gas and aerosol emissions from vegetation fires. National governments are required to report their greenhouse gas emissions. Natural resources managers and policy makers can benefit from a synoptic view of fire activity. The savannas of Africa are thought to experience the most extensive biomass burning in the world, for example, contributing an estimated 49% of the carbon lost from fires worldwide (Scholes and Andreae 2000, Dwyer *et al.*, 2000; van der Werf *et al.*, 2003). Savanna fires in southern Africa play an important role in the regional atmospheric distribution of trace gases and aerosols, ecosystem functioning and biogeochemical cycles (Scholes *et al.*, 1996a; Frost and Robertson, 1987).

SAFARI 2000 was an international scientific campaign aimed to study land-atmosphere interactions in southern Africa (Swap *et al.*, 2003). One of the main objectives of SAFARI 2000 was the characterization and quantification of regional emissions sources, including those from savanna burning. Within this context, a dynamic, spatially explicit emissions model is developed, which is applied here to estimate the pyrogenic emissions for a number of trace gases and particulates during the dry season field campaign in September 2000. In this chapter, a sensitivity analysis is performed to examine the geospatial relationship between burned area and emissions. Three recently developed moderate-resolution satellite burned area products from the MODIS, SPOT-VEGETATION and ATSR-2 sensors provide the basis for generating and comparing new

estimates of biomass burning emissions from woodland and grassland fires in southern Africa during September 2000. The different burned area products are in the process of being validated, through systematic accuracy assessment. This analysis is intended to show the importance of having an accuracy assessment associated with satellite products to be used in modeling.

4.2 Fire Emissions Modeling Methodology

Estimates of pyrogenic gas emissions require information on burned area, fuel load (the amount of fuel per unit area), completeness of combustion (the proportion of the fuel consumed during the fire) and emission factors (characteristic of the amount of the specific atmospheric species produced during the burning). Emissions are computed using spatially explicit input data following the well established Seiler and Crutzen (1980) model:

$$E_x = \sum_{i,j} A_{i,,j} \text{ x } F_{i,j} \text{ x } CC_{i,j} \text{ x } (EF_x)_{i,j} \quad (4.1)$$

where:

E_x total pyrogenic emissions for atmospheric species x (g)

$A_{i,,j}$ burned area (km^2)

$F_{i,j}$ fuel load ($kg\ km^{-2}$)

$CC_{i,j}$ the completeness of combustion (fraction)

$(EF_x)_{i,j}$ the emission factor for compound x ($g\ kg^{-1}$)

i,j spatial coordinates

x compound for which emissions are estimated

Equation (4.1) is used to compute emissions of major and minor gaseous compounds and particulate species for September 2000 for all of Africa south of the equator (not including Madagascar) at a pixel size of 1 km^2. The region is stratified spatially into grassland and woodland areas and the emissions are computed independently for these two land covers. The relative proportions of woody, grass and leaf litter fuels determine important aspects of fire behavior which impact factors including emission factors and the completeness of combustion (Shea *et al.*, 1996; Hoffa *et al.*, 1999). In grasslands the fuel layer is relatively homogeneous, whereas in woodlands the woody and grass fuel components coexist with more restricted grass production in the more closed-canopy woodlands (Scholes *et al.*, 2002). Different emission factors and combustion completeness parameterizations are applied for woodlands and grasslands. The IPCC guidelines for greenhouse gas emissions reporting also suggest the division of these two savanna land covers (IPCC, 1997a). The MODIS percent tree cover (PTC) product (Hansen *et al.*, 2002) is used to distinguish between grasslands and woodlands and define areas with PTC less than or equal to 10% as grasslands and areas with PTC greater than 10% as woodlands. The 10% PTC threshold is based on the Food and Agricultural Organization of the United Nations (FAO) definition of forest (FAO, 2001). This PTC-based land cover classification is illustrated in Figure 1. Using a high-resolution mapping approach combined with field measurements, Hansen *et al.* (in press) determined the accuracy of the MODIS PTC to be ± 5.2% compared with Landsat ETM+ in Western Province, Zambia. Preliminary validation efforts estimate the global MODIS PTC product accuracy to be ± 11.5%.

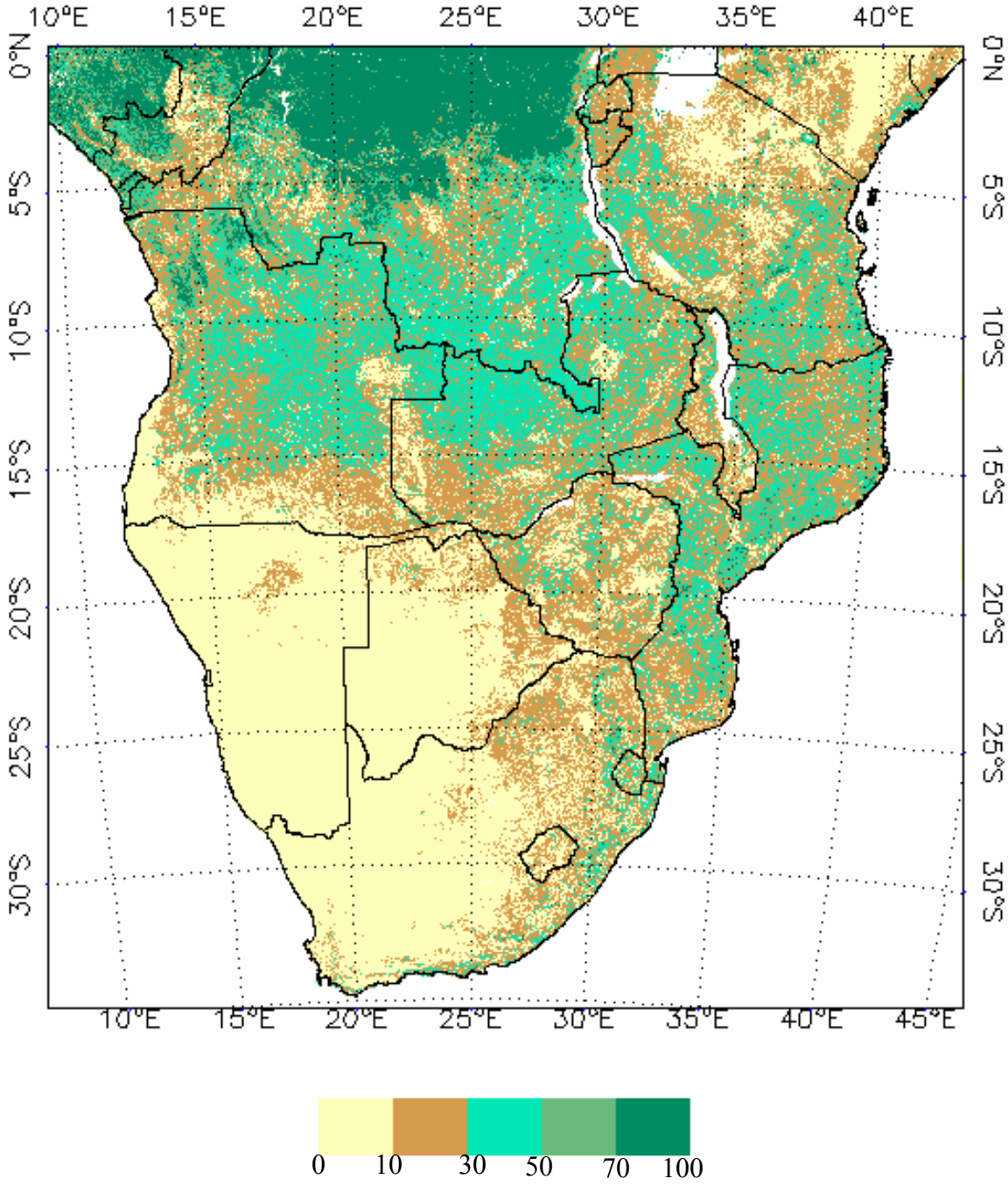

Figure 1. Southern Africa woodland–grassland classification derived from the MODIS Percent Tree Cover (PTC) product. Grasslands (PTC ≤ 10%). Woodlands (PTC > 10%). Lambert Azimuthal Equal Area projection (center longitude 25 degrees, center latitude -15 degrees).

4.2.1 Model Inputs

4.2.1.1 Fuel Load

Regional fuel load datasets of green grass, dry grass, leaf litter and twigs fuel types generated by Hély *et al.* (2003a) for southern Africa in support of SAFARI 2000 fire emissions modeling are used to compute spatially explicit total fuel load amounts and fuel load type mixtures. The modeled fuel load type outputs used in this chapter are available on the third SAFARI 2000 CD-ROM (Hély *et al.*, 2003b). The production of green and dry grass, and leaf litter fuel types is calculated using a satellite-driven Net Primary Productivity (NPP) model that incorporates ecophysiological processes, such as respiration and potential evapotranspiration, in conjunction with empirical relationships. Herbivory reduction of the grass fuel is also included (Hély *et al.*, 2003a). The twigs amount is not explicitly calculated by the NPP model but was determined empirically from the AVHRR derived PTC. Here, the modeled twigs data layer is improved using the MODIS PTC and the empirical relationship by Hély *et al.* (2003a). Fuel amount for each fuel type is computed for each 1 km^2 pixel every 15 days for the preceding growing season from September 1, 1999 to August 31, 2000. The total fuel load available for burning in September 2000 is determined by accumulating fuel load throughout this period. The fuel load ranges predicted by the model are generally in agreement with the limited published field measurements (Shea *et al.*, 1996; Trollope *et al.*, 1996; Hély *et al.*, 2003a). Several potential biases are recognized in the fuel load model, including: no modeling of fuel load reduction by people, fuel load accumulation and decay since the last fire occurrence, and that larger diameter woody fuels are not modeled even though smoldering following fires on these fuel types may be highly emissive (Bertschi *et al.*, 2003). The impact of these limitations on fuel load estimation is currently not possible

since only this particular fuel load dataset is publicly available. It is hoped that recognition of these issues will lead to the development of more robust fuel load models.

4.2.1.2 Combustion Completeness

Combustion completeness is defined as the fraction burned of the biomass fuel exposed to the fire (Shea *et al.*, 1996; Scholes *et al.*, 1996b). Combustion completeness depends on the fuel loading, type, moisture content, packing and meteorological parameters including wind speed, relative humidity and temperature. Fine and/or drier fuels typically burn more completely than coarser and/or moister fuels. The combustion completeness of all fuel types is generally thought to increase as the southern Africa dry season progresses (Hoffa *et al.*, 1999). In grasslands, the combustion completeness is determined from the percentage of green grass to total grass (PGREEN) for values of PGREEN equal or greater than 20%, to allow for the assessment of the effects of varied grass moisture content, and has a lower limit of 44% based on field measurements by Hoffa *et al.* (1999):

$$CC_G = -213.09(PGREEN) + 138.21 \quad (4.2)$$

For values of PGREEN below 20%, CC_G is computed using an empirical relationship derived from the late dry season measurements by Shea *et al.* (1996) during SAFARI 92:

$$CC_G = (0.99*\text{dry grass} + 0.98*\text{green grass} + 0.91*\text{leaf litter} + 0.48*\text{ twigs})/\text{total fuel} \quad (4.3)$$

In woodlands, the combustion completeness is determined from PGREEN for values of PGREEN equal or greater than 14%, and has a lower limit of 1% (Hoffa *et al.*, 1999):

$$CC_W = -114.792(PGREEN) + 52.704 \quad (4.4)$$

For PGREEN values below 14%, the CC_W is calculated using Equation (4.3).

For the most part, the fuel load modeled grass is predicted to be dry in September. For example, in September, PGREEN is typically lower than 20% in grasslands and lower than 14% in woodlands. Consequently, the combustion completeness is mainly computed using Equation (4.3) and the combustion is relatively complete.

4.2.1.3 Emission Factors

An emission factor is the amount of a specific trace substance emitted by the combustion per unit mass of dry fuel consumed (gkg^{-1}) (Ward *et al.*, 1996). Regional grassland and woodland emissions are estimated using ecosystem-specific emission factor algorithms for carbon dioxide (CO_2), carbon monoxide (CO), methane (CH_4), non-methane hydrocarbons (NMHC) and particulate matter with diameter less than 2.5 μm (PM2.5) for southern African savanna fires developed in Chapter 3. Most modeling studies report emissions for these key five carbon-containing species. Here, the emissions database for this region is expanded by incorporating emission factors for a variety of compounds, including oxygenated volatile organic compounds (OVOCs), halocarbons, nitrogen oxides (NO_x), ammonia (NH_3), hydrogen cyanide (HCN) and particulate ionic components measured during the SAFARI 2000 dry season field campaign (Yokelson *et al.*, 2003; Sinha *et al.*, 2003). A fuel carbon content of 50% is assumed in all emission factors calculations (Ward *et al.*, 1996). The term "products of incomplete combustion" is used to describe compounds reported in this study other than CO_2 and NO_x, *i.e.*, low oxidized emissions products that are mainly emitted during smoldering combustion.

Emission factors are usually computed as a linear function of the modified combustion efficiency (MCE) for a given fuel type (Ward *et al.*, 1996). The MCE is an index of the fire oxidation conditions, defined as the molar ratio of CO_2 to the sum of CO

and CO_2 released. In this work, models of emission factors versus MCE reported in the literature and developed in Chapter 3 for southern Africa fuels are used (Ward *et al.*, 1996; Sinha *et al.*, 2003; Yokelson *et al.*, 2003; Chapter 3). For woodlands, the MCE_W is computed from the ratio of the grass fuel to the sum of grass and litter fuels (Ward *et al.*, 1996).

$$MCE_W = 0.85 + 0.11[\text{grass}/(\text{litter}+\text{grass})]^{0.34} \quad (4.5)$$

"Grass" consists of green and dry grass. "Litter" consists of fallen tree leaves and twigs

For grasslands, the MCE_G is computed from PGREEN constrained by a lower limit of 0.912 and an upper limit of 0.974 (Hoffa *et al.,* 1999; Chapter 3):

$$MCE_G = 1.010 - 0.217(\text{PGREEN}) \quad (4.6)$$

In grassland locations dominated by litter (*e.g.*, where grass has been removed by herbivory) MCE_G is set to 0.85 (Ward *et al.*, 1996). These locations comprised small fractions of the grassland burned area (approximately, 6% of the GBA, 6% of MODIS, and 9% of the GLOBSCAR September grassland burned areas). As seen from Equations (4.5) and (4.6), the MCE varies as the vegetation conditions change. Thus, the emission factors algorithms provide a means of estimating the proportion of different compounds in the smoke mixture at any temporally and spatially defined pixel.

4.2.1.4 Burned Area

To compare the sensitivity of the emissions estimation to burned area, three regional moderate spatial resolution burned area products derived from Moderate Resolution Imaging Spectroradiometer (MODIS), SPOT-VEGETATION, and Along Track Scanning Radiometer (ATSR-2) satellite data are used. The MODIS active fire

product is also compared with these products, as prior to the generation of spatially explicit burned area products, active fire locations were the only regional data available for emissions estimation. All data sets were projected into a common Lambert Azimuthal Equal Area projection using nearest neighbor resampling.

The MODIS burned area product maps the 500 m location and approximate day of burning using a change detection algorithm based on a bi-directional reflectance model-based expectation method applied to the MODIS near-infrared and shortwave infrared bands (Roy *et al.*, 2002a). The algorithm was applied to recently reprocessed 500 m daily MODIS land surface reflectance data to produce burned area data sets for all of southern Africa for 2000 onwards. The MODIS burned area data used in this chapter are available on the third SAFARI 2000 CD-ROM (Roy, 2003a). In order to minimize geolocation errors associated with nearest neighbor resampling, the 500 m burned area data were reprojected into the Lambert Azimuthal Equal Area projection with an output pixel dimension of 500 m rather than 1 km. The reprojected data were then binned to 1 km pixels by counting how many burned 500 m pixels occur in each 1 km pixel (0 to 4), *i.e.,* in an 1 km^2 pixel with a count of 1 only 25% of the pixel is burned, whereas a 1 km^2 pixel with a count of 4 is assumed to be completely burned. This reduces nearest neighbor resampling pixel shifts (*i.e.*, position errors) (Dikshit and Roy, 1996) and provides a more accurate burned area assessment for subsequent analysis. Pixels labeled by the MODIS burned area product as "not considered" (either an area of ephemeral or inland water) or "unmapped" (due to insufficient MODIS data associated with persistent cloud and/or missing MODIS data) were not counted. The precise day of burning may not be certain because of cloudy and missing data. A conservative estimate of the area

burned in September 2000 is used by only considering pixels with burns occurring in September and on the last day of the previous month.

The MODIS active fire product maps the 1 km location of active fires detected at the time of satellite overpass using an established contextual hot-spot detection algorithm (Justice *et al.*, 2002a). The timing and spatial extent of burning cannot be estimated reliably from these orbital hot spot data, as the satellite may not overpass when burning occurs and because clouds may preclude active fire detection (Robinson, 1991; Justice *et al.*, 1993; Justice *et al.*, 2002a). Despite this limitation, a spatially explicit 1 km September active fire data set is computed by temporally compositing all the MODIS 1 km day and night September active fire detections over southern Africa. Both the MODIS active fire and burned area products were produced from the latest reprocessed MODIS Collection 4 data (Justice *et al.*, 2002b). It should be noted, that MODIS data sensed prior to November 2000 are less reliable compared with later data, due to some noisy and poorly performing MODIS detectors (Guenther *et al.,* 2002) which had a deleterious impact on MODIS land product quality (Roy *et al.,* 2002b).

Two regional SPOT-VEGETATION burned area products were initially considered; both map the 1 km location and month of burning. The first, produced by application of a supervised classification tree algorithm to 1 km near-infrared SPOT-VEGETATION data (Silva *et al.*, 2003) was superceded by a second SPOT-VEGETATION product computed using a supervised classification tree algorithm applied to the red, near-infrared and spectral band indices (Tansey *et al.*, 2002). In this study the second SPOT-VEGETATION burned area product is used, which is more recently distributed as part of the Global Burnt Area 2000 (GBA2000) initiative

developed at the Joint Research Centre of the European Commission (Grégoire *et al.*, 2003). The September 2000 GBA product is used and it is noted that the compositing algorithm used to generate this product (Stoppiana *et al.*, 2002) tends to discard areas that burned on the last two days of the month (Silva J., personal communication 2003).

The global ATSR-2 burned area product (GLOBSCAR) is based on the logical AND of two independent algorithms – one based on near infrared reflectance decrease and thermal band brightness temperature increase after a fire (Piccolini, 1998) and the other applying thresholds to spectral band indices and individual ATSR-2 bands (Eva and Lambin, 1998). Preliminary validation activities in southern Africa indicate that the seasonal distribution of burning is well matched but that there is an under detection of burning, caused primarily by the joint use of the two algorithms and the relatively low ATSR repeat cycle days interacting with persistent cloud (Simon *et al.*, in press).

4.3 Results and Discussion

4.3.1 Intercomparison of MODIS, GBA-2000 and GLOBSCAR Burned Area Products, Southern Africa, September 2000

Tables 1 and 2 summarize the regional differences between the MODIS, GBA-2000 and GLOBSCAR burned area products for September 2000. The total southern Africa area considered is 9,269,225 km^2. MODIS detects a regional September burned area amount of approximately 268,500 km^2, GBA-2000 detects approximately 173,100 km^2, and GLOBSCAR detects approximately 59,800 km^2. The MODIS active fire product detects an approximate area of 126,400 km^2, although as noted above this estimate is expected to be biased.

Table 1. MODIS and GBA-2000 burned area product intercomparison, southern Africa, September 2000. All burned areas to nearest 100 km^2. The burned areas are defined (a) with respect to MODIS 500m pixels, (b) with respect to 1 km GBA-2000 pixels.

	Burned Area (km^2 x 10^3)
Total MODIS	268.5[a]
Total GBA	173.1[b]
Detected by MODIS but not GBA	181.6[a]
Detected by GBA but not MODIS	60.4[b]
Detected by GBA, not mapped by MODIS	5.9[b]
Detected by both MODIS and GBA	86.9[a], 106.8[b]

Table 2. MODIS and GLOBSCAR burned area product intercomparison, southern Africa, September 2000. All burned areas to nearest 100 km^2. The burned areas are defined (a) with respect to MODIS 500m pixels, (b) with respect to 1 km GBA-2000 pixels.

	Burned Area (km^2 x 10^3)
Total MODIS	268.5[a]
Total GLOBSCAR	59.8 [b]
Detected by MODIS but not GLOBSCAR	254.4[a]
Detected by GLOBSCAR but not MODIS	33.7[b]
Detected by GLOBSCAR, not mapped by MODIS	6.2[b]
Detected by both MODIS and GLOBSCAR	14.1[a], 19.9[b]

Spatially explicit comparisons of these products are shown in Figures 2 and 3 and illustrate the large differences between products. Pixels labeled by the MODIS burned area product as "unmapped" (due to insufficient data associated with persistent cloud and/or missing data) are shown as white. The GBA-2000 and GLOBSCAR products are defined without an unmapped class, potentially increasing the possibility of burned areas being mapped as unburned rather than unmapped due to missing, infrequent, and/or cloudy data.

The MODIS product mapped a total burned area approximately 1.5 times greater than GBA-2000, and of the 173,100 km^2 mapped by GBA-2000 the summed area of GBA-2000 1 km pixels containing one or more 500m MODIS burned pixels is 106,800 km^2 (Table 1). Calculating the coincident area with respect to the MODIS data gives a smaller common area of 86,900 km^2, as many of the burned 1 km GBA-2000 pixels contain less than four 500 m MODIS burned pixels. Systematic differences are also present. For example, the GBA-2000 product has discontinuous linear stripes of burned pixels hundreds of kilometers long aligned in the SPOT orbit that are probably artifacts (although negligible for this analysis) and has extensive burning in the Kenya-Tanzania border (Figure 2) that are not found in the MODIS or GLOBSCAR products. The MODIS product mapped an area more than four times greater than GLOBSCAR, and of the 59,800 km^2 mapped by GLOBSCAR less than 20,000 km^2 were coincidently mapped by MODIS (Table 2).

Table 3 tabulates the total area burned for the three products broken down by woodland and grassland, as these land covers are used to parameterize the emissions model. Woodland fires (defined as PTC > 10%) account for the majority of the regional burned area rather than grasslands fires (defined as PTC <= 10%). MODIS and GBA-2000 map similar grassland burned areas and approximately six times more than GLOBSCAR. MODIS maps approximately twice as much burned area in woodlands as GBA-2000, which maps approximately twice as much burned area in woodlands as GLOBSCAR. The ratios between woodland to grassland area burned vary among products. GLOBSCAR presents the highest relative proportion of woodland burns

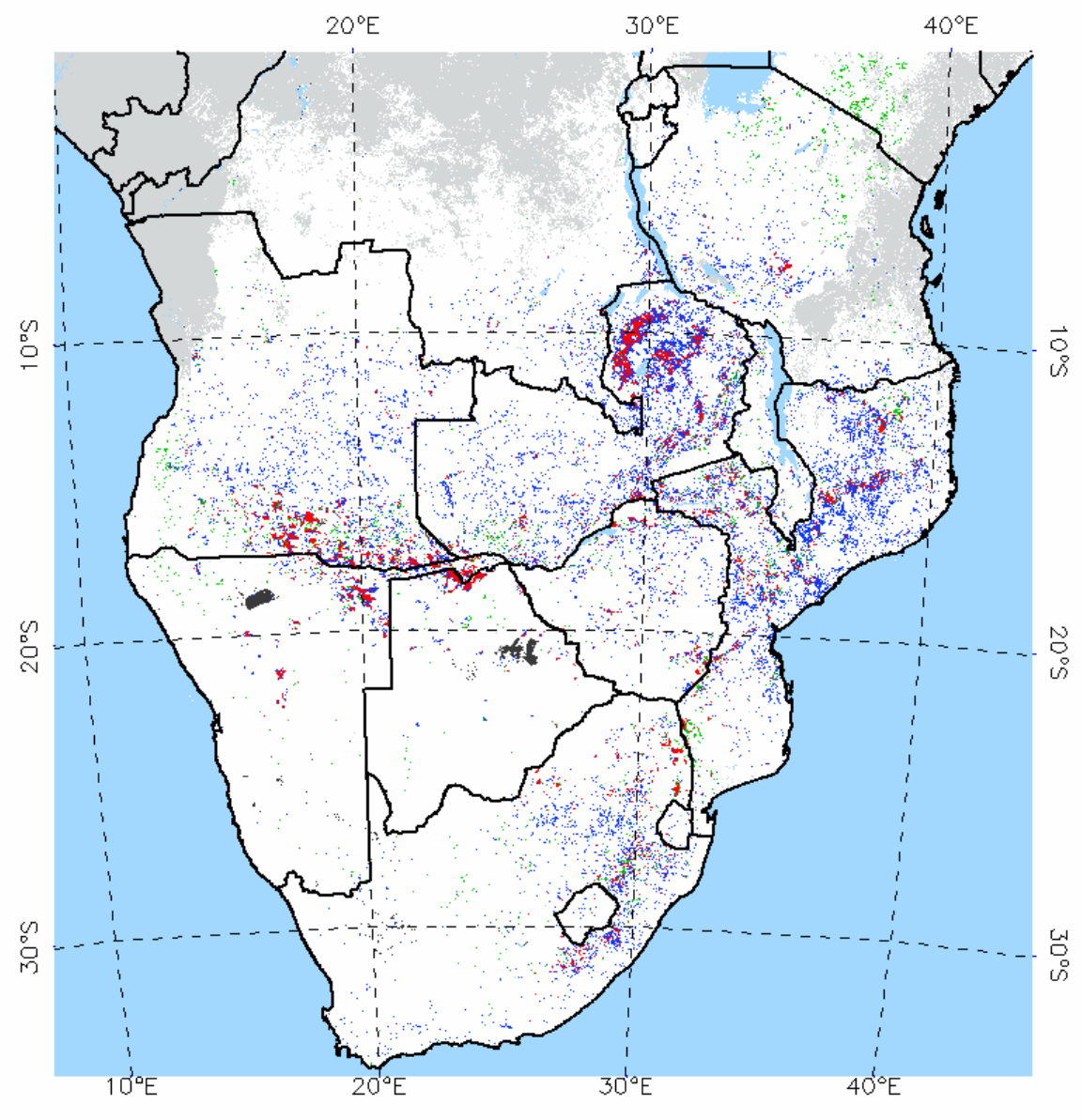

Figure 2. Intercomparison of the MODIS and GBA-2000 burned area products, southern Africa, September 2000. Dark blue = MODIS detections only, Light green = GBA-2000 detections only, Red = agreement, Light grey = Not mapped by MODIS due to insufficient cloud free observations, Dark grey = Not considered by MODIS due to ephemeral water or inland water, Light blue = water. Lambert Azimuthal Equal Area projection (center longitude 25 degrees, center latitude -15 degrees).

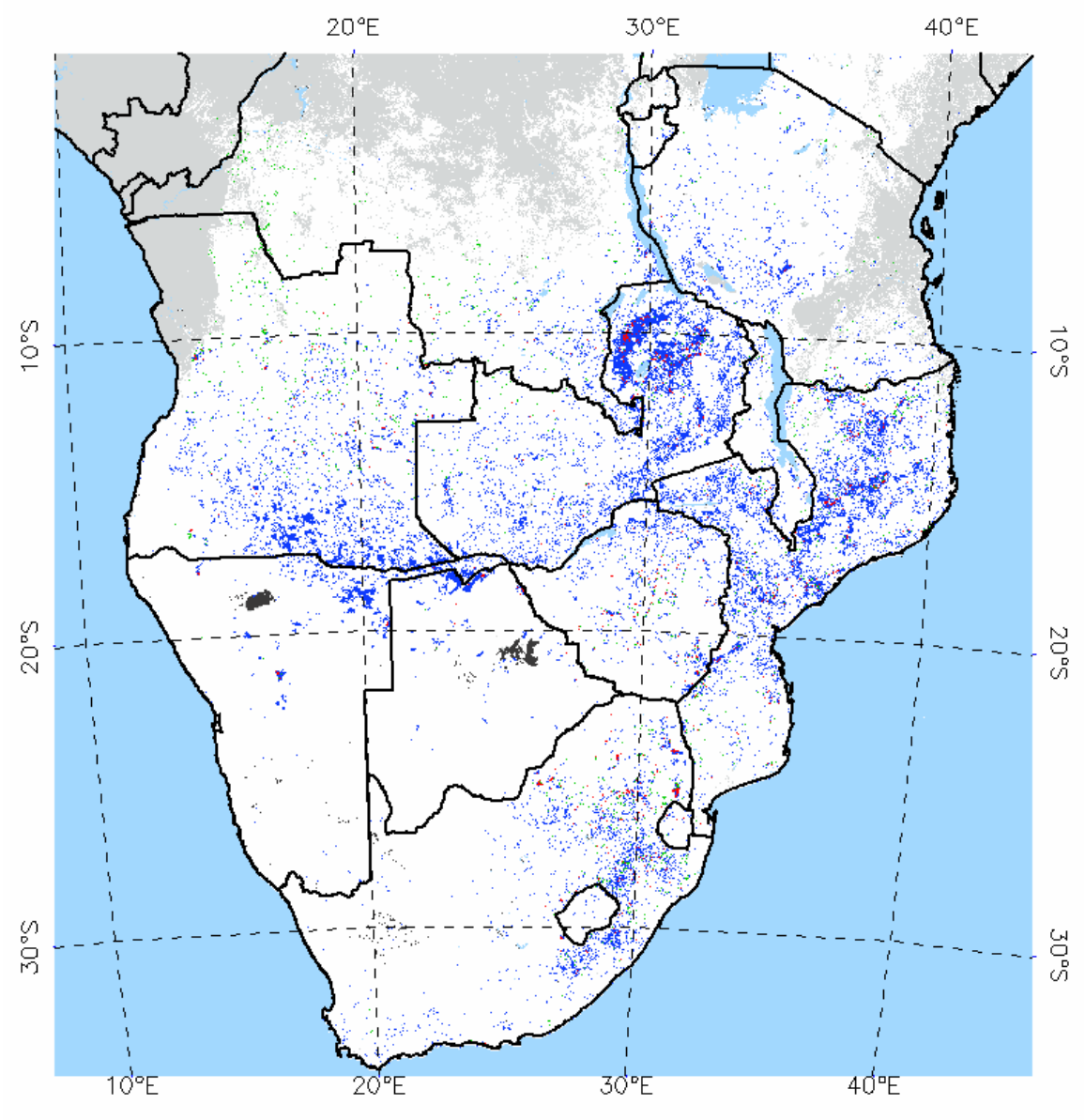

Figure 3: Intercomparison of the MODIS and GLOBSCAR burned area products, southern Africa, September 2000. Dark blue = MODIS detections only, Light green = GLOBSCAR detections only, Red = agreement, Light grey = Not mapped by MODIS due to insufficient cloud free observations, Dark grey = Not considered by MODIS due to ephemeral water or inland water, Light blue = water. Lambert Azimuthal Equal Area projection (center longitude 25 degrees, center latitude -15 degrees).

(~83%), followed by MODIS (~75%) and then GBA-2000 (~66%). Figure 4 illustrates the regional amount of area burned as a function of PTC greater than 10% for each burned area data set. MODIS detects a proportionally higher burned area than GBA-2000 or GLOBSCAR for PTC 40-50% and always has higher area burned up to 60% PTC. Both MODIS and GBA-2000 have approximately bimodal distributions with peaks at approximately 20% and 30% PTC indicating that they detect a similar regional distribution of woodland burning. The GLOBSCAR product has a uniform burned area distribution up to approximately 50% PTC and then decreases in a similar manner as the other burned area data sets.

Table 3. MODIS, GBA-2000 and GLOBSCAR burned areas in woodlands and grasslands.

Burned Area (km^2 x 10^3)	*Woodlands*	*Grasslands*	*Ratio (Woodlands/Grasslands)*
MODIS	201.6	66.9	3.0
GBA-2000	113.9	59.2	1.9
GLOBSCAR	49.6	10.2	4.9

None of the three 2000 satellite burned area products has been systematically validated. The extent to which differences among these products is due to commission and omission errors is unknown. Consequently, it is difficult to reliably explain differences observed between them, especially as different algorithms were used in their generation. All factors being equal, higher spatial resolution systems will more reliably detect burned areas (*i.e.*, have lower omission errors) than lower spatial resolution systems. This is because increasing the fraction of the observation area (sensed by a pixel) that burns, increases the change in reflectance that occurs after the passage of fire and thus, the detection likelihood (Roy and Landmann, in press). Similarly, higher spatial

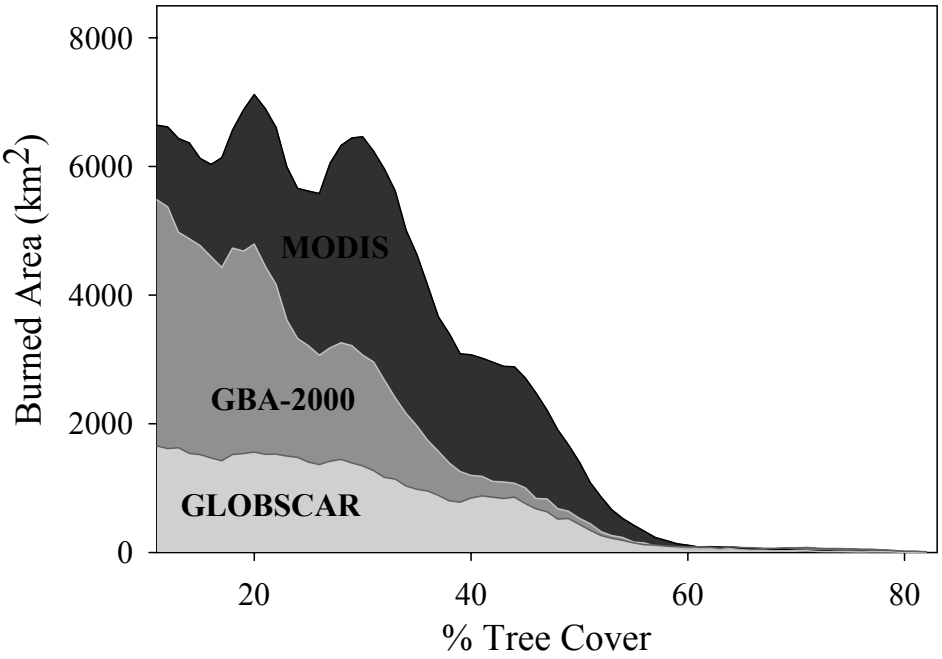

Figure 4. Distribution of burned area in woodlands in the MODIS, GBA-2000 and GLOBSCAR products by percent of tree cover for southern Africa, September 2000.

resolution data may allow more reliable detection of burned surfaces that are partially obscured by unburned overstorey vegetation, that are more common in dense woodlands. These factors may in part explain the more extensive burning detected using 500 m MODIS data than detected by the 1 km SPOT-Vegetation (GBA-2000) and the ATSR-2 (GLOBSCAR). Recent validation of the improved quality MODIS 2001 and 2002 burned area product, performed using Landsat ETM+ derived independent burned area data (Roy *et al.*, in press), indicates that the MODIS burned area is underestimating, rather than overestimating, the regional area burned (Roy *et al.*, 2003b). It is noted that calibration, data pre-processing, spectral characteristics, and algorithm differences may also be highly important factors. As the purpose of this study is an emissions sensitivity analysis, this chapter focuses more on the impact of the different burned area products on emissions rather than why the burned area data sets are different.

4.3.2 Sensitivity of Regional Fire Emissions to MODIS, GBA-2000 and GLOBSCAR

Figures 5 and 6 illustrate the September 2000 MODIS-based carbon dioxide (CO_2) and carbon monoxide (CO) emissions density (emissions per unit area). Intense, efficient (flaming) fires have more complete combustion and release more CO_2, whereas less efficient (smoldering) fires have less complete combustion and release more CO (Ward *et al.*, 1996). There are distinct differences between the spatial distribution of the estimated CO_2 and CO emissions. The highest CO_2 emissions densities are concentrated in the latitudinal belt between approximately 15^oS to 20^oS, whereas the highest CO emission densities are observed to occur from 8^oS to 13^oS. Examination of the MODIS PTC product reveals that areas with the highest CO_2 emissions densities are grasslands and/or open woodlands, whereas areas with the highest CO have higher PTC. The GBA-2000 CO_2 latitudinal distribution is comparable with MODIS but due to the more disperse burning in GBA-2000 there are no clear latitudinal belts of concentrated high CO emissions. For the same reason, there are no obvious latitudinal trends in the CO_2 and CO regional distribution in GLOBSCAR.

Tables 4-6 (Appendix B) summarize the regional September 2000 pyrogenic emissions for major and minor trace gases and particulate species computed using the MODIS burned area (Table 4), the GBA-2000 burned area (Table 5) and the GLOBSCAR burned area (Table 6) products. The regional pyrogenic emissions are highly sensitive to the burned area amounts. For example, the MODIS driven emissions estimate for CO_2 is approximately 134 Tg, the GBA-2000 emissions estimate 90 Tg and the GLOBSCAR estimate 30 Tg.

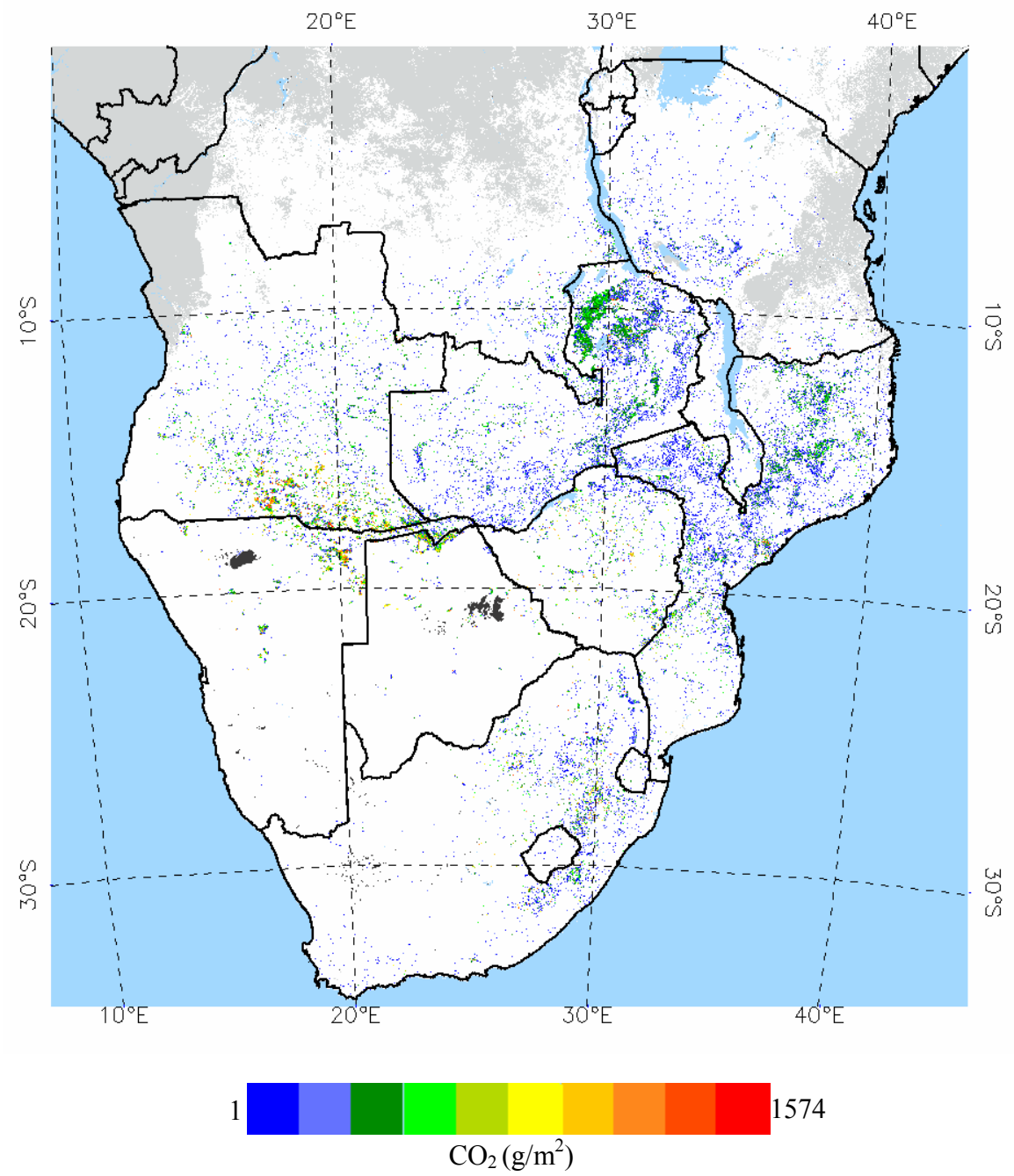

Figure 5. MODIS CO_2 emissions, southern Africa, September 2000. Light grey = not mapped by MODIS due to insufficient cloud free observations, dark grey = not considered by MODIS due to ephemeral water or inland water, light blue = water. Lambert Azimuthal Equal Area projection (center longitude 25 degrees, center latitude -15 degrees).

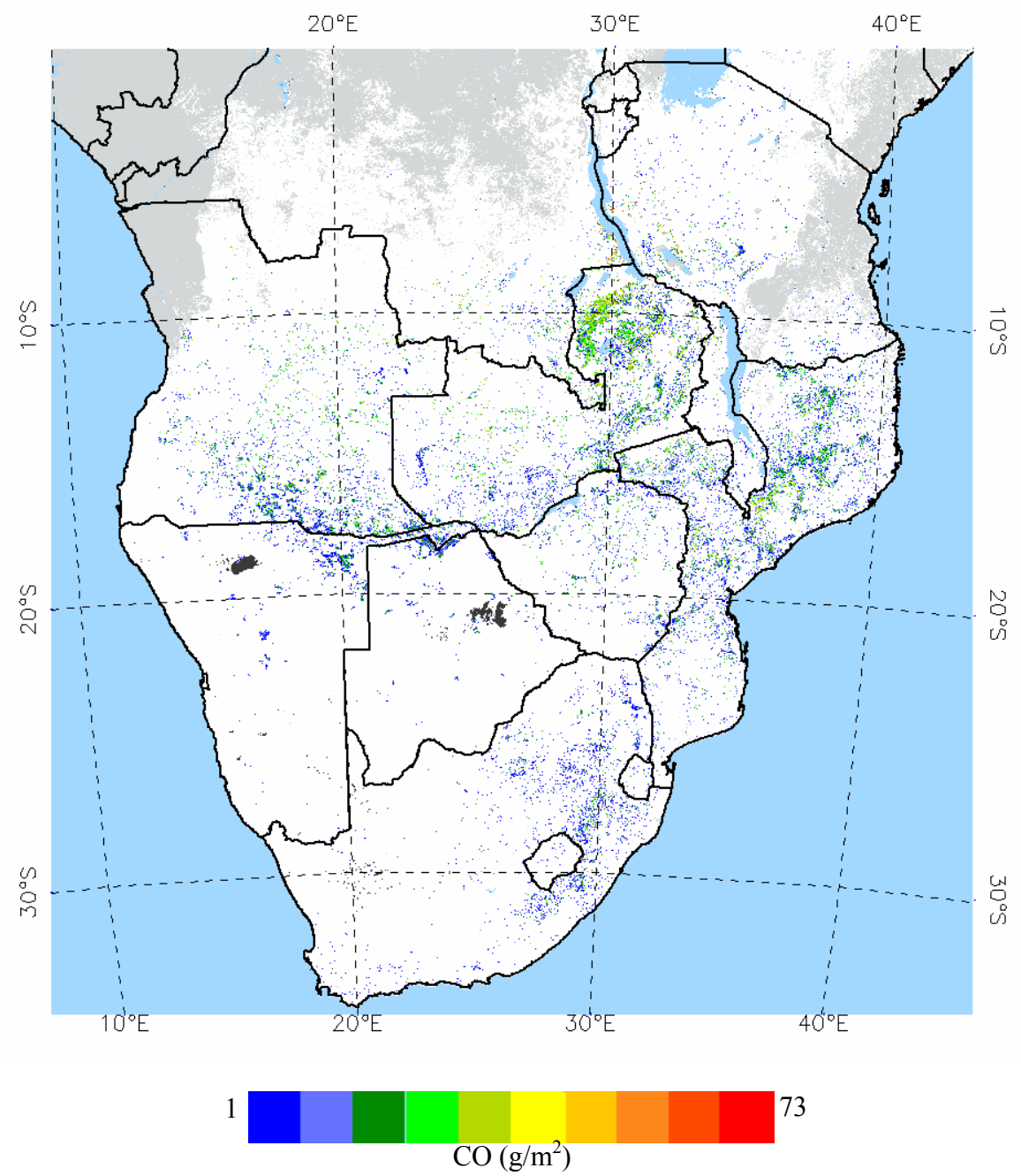

Figure 6. MODIS CO emissions, southern Africa, September 2000. Light grey = not mapped by MODIS due to insufficient cloud free observations, dark grey = not considered by MODIS due to ephemeral water or inland water, light blue = water. Lambert Azimuthal Equal Area projection (center longitude 25 degrees, center latitude -15 degrees).

Table 7 shows the regional amounts of biomass burned in woodlands and grasslands. The main difference between MODIS and GBA-2000 in terms of burned area (Table 3) and biomass burned (Table 7) is associated with woodland rather than grassland fires. GLOBSCAR detects substantially less burned area and biomass burned in both woodlands and grasslands compared with MODIS and GBA-2000, and the largest differences are found in the grasslands. In MODIS and GBA more biomass is burned in grasslands than woodlands relative to their respective burned area amounts. In GLOBSCAR the ratio of biomass burned-woodlands over grasslands is slightly higher than the corresponding burned area ratio. Figures 7a-7c illustrate the regional amounts of biomass burned, CO_2 and CO emissions in woodlands as a function of PTC, defined within 1% PTC ranges greater than 10%. The distribution of the biomass burned by PTC for all three products is similar to that of the burned area. The CO_2 emissions distribution also closely follows that of the biomass and area burned distribution. The CO emissions are different in that they increase up to approximately 30% PTC before decreasing in the same way as CO_2, and biomass burned. It is hypothesized that this is because of increasing litter fuel load for PTC up to 30% and then decreasing total biomass burned at higher PTC.

Table 7. MODIS, GBA-2000 and GLOBSCAR biomass burned in woodlands and grasslands.

Biomass Burned (Tg)	*Woodlands*	*Grasslands*	*Total*	*Ratio (Woodlands/Grasslands)*
MODIS	56.5	22.9	79.4	2.5
GBA-2000	32.4	20.6	53.0	1.6
GLOBSCAR	15.0	3.0	18.0	5

Vegetation burning in the two land cover types emits various quantities of different atmospheric species that are not necessarily proportional to their correspondent burned area. In MODIS, whereas woodland fires account for approximately 75% of the regional area burned, they contribute approximately 70% of the regional CO_2, 73% of the regional NO_x, and anywhere from 77% to 98% of the regional budgets for the remaining trace gas and particulate species (Table 4, Appendix B). In GBA-2000, woodland fires account for approximately 66% of the regional area burned, but they contribute approximately 60% of the regional CO_2, 63% of the regional NO_x, and anywhere from 67% to 97% of the regional budgets for products of incomplete combustion (Table 5, Appendix B). In GLOBSCAR, woodland fires account for approximately 83% of the regional area burned, and they contribute approximately 82% of the regional CO_2, 79% of the regional NO_x, and anywhere from 87% to 98% of the regional budgets for products of incomplete combustion (Table 6, Appendix B).

Furthermore, when comparing the differences in regional emissions arising from using the different burned area products, it is also evident that they are not directly proportional to differences in burned area amount changes between products and that they vary among atmospheric species (Tables 1-2 and 4-6 in Appendix B). The approximately 55% regional increase in burned area detected by MODIS compared with GBA-2000 (Table 1), results in a proportionally smaller increase in emissions of products of complete combustion, such as CO_2 (48%) and NO_x (52%), compared with the emissions of products of incomplete combustion, such as CO (73%) and CH_4 (87%) (Tables 4-5, Appendix B). The MODIS-based emissions of the products of incomplete

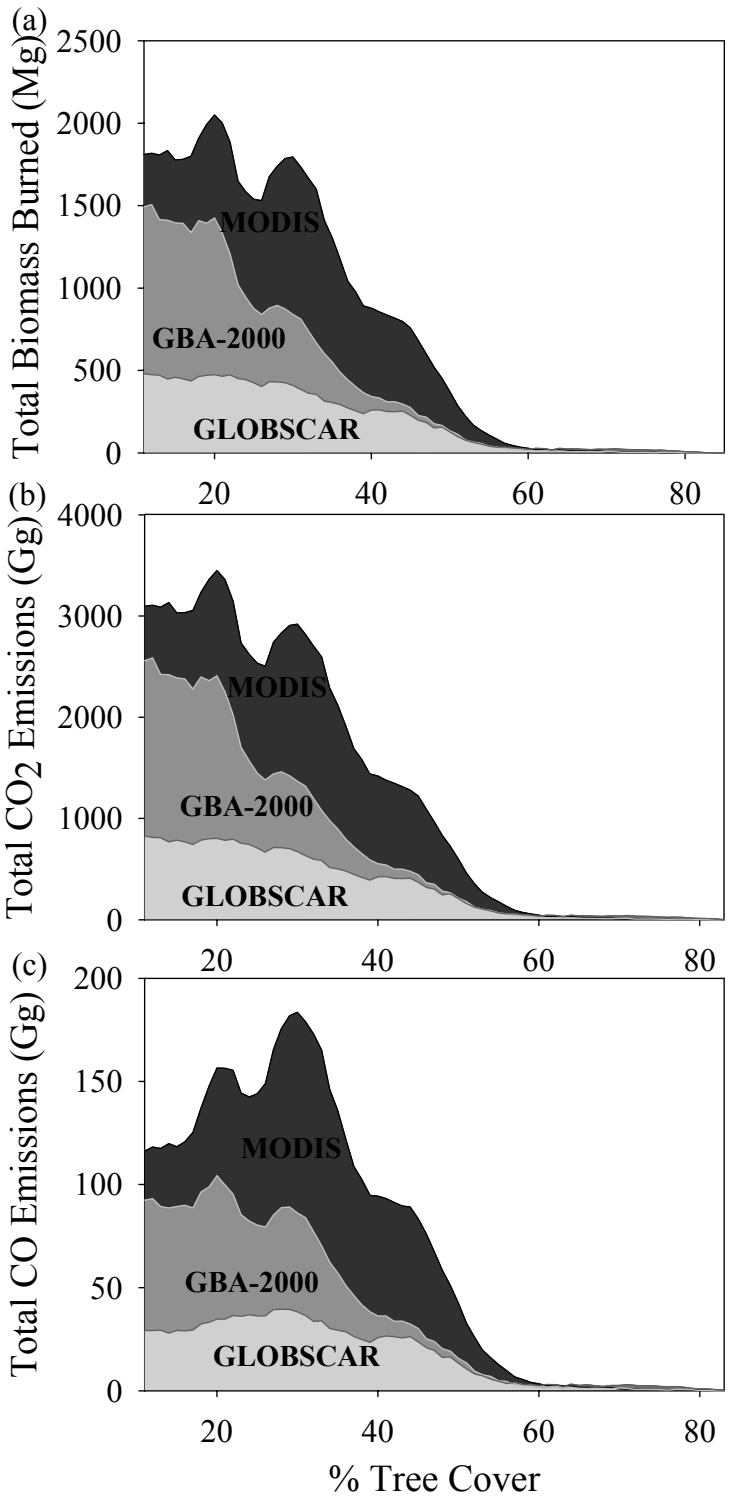

Figure 7. Distributions by Percent Tree Cover (PTC) of woodland (a) biomass burned, (b) CO_2 emissions, and (c) CO emissions, southern Africa, September 2000, The distributions are binned at 1% PTC intervals, starting at 11% PTC.

combustion are higher by approximately 57% to 98% compared with the GBA-2000 equivalents. Comparison of MODIS with GLOBSCAR yields the opposite results. The MODIS burned area product maps approximately 349% more area burned than the GLOBSCAR product (Table 2). In this case, MODIS CO_2 and NO_x emissions are higher by approximately 341% and 338%, than the corresponding GLOBSCAR emissions, respectively (Tables 4 and 6, Appendix B). The MODIS-based emissions of products of incomplete combustion are higher by mostly smaller proportions than CO_2 and NO_x, ranging from 310% to 336%, compared with the respective GLOBSCAR-based emissions. Examination of Equations (4.1-4.6) indicates that burned area differences will produce different emissions estimates, and that these differences will be dependent on the spatial distribution of burning relative to the fuel load amount and composition in grasslands and woodlands.

To address the effects of the different spatial distribution of the three burned area products on emissions and verify the model's behavior to the various burned area inputs, the variations in fuel load density, biomass burned density, combustion completeness, emission factors for CO_2 ($EFCO_2$) and CO (EFCO), CO_2 and CO emissions densities, are examined for each burned area product. Figures 8-10 show for MODIS, GBA-2000 and GLOBSCAR, respectively, the variations in these variables as a function of PTC defined within 5% PTC ranges. The suppressive effect of increasing PTC on grass production is apparent in Figures 8a, 9a and 10a and is well documented for southern African savannas (Frost, 1996; Scholes *et al.*, 2002).

The average biomass burned density in woodlands in MODIS is very similar up to 40% PTC and decreases slightly afterwards (Figure 8b). This is the outcome of the

combined, and in most cases canceling, effects of the fuel load density and the combustion completeness in the woodland locations mapped by MODIS (Figures 8a and 8c). In general, fuel load density increases up to about 40% PTC from an average of about 297 gm^{-2} to 370 gm^{-2}. At the same time, the combustion completeness decreases from an average of about 0.92 to 0.76. For PTC values higher than 40% the fuel load density decreases up to about 70% PTC and increases again at higher PTC values, while combustion completeness increases slightly up to 65% and decreases after that.

The average biomass burned density in woodlands in GBA shows a similar distribution and values (Figure 9b) with MODIS (Figure 8b) up to 65% PTC. At higher PTC values slightly more biomass is consumed per unit area in GBA compared with MODIS due to higher fuel load densities (Figures 8a and 9a) and higher combustion completeness values (8c and 9c). Despite the higher litter loads per unit area in GBA (Figure 9a) compared with MODIS (Figure 8a) at PTC values greater than 65%, the higher combustion completeness occurs because of the smaller contribution of the twigs to the total fuel load per unit area.

The general trend observed in the GLOBSCAR woodland biomass burned densities is that they are slightly higher compared with MODIS and GBA up to 40% with somewhat larger differences occurring between 40% and 75% (Figures 8b, 9b, 10b). This is mainly because of the increased grass contribution in the fuel load mixture (Figures 8a, 9a, 10a) at that PTC range, resulting in higher fuel consumption by the fires (Figures 8c, 9c, 10c). The average biomass burned consumed per unit area in woodlands in GLOBSCAR is very similar up to about 65% PTC and increases slightly afterwards again as a net effect of decreasing/increasing fuel load densities and combustion completeness.

At the regional level the majority of the burned biomass in woodlands occurs at PTC values below 50% (Figure 7a). Considering that the amounts of biomass burned in woodlands for each burned area product are more or less similar across PTC values below 50%, and that small differences exist in the biomass burned density values among the three products, it is concluded that biomass burned density in not a significant source of variation for emissions from woodland fires at the regional level. It needs to be emphasized though, that this is the case only for the specific month and year of study. Examination of seasonal and interannual differences in the burned area distribution in woodlands among the three products may yield different results.

For all burned area products, the $EFCO_2$ decrease somewhat with increasing PTC by a maximum of about 10% in MODIS and GBA and 7% in GLOBSCAR (Figures 8d, 9d, 10d). Therefore, the CO_2 emissions densities in woodlands closely follow the trends of the biomass burned (Figures 8e, 9e, 10e). CO_2 emissions per unit area from woodland fires in GLOBSCAR are generally higher than the correspondent CO_2 emissions in MODIS and GBA. There is a pronounced increase in CO emission densities with increasing PTC which is linked to the increase in EFCO (Figures 8f, 9f, 10f). Average CO emission densities increase by maximum factors of 1.9 in MODIS, 3.1 GBA and 2.3 in GLOBSCAR (Figures 8g, 9g, 10g). This is due to the decreasing contribution of grasses to the fuel bed with increasing PTC and the more smoldering combustion of the woody components in the fuel.

Grassland burns have higher combustion completeness than woodland burns in all burned area products, which is the main reason for the generally higher average biomass burned densities in the MODIS and GBA grasslands compared with the woodlands

(Figures 8c, 9c, 10c). In GLOBSCAR, as a result of the lower fuel loads in grasslands compared with woodlands, comparable amounts of biomass are burned per unit area in both land cover types. Consequently, the net effect at the regional level, is that slightly more biomass is burned in woodlands than grasslands, relative to their correspondent burned area ratio (Tables 3 and 7). Field studies have also shown higher combustion completeness in grassland compared with woodland fires and increasing combustion completeness as the dry season progresses (Shea *et al.*, 1996; Hoffa *et al.*, 1999). It is also apparent that $EFCO_2$ Figures (8d, 9d, 10d) are higher for these very efficient mostly dry grassland fires compared with woodlands. More CO_2/CO is released per unit area in grasslands compared with woodlands in all burned area products (Figures 8e/8g, 9e/9g, 10e/10g). EFCO (Figures 8f, 9f, 10f) in grasslands are lower by up to a factor of 2 compared with EFCO in woodlands. The differences in EFCO, rather than the differences in biomass burned, is the fundamental reason for the significantly lower CO emission densities in grasslands compared with woodlands (Figures 8g, 9g, 10g).

The emissions profile for woodlands and grasslands fires, regardless of the satellite burned area product used, predicted by the model developed here is supported by the general fire emissions patterns for these two land cover types in the late dry season when fuel types are fairly dry (Ward *et al.*, 1992; Ward *et al.* 1996; Yokelson *et al.*, 2003; Sinha *et al.*, 2003). Dry savanna fires, including grasslands and woodlands, are typically efficient fires that have higher emissions factors for fully oxidized species, such as CO_2 and NO_x, compared with forest fires (Andreae, 1997; Andreae and Merlet, 2001). At the same time, within the savanna vegetation continuum formations, ranging from pure grasslands to closed-canopy woodlands, there is great variability in fuel composition,

which among other important factors such as fuel condition (*e.g.*, moisture content, packing density) and environmental conditions (*e.g.*, relative humidity, wind direction, wind speed), determine the relative proportions of flaming and smoldering combustion. Combustion of predominantly grass fuel in grasslands favors the generation of fully oxidized products, such as CO_2 and NO_x. On the other hand, the leaf litter and twig components in the woodland fuel beds tend to involve more smoldering combustion, compared with the grass, favoring the generation of products of incomplete combustion. As the amount of combustible litter increases, and `the amount of grass decreases, the emission factors for products of incomplete combustion generally increase. The results presented above verify that the emissions model responds in a reasonable fashion to different burned area inputs. Furthermore, they explain why the regional emissions of smoldering compounds from woodland fires are disproportionately high relative to their burned areas for each burned area product.

The aforementioned analysis on the impact of the spatial distribution on emission densities provides the basis to also understand the disproportionate response of emissions for certain atmospheric species, to changes in the burned area amounts at the regional level. This non-linear response is related to the differences in the relative proportion and location of woodland and grassland burns mapped in each product. The main underlying reason is that, variations in fuel composition lead to different fire behaviors in these two land cover types, involving more smoldering combustion in woodlands compared with grasslands. The differences in the relative amounts among the different atmospheric species are related to the fact that they are emitted at different molar ratios.

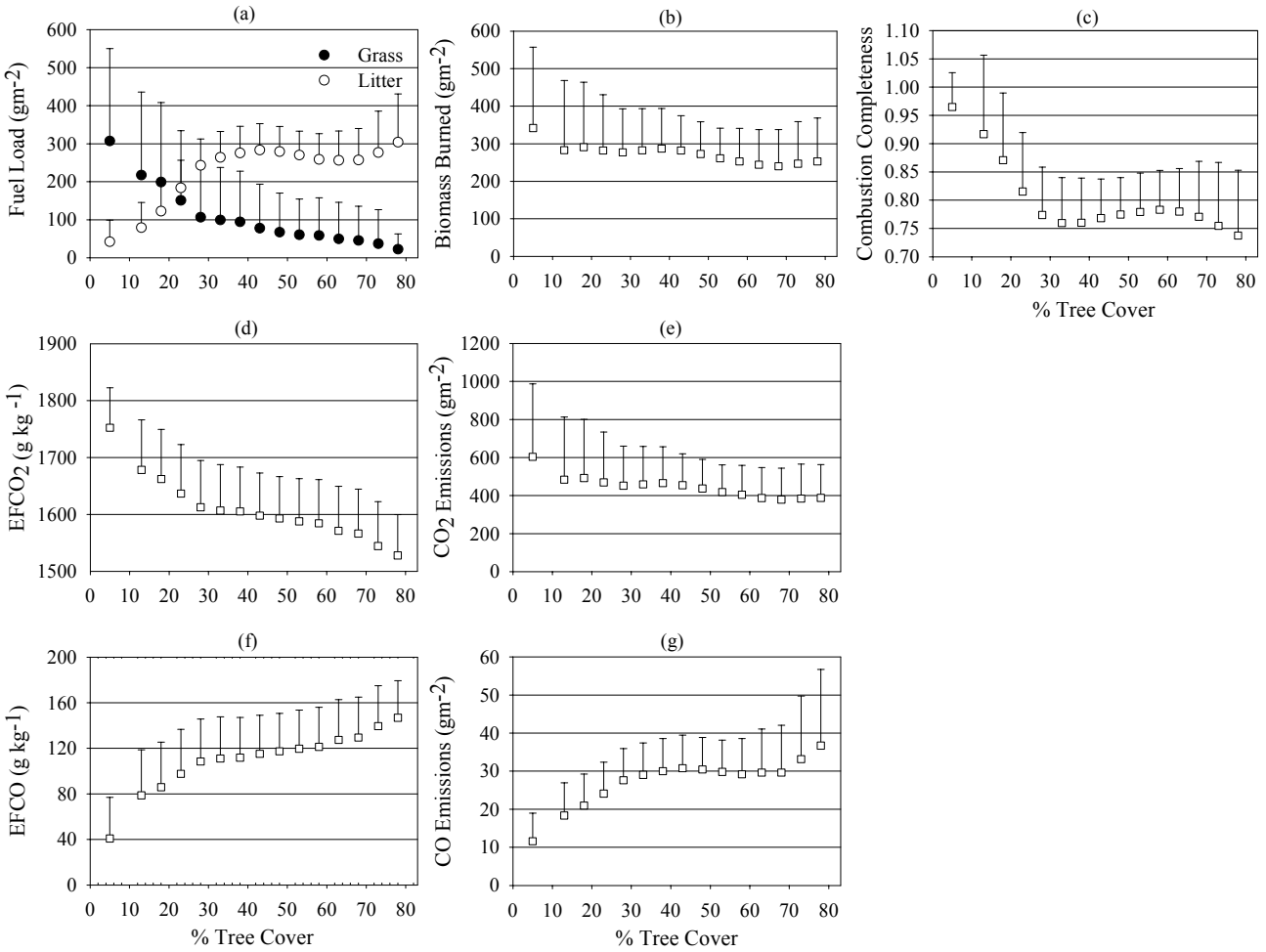

Figure 8. Mean (symbol) and one standard deviation statistics computed from the southern Africa, September 2000, MODIS burned pixels of (a) fuel load, (b) biomass burned, (c) combustion completeness, (d) CO_2 emission factors, (e) CO_2 emissions, (f) CO emission factors, and (g) CO emissions. The grassland (0% <= PTC <= 10%) statistics are shown at PTC = 5%. The woodland (PTC > 10%) statistics are defined over 5% PTC intervals.

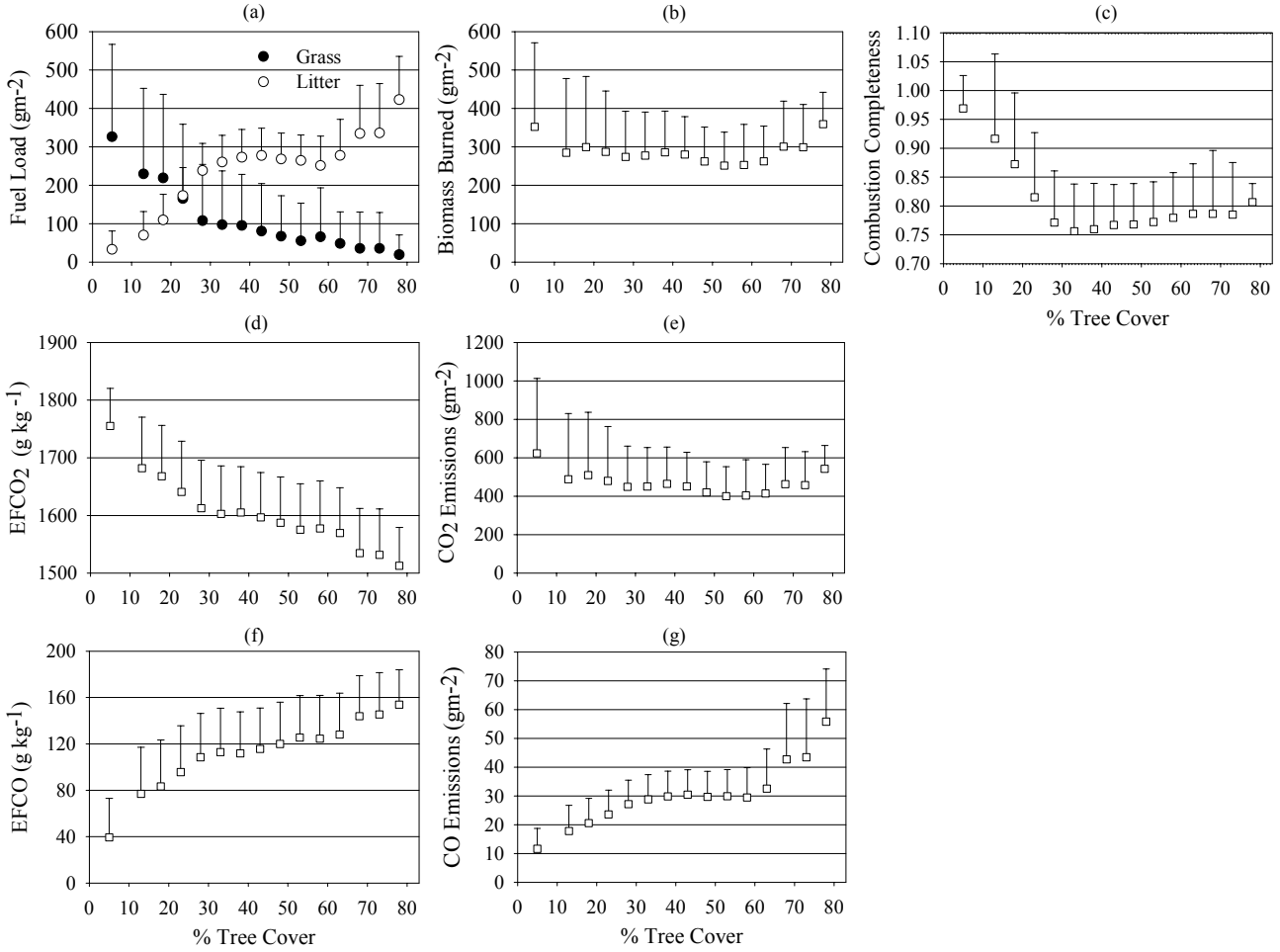

Figure 9. Mean (symbol) and one standard deviation statistics computed from the southern Africa, September 2000, GBA-2000 burned pixels of (a) fuel load, (b) biomass burned, (c) combustion completeness, (d) CO_2 emission factors, (e) CO_2 emissions, (f) CO emission factors, and (g) CO emissions. The grassland (0% <= PTC <= 10%) statistics are shown at PTC = 5%. The woodland (PTC > 10%) statistics are defined over 5% PTC intervals.

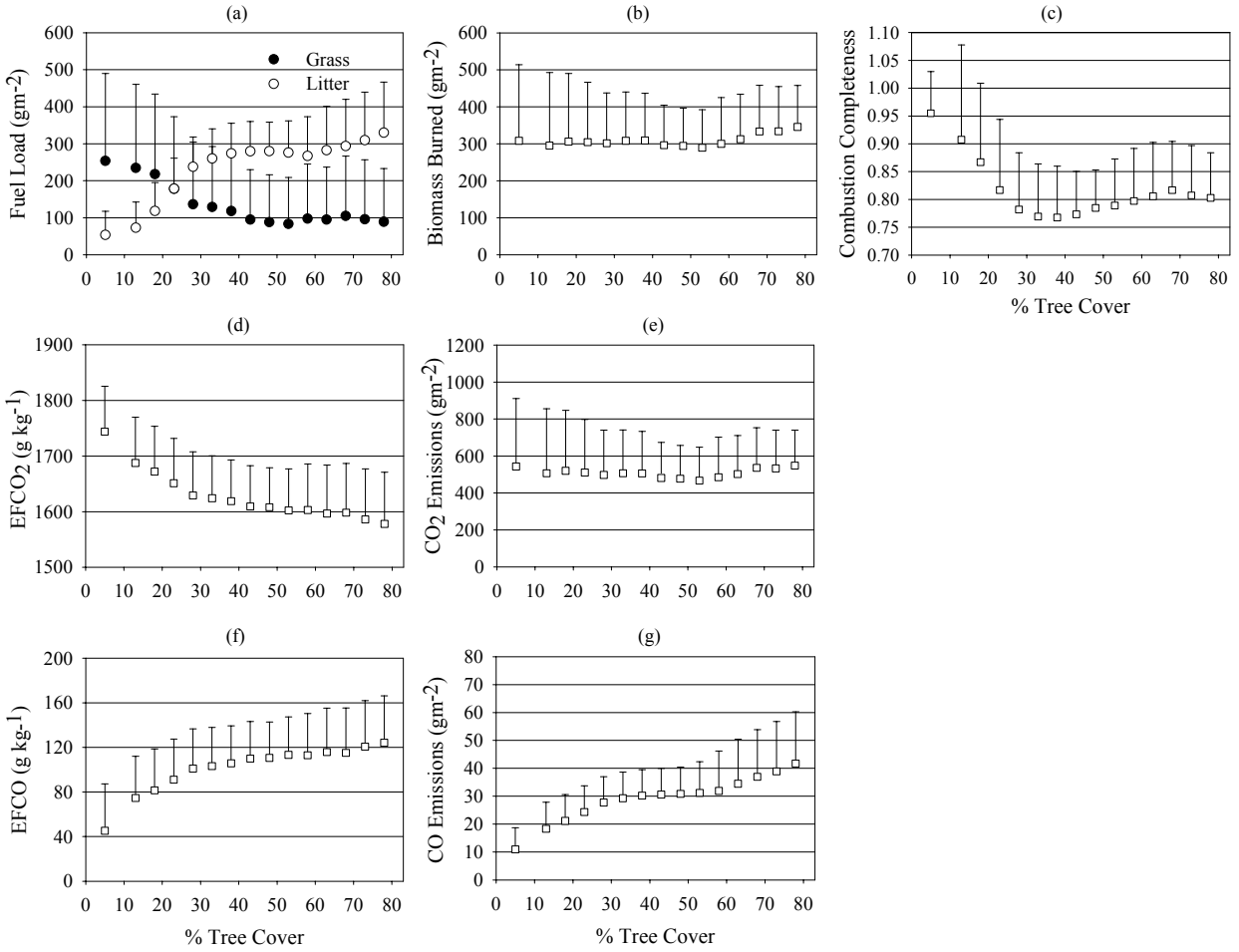

Figure 10. Mean (symbol) and one standard deviation statistics computed from the Southern Africa, September 2000, GLOBSCAR burned pixels of (a) fuel load, (b) biomass burned, (c) combustion completeness, (d) CO_2 emission factors, (e) CO_2 emissions, (f) CO emission factors, and (g) CO emissions. The grassland (0% <= PTC <= 10%) statistics are shown at PTC = 5%. The woodland (PTC > 10%) statistics are defined over 5% PTC intervals.

Figure 11 illustrates that regional average fuel loads, combustion completeness, $EFCO_2$ and EFCO for grasslands and woodlands are comparable among burned area products. However, at the regional level, MODIS maps a higher percentage of burned area/biomass burned for woodland fires compared with GBA-2000 (Tables 3 and 7). Since burning in woodlands involves more smoldering compared with grasslands (Figure 11d), the increase of the MODIS over the GBA-2000 is proportionally higher for products of incomplete combustion than the corresponding increase for the fully oxidized emissions products, such as CO_2 and NO_X. The opposite is found when comparing MODIS with GLOBSCAR. MODIS maps a higher proportion of grasslands compared with GLOBSCAR. As seen above, burning in grasslands at the end of the dry season favors emissions of fully oxidized products, such as CO_2 and NO_X. Therefore, the increase in burned area of MODIS over GLOBSCAR results in proportionally larger differences for products of complete combustion compared with products of incomplete combustion. Variations in the fuel load amounts, between woodlands and grasslands, and between the respective woodland and grassland locations mapped in each burned area appear to be of lesser importance at the regional level.

To assess the sensitivity of the emissions estimation process to different PTC thresholds, CO_2 and CO emissions are quantified using 5% and 15% PTC values to stratify the grasslands and woodlands for each burned area product. As seen in Table 8, insignificant differences in the emissions estimates arise at the regional level as a result of applying the different thresholds. It is also conspicuous, that the differences in emissions among burned area products are considerable and that they follow the same trends as with the 10% PTC used in the analysis above (Tables 4-6, Appendix B).

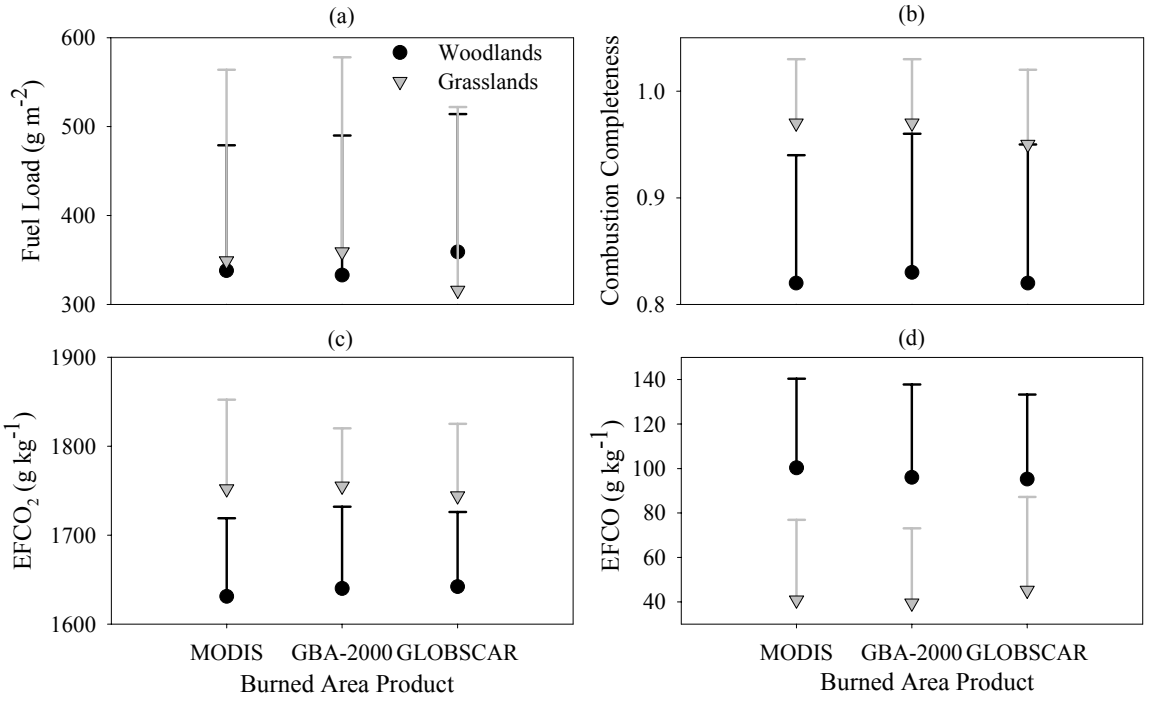

Figure 11. Mean (symbol) and one standard deviation (error bar) statistics computed from the southern Africa, September 2000, MODIS, GBA-2000 and GLOBSCAR burned area products for (a) fuel load, (b) combustion completeness, (c) CO_2 emission factors, and (d) CO emissions factors.

The results of this study indicate that reliable information on the burned area spatial distribution in addition to the amount is required to increase the accuracy of emissions models. Approaches designed to obtain burned area error information and patterns should be at least ecosystem-specific. Development of increasingly sophisticated and more robust emissions modeling frameworks will require spatially-explicit uncertainty measures of burned area. Furthermore, the results suggest that emissions estimation based on extrapolations of the burned area amounts without spatially explicit consideration of impacts of the fuel characteristics on emissions (*e.g.*, using average emission factors for savanna burning) will result to various degree of uncertainty for different atmospheric species. Obviously, accurate fuel load information is pertinent to

the spatial distribution of burned area and their complex interrelation and associated impact on emissions quantification needs to be explored further.

Table 8. Emissions estimates for different Percent Tree Cover (PTC) thresholds for the grasslands-woodlands classification, southern Africa, September 2000.

Regional Emissions (Gg)	*5% PTC*	*15% PTC*
MODIS		
CO_2	133369	134279
CO	6072	5626
GBA-2000		
CO_2	89828	90690
CO	3561	3215
GLOBSCAR		
CO_2	30213	30455
CO (Gg)	1438	1334

4.3.3 Implications of the Spatial Distribution of Burned Area for National Emissions

Party countries to the United Nations Framework Convention on Climate Change (UNFCC) are obliged to report their national greenhouse gas emissions, including those from savanna burning (Braatz *et al.*, 1995). The spatial differences in the burned area products discussed in the previous section become especially important within this context, since some countries might be more susceptible to these uncertainties in the burned area mapping than others. The discussion is limited to larger countries since emission estimates for small countries likely have higher uncertainties. Table 9 (Appendix B) lists the country-level burned area and emissions for selected trace gases and particulates for the three burned area products. Figure 12 illustrates the corresponding woodland to grassland ratios for the three burned area products.

As can be seen in the case of Tanzania, despite the practically equal MODIS and GBA-2000 burned area amounts, the MODIS derived estimates for products of incomplete combustion are higher by approximately 30% to 58%. The differences are

primarily due to the fact that MODIS maps more burns in woodlands compared with GBA-2000. The ratio of woodland over grassland fires mapped in MODIS is 5.5 whereas in GBA-2000 it is 1.9. The variations in fuel load, combustion completeness and emission factors between woodlands and grasslands primarily, and between the respective woodland and grassland locations mapped in each burned area product, secondarily, result in these differences in emissions. In the MODIS-driven emissions model the average values for woodlands and grasslands in Tanzania are 317 gm^{-2} and 241 gm^{-2} for fuel load, 0.78 and 0.94 for combustion completeness, 1587 gkg^{-1} and 1685 gkg^{-1} for emission factors for CO_2, 120.1 gkg^{-1} and 75.2 gkg^{-1} for emission factors for CO, 4.646 gkg^{-1} and 2.169 gkg^{-1} for emission factors for CH_4, 3.028 gkg^{-1} and 3.335 g kg^{-1} for emission factors for NMHC and 16.198 gkg^{-1} and 4.716 gkg^{-1} for emission factors for PM2.5, respectively (Tables 10-11).

Table 10. Average values and ($|\pm\sigma|$) of fuel load (gm^{-2}), combustion completeness (CC), and emission factors (EF) (gkg^{-1}) for woodland fires in Tanzania, September 2000, using MODIS and GBA-2000.

	Fuel load	*CC*	*$EFCO_2$*	*EFCO*	*$EFCH_4$*	*EFNMHC*	*EFPM2.5*
MODIS	317	0.78	1587	120.1	4.646	3.028	16.198
	(155)	(0.16)	(104)	(47.4)	(2.469)	(0.936)	(9.243)
GBA-2000	297	0.81	1607	110.9	4.168	2.847	14.409
	(179)	(0.18)	(114)	(51.8)	(2.697)	(1.022)	(10.098)

Table 11. Average values and (|±σ|) of fuel load (gm^{-2}), combustion completeness (CC), and emission factors (EF) (gkg^{-1}) for grassland fires in Tanzania, September 2000, using MODIS and GBA-2000.

	Fuel load	*CC*	*$EFCO_2$*	*EFCO*	*$EFCH_4$*	*EFNMHC*	*EFPM2.5*
MODIS	241	0.94	1685	75.2	2.169	3.335	4.716
	(182)	(0.06)	(126)	(64.9)	(2.474)	(3.800)	(4.319)
GBA-2000	250	0.95	1715	60.3	1.600	2.462	3.724
	(183)	(0.07)	(110)	(56.8)	(2.166)	(3.326)	(3.782)

In comparison, the GBA-2000 driven average values for woodlands and grasslands in Tanzania are 297 gm^{-2} and 250 gm^{-2} for fuel load, 0.81 and 0.95 for combustion completeness, 1607 gkg^{-1} and 1715 gkg^{-1} for emission factors for CO_2, 110.9 gkg^{-1} and 60.3 gkg^{-1} for emission factors for CO, 4.168 gkg^{-1} and 1.600 gkg^{-1} for emission factors for CH_4, 2.847 gkg^{-1} and 2.462 gkg^{-1} for emission factors for NMHC and 14.409 gkg^{-1} and 3.724 gkg^{-1} for emission factors for PM2.5, respectively (Tables 10-11). In comparison, in other countries where major biomass burning occurs, such as Mozambique, differences in emissions closely follow the differences in burned area amounts, because of the similar woodland over grassland ratios in MODIS (11.2) and GBA-2000 (10.0) for this country and the similar fuel load distribution.

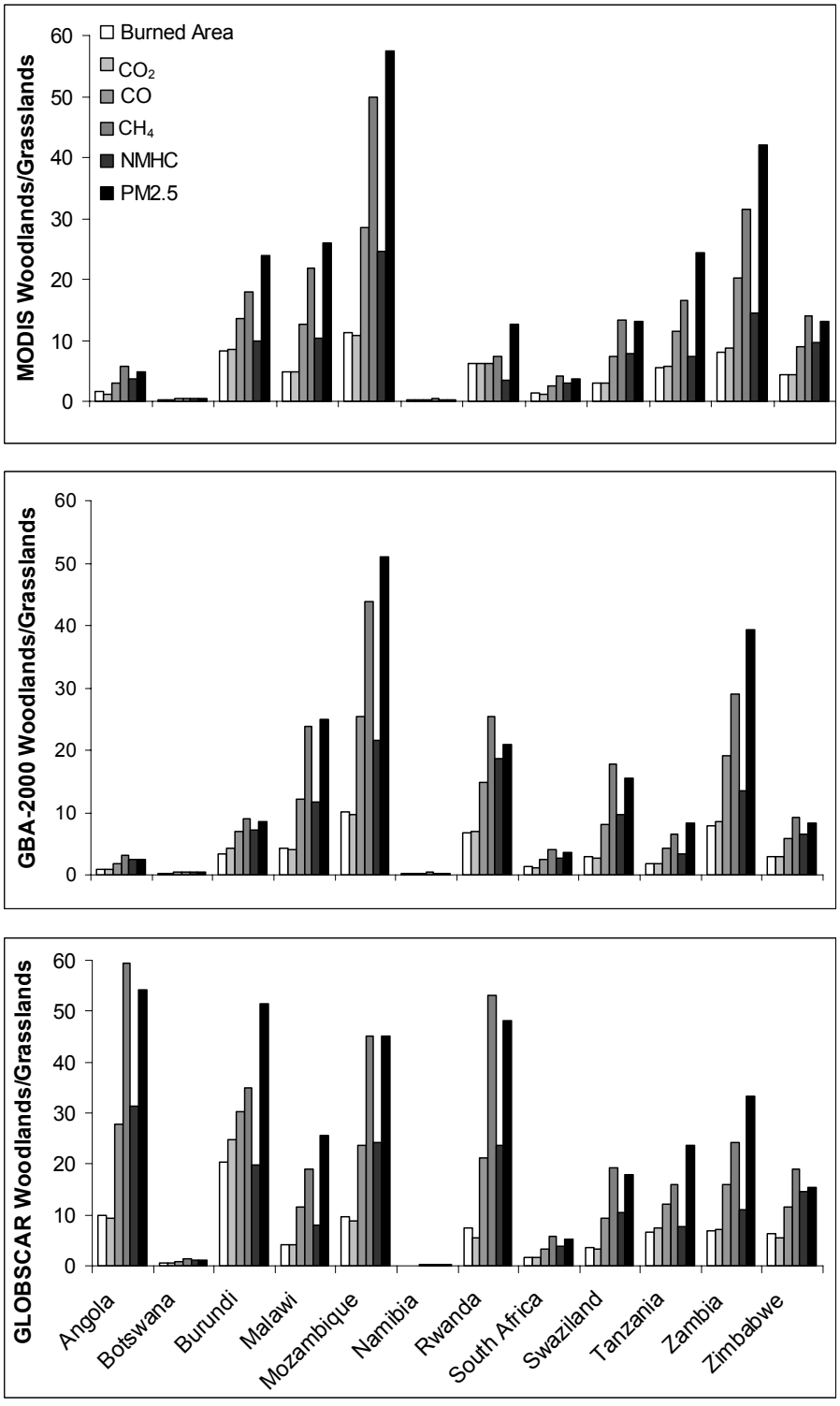

Figure 12. MODIS, GBA-2000 and GLOBSCAR woodland over grasslands ratios for burned area, and selected trace gas and particulate emissions for September 2000. Only those southern African countries situated completely south of the Equator are reported.

4.4 Conclusions

This one-variable sensitivity study contributes to a better understanding of the relationship between burned area and emissions. The model's predictions, regardless of burned area, are consistent with published field studies of emission patterns from woodland and grassland fires (Ward *et al.*, 1996; Hoffa *et al.*, 1999). These studies show that burning in woodlands favors emissions of products of incomplete combustion compared with grasslands. It appears from this study that uncertainties in the regional emissions predictions are due to uncertainties in the input variables (in this case burned area) rather than the model's structure and specifications. Changes to the burned area amounts lead to significant changes in the emissions output. However, due to the different emission profiles in woodlands and grasslands, these changes are not necessarily proportional to the differences in the burned area amounts. The nonlinearity of emissions to burned area highlights the fact, that Equation (4.1) needs to be applied within a spatially explicit context and that simple extrapolations based on burned area amounts can lead to different uncertainties for different emissions products. Information on the spatial distribution of burned area is essential to reducing uncertainty in emissions estimates. Validation of burned area datasets is a priority for satellite data providers, for a variety of usages, including reduction of emissions models uncertainties. This is especially the case, if derived satellite products are to be used for national greenhouse gas emissions reporting. There is some urgency for the international satellite community to develop the appropriate protocols and procedures for land data product validation (Justice *et al.*, 2002b; Morisette *et al.*, 2002). From an emissions modeling perspective, spatially explicit maps of burned area uncertainty are desirable since the spatial distribution of the burning has significant implications for emissions quantifications. This information is

pertinent not only for improvement of the satellite burned area products but it will also provide the base information for proper capture of uncertainty in emissions models. Failing the availability of spatially explicit uncertainty information, the results in this chapter indicate that ecosystem-specific uncertainty information will provide a step forward. Even though this study focused on one month at the end of the 2000 dry season, it is very likely that uncertainty in the burned area also varies through time and should also be quantified within the context of seasonal emissions modeling.

Chapter 5: Regional Seasonal Vegetation Fire Emissions for 2000

5.1 Introduction

Vegetation fires may produce an interannual modulation in global greenhouse gas levels (Langenfelds *et al.*, 2002; Page *et al*; 2002; Schimel and Baker, 2002; van der Werf *et al.*, 2004). To generate more realistic patterns of the transformation and deposition of atmospheric species, atmospheric chemistry models require spatially and temporally explicit estimates of trace gas and particles (Scholes and Andreae, 2000, Bergamaschi *et al.*, 2000; Duncan *et al.*, 2003). A thorough understanding of the seasonal variations in fire emissions, that likely differ from year-to-year, is required to decipher the role of vegetation fires on global land-atmosphere carbon exchanges. Existing regional and global emissions modeling approaches, including land-based and inverse atmospheric chemistry and transport models, have largely ignored the seasonal variations in combustion efficiency and combustion completeness and the resulting implications for both the type and quantity of trace gases and particulates.

Although, seasonal trends of southern African savanna fire emissions relating to the fuel moisture condition have been shown to significantly affect fire behavior and the annual emissions estimation for grassland fires at the site and landscape levels, particularly for products of incomplete combustion (Hoffa *et al.*, 1999; Chapter 2; Chapter 3), a similar evaluation at the regional level has not been performed yet. At the landscape level, the combustion efficiency of grassland fires increases, as the fuel becomes drier towards the end of the dry season. Hoffa *et al.* (1999) hypothesized, that similar seasonal trends may also occur for woodland as for grassland fires. However, due to the larger fuel heterogeneity in the experimental woodland burns, which they

conducted, no definite trends in seasonal combustion efficiency could be determined. The significance of the differences in fire behavior for emission of trace gases and particulates at large scales has yet to be determined and the aim of this study is to address this gap in our knowledge.

In this chapter the regional emissions model presented in Chapter 4 is applied with slight modifications described below to estimate monthly early (April-July) and late (August-October) dry season emissions from grassland and woodland fires in southern Africa for the year 2000. A wide variety of chemical species that are important in global atmospheric chemistry, including Oxygenated Volatile Organic Compounds (OVOCs), are modeled here for the first time for southern African vegetation fires. To make the emissions results from this study comparable with previous studies (Scholes *et al.*, 1996a; Barbosa *et al.*, 1999), the analysis is undertaken for the months of April through October. Vegetation fire emissions are compared with other regional sources of pyrogenic trace gases and particulates, as well as global biomass burning and fossil fuel emissions to assess their importance.

5.2 Seasonal Vegetation Fire Emissions Modeling Methodology

The regional model and the equations used to evaluate the seasonal emission patterns from grassland and woodland fires in southern Africa are described in Chapter 4. A flowchart of the regional emissions model is presented in Figure 1 and the data sets used as inputs are presented in Table 1. Fuel moisture condition computed as the percentage of green grass relative to the total grass (PGREEN) is derived in two ways. The first, referred to as the "fuel-load based method" is derived from the fuel load

modeled dead and green grass outputs. The second, referred to as the "NDVI-based method" is derived from NDVI time series data and is described in Section 5.2.1.

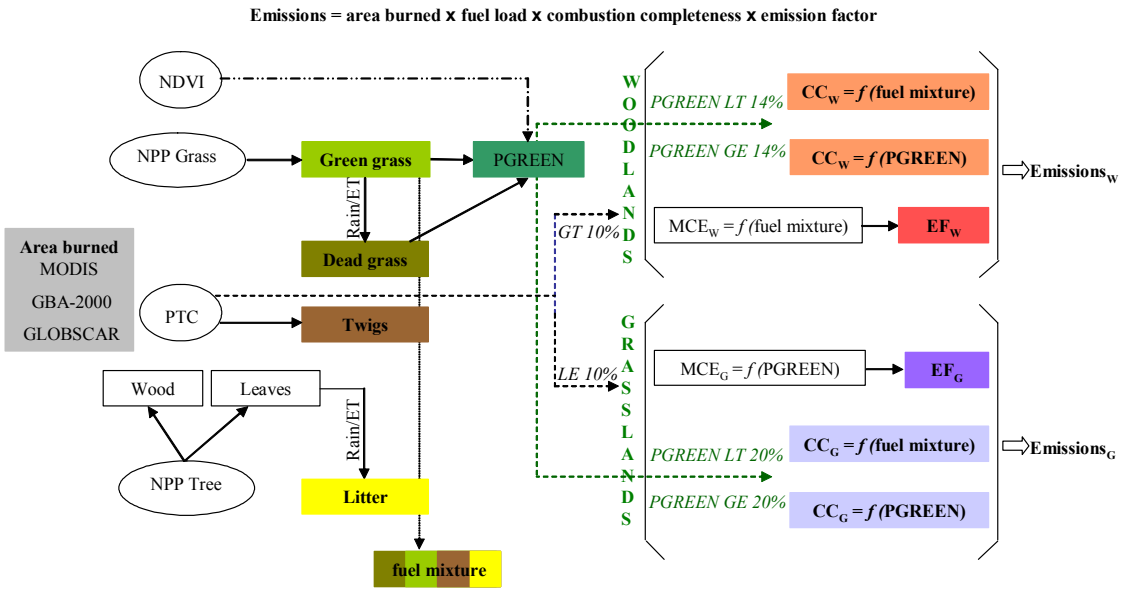

Figure 1. Overview of monthly regional spatially-explicit emissions model for grassland (G) and woodland (W) fires. Emissions variables are denoted by colored rectangles. Important input data used to derive various emissions variables are denoted by ovals. Thresholds applied to the MODIS Percent Tree Cover (PTC) and the percentage of green grass relative to the total grass (PGREEN) are shown in italics (LT = less than, GE = greater than or equal, GT = greater than, LE = less than or equal). CC is the combustion completeness, MCE the modified combustion efficiency and EF the emission factors.

Table 1. Summary of data sets and parameterizations used in the estimation of spatially-explicit seasonal regional vegetation fire emissions.

Variables	Source	Method
Green grass, dead grass, litter and twigs fuel loads	Hély *et al.* (2003)	NPP model ⟶ allocation *herbivory, evapotranspiration*
MODIS burned area	Roy *et al.* (2002)	BRDF model based change detection
Global Burned Area-2000	Tansey *et al.* (2002)	Supervised classification tree
GLOBSCAR	Simon *et al.*, in press	Logical AND of two threshold based algorithms
[a]CC grasslands	Hoffa *et al.* (1999); Shea *et al.* (1996)	Linear regression + PGREEN[b] Average of field measurements
[a]CC woodlands	Hoffa *et al.* (1999); Shea *et al.* (1996)	Linear Regression + PGREEN[b] Average of field measurements
[c]EF grasslands	Chapter 3	Linear Regression + MCE_G[d]
[c]EF woodlands	Chapter 3	Linear Regression + MCE_W[e]
Percent tree cover	Hansen *et al.* (2002)	Regression tree
NDVI	Tucker *et al.* (1994)	Maximum value compositing

[a]CC = Combustion completeness; [b]PGREEN = (green grass/ total grass); [c]EF = Emission factor; [d]MCE_G = Modified combustion efficiency for grassland fires from Chapter 3; [e]MCE_W = Modified combustion efficiency for woodland fires from i) Ward *et al.* (1996) and ii) Section 5.2.1.2. These variables are calculated using the i) fuel load-based method and ii) the NDVI-based method described in Section 5.2.1.1, to assess the contribution of dry and green grass in the fuel mixture.

The NDVI-based method is developed because in the early stages of the research it was observed that the fuel load model under-predicted the amount of green grass relative to dead grass. This occurred particularly in the early dry season. The 1999-2000 growing season has been classified as a La Niña year and was the wettest year compared to the previous 20+ years both in amount and spatial extent (Anyamba *et al.*, 2003). Persistent greenness during the 2000 dry season was evident both in satellite imagery (Anyamba *et al.*, 2003) and was observed in the field by numerous SAFARI 2000 researchers (T. Landmann, personal communication). Furthermore, comparison of the fuel-based and NDVI-based methods allows for an assessment of the sensitivity of the emissions results to different levels of fuel greenness. To account for the seasonal

changes in emission factors for woodland fire, that were not modeled in the work reported in Chapter 4, the woodland modified combustion efficiency is now parameterized in a way to also consider the proportion of green grass in the fuel mixture (see Section 5.2.2).

5.2.1 Assessment of Fuel Moisture Condition Using NDVI Time Series

Fuel moisture is required to assess seasonal changes in combustion completeness and emission factors. The paucity of available information on the effects of non-grass fuel moisture on MCE and combustion completeness precludes meaningful modeling at this time. In this study, only grass fuel moisture is considered since empirical fire behavior studies indicate that moisture changes in grass are primarily important (Hoffa *et al.*, 1999). Although techniques have been developed to derive vegetation moisture from optical wavelength data (*e.g.*, Gao and Goetz, 1990; Gao, 1996; Ceccato *et al.*, 2002), and radar data (*e.g.,* Brisco *et al.*, 1990; Hochschild and Herold, 2001) their utility for reliable regional scale analyses has not been proven. Consequently, in this study temporal analysis of the robust Normalized Difference Vegetation Index (NDVI) is used to assess the fuel moisture condition.

The NDVI is calculated as the difference in reflectance between the near-infrared and visible red wavelengths divided by their sum (Tucker, 1979). As vegetation dries out, its chlorophyll content is reduced and the visible red reflectance increases and the near-infrared reflectance decreases. Therefore, the NDVI is sensitive to the presence of actively photosynthesizing biomass. A number of remote sensing studies have employed spectral vegetation indices to gain an understanding of savanna productivity, biomass and curing (*e.g.*, Justice and Hiernaux, 1986; Fuller and Prince, 1996). Fuller *et al.* (1997)

analyzed the contributions of the surface and the tree layers to the NDVI in savanna woodlands in eastern Zambia. They found that the ground surface layer was the largest contributing component to the NDVI throughout most of the seasonal cycle. The radiometric contribution from the green canopy tree layer becomes relatively more important (20-40%) during the dry season when the ground surface layer is largely senescent. It appears thus, that even during the dry season, the majority of the NDVI signal may be attributed to the below-canopy surface layer. This supports the application of NDVI to assess the grass fuel moisture condition in this study, since the majority of fires in southern Africa are surface fires (Frost, 1996; Trollope and Trollope, 2002). The United States Forest Service (USFS) uses NDVI to assess relative fuel greenness (Burgan *et al.*, 1998; Hardy and Burgan, 1999) and significant relationships between ground- and NDVI-based estimates of fuel curing have been derived for Australian savanna fire management applications (Paltridge and Barber, 1988; Allan *et al.*, 2003).

The percentage of green grass over total grass (PGREEN) is determined independently at each pixel using Equation (5.1) (Kogan, 1997; Burgan *et al.*, 1998):

$$PGREEN_t = ((NDVI_t - NDVI_{min}) / NDVI_{range}) * 100.0 \quad (5.1)$$

where, t = time step

$NDVI_{min}$ = minimum of all NDVI values at the pixel over the year

$NDVI_{max}$ = maximum of all NDVI values at the pixel over the year

$NDVI_{range} = NDVI_{max} - NDVI_{min}$

The PGREEN values range from 0 to 100 reflecting changes in the moisture condition of the grass fuel at that pixel from extremely dry to wet. The NDVI datasets

used here were derived from AVHRR data processed by the Global Inventory Monitoring and Modeling Studies (GIMMS) group at NASA's Goddard Space Flight Center (Tucker *et al.*, 1994). NDVI monthly data composites at 8 km spatial resolution were generated using the maximum value compositing procedure to minimize aerosol and residual cloud contamination effects (Holben, 1986). Artifacts in the NDVI due to satellite drift have been corrected using empirical mode decomposition (Pinzón *et al.*, 2004). Calibration based on invariant desert targets has been applied to the data to minimize the effects of sensor degradation (Los, 1993).

The NDVI-based method to assess PGREEN will be unreliable for pixels with persistently high NDVI throughout the year, for example, equatorial evergreen forests, and in regions with persistently low NDVI values, for example deserts and salt pans. For these reasons, evergreen and desert masks are used to define pixels where the PGREEN is not derived using Equation (5.1). The PGREEN evergreen and desert masks are defined as:

$$\text{PGREEN-evergreen} = \text{NDVI}_{\text{mean}} > 0.6 \text{ AND } \text{NDVI}_{\text{range}} < 0.3 \quad (5.2)$$

$$\text{PGREEN-desert} = \text{NDVI}_{\text{mean}} < 0.1 \text{ AND } \text{NDVI}_{\text{range}} < 0.04 \quad (5.3)$$

where, $\text{NDVI}_{\text{mean}}$ = mean of all NDVI values at the pixel over the year

The thresholds used in Equations (5.2) and (5.3) were derived interactively by visual examination of the NDVI data and approximate NDVI values for desert and evergreen land covers found in the literature (*e.g.*, Anyamba *et al.*, 2003).

In the NDVI method, pixels that are masked are used to derive emissions but with PGREEN values determined from the fuel load method (described in Section 4.2.1.1). For all other pixels, the NDVI-based PGREEN values are used to adjust the fuel-load

modeled estimates of green and dry grass using Equations (5.4) and (5.5). In this adjustment, it is assumed, that the amount of twigs and litter remains the same, only the relative proportions of the green and dry grass to the total grass change.

$$\text{Adjusted } GG_t = (PGREEN_t / 100) * (GG_t + DG_t) \quad (5.4)$$

$$\text{Adjusted } DG_t = (1 - (PGREEN_t / 100)) * (GG_t + DG_t) \quad (5.5)$$

where, t = time step

GG_t = Fuel load modeled green grass at time step t (gm^{-2})

DG_t = Fuel load modeled dry grass at time step t (gm^{-2})

$PGREEN_t$, defined by Equation (5.1)

5.2.2 Modified Combustion Efficiency in Woodlands

Some emitted compounds can generally be attributed to flaming or smoldering combustion based on a linear correlation with the degree of oxidation, and thus the production of CO and CO_2 (Yokelson *et al.*, 1996). Combustion conditions that decrease the products of incomplete combustion, increase simultaneously the production of fully oxidized products such as CO_2 (Ward and Radke, 1993). The modified combustion efficiency (MCE) (see Chapter 3) adds considerable predictive value to estimates of fire emissions for particular atmospheric species. The efficiency of a fire is controlled by the moisture content, the chemical composition, the amount and packing of the fuel, among other factors, together with the environmental conditions that prevail during the burn (Ward and Hao, 1991). Although the impact of fuel moisture on the efficiency of grassland fires has been described (Hoffa *et al.*, 1999), a similar assessment for woodlands is not available. The dependence of MCE on fuels composed from dry fine fuel types has been determined for southern African woodlands (Ward *et al.*, 1996; see

Chapter 4). However, this relationship may not be representative of early dry season burning when the fuels are wetter (Hoffa *et al.*, 1999). A reanalysis of late dry season field measurements by Shea *et al.* (1996) and Ward *et al.* (1996), and the only available early dry season field measurements by Hoffa *et al.* (1996), provides the following relationship for MCE as a function of grass moisture condition and fuel composition (R^2 =0.98, SEE=0.028, p<0.001, n= 17):

MCE_W = (0.938*Pgreengrass+0.963*Pdeadgrass+0.940*Plitter+0.860*Ptwigs)/total fuel (5.6)

where, "P" denotes the proportion of each fuel type in the fuel mixture and the four proportions sum to 1.

The plitter and ptwigs are the same for both the fuel load- and the NDVI-based methods but pgreengrass and pdeadgrass are different between the two methods as described in Section 5.2.1.

5.2.3 MODIS-based Regional Burned Area and Emissions

Due to initial sensor gain and offset problems (Guenther *et al*., 2002), generation of a full time series of MODIS-derived burned area for the 2000 dry season was not possible. For this reason, the seasonal patterns of emissions are examined using monthly GBA-2000 burned area products generated from SPOT-VEGETATION data (Tansey *et al*., 2002). However, the MODIS burned area is available for July and September 2000 (Roy, 2003). Based on the results of Chapter 4, the GBA-2000 will likely underestimate regional emissions estimates. Therefore, in an attempt to obtain a more realistic estimate of the early and late dry season burned area and fire emissions using the available MODIS information, the following extrapolations are made.

MODIS early and late dry season burned area estimates for the woodland and grasslands are extrapolated using Equation (5.7). This equation is applied independently with respect to the burned areas in the grasslands and woodlands (*i.e.*, to give separate woodland and grassland MODIS early and late dry season burned area estimates).

$$MODIS_{early} = GBA_{early} * (MODIS_{July} / GBA_{July}) \quad (5.7)$$

$$MODIS_{late} = GBA_{late} * (MODIS_{September} / GBA_{September})$$

where,

$MODIS_{early}$ is the MODIS-based early dry season regional burned area

GBA_{early} is the sum of the GBA-2000 April-July total burned areas

$MODIS_{July}$ and GBA_{July} are the total areas burned in the MODIS and GBA-2000 July data sets respectively.

$MODIS_{late}$ is the MODIS-based late dry season regional burned area

GBA_{late} is the sum of the GBA-2000 August-October total burned areas

$MODIS_{September}$ and $GBA_{September}$ are the total areas burned in the MODIS and GBA-2000 September data sets, respectively.

Similarly, MODIS early and late dry season emissions estimates for a particular atmospheric species in the woodland and grasslands, and computed for the NDVI and the fuel load-based methods are extrapolated using Equation (5.8). This equation is applied independently to give grassland and woodland estimates for both the NDVI and the fuel load-based methods for a given atmospheric species.

$$E\_MODIS_{early} = E\_GBA_{early} * (E\_MODIS_{July} / E\_GBA_{July}) \quad (5.8)$$

$$E\_MODIS_{late} = E\_GBA_{late} * (E\_MODIS_{September} / E\_GBA_{September})$$

where,

E_MODIS_{early} is the MODIS-based early dry season emission

E_GBA_{early} is the sum of the GBA-2000 April-July emissions

E_MODIS_{July} and E_GBA_{July} are the total emissions defined using MODIS and GBA-2000 July data sets respectively.

E_MODIS_{late} is the MODIS-based late dry season emissions

E_GBA_{late} is the sum of the GBA-2000 August-October emissions

$E\_MODIS_{September}$ and $E\_GBA_{September}$ are the total emissions defined using the MODIS and GBA-2000 September data sets, respectively.

The MODIS-based early dry season emission estimate for a given atmospheric species for grasslands is then taken as the average of the NDVI and the fuel load-based E_MODIS_{early} emissions computed for grasslands. The MODIS-based woodland early dry season emissions and the MODIS late dry season emissions for grasslands and woodlands are computed similarly. The average of the NDVI and fuel load-based emissions is taken, in an attempt to provide a conservative estimate. Country-level burned area and emissions estimates are extrapolated in the same way by assuming, that the contribution of each country to the MODIS regional burned area and emissions for each atmospheric species is the same as that to the GBA-2000 regional burned area and emissions.

5.3 Results and Discussions

5.3.1 Seasonal Burned Area

5.3.1.1 GBA-2000

The analysis of the GBA-2000 shows that a total area of approximately 1,042,000 km^2 burned in southern Africa in 2000. The burning in grasslands and woodlands amounted to approximately 244,000 km^2 and 798,000 km^2, respectively. About 47% of the burning in grasslands, and 62% of the burning in woodlands, occurs during the early

dry season. The contribution of the monthly burning to the total burned area in each land-cover type is shown in Figure 2. Woodland burning peaks in July and grassland burning peaks in September. Early dry season burning accounts for the majority of the burning (58%) during the 2000 dry season at the regional level (Figure 3). July shows the most extensive burning due to heightened burning activity in woodlands that month. Previously, it was observed that August and September were the peak biomass burning months in the region (Scholes *et al.*, 1996a; Barbosa *et al.*, 1999). This supports the hypothesis that there is interannual variation in the fire occurrence and timing throughout southern Africa (Justice *et al.*, 1996; Barbosa *et al.*, 1999).

Extensive early dry season burning occurs in the moist/infertile miombo woodlands covering a broad belt between 5^{o}S and 15^{o}S, from Angola to Tanzania (Figures 4-5). In moist/infertile savannas, grass production is high but a smaller fraction of the grass is consumed by herbivory, compared with the fertile savannas, due its low nutrient content (Van Wilgen and Scholes, 1997). This allows the fuel to accumulate and burn (Frost, 1996). In the late dry season, fires predominate in the semiarid woodlands and grasslands in the southern and eastern half of the region and the Namibia/Angola

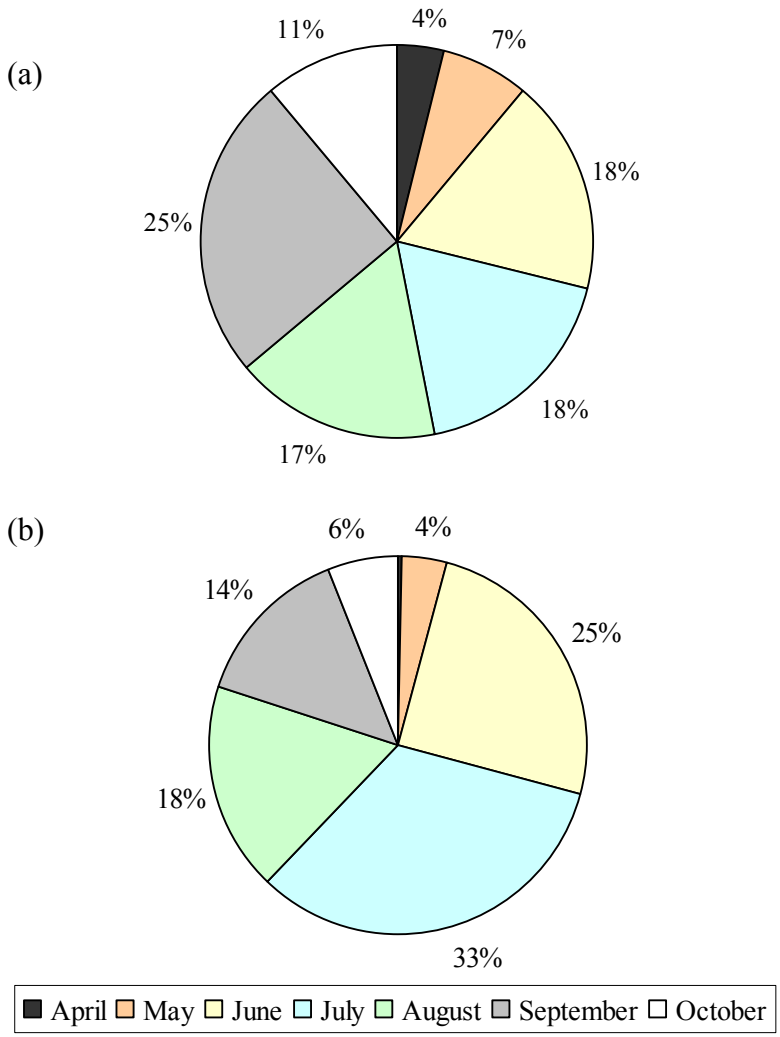

Figure 2. Contribution of seasonal burned area to total burned area in a) grasslands and b) woodlands using GBA-2000.

border. In these semiarid regions, where rainfall significantly affects the annual production, fire activity increases in wetter years, such as 2000, due to the increased availability of fuel (Justice *et al.*, 1996; Anyamba *et al.*, 2003). Fire incidence is very low in the arid regions of the southwest because of the insufficient amount of fuel to support a fire (Bond, 1997). Similar spatial progression of burning as the dry season proceeds has been reported for previous fire seasons (Cahoon *et al.*, 1992; Justice *et al.*, 1996; Dwyer *et al.*, 2000).

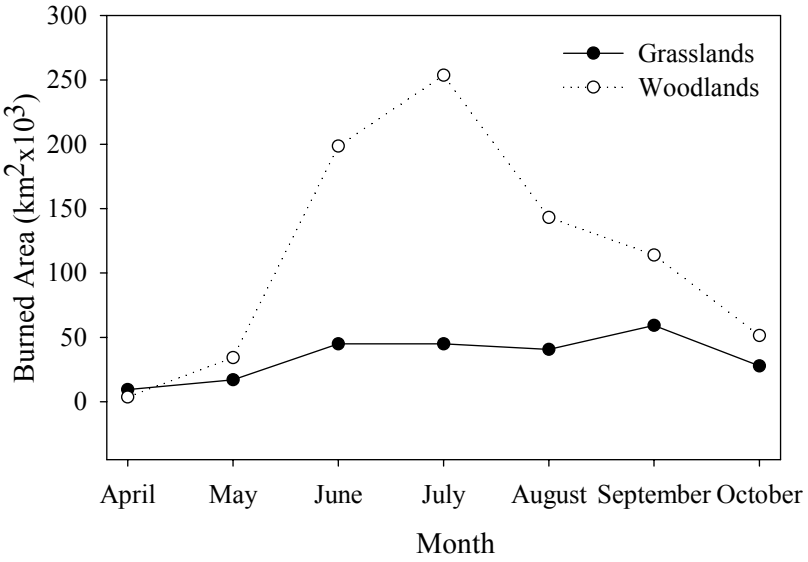

Figure 3. Seasonal GBA-2000 burned area in grasslands and woodlands in southern Africa, 2000.

A comparison of the monthly distribution of burning with the NDVI-derived PGREEN, shows that burning tacks closely the drying out of the vegetation (Figure 6). From Figures 3 and 7, it appears that in 2000 burning commences mostly in grasslands and relatively open canopy woodlands, and as the dry season evolves the burning tends to gradually also take place under more closed canopy woodlands. This may be because fuels beneath the more closed vegetation canopies in the moist woodland savannas take longer to cure. After August, the spatial distribution of the burning in woodlands tends to be skewed again towards lower PTC values. Overall, very little burning occurs at PTC values higher than 50%. Closing the tree canopy suppresses grass growth at sites receiving rainfall higher than about 600 mm (Chapter 4, Figures 8-10), thereby decreasing the likelihood of a site to be able to sustain a fire (Frost, 1996; Scholes *et al.*, 2002). Another plausible explanation for the scarcity of burning at higher than 50% PTC in GBA-2000 may be related to the difficulty of detecting burned areas underneath dense woodland canopies. Also, these areas are often persistently cloudy precluding burned

area mapping using optical wavelength satellite data (Roy *et al.*, 2002a). In the evergreen forests occurring along the northern limit of the miombo woodlands in the Democratic Republic of Congo, the persistent wetness of the fuel may also decrease the probability of burning (Van Wilgen and Scholes, 1997).

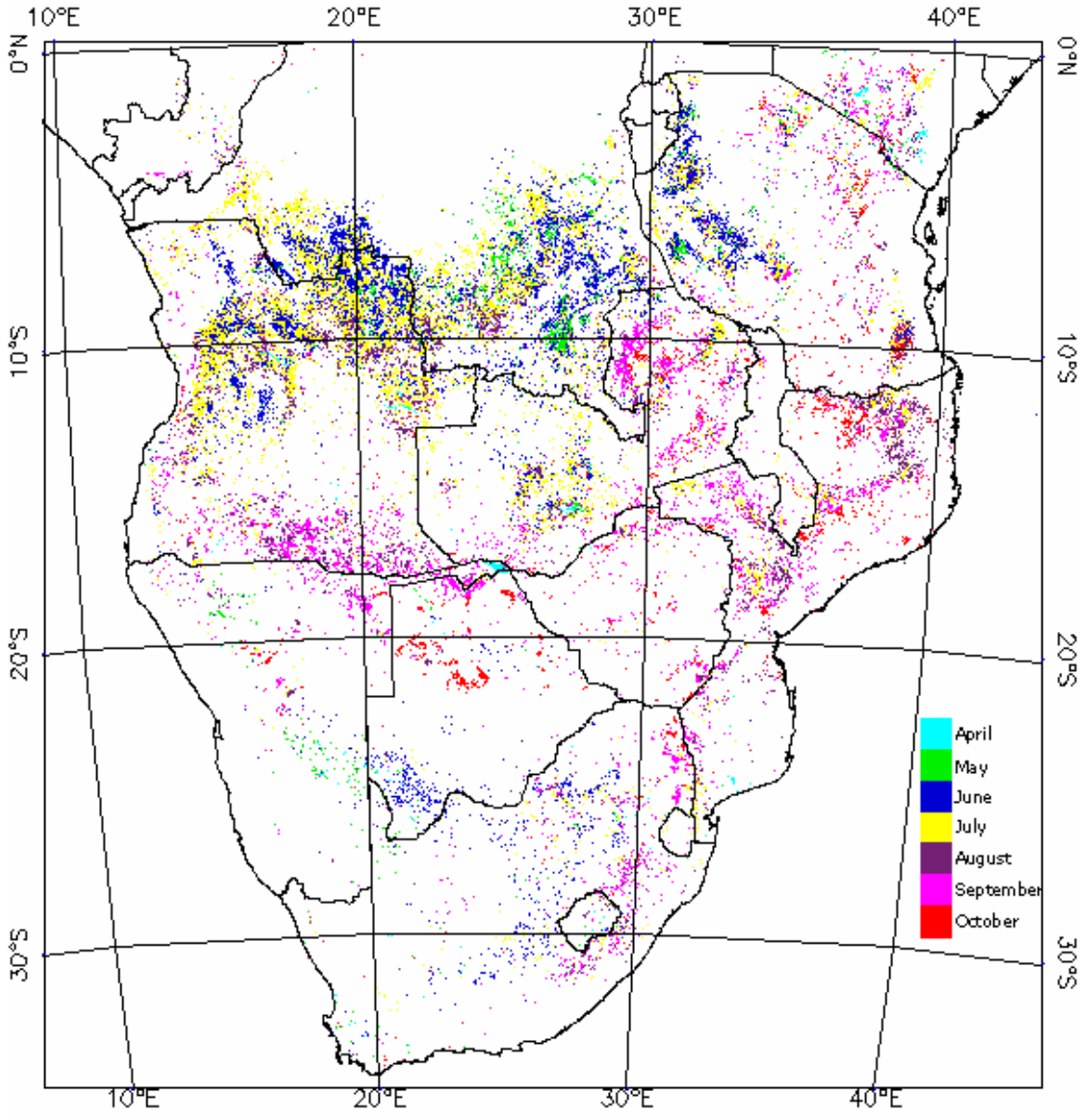

Figure 4. Seasonal spatial distribution of GBA-2000 burned area in southern Africa.

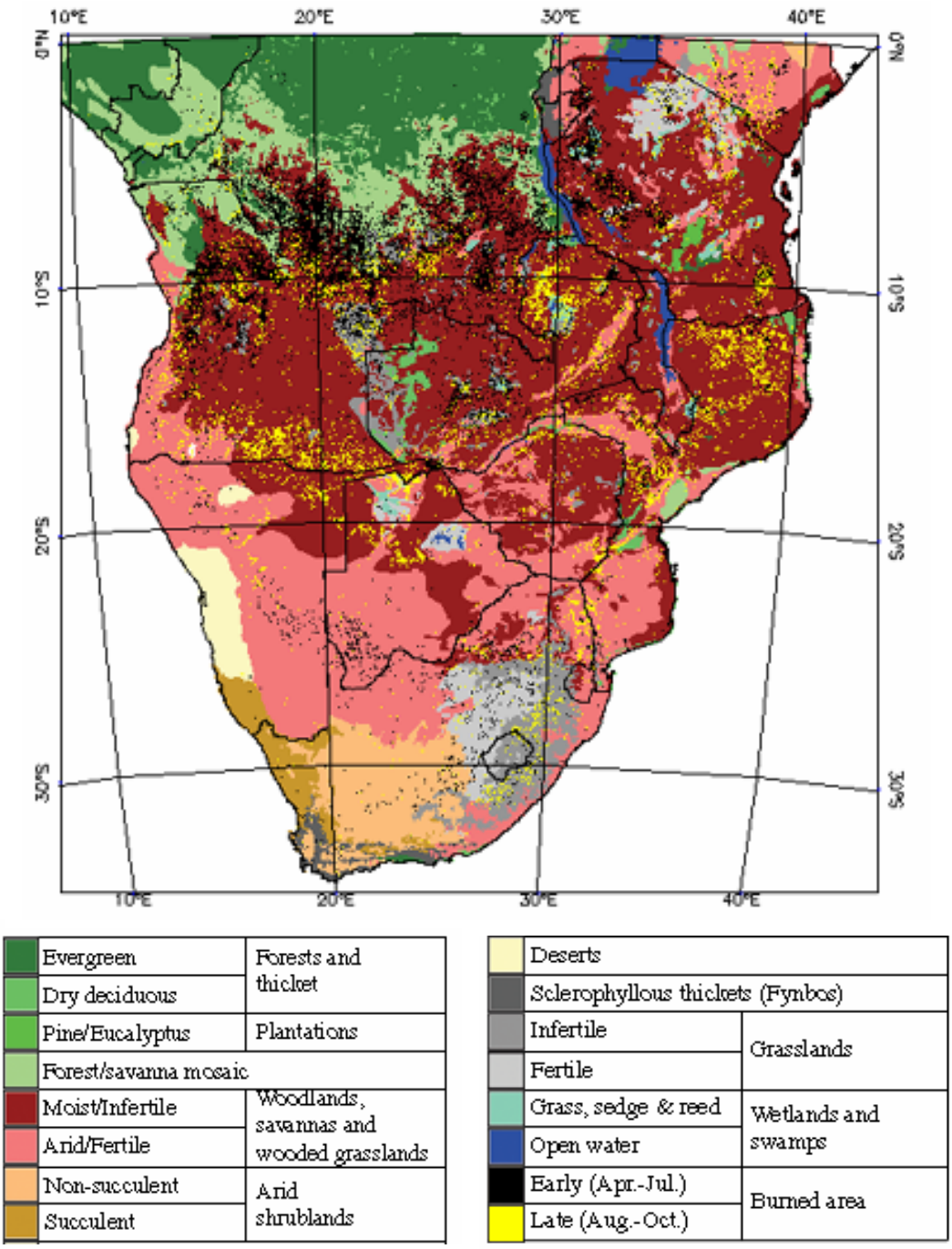

Figure 5. Early and late dry season GBA-2000 burned area overlayed on a fire regime map by Scholes *et al.* (1996b) for major vegetation types in southern Africa.

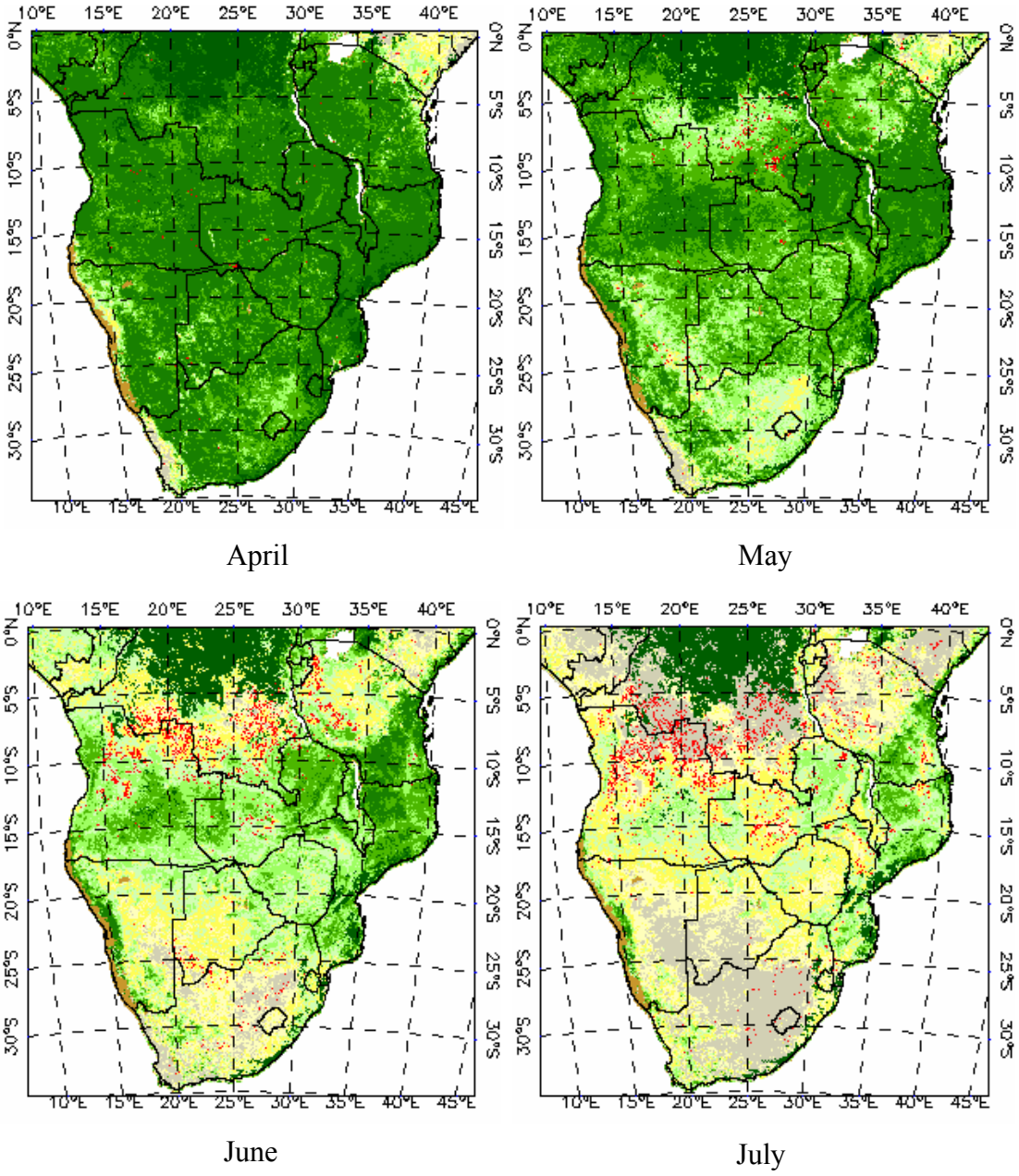

Figure 6. NDVI-based PGREEN showing the seasonal drying out of vegetation in the 2000 dry season in southern Africa. The monthly distribution of the GBA-2000 burned area, shown in red dots, is overlayed on the PGREEN maps. Dark green = NDVI-based evergreen mask, brown = NDVI-based desert mask.

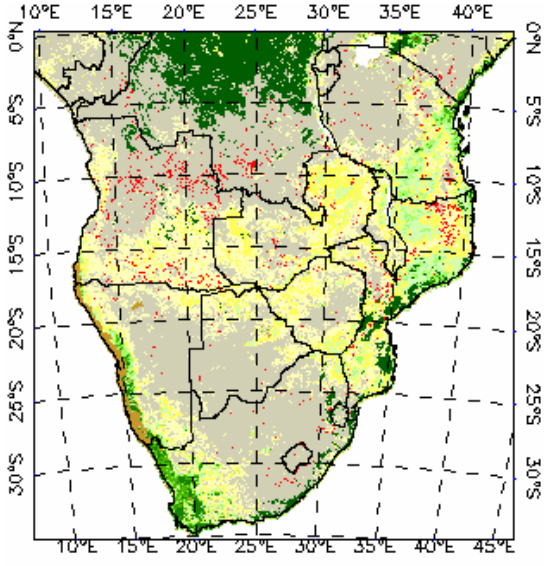

August

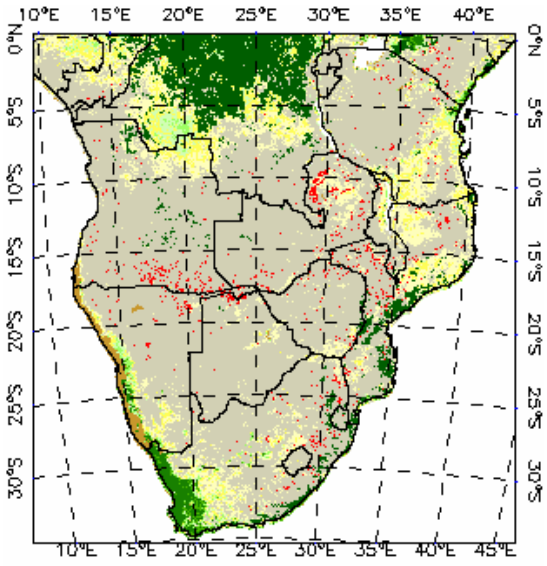

September

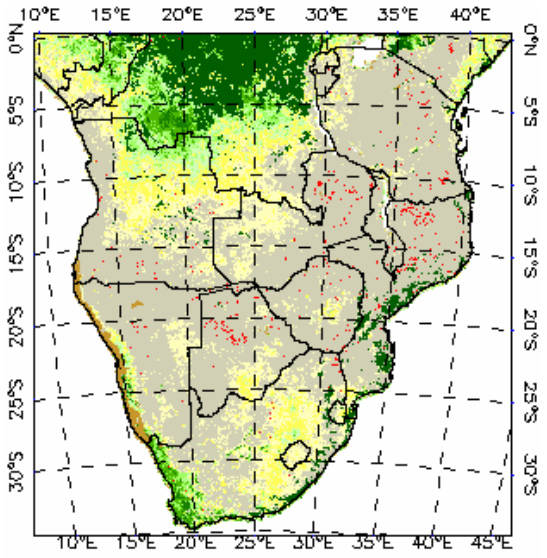

October

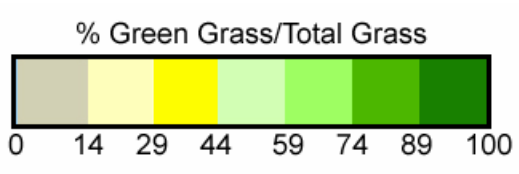

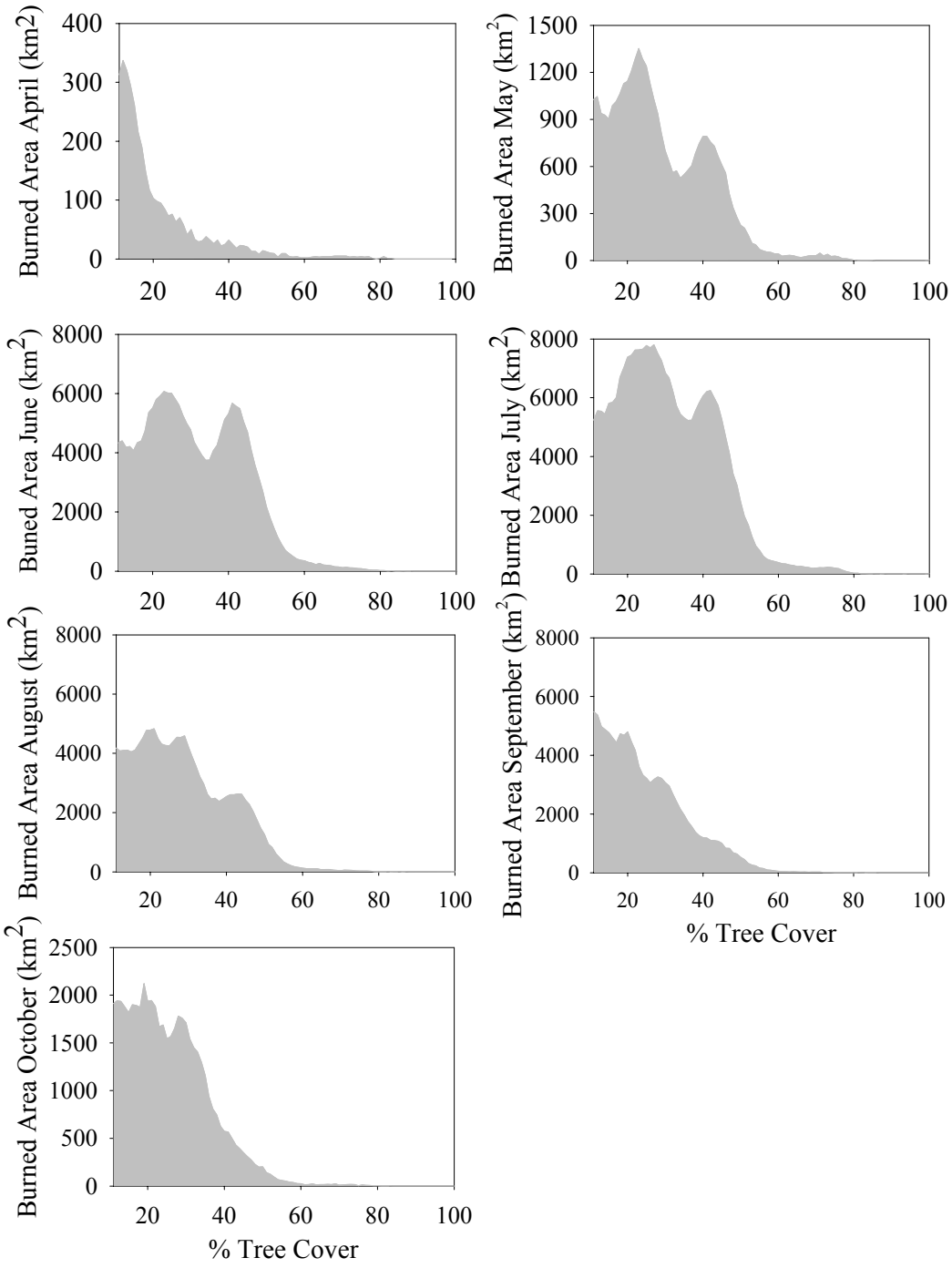

Figure 7. Seasonal distribution of the GBA-2000 burned area as a function of percent tree cover in southern Africa, 2000.

5.3.1.2 MODIS Burned Area Extrapolation

Table 2 summarizes the quantitative intercomparison of the MODIS and GBA-2000 burned areas in July. MODIS maps about 42% more burning than GBA-2000 in July, similar to the 55% difference found in September (Chapter 4, Table 1). Woodland burning accounts for 87% of the total area burned in July in MODIS, similar to the 85% in GBA-2000 for the same month. Comparable amounts are mapped for grasslands in the two burned area products in both July and September. The distribution of the MODIS burned area in July as a function of PTC (Figure 8) resembles that of GBA-2000 for the same month. Similar distribution between MODIS and GBA-2000 are also found for September (Chapter 4). Based on the MODIS extrapolation from GBA, approximately 1,543,000 km^2 burned in southern Africa in the 2000 dry season (Table 3).

Table 2. Comparison of MODIS and GBA-2000 burned areas in woodlands and grasslands for July 2000.

Burned Area (km^2 x 10^3)	*Grasslands*	*Woodlands*	*Regional*
MODIS	56.7	366.8	423.5
GBA-2000	44.9	253.6	298.5

Table 3. MODIS extrapolated regional burned area, April-October, 2000.

Burned Area (km^2 x 10^3)	*Grasslands*	*Woodlands*	*Regional*
Early	146.6	708.7	855.3
Late	143.9	543.4	687.3

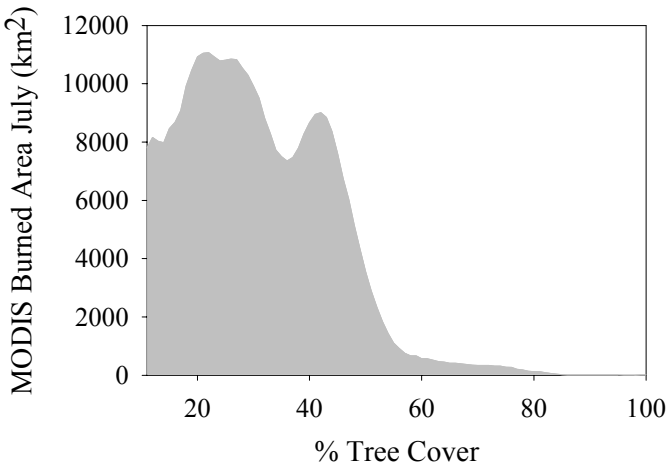

Figure 8. MODIS burned area distribution as a function of percent tree cover in southern Africa, July 2000.

5.3.2 Grassland and Woodland Seasonal Regional Emissions

5.3.2.1 Grassland Fires

The patterns of temporal change in regional average PGREEN in grasslands are illustrated in Figure 9a. Whereas, both the NDVI-based and the fuel load-based methods for PGREEN estimation predict the seasonal curing of the fuel, the NDVI-based method predicts generally higher regional average PGREEN values. The two methods differ mostly in the early dry season and converge as the dry season progresses. The NDVI-based PGREEN values are in good agreement with the limited number of seasonal field measurements in Western Province, Zambia for the average rainfall year of 1996 (Hoffa *et al.*, 1999) (Table 4). Mean annual rainfall at the study sites of Hoffa *et al.* (1999) ranges between 900-1000 mm/yr. Considering that the majority of burning in the region for 2000 occurs north of the Hoffa *et al.* (1999) sites, in the wet miombo region between 5^{o}S and 15^{o}S, that receives comparatively more rainfall (Chapter 1, Figure 1), it appears that in general, the fuel load-based method under-predicts the presence of green grass in the fuel mixture.

In both the NDVI-based and the fuel-load based methods, seasonal increases of combustion completeness are observed in grasslands (Figure 9b). This is consistent with field observations of higher consumption of the fully cured fine grassy fuel by the end of the dry season (Shea *et al.*, 1996; Trollope *et al.*, 1996; Stocks *et al.*, 1996). Overall, the NDVI-based and fuel load-based combustion completeness increases seasonally by a factor of 2 and 1.3, respectively. Differences in the PGREEN between the two methods affect considerably the estimation of the combustion completeness. The NDVI-based method predicts lower combustion completeness compared with the fuel load-based method until about August. After this, both methods predict similar combustion completeness. The maximum difference in combustion completeness between the fuel load-based and the NDVI-based methods is found in May (about 82%).

Table 4. Comparison of field-derived PGREEN (Hoffa *et al.*, 1999) with the average regional NDVI-based and fuel load-based modeled values of PGREEN for grasslands (G) and woodlands (W).

Month	*Hoffa et al* (G)*	*NDVI-based (G)*	*Fuel load-based (G)*	*Hoffa et al.* (W)*	*NDVI-based (W)*	*Fuel load-based (W)*
June	37	34	12	32	38	15
July	26	25	8	24	21	7
August	20	15	4	-	-	-

* Average of the measurements taken within the specific month

The amount of biomass burned in grasslands increases considerably from April to September (by about 15 times in the NDVI-based method and 10 times in the fuel load-based method). This is generally expected, as late dry season fires are likely to be larger and more intense than in the wet or early dry season, since more dry fuel load is available, and because the often hot and windy conditions cause fires to spread more easily and make them difficult to control (Frost, 1996). The amount of biomass burned

drops in October (Figure 9c) driven by a commensurate drop in burned area (Figure 9e). This reduction may be because by that time, at the regional level, lesser quantities of biomass are left over to promote large fires, and perhaps because of the onset of wet season rainfall. Litter constitutes less than 6% in the areas classified as grasslands in this study, thus the fuel loads consist mostly of grass. Seasonal variations in the pre-fire grass fuel loads in the locations that burn are negligible at the regional scale (323-379 gm^{-2}) (Figure 9d). Therefore, the increasing biomass burned from April to September is essentially due the increasing burned area (by a factor of 6, approximately) (Figure 9e), and to a lesser extent due to the increasing combustion completeness (Figure 9b). Despite the high combustion completeness in October, the biomass burned declines because of the smaller area affected by fires. The amount of biomass burned in grasslands is 31.5 Tg and 42.5 Tg during the early and late dry season, respectively, in the fuel load based method. In the NDVI-based method, 23.8 Tg and 41.7 Tg of biomass is burned in the dry and late dry season, respectively. The differences observed in biomass burned between the NDVI-based and fuel-load based methods, are solely due to the differences in combustion completeness.

Emission factors (EF) for CO_2 increase seasonally because of the higher oxidation of the progressively drier predominantly grass fuels (Figure 10a). Emission factors for products of incomplete combustion, (*e.g.*, CO and CH_4) are significantly higher in the early dry season when the fuel is moister (Figures 10b-c). EFCO are higher by a maximum factor of 2.6 and 1.8 in the NDVI-based and fuel load-based methods, respectively. $EFCH_4$ are higher by a maximum factor of 3.9 and 2.4 in the NDVI-based and fuel load-based methods, respectively. The NDVI-based average regional MCE for

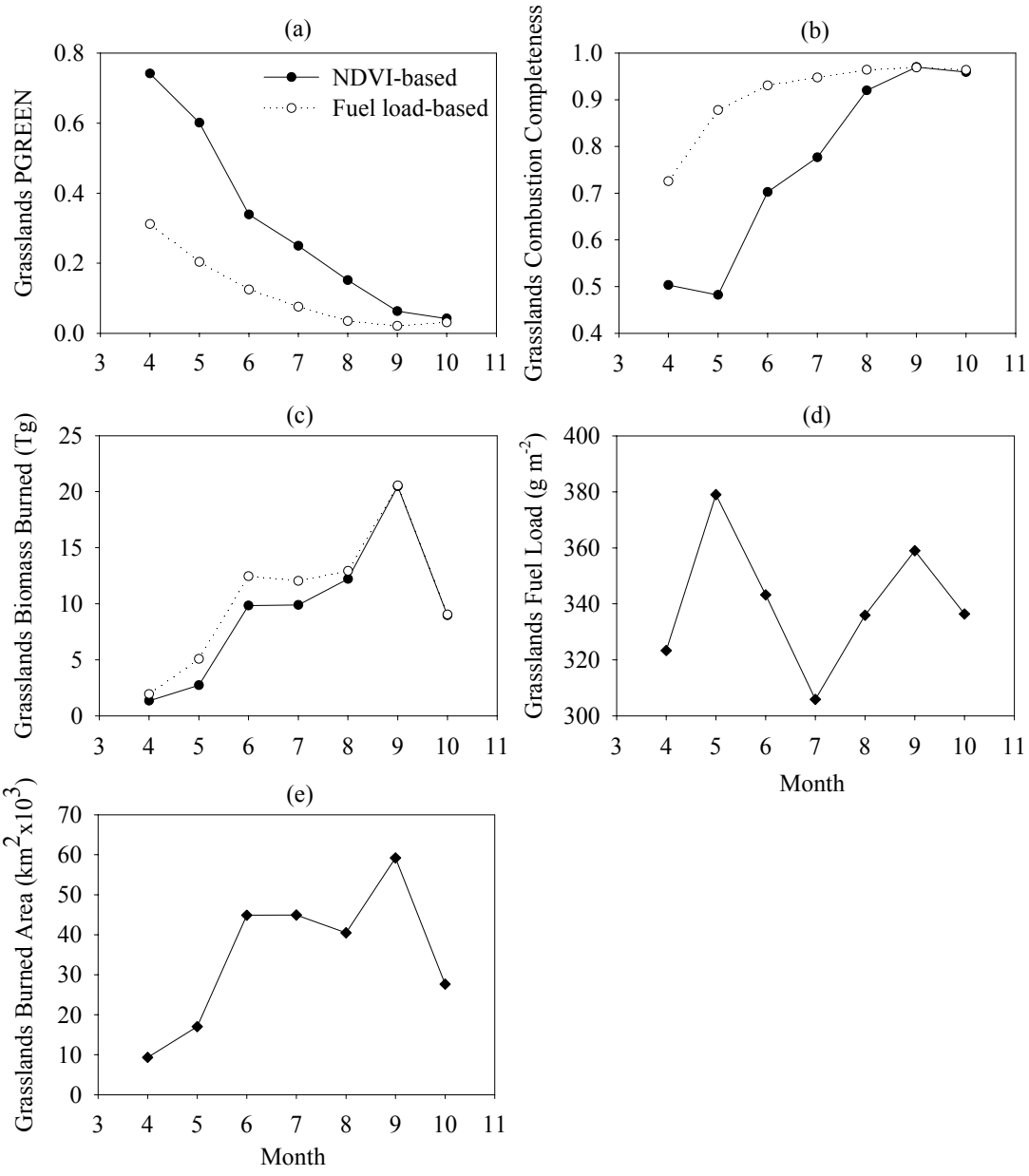

Figure 9. Seasonal regional trends for grassland burned areas in a) average PGREEN, b) average combustion completeness c) total biomass burned d) average fuel load and e) total burned area using GBA-2000.

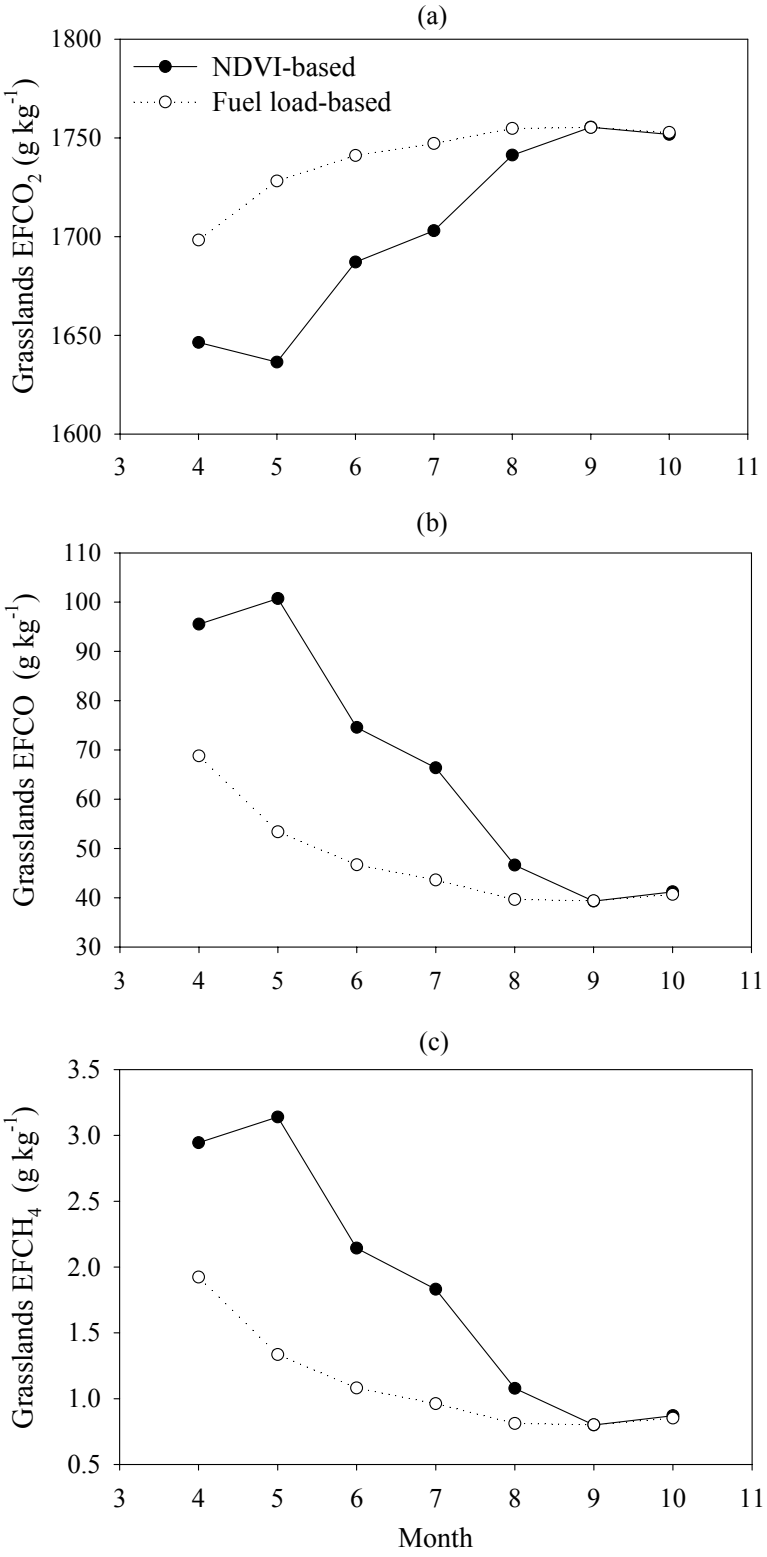

Figure 10. Seasonal progression for grassland fires of regional average emissions factors for a) CO_2, b) CO and c) CH_4, using GBA-2000.

grassland fires is lowest in May (0.912±0.020) and highest in September (0.966±0.029). These values are comparable with field measurements of MCE (see Chapter 3; Yokelson *et al.*, 2003). In general, the fuel load-based method predicts higher MCE values compared with the NDVI method since the fuel is relatively dry throughout the dry season. The average regional MCE is lowest in April (0.940±0.027) and highest in September (0.966±0.029). The increased greenness predicted in the NDVI-based method compared with the fuel load-based method, especially during the early dry season, amplifies the emission factors for products of incomplete combustion. Due to the similar PGREEN values for September and October between the NDVI-based and the fuel load-based methods similar emission factors are predicted (Figure 10a-c).

A summary of the maximum differences found between early and late dry season grassland emission factors for all species is presented in Tables 5-6 (Appendix C) for the fuel load and NDVI methods, respectively. The differences among atmospheric compounds originate from the fact that they are emitted in various proportions in the smoke mixture (Chapter 3, Chapter 4). The modeled results are consistent with the emission factor measurements for grassland fires in Chapter 3, which showed that higher emission factors for products of incomplete combustion and simultaneously lower emission factors for products of complete combustion are more likely to occur in the early dry season compared than later in the dry season.

The following exception should be noted. In this study, early dry season emission factors for NOx (3.25 g kg^{-1} and 3.41 g kg^{-1} in the fuel load- and NDVI-based method, respectively) are higher than in the late dry season (3.10 g kg^{-1} in the fuel load- and NDVI-based method, respectively). Laboratory studies have indicated that NO_x is

preferentially released during flaming combustion (Lobert and Warnatz, 1993; Andreae and Merlet, 2001). This implies that the opposite of the relationship found here between early and late dry season EFNOx should occur, since late dry season burns are more efficient. The EFNOx modeled here are based on airborne measurements by Sinha *et al.*, 1996 and are poorly correlated with MCE. It is known, that $EFNO_x$ are linearly related to the nitrogen content of the fuel (Lacaux *et al.*, 1996; Kuhlbush *et al.*, 1996). The nitrogen content of the fuels may vary considerably in space and time, as a function of rainfall, land use, fire regime and vegetation type (Lacaux, *et al.*, 1996; Kuhlbusch *et al.*, 1996; Feral *et al.*, 2003). Considering that fire is a primary mechanism of nitrogen loss in the moist, nutrient poor savannas (Figure 4), future efforts in regional emissions modeling should be allocated to developing the underlying spatially and temporally explicit regional databases of fuel nitrogen content.

When the fuel is sufficiently wet, early burning in grasslands tends to involve more smoldering combustion compared with the late dry season. This is supported by the results tabulated in Table 7 which show regional emission densities (defined as the total emissions/total burned area). The regional average CO_2 emission densities increase from 350 gm^{-2} and 476 gm^{-2} and in the early dry season to 576 gm^{-2} and 590 gm^{-2} in the late dry season for the NDVI and fuel load based-methods, respectively. The regional average CO and CH_4 emission densities for grassland fires decrease from 12.6 gm^{-2} and 0.34 gm^{-2} in the early dry season to 11.7 gm^{-2} and 0.22 gm^{-2}, respectively, in the NDVI-based method. In the fuel load-based method the corresponding differences between early and late dry season fires are lower, or even slightly reversed, because mostly dry grass is predicted. CH_4 emission densities decrease from 0.22 gm^{-2} to 0.19g m^{-2}, whereas a slight

increase is predicted in CO emissions densities from 10.8 gm^{-2} to 11.1 gm^{-2}. The hypothesis by Hoffa *et al.* (1999) that early dry season burning will have a different effect on the quantity and type of emissions from grassland fires compared with late dry season fires is partially substantiated by the NDVI-based large scale, regional results. However, what is important to note here, is that these trends will depend on the seasonal moisture changes of the grass fuel and will likely vary from year to year at the regional scale. So, in dry seasons where the grass fuels are relatively dry for the most part of the dry season, emission densities are expected to be more similar seasonally.

Table 7. Fuel load- and NDVI-based average regional emission densities (emissions/burned area) in (gm^{-2}) for early (April-July) and late dry season grassland fires using GBA-2000.

Emission Densities	*Early Fuel-load*	*Late Fuel-load*	*Early NDVI*	*Late NDVI*
CO_2	476	590	350	576
CO	10.8	11.1	12.6	11.7
CH_4	0.22	0.19	0.34	0.22

The seasonal progression of regional emission from grassland fires is illustrated in Figures 11a-c. Seasonal emissions follow somewhat similar trends to the biomass burned (Figure 9c). In general, there is a trade-off between lower amounts of biomass burned and higher emission factors for products of incomplete combustion in the early dry season and between higher amounts of biomass burned and lower emission factors for products of incomplete combustion in the late dry season. Therefore, the significant seasonal fluctuation in biomass burned is dampened by the counteracting effect of the emission factors for products of incomplete combustion and is slightly accentuated by the similar effect of the emission factors for products of complete oxidation. As a result, CO_2 emissions increase from April to September by about 16 and 11 times in the NDVI-based

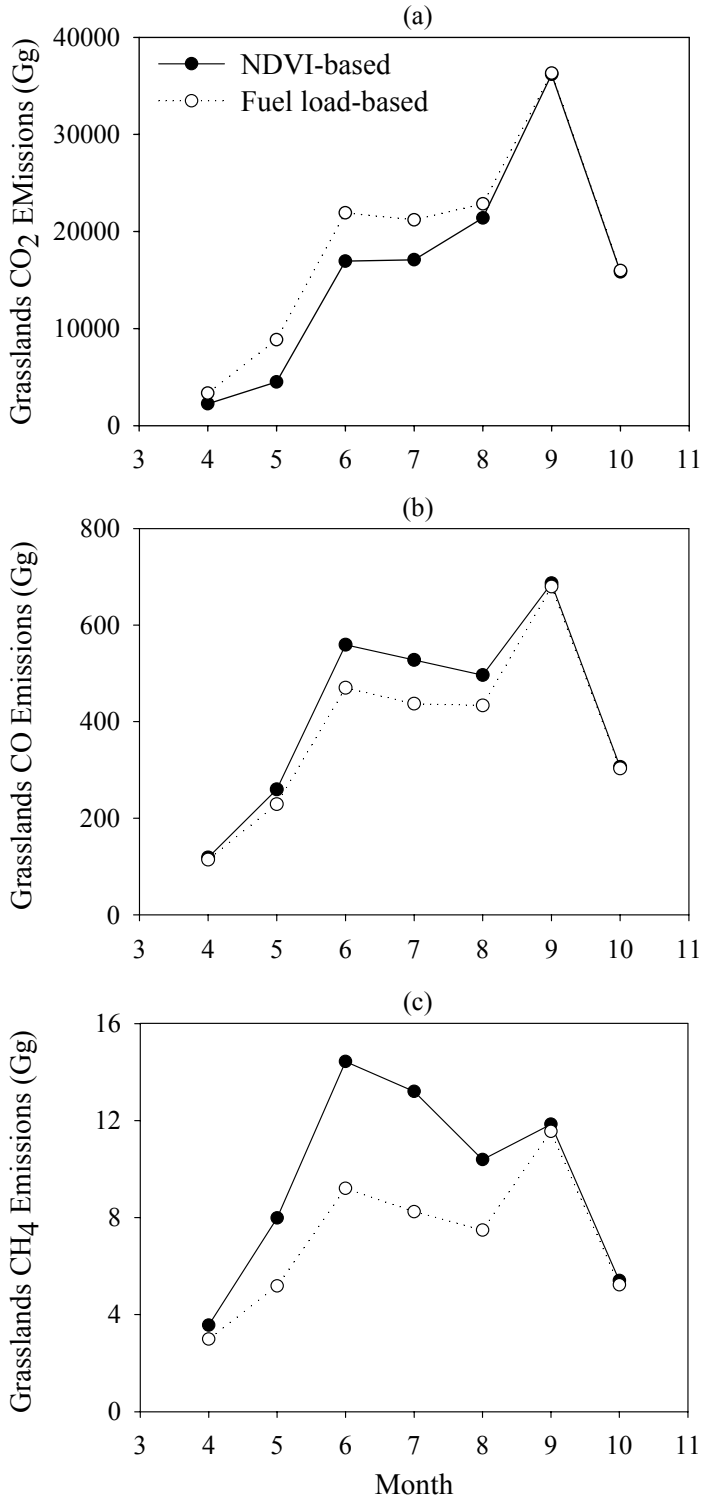

Figure 11. Seasonal progression for grassland fires of a) CO_2, b) CO and c) CH_4, using GBA- 2000.

and fuel-load based methods, respectively (Figure 11a). For the same time period, CO emissions increase by about 5.8 and 6 times, for the two methods, respectively (Figure 11b). In the fuel load-based method, CH_4 emissions increase by 3.9 times from April to September (Figure 11c). In the NDVI method, the peak of CH_4 emissions is shifted to earlier in the season (June) relative to the peak in biomass burned, because of the large impact of the increased emission factor for CH_4.

Despite the lower amounts of biomass burned in the NDVI-based method compared with the fuel load–based method (Figure 9c) in the early dry season, higher quantities of the products of incomplete combustion are predicted (Figures 11b-c). This suggests that at the regional scale, the effect of increased moisture content on lowering MCE and the resulting effect on emission factors for products of incomplete combustion is greater than the effect of moisture content on combustion completeness. Furthermore, it indicates that burning in wetter grass fuel tends to involve more smoldering combustion. The NDVI-based CO emissions are slightly higher than the fuel load model-based CO emissions mostly during June-July (about 20%) (Figure 11b). A more pronounced difference, is seen in CH_4 emissions between the two methods mostly in the early part of the dry season, reaching a maximum of 60% difference in July (Figure 11c). The NDVI-based CO_2 emissions are lowered in the early dry season compared with the corresponding fuel load- based ones by a maximum of 49% in May (Figure 11a).

5.3.2.2 Woodland Fires

Similar seasonal patterns are observed in the regional average PGREEN in woodlands, as in grasslands (Figure 12a). In both the NDVI-based and the fuel load-

based methods, there is a seasonal decrease in PGREEN. Here again, higher levels of grass moisture are predicted by the NDVI-based method compared with the fuel load-based method. The discrepancy in PGREEN between the two methods decreases seasonally. A higher level of agreement is found between the NDVI-based PGREEN values in woodlands and the seasonal field measurements in Western Province, Zambia, by Hoffa *et al.* (1999) compared with the fuel load based method (Table 4).

The combustion completeness for woodlands also follows a seasonal gradient of progressively increasing values (Figure 12b). The regional average fraction of fuel consumed in the late dry season is higher by a maximum of 23 and 2.6 times, in the NDVI- and the fuel load-based methods, respectively, compared with the early dry season. The very large seasonal difference between the two methods is clearly because of the higher greenness levels predicted by the NDVI-based method. The combustion completeness in woodlands in the early dry season in this model is parameterized using the relationships established empirically by Hoffa *et al.* (1999). Considerable uncertainty remains in the evaluation of combustion completeness in woodlands, especially during the early dry season. For example, in the Hoffa *et al.* (1999) study, burns that were conducted 12 days apart showed a 22-fold difference in combustion completeness. This was mostly due to heterogeneity in the fuel loadings and moisture. Clearly, a larger number of early dry season studies, in woodlands with diverse vegetation structure and fuel characteristics are needed to improve characterization of the fuel consumption process.

Similar trends are observed in the biomass burned in both methods from April to July (Figure 12c). The biomass burned increases dramatically, by 264 and 183 times in

the NDVI- and the fuel load-based methods, respectively. Variations in pre-fire fuel load reflect the increasing leaf litter fall as the dry season progresses, but they do not influence the biomass burned significantly, since the overall range is between 281 and 343 gm^{-2} (Figure 12d). The dramatic increase in biomass burned from April to July is principally due to the significant increase in burned area (Figure 12e) and to a lesser extent due to the increasing combustion completeness in the fuel load-based method (Figure 12 b). From May to July the increase in combustion completeness becomes more significant than the increase in burned area in the NDVI-method. After July, the amount of biomass burned steadily drops for the remainder of the dry season in the fuel load-based method. This is caused by the minor proportional increase in combustion completeness (about a factor of 1.1) relative to the large decrease in burned area (about a factor of 4.9), from July to October (Figure 12e). A different pattern in the biomass burned is seen in the NDVI-based method. After July, the biomass burned remains at similar levels until September and then declines in October. In this case, the impact of the decreasing burned area from July to September (by a factor of 2.2) offsets the simultaneous increase in combustion completeness (by a factor of 1.9). About 103 Tg and 87.5 Tg of biomass is burned in woodlands in the early and late dry season, respectively, in the fuel load based method. In the NDVI method 38.0 Tg and 70.4 Tg of biomass is burned during the early and late dry season, respectively.

Emission factors for fully oxidized products, such as CO_2, decrease initially until June and generally increase afterwards (Figure 13a). As expected, the inverse happens

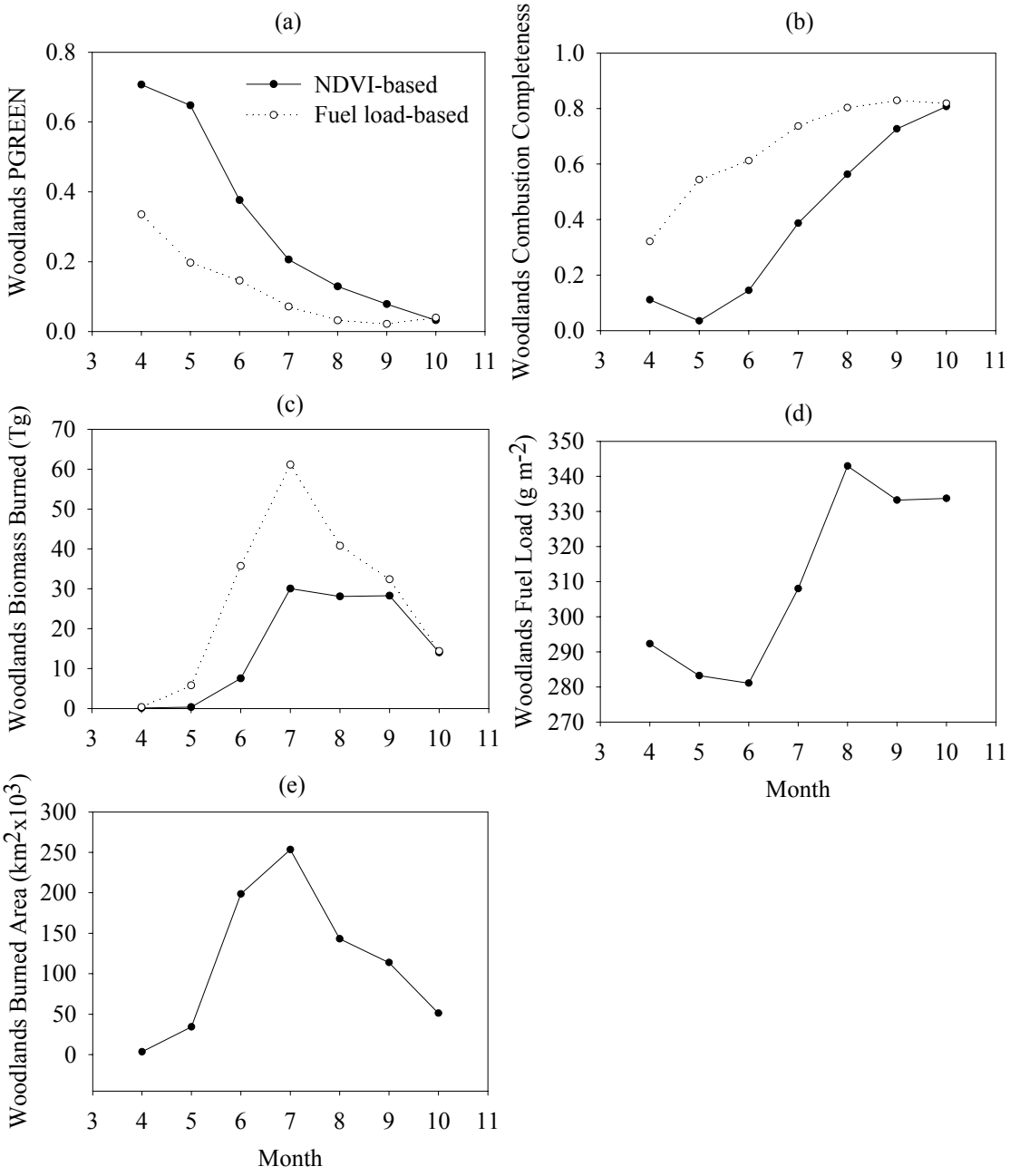

Figure 12. Seasonal regional trends in woodland burned areas of a) average PGREEN, b) average combustion completeness c) total biomass burned d) average fuel load and e) total burned area using GBA-2000.

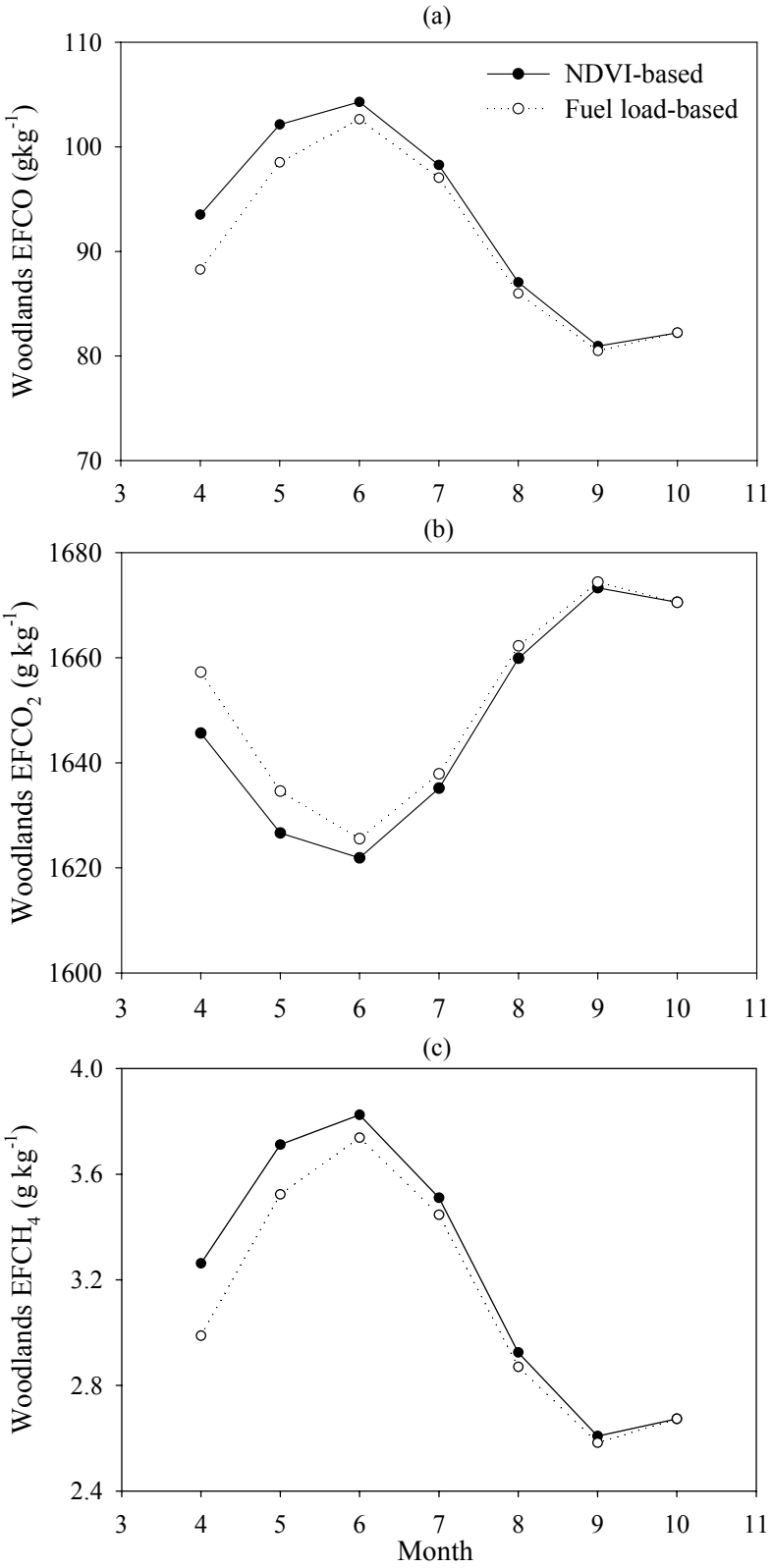

Figure 13. Seasonal progression of emissions factors for a) CO_2, b) CO and c) CH_4 for woodland fires.

with emission factors for products of incomplete combustion Figures 13b-c. Emission factors of CO are higher by 29% and 28% in June compared with September, in the NDVI and fuel load-based methods, respectively. The corresponding differences in the emission factors for CH_4 are 47% and 45%. The MCE for woodland fires in the NDVI-based method ranges from 0.908±0.027 in June to 0.929±0.021 in September. The MCE for woodland fires in the fuel load-based method ranges from 0.910±0.029 in June to 0.930±0.021 in September. Tables 8-9 (Appendix C) summarize the maximum variations between early and late dry season emission factors for the two methods. The fuel load and the NDVI-based methods provide similar values and differences in emission factors between early and later dry season woodland fires. Emission factors for NO_x are correlated with CO_2 and therefore, a higher NO_x in September than in June is anticipated. As with grasslands, the opposite occurs here, and it may be attributed to the same reasons discussed in Section 5.3.2.1.

Woodland emission factors are determined by the fuel composition. As seen in Figure 14, the proportion of twigs and litter in the fuel mixture increases gradually from April through June, relative to the grass fuels, providing a lower MCE. The increasing burning in more closed canopy woodland in this period, discussed in Section 5.3.1.1, is perhaps related to this fuel composition trait. After June, the proportion of the twigs drops whereas, the proportion of dry grass increases, thus providing a more efficient burn. This is consistent with field measurements (Ward *et al.*, 1996). Emission factors for products of incomplete combustion for early and late dry season woodland fires are higher than the corresponding emission factors for grassland fires (Tables 5-6 and 8-9, Appendix C), due to the more smoldering combustion of the litter and twigs

material. As mentioned in Section 5.2.2, a shortcoming in the MCE relationship is that it does not account for moisture-driven seasonal changes in the flaming versus smoldering combustion of the litter and twigs.

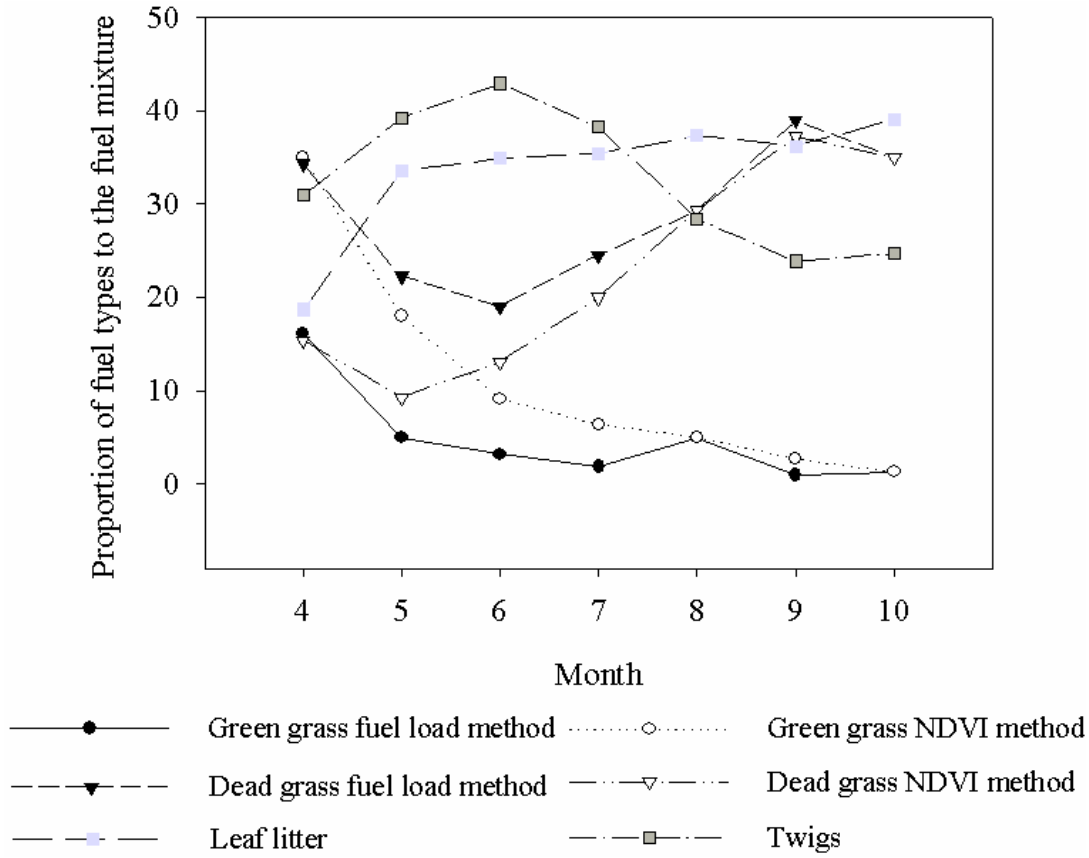

Figure 14. Seasonal average composition of the fuel mixture in woodlands.

When comparing the emission factors predicted by the NDVI- and the fuel load-based method, it appears that the increased greenness does not significantly affect emission factors in woodlands (Figures 13a-c). For example, the maximum difference in emission factors for CH_4 occurs in April and is only 9%. However, the impact of the increased greenness on emission factors is obscured by the seasonal changes in the fuel

composition (Figure 14). To demonstrate this, four scenarios are examined, ranging from low to high litter and twigs. Figure 15 displays the emissions factor of CH_4 as a function of the percent green grass for these scenarios. The CH_4 emission factor is more sensitive to the presence of green grass when the contribution of the twigs and litter to the fuel mixture is low. Depending on the PGREEN, the CH_4 emission factor can vary by more than a factor of 2 at low litter and twigs proportions in the fuel mixture, whereas, there is negligible variation at high proportions of litter and twigs in the fuel mixture. The MCE for the scenario of low litter and twigs (Plitter = 0.05 and Ptwigs = 0.05) ranges from 0.930 to 0.957. Emission factors for other products of incomplete combustion besides CH_4, may vary to different degrees according to this MCE range.

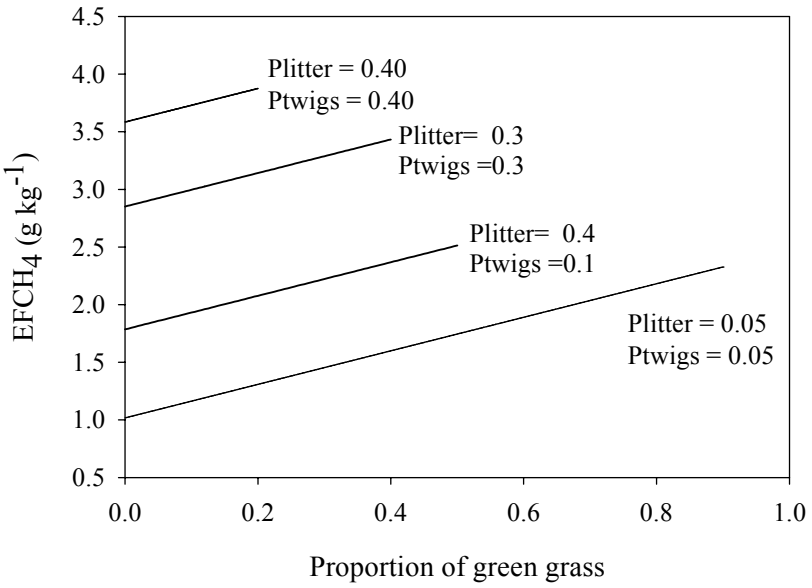

Figure 15. Variation in CH_4 emission factors as a function of proportion of the green grass for different fuel mixture scenarios. The dry grass proportion is not shown; at each graphed point the dry grass, green grass, twig and litter fuel proportions sum to unity (Equation 5.6).

The seasonal dynamics of regional emissions from woodland fires are illustrated in Figures 16a-c. Similar trends are observed as for the biomass burned (Figure 12c). In the early dry season, the increase in emissions of the products of incomplete combustion is proportionally higher to that of the biomass burned because of the higher emission factors, compared with the late dry season. Early burning in woodlands generally releases lower amounts of trace gases compared with the late dry season (Table 10). The differences between early and late dry season emission densities are more pronounced in the NDVI method due to increased greenness. The regional average CO_2 emission densities increase from 128 gm^{-2} and 350 gm^{-2} in the early dry season to 384 gm^{-2} and 478 gm^{-2} in the late dry season for the NDVI- and fuel load based-methods, respectively. The regional average CO and CH_4 emission densities increase from 6.9 gm^{-2} and 0.24 gm^{-2} in the early dry season to 17.5 gm^{-2} and 0.55 gm^{-2}, respectively, for the NDVI-based method. The regional average CO and CH_4 emission densities increase from 17.9 gm^{-2} and 0.59 gm^{-2} in the early dry season to 21.6 gm^{-2} and 0.67 gm^{-2}, respectively, for the fuel load-based method. These results indicate, that the effect of increased moisture content in the early dry season on lowering the combustion completeness is greater than the effect of moisture content on MCE, and thus on emission factors for products of incomplete combustion. This is the opposite of what was found for grassland fires. These results also suggest that the effect of greenness on emissions is more significant for woodlands than for grasslands (Tables 7 and 10).

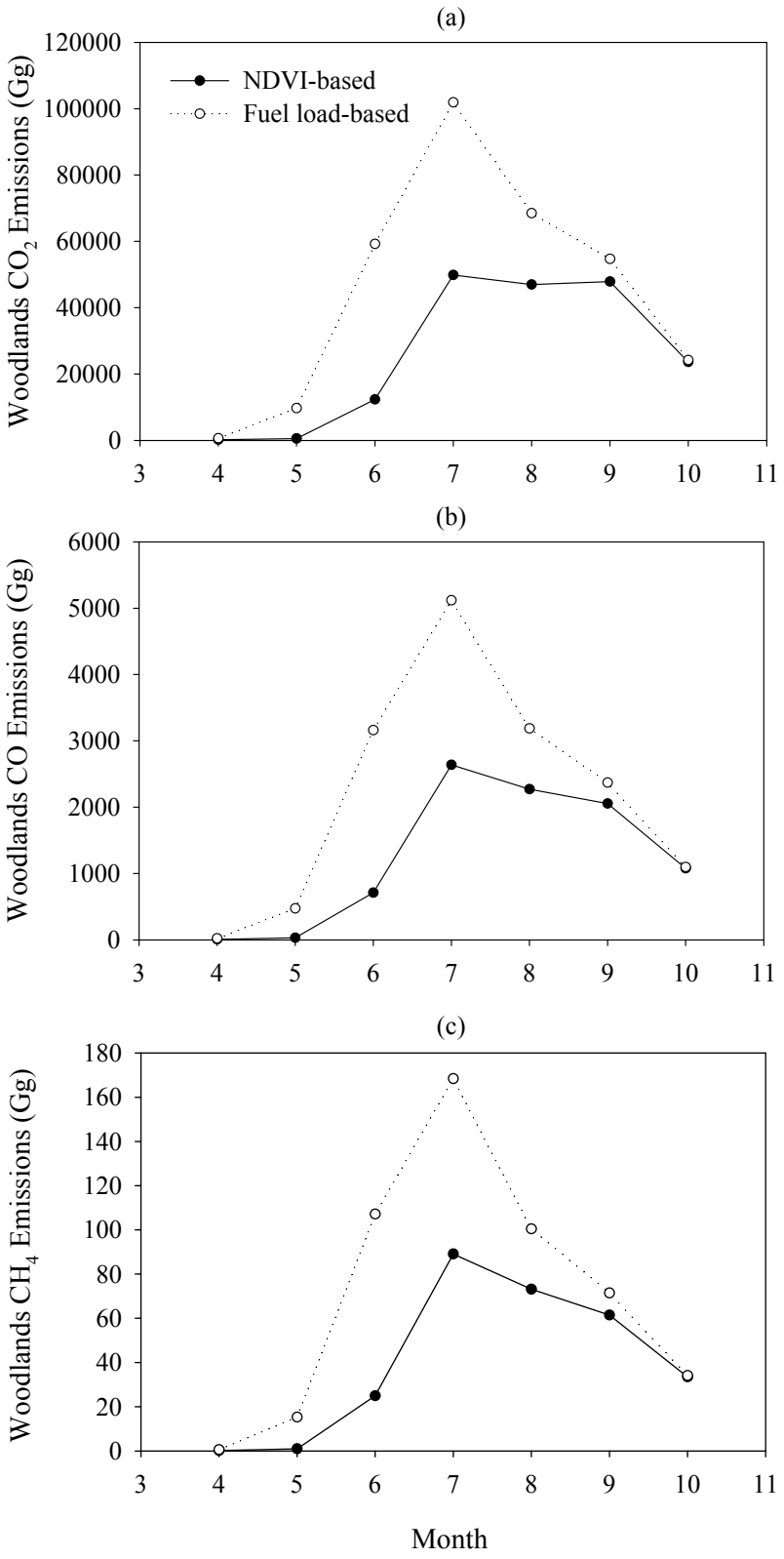

Figure 16. Seasonal progression of regional emissions of a) CO_2, b) CO and c) CH_4 from woodland fires.

Table 10. Fuel load- and NDVI- based average regional emission densities (emissions/burned area) in (gm^{-2}) for early (April-July) and late dry season woodland fires using GBA-2000.

Emission Densities	*Early Fuel-load*	*Late Fuel-load*	*Early NDVI*	*Late NDVI*
CO_2	350	478	128	384
CO	17.9	21.6	6.9	17.5
CH_4	0.59	0.67	0.24	0.55

5.3.2.3 Seasonal Regional Emissions

5.3.2.3.1 Regional Biomass Burned

A total of 265 Tg of biomass is estimated to have burned in 2000 using the fuel load-based method, half of which burned during the early dry season. A total of 174 Tg of biomass is estimated to have burned using the NDVI-based method, 36% of which burned during the early dry season. The largest fraction of biomass burned in southern Africa occurs in woodlands, 72% and 62% in the fuel load- and NDVI-based methods, respectively. The difference in biomass burned between the two methods reflects the effect of increased grass moisture on combustion completeness.

5.3.2.3.2 Regional Emissions

The GBA-2000-based early and late dry season emissions from grassland and woodland fires in southern Africa are summarized in Tables 11 and 12 (Appendix C) for the fuel load and NDVI methods, respectively. Lower average emissions per unit area result from burning during the early dry season for all atmospheric species because woodland fires constitute the majority of the regional budgets. The average regional emission densities for CO_2, CO and CH_4, respectively, increase from 171 gm^{-2}, 8.0 gm^{-2} and 0.25 gm^{-2} in the early dry season to 439 gm^{-2}, 15.8 gm^{-2} and 0.45 gm^{-2} in the late dry

season, in the NDVI- based method. These differences are much smaller in the fuel load-based method since the grass fuel is predicted to be relatively dry even during the early dry season. The average emission densities for CO_2, CO and CH_4, respectively, increase from 374 gm^{-2}, 16.5 gm^{-2} and 0.52 gm^{-2} in the early dry season to 511 gm^{-2}, 18.5 gm^{-2} and 0.53 gm^{-2} in the late dry season, in the fuel load-based method. At the regional level, the fuel load-based emissions estimates are 52-61% higher than the corresponding NDVI-based emissions. These results suggest that the wetness of the fuel significantly affects emissions but contest the hypothesis by Hoffa *et al.* (1999) that incorporation of early season burning will increase the estimates of products of incomplete combustion.

The MODIS July and September emissions for grasslands and woodlands using the fuel load and NDVI methods for PGREEN are summarized in Tables 13 and 14 (Appendix C), respectively. It should be noted that the differences in the September MODIS woodland emissions between the fuel load method presented here and the results presented in Chapter 4 (Table 4, Appendix B) are solely due to the different MCE relationships used. In general, there is good agreement between these two approaches to deriving the MCE. There is practically no difference in the CO_2 and NO_X emissions from woodland fires. The emissions for products of incomplete combustion from woodland fires presented here are on average lower by 13%. The MODIS-based extrapolated annual regional emissions are summarized in Table 15 (Appendix C) and annual emissions by country are shown in Table 16. Based on the MODIS extrapolation, about 316 Tg of biomass was consumed from vegetation fires in southern Africa in the 2000 dry season. It is estimated that these fires released approximately 537 Tg of CO_2, 23.2 Tg

of CO, 726 Gg of CH_4, 661 Gg of NMHC, 2.4 Tg of PM2.5 and 1.0 Tg of NOx. Especially high is the previously undetermined contribution of OVOCs (1.8 Tg).

Table 16. Vegetation fire emissions and burned area in African countries south of the equator for the 2000 dry season, based on the MODIS extrapolation.

Country	*Burned Area* ($10^3 xkm^2$)	*CO_2* (Tg)	*CO* (Gg)	*CH_4* (Gg)	*NMHC* (Gg)	*PM2.5* (Gg)
Angola	437.8	164.6	7069.4	219.8	198.4	720.1
Botswana	47.9	29.0	653.3	12.7	18.6	40.0
Burundi	1.1	0.3	15.3	0.5	0.4	1.5
Malawi	7.7	2.8	123.3	3.8	3.6	12.3
Mozambique	152.5	51.8	2644.5	88.4	73.5	292.6
Namibia	46.8	27.9	716.7	15.8	22.9	45.1
Rwanda	0.8	0.2	8.1	0.3	0.2	0.8
South Africa	97.5	43.5	1240.7	29.1	36.4	89.8
Swaziland	0.7	0.3	12.5	0.4	0.3	1.3
Tanzania	171.1	43.4	2146.0	70.0	64.4	222.0
Zambia	163.7	48.9	2492.2	83.2	71.6	271.0
Zimbabwe	24.7	12.9	454.8	11.9	13.6	36.4
Others	390.9	111.4	5651.3	189.7	157.6	628.0

* Only countries contained completely within the study area are individually listed.

5.3.3 Error Analysis

Currently, the lack of spatial and temporal information on the accuracy of the variables used to calculate the emissions impedes a rigorous error analysis. An approximation of the error propagation in the regional emissions estimates based upon standard propagation of variance formula (Cooper 1987) applied to Equation (4.1), and assuming that the fuel load, area burned, combustion completeness and emission factor variables are independent, is given in percentage (%) units by:

$$e_{\text{total}} = (e^2_{\text{fuel load}} + e^2_{\text{area burned}} + e^2_{\text{combustion completeness}} + e^2_{\text{emission factor}})^{1/2} \quad (5.9)$$

where,

$e_{\text{total}} =$ total emissions error for a given trace gas

$e_{\text{fuel load}} = (\sigma_{\text{fuel load}} / \text{Fuel Load}) * 100.0$

$e_{\text{area burned}} = (\sigma_{\text{area burned}} / \text{Area burned}) * 100.0$

$e_{\text{combustion completeness}} = (\sigma_{\text{combustion completeness}} / \text{Combustion Completeness}) * 100.0$

$e_{\text{emission factor}} = (\sigma_{\text{emission factor}} / \text{Emission Factor}) * 100.0$

σ_x = standard deviation of variable x

The total emissions error (e_{total}) defines the percentage emissions estimate at the one sigma level (*i.e.*, the error is expected to fall within $\pm e_{\text{total}}$ approximately 68% of the time). Scholes *et al.* (1996a; 1996b) and Barbosa *et al.* (1999) used a similar approach to get a conservative estimate of their emissions uncertainties. The errors are calculated here for the July and September MODIS-based CO_2, CO and CH_4 emissions for grasslands and woodlands and for the fuel load and NDVI-based methods. The month of July provides an approximation of the errors in the early dry season emissions, whereas the month of September is representative of the errors in the late dry season emissions.

The error estimates are derived independently for each woodland and grassland land cover and for the two months. The total MODIS burned area, and the average emission factor, combustion completeness, and fuel load for each land cover type and month are used. The $\sigma_{\text{area burned}}$ is defined by the difference between the MODIS and GBA-2000 burned area divided by three (i.e., this difference is assumed to correspond to a 3σ range). The $\sigma_{\text{emission factor}}$ is determined from the regression model used to derive the emission factors described in Chapter 3 (the standard deviation of the residuals are used). The September $\sigma_{\text{combustion completeness}}$ values are derived from the standard deviation of the late dry season published combustion completeness measurements by Shea *et al.* (1996). The July $\sigma_{\text{combustion completeness}}$ values are determined from the regression models from

Hoffa *et al.* (1999) (again, the standard deviation of the residuals are used). The $\sigma_{\text{fuel load}}$ is unknown and arbitrarily assumed to be 30%.

The results of the error analysis are summarized in Table 17 (Appendix C). The average monthly emissions calculated by applying Equation (4.1) using the total MODIS burned area, average emission factor, combustion completeness and fuel load for each land cover type and month are also shown with the spatially explicit monthly modeled emissions and their difference expressed as a ratio. The average monthly CO_2 and CO emissions are comparable with the corresponding spatially explicit monthly CO_2 and CO modeled values. For CH_4, the average total emissions are also comparable with the corresponding spatially explicit monthly modeled values for woodland fires but higher than the corresponding spatially explicit monthly modeled values for both early and late dry season grassland fires. The reasons for this are discussed below. Based on this analysis, the e_{total} values are assumed to be indicative of the error in the spatially explicit emissions estimates as well as the average values.

The estimated 1σ error in grassland and woodland emissions ranges from approximately 34% to 99% (Table 17, Appendix C). These large errors indicate the need for a rigorous error assessment. The error estimates in Table 17 (Appendix C) provide a limited understanding of the most influential variables on the resulting uncertainties in total emissions. Obviously, the arbitrary 30% fuel load error contributes largely to the uncertainty in the current emissions modeling methodology. The combustion completeness also accounts for a significant portion of the uncertainty, with higher errors in the early dry season mainly for woodland fires. The combustion completeness is equally important with respect to error contribution for early dry season woodland fires

and in fact, becomes the most critical error variable in the estimation process of the NDVI-based early dry season woodland fire emissions, when the fuel moisture content is high. The errors in area burned are better constrained than previously (*e.g.*, Scholes *et al.*, 1996a; Barbosa *et al.*, 1999) due to the current availability of comparable burned area datasets. However, as also noted in Chapter 4, the actual accuracy of these burned area datasets is not known. Consistent with what was found in this study from the comparison of the MODIS and GBA-2000 products, the errors in area burned are larger in woodlands than in grasslands. The emission factors for CO_2 and CO are not significant error sources, in contrast to the very high uncertainty for the CH_4 emission factor for grassland fires. The high errors in CH_4 emission factor errors are likely because CH_4 is emitted at very small amounts from highly efficient grassland fires, and this is also reflected in the fact that CH_4 emission factors in the late dry season have higher uncertainties compared with the early dry season. The grassland CH_4 emissions, are significantly smaller compared with the woodland CH_4 emissions (by factors 5-17) and therefore, have a smaller weight on the overall regional emission errors compared with woodland CH_4 fire emissions.

The fuel load-based and NDVI-based overall errors are similar for woodland and grassland fires in the late dry season because both methods predict similar fuel moisture conditions (Figures 9a and 12a). In the early dry season woodland fires the NDVI-based overall emissions errors are higher than for the fuel load method, due to the higher uncertainty in combustion completeness of the wetter fuels. For early dry season grassland fires the errors are slightly higher for the NDVI than the fuel load method for CO_2 and CO emissions, due to the higher uncertainty in combustion completeness. On the other hand, lower errors occur when using the NDVI-based method to estimate CH_4

emissions from early dry grassland fires, mainly because of the higher CH_4 emission factors predicted for the combustion of the wetter grass fuels (Figure 10c).

The main implications of this limited exercise are that it may (i) facilitate the selection of the most critical variables in the emissions estimation process and so, provide an indication of priorities for field measurements, and (ii) identify which variables need more reliable predictive models in the emission model. A spatially explicit Monte Carlo error simulation (Heuvelink *et al.*, 1989) may help to define this more rigorously than the first order error analysis defined here. The results in Table 17 (Appendix C) indicate that attention should be particularly given to create fuel load datasets that have associated uncertainty information. Early dry season combustion completeness field measurements, especially for woodland fires, are also needed with high priority. Furthermore, since the seasonal, ecosystem-specific emission factors (Chapter 3) are derived from a limited number of field measurements, a larger database needs to be created to properly examine the ecosystem differences. Improved characterization of emission factors for products of incomplete combustion from grassland fires is also recommended.

5.3.4 Intercomparison with Previous Studies

While results from this study are not directly comparable with the findings of previous studies due to interannual variability and the different methodologies used, it is worth comparing this study with previous studies that have used satellite observations to parameterize their emissions models (Table 18). Regional emission estimates are within the range predicted by the studies of Scholes *et al.* (1996a) and Barbosa *et al.* (1999) and are in agreement, in the sense that they all predict lower emissions compared with the classification emissions estimation approach (Hao *et al.*, 1990; Hao and Liu, 1994). On

the other hand, emissions results from this study are significantly lower compared with the two bottom-up estimates made by van der Werf *et al.* (2003, 2004). The main reason for the discrepancy between this study and the earlier van der Werf (2003) study may be attributed mostly to the higher fuel loads for above ground woody vegetation used by van der Werf (2003). The fuel load in this study likely presents a lower bound, since it does not account for fuel accumulation, living wood, and dead wood more than 5 cm in diameter. None of the methods accounts for fuel load removal by people. As noted by van der Werf *et al.* (2003), it does appear that their method overestimates fuel loads compared with literature values. In their later study, van der Werf *et al.* (2004) significantly increased their burned area estimates.

Most of the top-down CO inversion studies to date have suggested that bottom-up approaches underestimate the CO produced from vegetation fires and that they are at least as high as the Hao and Liu (1994) estimates (*e.g.*, Chatfield *et al.*, 1996; Chatfield *et al.*, 1997; Bergamaschi *et al.*, 2000). However, recently available 2000 tropospheric CO retrievals from the Measurements Of Pollution In The Troposphere (MOPITT) instrument for the year 2000 range from 51-63 Tg of CO for southern Africa (Arellano *et al.*, 2004) and are lower than the Hao and Liu (1994) estimates. The average MODIS-based CO estimate of 23 Tg in this study (Table 18) is still lower than MOPITT CO retrievals. At the same time, when taking the maximum CO error of 72% from Table 17 (Appendix C) for woodland fires (since these contribute mostly to regional emissions) the MODIS-based CO estimate falls in the range 23±17 (1σ) Tg. Furthermore, the true uncertainty in the MOPITT CO estimates is not known, since these results are driven by

Table 18. Intercomparison of different annual estimates of burned area, biomass burned and emission estimates for southern Africa.

Study	*Burned area (10^6 km^2/yr)*	*Biomass burned (Tg/yr)*	*CO_2 (Tg/yr)*	*CO (Tg/yr)*
Hao *et al.* (1990)	-	1200	1560	99 [a]
Hao and Liu (1994)	-	827	-	68 [b]
Hao *et al.* (1996)	-	1000 [c]	-	75
Scholes *et al.*(1996a) (year 1989)	1.68	177	324	14.9
Scholes *et al.* (1996b) classification method	3.99	1152	-	-
Barbosa *et al.* (1999) (year 1989)	1.54	456	748	31.0
van der Werf *et al.* (2003) (years 1998-2001)	1.16	1147	1848 [d]	76.8 [d]
van der Werf *et al.* (2004) (years 1997-2001)	-	2040	3286	136.7
This study GBA-2000 (year 2000) [e]	1.04	254	372	14.9
This study MODIS (year 2000) [e]	1.54	316	537	23.3

[a] Assuming molar ratio of CO to CO_2 is 0.1 from Hao *et al.* (1990). The calculations assume 50% carbon content.
[b] Based on extrapolation from Hao *et al.* (1990)
[c] Calculated based on the contribution of southern Africa to continental Africa from Hao *et al.* (1990)
[d] Using the emissions factors from van der Werf *et al.* (2004)
[e] Average of fuel load and NDVI-based methods

an *a priori* CO estimate of 147 Tg from van der Werf *et al.* (2004) and the assumed errors in the datasets used in their methodology. The true uncertainties are likely larger than reported since these factors will affect the inversion results (Arellano *et al.*, 2004). It appears thus, that the discrepancy that has been previously noted between bottom-up and top-down based approaches (*e.g.*, Scholes *et al.*, 1996a; Barbosa *et al.*, 1999; Chatfield *et al.*, 1997) still persists, even though more recent results suggest a smaller biomass burning CO source strength from southern African savanna fires. It should be noted, that from this study it appears, that incorporation of the seasonal dynamics of vegetation fire emissions will affect regional emissions estimation by lowering emissions estimates even more rather than increasing them.

5.3.5 Synthesis of Regional Trace Gas Emissions

Besides vegetation fires, other important sources of trace gases in southern Africa include biogenic emissions, industrial emissions and emissions from domestic biofuel use. Where readily quantifiable, these sources are compared in Table 19. Synthesis results, such as the ones presented in Table 19, are important for assessing the impact of different processes on regional atmospheric chemistry and composition and for an improved estimation of global trace gas budgets. These results suggest that regional sources are important to varying degrees for the different atmospheric species of interest. In addition to their source strength, the temporal variation of these emissions plays a key role in regional atmospheric chemistry (Scholes and Scholes, 1998). An overview of the biogenic, fossil fuel and biofuel emissions is provided below.

5.3.5.1 Biogenic Emissions

Due to their high temperatures and radiation fluxes, tropical ecosystems are a significant source of NMHC, especially for isoprene and monoterpenes (Otter *et al.*, 2003). In the warm, humid tropical regions of central Africa with high plant productivity, emissions are high throughout the year. Annual regional hydrocarbon emissions from vegetation are significantly higher than those from vegetation fires, however vegetation emissions decline significantly during the leafless period, coincident with the biomass burning season. CO_2 is released through soil respiration and decomposition of dead organic material. Soil moisture is a greater controlling factor than temperature (Levine *et al*., 1996). Soil CO_2 emissions are low during the dry season and have shown to increase by a factor of 20 during the wet season. Estimated soil CO_2 fluxes for African savannas range between 0.4-0.8 $gCm^{-2}day^{-1}$ (Otter *et al.*, 2001). CO is emitted from green plants, dead vegetation and litter. CO production can be induced both photochemically and

thermally (Shade and Crutzen, 1999). Vegetation in southern Africa is estimated to release at least 1.2 Tg CO (Otter *et al.*, 2001). Soils are considered to be a sink for CO on a global basis, however CO flux measurements from savannas are conflicting, with some sites showing net emissions (Conrad and Seiler, 1982; Zepp *et al.*, 1996). Burning tends to increase CO fluxes from soils for a few days, and rain on the burned site has an additional stimulating effect (Zepp *et al.*, 1996). Vegetation fires make a larger contribution to regional CO_2 and CO budgets compared with biofuel and fossil fuel burning.

Table 19. Sources of trace gas emissions in southern Africa (TgC/yr or TgN/yr). Brackets show range of values.

Trace gas	*MODIS Vegetation Fires*	*Biogenic*	*Biofuel*	*Fossil Fuel*
CO_2	146.5 (~52.7%)	NAV	47.1[a] (~17.0%)	84.2 (~30.3%)
CO	10.0 (~52.0%)	0.21[c] (~1.1%)	5.8[a] (~30.2%)	3.2[d] (~16.7%)
CH_4	0.54	(0.29-7.5)[a]	0.22[a]	0.32
NMHC	1.2 (~1.5%)	80[b] (~98%)	0.45[a] (~0.5%)	NAV
NO	0.49 (~25.0%)	0.49[c] (~25.0%)	0.06[a] (~3.1)	0.92[c] (~46.9%)

NAV. Not available

[a] From Otter *et al*, 2001 not including Madagascar, Seychelles, Mauritius.

[b] From Otter *et al.*, 2003.

[c] Soil NO_x from Scholes and Scholes, 1998. Lightning is included in the NO_x biogenic estimates.

[d] South African data from Scholes and van der Merwe, 1996. Emissions from international bunkers should be excluded from the national reports as they are calculated on a global basis. Scholes and van der Merwe include the emissions from international bunkers under the transport sector. To estimate CO emissions from transportation, excluding international bunkers, the CO estimates by Scholes and van der Merwe are adjusted based on the relative proportions of transportation and international bunkers in the IPCC CO_2 estimates for 1994.

Savanna soils have a clear seasonal pattern regarding CH_4, being a sink during the dry season and a weak source during the wet season (Otter and Scholes, 2000; Otter *et al.*, 2001). Savannas in southern Africa are estimated to consume about 0.23 Tg CH_4 yr^{-1} (Otter *et al.*, 2001). Methanogenesis by the seasonal wetlands (*dambos*) dominates the regional CH_4 budgets, as it is estimated to range between 0.3 and 10 Tg CH_4 yr^{-1} (Otter *et al.*, 2001). CH_4 emissions from enteric fermentation in large herbivores in southern Africa are estimated to be 0.32 Tg CH_4 yr^{-1} (Scholes *et al.*, 1996a).

Microbial production of NO from soils in southern Africa is enhanced during the wet, summer months, whereas production of nitrous oxide (N_2O) is insignificant even after rainfall (Parsons *et al.*, 1996; Levine *et al.*, 1996). NO emissions show a large pulse after the onset of the first rains in the spring, but this is short lived and does not significantly contribute to the overall NO budgets. However, it has been postulated, that the timing of these biogenic NO emissions pulse is such, that in combination with the NMHC and CO produced from vegetation fires, it may contribute significantly to the annual spring midtropospheric ozone maxima, observed over the tropical South Atlantic typically during September to October (Scholes and Scholes, 1998; Scholes and Andreae, 2000). Lightning activity may also be a significant source of tropospheric NO_x (Price *et al.*, 1997). It is estimated that lightning produces about 0.35 Tg N-NO_x in southern Africa (Horowitz *et al.*, 2003; L. Emmons, pers. comm.). Lightning has been suggested as being the culprit for the "ozone-paradox", *i.e.*, the O_3 maxima observed over the tropical Atlantic during the early part of the year, outside the southern African biomass burning season (Edwards *et al.*, 2003). The seasonality of NO_x production from lightning is such, that it sharply increases during September/October and peaks during January/February.

The combined lightning and soil NO_x are comparable to NO_x emissions from vegetation fires (Table 19). The majority of annual NO_x emissions from vegetation (about 57%) fires are concentrated during the months of August through October (Table 15). The timing and quantitative predominance of vegetation fires and lightning NO_x over soil NO_x, contest the hypothesis that soil NO_x significantly contribute to the austral spring mid-tropospheric ozone maxima. However, large uncertainties still exist in quantifying all of these sources and it may be that soil NO_x may be larger than currently thought.

5.3.5.2 Fossil Fuel Emissions

The fossil fuel emissions in Table 19 are compiled from the latest available IPCC national communications to the United Nations Framework Convention on Climate Change (UNFCC) for all countries contained completely within the study region, besides Angola and Zambia. The reports, were obtained from the United Nations Framework Convention on Climate Change (UNFCC) web site (Table 20, WWW1). To the knowledge of this author, the Angolan and Zambian IPCC reports are unavailable at this time. South Africa is the dominant regional source (about 88%) of atmospheric pollutants from fossil fuel combustion (Scholes and Scholes, 1998). The most significant contribution to fossil fuel emissions in South Africa is from the generation of electricity in coal-burning power stations. South Africa produces and consumes over 60% of the total electrical energy of the African continent, and is ranked twelfth in the world in terms of carbon emissions (Table 20, WWW2). Other sources include emissions from transportation, petroleum refining, coal mining, and industrial production of minerals, chemicals and metal. Mining and metallurgical operations in the Zambian Copperbelt are also important with respect to regional fossil fuel emissions, but to a lesser extent than

South Africa. In general, the uncertainties associated with fossil fuel emission are small (about 20%) relative to those associated with biogenic and vegetation fire emissions (Scholes and Scholes, 1998).

Table 20. World Wide Web sites referenced.

WWW1-National Communications to the United Nations Framework Convention on Climate Change. http://unfccc.int/resource/natcom/nctable.html
WWW2-Energy Information Agency, US Department of Energy Data Tables, 2002. http://www.eia.doe.gov/pub/international/iealf/tableh1.xls
WWW3-ISI Essential Science Indicators, 2003. http://www.esi-topics.com/

5.3.5.3 Biofuel Emissions

The majority of southern Africa's rural population (over 90%) relies on biofuels (mostly wood and charcoal but also dung and agricultural residues) for domestic heating and cooking (Ludwig *et al.*, 2003). About half of the charcoal production globally occurs in Africa (Yevich and Logan, 2003). Unlike vegetation fires which are a seasonal phenomenon, domestic biofuel consumption provides a steady input of trace gases and particulates into the atmosphere (Ludwig *et al.*, 2003). Fuelwood burning favors the production of smoldering compounds such as CO, whereas about 98% of the total carbon released is in the form of CO_2 and CO (Brocard and Lacaux, 1998). Because the nitrogen content of fuelwood is low, the contribution of domestic biomass burning to regional NOx budgets is relatively low.

5.3.6 The Global Significance of Southern African Vegetation Fires

To situate southern African savanna vegetation fire emissions within the global context, the MODIS-based estimates of this study are compared with the annual global inventories of emissions from savanna fires and all biomass burning sources estimated by Andreae and Merlet (2001) and global emissions from fossil fuel combustion compiled by Yevich and Logan (2003). The Andreae and Merlet (2001) study is chosen, as it is mostly cited in biomass burning emissions studies and is believed to provide the best available synthesis on global emissions from vegetation fires (Table 20, WWW3). The Yevich and Logan (2003) study is chosen because it provides the most up-to-date synthesis on global fossil fuel emissions.

5.3.6.1 Differences in Emission Factors

To examine the reasons for agreement or discrepancy between the savanna emissions estimates of this study and those by Andreae and Merlet (2001), the maximum range in seasonal emission factor values for grassland and woodland fires computed in this work are compared with the ranges of emissions factors for savanna fires globally compiled by Andreae and Merlet (2001) in Figures 17-19. The NDVI-based emission factors are not illustrated here, since they are very similar to the fuel load-based emission factors (Tables 8-9, Appendix C). In some cases, Andreae and Merlet computed emission factors assuming 45% carbon content in the fuel. Therefore, disagreement in emission factors is deemed when differences exceed 10%. Figures 17-19 have logarithmic y axes to visualize the wide range of emission factors values reported in Tables 5-6 (Appendix C) and in Table 8 (Appendix C). Regional average early and late dry season emissions factors for dimethyl sulfide, methyl nitrate, 3-methyl-1-butene, t-2 pentene, c-2-pentene, 2-methyl-2-pentene and *n*-heptane, based on airborne measurements by Sinha *et al.*

(2003), have not been reported previously. Taking into account the standard deviations of the measurements, the mean emission factors for grassland and woodland fires modeled in this study are similar to the values reported by Andreae and Merlet (2001) except for ammonia, formaldehyde, hydrogen cyanide and methyl iodide. Emission factors for acetic acid, formaldehyde, and potassium for early and late dry season woodland fires and the NDVI-based early dry season grassland fires are higher compared with Andreae and Merlet (2001). Furthermore, emission factors for total particulate matter for early dry season woodland fires and the NDVI-based early dry season grassland fires are also higher compared with Andreae and Merlet (2001).

These differences between this study and the Andreae and Merlet (2001) compilation for the species mentioned above may be attributed to several reasons. In some cases the emission factors proposed by Andreae and Merlet (2001) are based on only one or two measurements, whereas in this study emission factors are calculated based on a larger database provided by the SAFARI 2000 campaign (Yokelson *et al.*, 2003; Sinha *et al.*, 2003). Whereas the emission factors of this study are parameterized by measurements of nascent smoke, the average emission factors by Andreae and Merlet (2001) are also based on measurements of "older" smoke, of unknown age (Yokelson *et al.*, 2003). Recently, Hobbs *et al.*, (2003) showed that significant post-emission transformations in smoke composition occur as the smoke ages due to photochemistry and cloud processing. In addition, as mentioned previously, emission factors depend on the chemical composition of the fuel which was not accounted for in this modeling study. Finally, differences may also be attributed to the fact that seasonal variations of emissions

factors are accounted for in this study, whereas the values presented by Andreae and Merlet (2001) are based on measurements conducted during the late dry season.

When comparing the ecosystem-dependent emissions factors derived from the two methods in this study with the Andreae and Merlet (2001) values, the following additional points are observed. The compilation by Andreae and Merlet (2001) is based on measurements from fires in locations with mixed fuel types, which tend to fall largely under what is defined in this study as woodlands. As noted in Section 5.3.2.2, the differences between early and late dry season emission factors for woodland fires in this study are mostly driven by the presence of woody and litter fuels rather than the moisture content of the grass. The wide range of measurements used in the Andreae and Merlet (2001) compilation likely encompasses this variety in fuel mixture that drives the early and late dry season emission factors of this study. Therefore, mean values of the fuel-load based emission factors for both early and late dry season woodland fires tend to be close to the mean values by Andreae and Merlet (2001), except for the species noted above (Figure 17). This is similar for the NDVI-based emission factors, due to the similarity with the fuel load-based emission factors (Tables 8-9, Appendix C). As discerned from Tables 5-6 (Appendix C) and 8-9 (Appendix C), the early dry season emissions factors for grassland fires tend to be similar to late the dry season emission factors for woodland fires in the fuel load-based method, and similar to the early dry season emission factors for woodland fires in the NDVI-based method. This may explain why for grassland fires, a number of mean values of early dry season emission factors for products of incomplete combustion tend to agree better with the mean values in Andreae and Merlet (2001), except for the species mentioned above (Figures 17-18). On the same

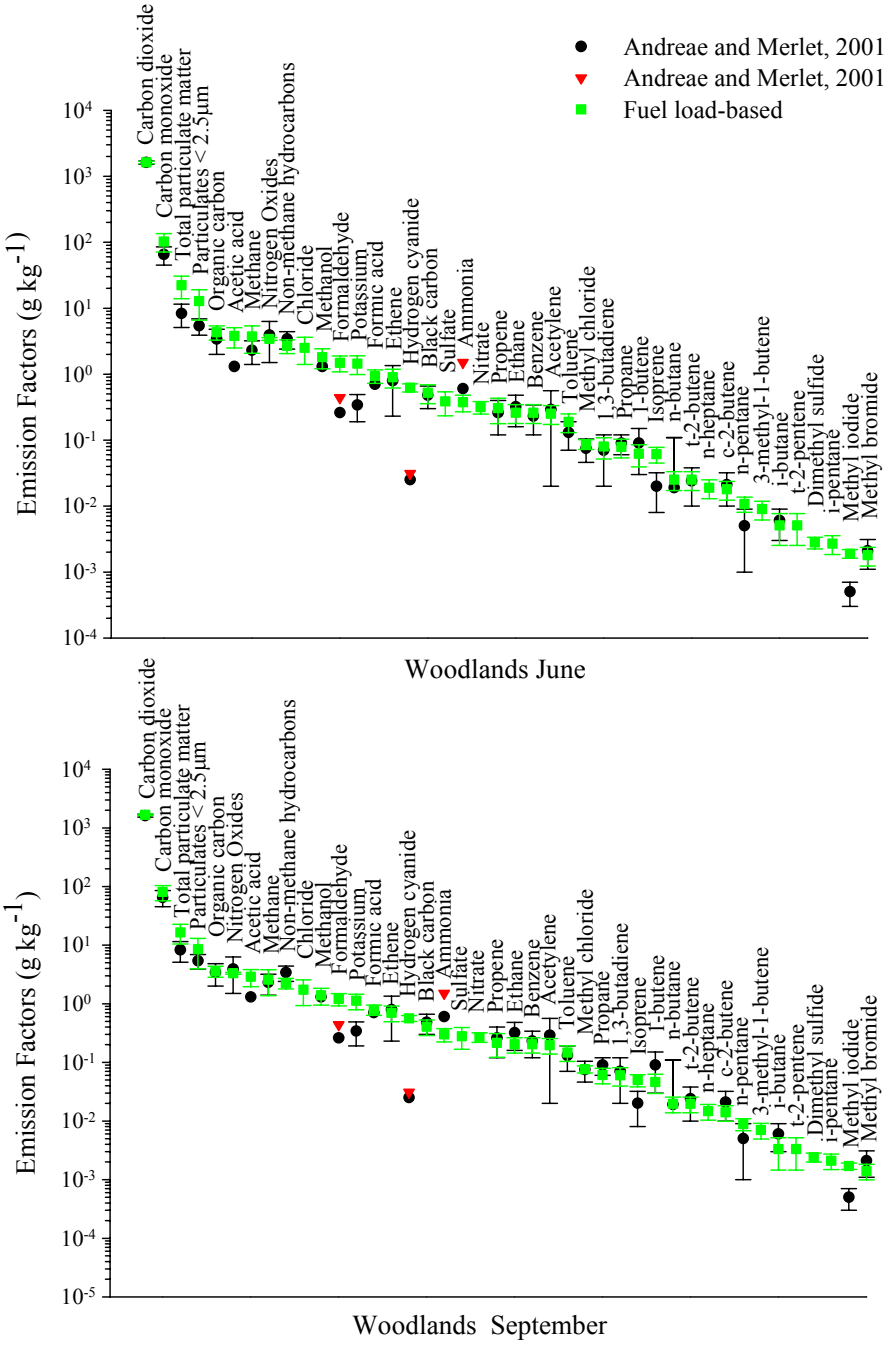

Figure 17. Comparison of mean and standard deviation of the fuel load-based emission factors for several trace gases and particulates in order of decreasing magnitude for woodland fires in June and September, 2000 with a compilation of field measurements by Andreae and Merlet (2001). Individual measurements are shown as black circles without the standard deviation and as red triangles.

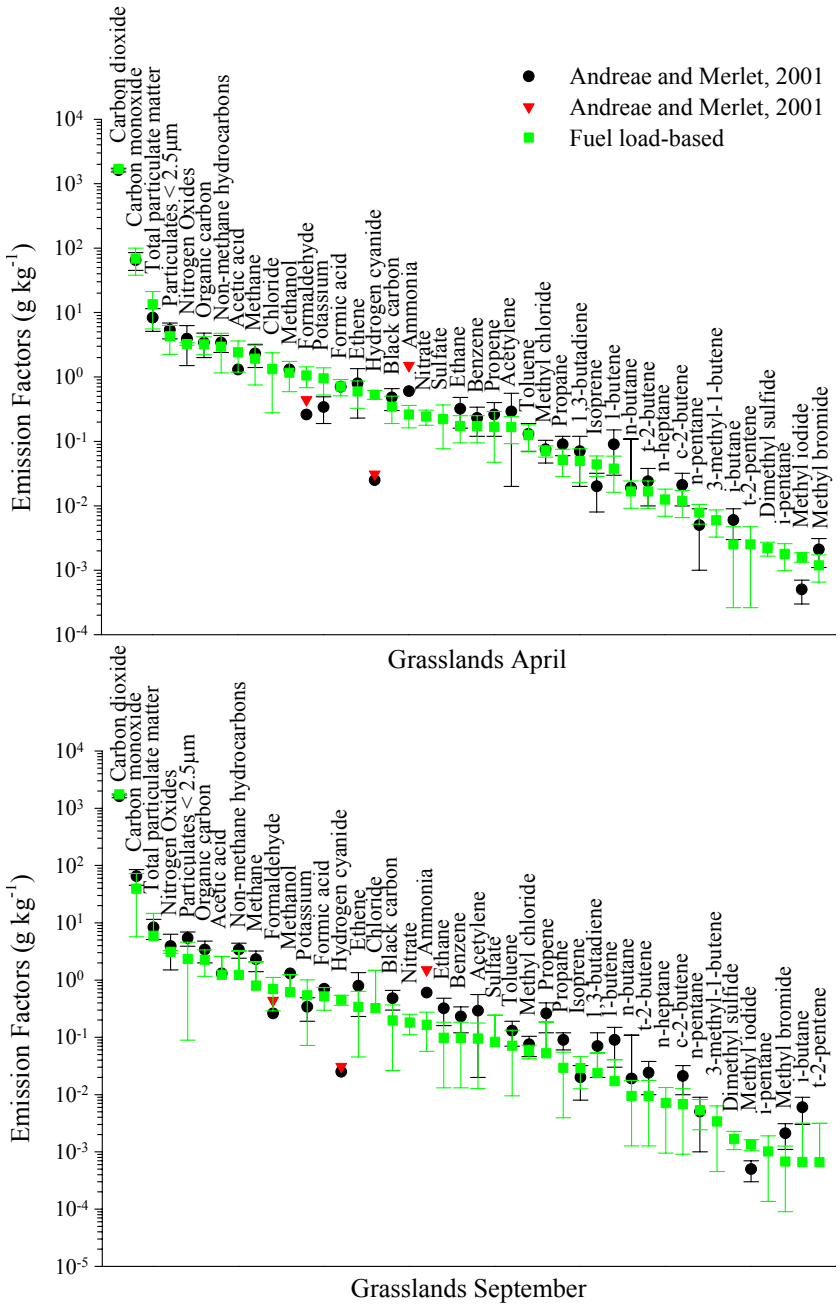

Figure 18. Comparison of mean and standard deviation of the fuel load-based emission factors for several trace gases and particulates in order of decreasing magnitude for grassland fires in April and September, 2000 with a compilation of field measurements by Andreae and Merlet (2001). Individual measurements are shown as black circles without the standard deviation and as red triangles.

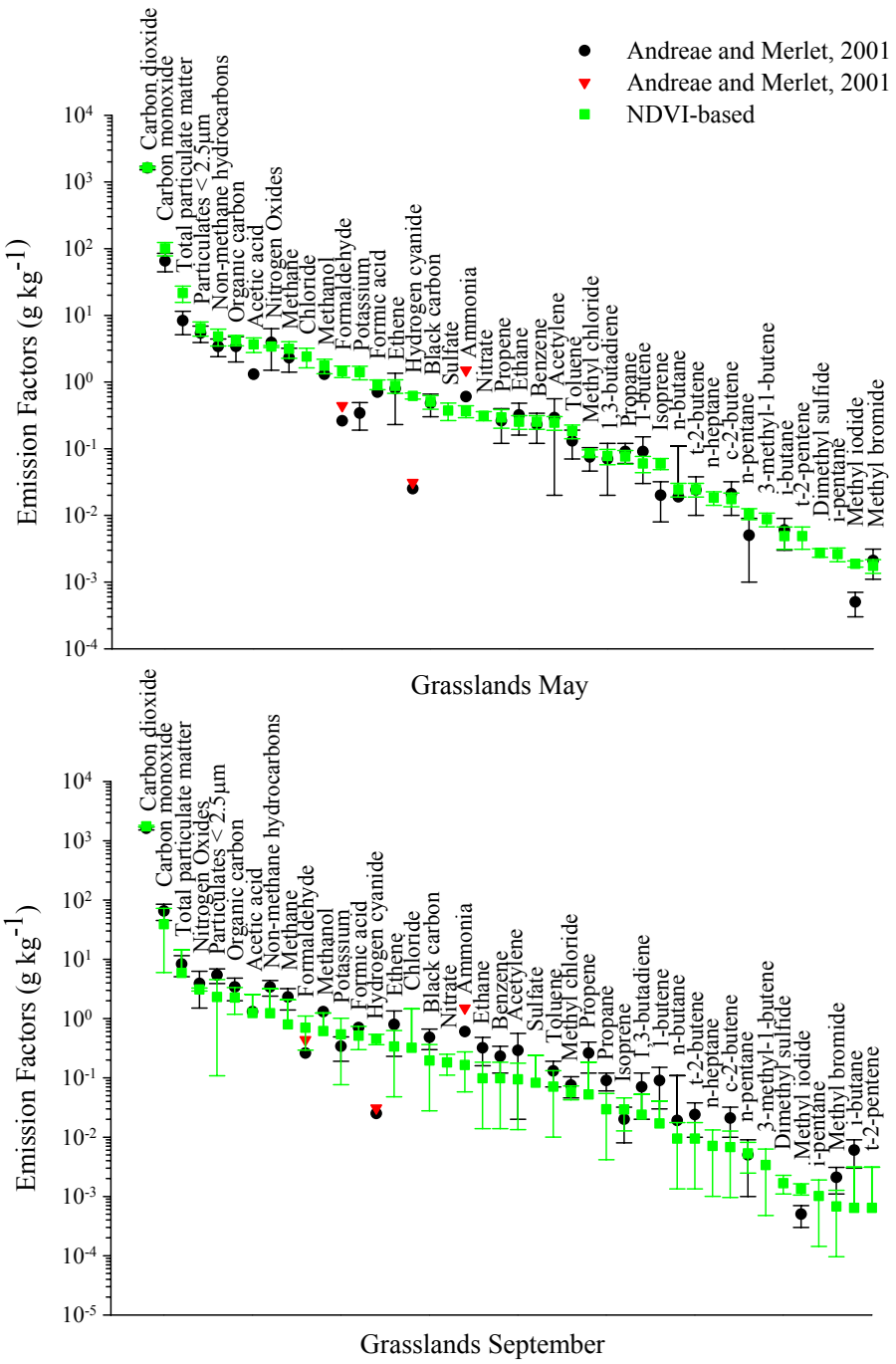

Figure 19. Comparison of mean and standard deviation of the NDVI-based emission factors for several trace gases and particulates in order of decreasing magnitude for grassland fires in May and September, 2000 with a compilation of field measurements by Andreae and Merlet (2001). Individual measurements are shown as black circles without the standard deviation and as red triangles.

basis, because of the generally more efficient burning in grasslands compared with woodlands in the late dry season, mean values of late dry season emission factors for several products of incomplete combustion in grassland fires tend to be lower than the mean values in Andreae and Merlet (2001).

5.3.6.2 Contribution of Vegetation Fires in Southern Africa to Global Emissions

The contribution of southern African savanna fire emissions to global savanna burning and global biomass burning is assessed for the species for which estimates are reported by Andreae and Merlet (2001) (Table 21, Appendix C). Global savanna emissions for those species for which the more recent SAFARI 2000 field measurements (Yokelson *et al.* 2003; Sinha *et al.* 2003) showed significant differences with the Andreae and Merlet (2001) values are recalculated here. These species include hydrogen cyanide, ammonia, acetic acid and formaldehyde.

Vegetation fires in southern Africa savannas account for ~10% of the biomass burned annually in savannas globally and ~3.7% of the total biomass burned globally (Table 21, Appendix C). The contribution of southern African woodland and grassland fires to annual emissions of CO_2, CO, CH_4, NMHC and NO_x from global savanna burning is ~10.5%, 11.3%, 9.8%, 6.1%, and 8.5%, respectively. The corresponding percentages to global pyrogenic emissions from all the above sources are ~4.0%, 3.4%, 1.9%, 1.3%, 5.0%. The CO_2, CO, CH_4 and NO_x released from vegetation fires in southern Africa represent ~2.8%, 5.8-7.7%, 0.7-1.0%, and ~2.3% of the corresponding global fossil fuel emissions (Yevich and Logan, 2003), respectively.

Hydrogen cyanide (HCN) has been proposed as a useful tracer of biomass burning since it can be determined by remote sensing (Li *et al.*, 2000). The HCN estimates for

southern Africa are 1.9 times higher than the global emissions from savanna burning. However, Andreae and Merlet's (2001) estimates (0.025-0.031 gkg^{-1}) are based on two savanna fire measurements in Australia (Hurst *et al.*, 1994a, 1994b), the only data available at that time, which had an emission factor for HCN ~20 times lower than the average (0.53±0.15 gkg^{-1}) measured by Sinha *et al.* (2003). Recalculating global emissions of HCN using an average emission factor for the range of values reported by Andreae and Merlet (2001) and Sinha *et al.* (0.48±0.24 gkg^{-1}) yields a value of ~1.5 Tg/yr for global savanna burning and 2.3 Tg/yr for global biomass burning from all sources. HCN from southern African savanna fires account for ~11.5% and ~7.5% of the adjusted global savanna fires and global pyrogenic emissions, respectively.

Oxygenated Volatile Organic Compounds (OVOCs) are of particular importance to atmospheric chemistry, due to their influence on hydrogen radicals OH and HO_2 (collectively known as HO_x), hydrogen peroxide, ozone and particulate formation (Andreae and Crutzen, 1996; Wennberg *et al.*, 1998; Mason *et al.*, 2001). The origin of OVOCs from savanna fires was largely unexplored prior to the SAFARI-2000 campaign (Yokelson *et al.,* 2003). As seen in Table 21 (Appendix C) the sum of the four OVOCs is about 2.7 times larger than the NMHC. Therefore, OVOCs need to be routinely integrated in modeling studies of savanna fire emissions. The single emission factor values for the different OVOC species reported by Andreae and Merlet (2001) are close to the average of the measurements by Yokelson *et al.* (2003) for CH_3OH (1.2) and HCOOH (0.62), but factors of 2 and 3 lower for CH_3COOH (2.4) and HCHO (1.0). Thus, the global pyrogenic emissions for CH_3COOH and HCHO are recalculated based on average emission factors of 2.32±0.83 g kg^{-1} for CH_3COOH and 1.05±0.59 g kg^{-1} for

HCHO. Emissions of CH_3COOH, HCHO, CH_3OH and HCOOH account for ~11.2%, 10.7%, 10.5% and 11.2% of those from global savanna fire emissions, respectively. They are estimated to make up ~5.2%, 4.6%, 3.1% and 4.0% of total global pyrogenic sources, respectively.

The Andreae and Merlet (2001) emission factor values for NH_3 (0.6-1.05) are 2 to 4 times higher than the average value (0.26±0.14 g kg^{-1}) by Sinha *et al.* (2003). Based on an average emission factor of 0.41±0.26 g kg^{-1} for NH_3, derived from the integration of the two literature sources, NH_3 from southern African fires account for ~6.8% of the global savanna burning and ~1.1% of the global biomass burning. The acetylene released from southern African vegetation fires is ~6.1% that of the global savanna burning and ~1.1% that of the global biomass burning.

The total particulate matter (TPM), particulates in the size range up to 2.5 μm (PM2.5), organic carbon (OC) and black carbon (BC) constitute ~17.7%, 14.7%, 10.0%, 7.8%, of the global savanna fire emissions and ~5.6%, 4.0 %, 3.0%, 2.4%, and 17.0% of global pyrogenic emissions, respectively. The large contribution of savanna fires to TPM and PM2.5 may be related to uncertainties associated with emission factors for aerosols (Andreae, 1997; Andreae and Merlet, 2001).

Andreae (1997) estimated that African savanna fires emissions account for ~54% of the global savanna fire emission for various trace gases. Southern African fires account for approximately 50% of the carbon released from all African savanna fires at the continental scale (van der Werf *et al.*, 2003). Based on the results found here for southern Africa, the contribution of African savanna fires to global savanna fire emission is ~20% for biomass burned, 20% for CO_2, 22% for CO, 20% for CH_4 and 17% for NO_x. This

would imply that African savanna fires are a smaller source of trace gases and particulates than suggested by Andreae *et al.* (1997). However, it needs to be pointed out, that the Andreae (1997) and Andreae and Merlet (2001) estimates are also based on FAO statistics and the Hao *et al.* (1990) estimates as described in Andreae (1993), which suggest that about two thirds of the global savanna biomass burning occurs in Africa. Therefore, Andreae (1997) and Andreae and Merlet (2001) may be overestimating the amount of biomass burned.

5.4 Conclusions

What emerges clearly from the results of this study is the complexity of the interactions among the different parameters that determine the seasonal trends in vegetation fire emissions. The emissions model developed here has the advantage of accounting for explicit variations of emissions from vegetation fires as a function of space, time, land cover and the type of combustion. Not accounting for the seasonal variations in the fuel condition may introduce large errors in the emissions quantification process, since significant differences are found between early and late dry season fire behavior in grasslands and woodlands. In grasslands, early burning emits more products of incomplete combustion per unit area compared with the late dry season, whereas the opposite is found for woodlands. The variable seasonal mixture of grassland and woodland fires, which also likely changes from year to year, will determine the net regional emissions. From an atmospheric perspective, it appears that early dry season burning at the regional level, when the fuel is wetter, may even reduce the annual regional trace gas and particulate budgets.

The significance of vegetation fires for the regional trace gas and particulate budgets remains prominent, even if other major sources are considered. Regional emissions for a number of reactive atmospheric species, including Oxygenated Volatile Organic Compounds (OVOCs), are estimated for the first time at the regional scale and their high contribution to regional emissions indicates that they need to be routinely integrated into future emissions modeling studies. Large uncertainties still likely persist with regard to the amount of fuel load. Considering the new advances in satellite burned area mapping and the fact that rigorous validation is underway (Roy *et al.*, 2003), future research efforts should focus on accuracy assessment of fuel load models. Additional early dry season studies are needed to improve our understanding of fire behavior in diverse savanna woodlands, and enable further refinement of predictive models for combustion completeness and emission factors. A compelling need for the prediction of combustion completeness and emission factors at the regional level is the reliable assessment of the fuel moisture content. The development of seasonal fuel chemistry databases will improve the characterization of nitrogen emission compounds. Likewise, for halogen, and sulfur-containing species, an approach that considers the regional fuel chemistry, in addition to type of combustion, will increase the accuracy of the predicted emissions estimates (Menaut *et al.*, 1991; Kuhlbusch *et al.*, 1996; McKenzie *et al.*, 1996).

Chapter 6: Applications of the Research

6.1 Introduction

The research presented in Chapter 5 has significant implications for applications including, IPCC national greenhouse gas emissions reporting, regional air quality monitoring, and fire management policy development. Particularly, in regards to the IPCC assessments, this research has the potential to make a significant contribution to the development of improved harmonized methodologies for greenhouse gas estimation from savanna fires. Results from the comparisons of IPCC reports for selected countries with the respective MODIS-extrapolated emissions are discussed.

6.2 National Greenhouse Gas Emissions Reporting

The Intergovernmental Panel on Climate Change (IPCC) was established in 1988 under the auspices of the United Nations Environment Programme (UNEP) and the World Meteorological Organization (WMO), in response to almost two decades of growing environmental concern, both in the scientific and political arena (Agrawala, 1998). Its purpose is to assess "the scientific technical and socioeconomic information relevant for the understanding of the risk of human-induced climate change" (Table 1, WWW1). The IPCC was formed specifically to inform international policy and negotiations on climate issues. The IPCC is divided into three working groups (WG) and a Task Force. WG 1 concentrates on the scientific aspects of climate change; WGII assesses the consequences of climate change; and WGIII examines options for mitigating climate change. The Task Force oversees the IPCC National Greenhouse Gas Inventories Programme (IPCC-NGGIP), which develops methodologies and software tools to calculate and report national greenhouse gas emissions and sinks.

Party countries to the UNFCC are obliged to report their national anthropogenic greenhouse gas emissions, including those from savanna burning. The IPCC is recognized as the most authoritative scientific and technical voice on climate change and its assessments influence the negotiations taking place under UNFCC. The reports should include a national inventory of anthropogenic emissions by sources and removals by sinks of all greenhouse gases not controlled by the Montreal Protocol (Table 1, WWW2). Information should be provided on CO_2, CH_4 and N_2O. Provision of CO, NO_x, NMOVOC, SO_2 and PM2.5 information is optional for non-industrialized countries. CO_2 emissions from savanna fires are not reported, since it is assumed that these fires result in no net change in carbon stocks (IPCC, 1997a). Later, a 1997 IPCC expert group meeting concluded that "this a justifiable assumption where there has been no change in fire regime, but is demonstrably untrue where the fire regime has changed over a longer time frame in both savannas and other recovering vegetation types such as forests" (IPCC 1997b). Considering that vegetation fires contribute significantly to regional CO_2, a more comprehensive account of carbon fluxes, including CO_2, is required to assess the potential long term effects of changing atmospheric CO_2 on savanna composition and structure. Simulations suggest that current trends of increased tree cover in South African savannas may be partially attributed to CO_2 fertilization from pre-industrial (270 ppm) to current CO_2 levels (360 ppm) (Bond *et al*., 2003). The proposed mechanism is that under elevated CO_2 levels, young trees can recover faster from fire, to eventually reach the heights that allow them to survive frequent fires in mesic savannas (Bond and Midgley, 2000).

Table 1. World Wide Web sites referenced.

WWW1-Intergovernmental Panel on Climate Change. http://www.ipcc.ch/
WWW2-United Nations Framework on Climate Change. http://unfccc.int/resource/docs/convkp/kpeng.html
WWW3-National Communications to the United Nations Framework Convention on Climate Change. http://unfccc.int/resource/natcom/nctable.html
WWW4-Regional air pollution in developing countries (RAPIDC). http://www.york.ac.uk/inst/sei/rapidc2/rapidc.html

Several countries in southern Africa, including Botswana, Malawi, Namibia, South Africa, Tanzania, and Zimbabwe, have provided their initial greenhouse gas emissions inventories to the IPCC (Table 1, WWW3). There appears to be a lack of uniform reporting of greenhouse gases from savanna burning among these southern African countries. This is in large part because of inconsistent interpretation of what constitutes anthropogenic savanna burning (IPCC, 1997b). There are not well defined limits of the anthropogenic influence on natural systems. As a result, some countries, such as South Africa and Malawi, report only the emissions resulting from the prescribed controlled burning of savannas, whereas other countries such as Botswana, Namibia, Tanzania and Zimbabwe report emissions from all savanna burning, since they consider it to be mostly human-induced.

Distinguishing between "natural" and "anthropogenic" fires is a challenging task in African savannas, and requires first and foremost a clarification on the definition of these terms. For example, the term "natural" is commonly used to imply lightning fires and it has been avowed that the term "anthropogenic" should be used for all savanna fires, unless they can be demonstrated to be natural (Braatz *et al*., 1995). Satellite

information on active fires and burned area does not indicate the cause of a fire. However, a combination of satellite observations of lightning (Christian *et al*., 1999) and biomass burning (Justice *et al*., 2002a) may furnish the information needed to move towards a more comprehensive accounting of anthropogenic versus natural fires due to lightning. Alternatively, it has been argued that the term ”anthropogenic” should be used to describe net emissions that result from increased human-induced burning, above a background, “natural” pre-industrial fire regime (IPCC, 1997b). This would require the construction of “natural” fire regime data based on the long human history of burning in the region. Whereas, in some savanna regions of the world (*e.g.,* Australia) this may be feasible, in some other areas (*e.g*., South Africa) this may be difficult, since very little archeological or ethnographic information exists to permit the re-creation of “natural” fire regime maps (Bond and Archibald, 2003). Other methodological problems that have been identified in the current IPCC guidelines with regards to savanna burning emissions reporting, include high uncertainties in the data used for reporting, lack of appropriate data, and the inadequate current IPCC definition of savannas that encompass also woodland savannas (IPCC, 1997b).

The IPCC methodology recommends the use of three-year averages of burned area, either from national or FAO statistics, to avoid anomalous results. If statistics are not available, then the guidelines recommend multiplying the savanna area in the country by the percentage of the savanna area that is burned annually. It should be noted though, that IPCC advocates the use of regionally applicable fuel load estimates, combustion completeness and emission factors where available, and therefore, the countries mentioned below have not necessarily used all IPCC general default values, but average

values based on limited national data. The general default IPCC assumes that 75% of total savanna area burns annually. The general default fuel load value is 660 ± 160 gm^{-2}, derived from Hao *et al*. (1990). A combustion completeness of 0.8 and 1.0 for green and dry fuel, respectively, is recommended. A fuel carbon content of 0.45 and 0.4 is recommended for green and dry fuel, respectively. IPCC provides default emission ratios (ER) for different species which are equivalent with the emission factors calculated in Table 2 assuming 0.45 fuel carbon content and 0.006 fuel nitrogen content. The IPCC recommends reporting the uncertainties in the emissions. However, currently most countries use expert judgment to specify their uncertainties qualitatively rather than quantitatively.

Table 2. Default IPCC Emission Ratios (ER) and Emission Factors (EF). Brackets show the range of values.

Species	*IPCC ER*[a]	*IPCC EF (g kg^{-1})*
CH_4	0.004	2.4
	(0.002-0.006)	(1.2-3.6)
CO	0.06	63
	(0.04-0.08)	(42-84)
N_2O	0.007	0.066
	(0.005-0.009)	(0.047-0.085)
NO_x (NO_2-based)[b]	0.121	2.385
	(0.094-0.148)	(1.853-2.918)
NO_x (NO-based)[b]	0.121	1.556
	(0.094-0.148)	(1.209-1.903)

[a] Emission ratio is the mass of carbon or nitrogen compound released as carbon or nitrogen relative to the total carbon or nitrogen released from burning.
[b] NO_2 is used as the reference gas for NO_x. In the modeling study NO is used as the reference gas for NO_x. Therefore, both are presented to allow for conversion.

The general IPPC default methodology appears to exaggerate both the area burned and the fuel load compared with this modeling study. Woodland and grassland savannas globally are estimated to occupy at least 16.1 million km^2, and approximately 48% of these (7.8 million km^2) are located in southern Africa (Scholes and Hall, 1996;

Scholes *et al*., 1996a). Based on the MODIS burned area in this study only about 20% of the total savanna area burns annually compared with the 75% of the IPCC default value. The average regional fuel loads in the locations that burned in 2000, predicted in this study (340 gm^{-2} for grasslands and 311 gm^{-2} for woodlands), are about half of the default IPCC values. The average combustion completeness at the regional level is also lower (0.57) compared with the IPCC default value, since the IPPC values are based on late dry season measurements. The regional average emission factors for CO (69.8 gkg^{-1}) and CH_4 (2.1 gkg^{-1}) are within the IPCC range. In general, large differences are found between the modeled estimates and the IPCC estimates.

Table 3 compares the latest national IPCC reports with the national emissions results from this study. Since the modeled estimates for small countries may possess a higher level of error, this intercomparison is limited to larger countries. From the results presented in Table 3 it appears, that the IPCC reports tend to largely underestimate or overestimate the emissions compared with the modeled results.

Table 3. Comparison of IPCC reported vegetation fire emissions and MODIS extrapolated emissions predicted from this study.*

Country	*IPCC CO (Gg)*	*This study CO (Gg)*	*IPCC CH_4 (Gg)*	*This study CH_4 (Gg)*
Botswana[b]	2057	588.0	76.0	11.4
Malawi[a]	11.06	111.0	0.42	3.4
Namibia[b]	1236	645.0	47	14.2
South Africa[a]	-	1116.6	12.63	26.2
Tanzania[b]	1255.4	1931.4	47.8	63.0
Zimbabwe[b]	1363	409.3	49	10.7

* Results of this study adjusted for 45% carbon content
[a] Only prescribed burning of savannas
[b] Total burning in savannas

6.2.1 Countries For Which Modeled Results Are Higher Than The IPCC Assessments

The modeled CH_4 emissions of this study for Malawi and South Africa are about 8 times and 2 times higher than the IPCC equivalents (Table 3). Furthermore, the modeled CO emissions for Malawi are about 10 times the IPCC CO emissions. The reason is, that these countries report to the IPCC only the emissions resulting from savanna prescribed burning, therefore, underestimating the total emissions from savanna fires. No specific details are provided by either country about the values used to derive their estimates. In the case of South Africa, it is interesting to note, that a report undertaken on behalf of the government, estimates the CH_4 emissions from savanna fires to be an order of magnitude higher than the modeled estimates of this study (Scholes and van der Merwe, 1996).

The IPCC emissions estimates for "un-prescribed" burning of savannas reported by Tanzania are lower by 24% compared with the modeled emissions of this study (Table 3). The Tanzanian IPCC estimates are derived assuming that 32% of the national savanna area burns (51.2×10^3 km^2) and that about 86% of the burning occurs in humid savannas (Table 4). Based on this study, approximately 3.3 times more area burned in Tanzania in 2000 (171×10^3 km^2). In humid savannas, the IPCC value for fuel consumed is 465 gm^{-2} whereas in semi-arid savannas the respective IPCC value is 351 gm^{-2}. In comparison, the respective modeled average value for biomass consumed per unit area is 151 gm^{-2}. The modeled average emission factors for CO and CH_4 in Tanzania are 75 gkg^{-1} and 2.4 gkg^{-1}, respectively, and are within the range of the default IPCC values shown in Table 2. This is an example of how large offsetting differences in the fuel load and burned area may produce relatively similar emissions results between methods.

Undoubtedly, this becomes a critical issue when the aim moves away from solely producing an emissions number, towards understanding the interactions of the key processes that affect fire emissions or when fire management features in carbon trading.

6.2.2 Countries For Which Modeled Results Are Lower Than The IPCC Assessments

Large discrepancies are also found for Botswana, Namibia and Zimbabwe, between the IPCC estimates and the modeled results of this study. For these countries, the IPPC values are higher than the modeled values (Table 3). The IPCC CH_4 estimates are 6.7, 3.3 and 4.6 times higher for the corresponding countries. The IPCC CO estimates for Botswana, Namibia and Zimbabwe are 3.5, 1.9 and 3.3 times higher than the

Table 4. Comparison of national IPCC values for burned area, fuel load, combustion completeness (CC) and emission factors (EF) with the respective average regional values for the MODIS extrapolated results. Only countries that explicitly report the values used to derive emissions are reported. Average regional fuel load values for this study are derived from the GBA-2000 results.

	Tanzania	*Botswana*	*Namibia*
IPCC burned area	33.3[a],17.9[b]	87.9	51.1
This study burned area	171	47.9	46.8
IPCC fuel load	561[a], 405[b]	360	600
This study fuel load	226	473	494
IPCC CC	0.80[c],0.99[d]	1.0	0.80
This study CC	0.67	0.73	0.69
IPCC EFCO	63	65	63
This study EFCO	75	39.5	40.4
IPCC $EFCH_4$	2.4	2.4	2.4
This study $EFCH_4$	2.4	0.77	0.89

[a] humid savannas, [b] semi-arid savannas, [c] living biomass, [d] dead biomass

corresponding modeled CO emissions. The estimates in Botswana are derived using an average fuel load of 360 gm^{-2} and assuming that on average 15 % of the land area of

Botswana ($87.9x10^3$ km^2) burns annually (Table 4). CO emissions are not explicitly reported in the IPCC but calculated here based on the emission factors by Delmas *et al*. (1995). The default combustion completeness for dry fuels (100%) is assumed. This implies that the average biomass burnt in this case is equal to the average fuel load value. The average combustion completeness for Botswana from this study is 0.73. The average biomass burnt predicted for Botswana of 345 gm^{-2} in this study is very similar to the default IPCC value but the burned area predicted is much lower ($47.9x10^3$ km^2). The average $EFCH_4$ from this study is 0.77 gkg^{-1} and is about 3.1 times lower than the 2.4 gkg^{-1} IPCC value by Delmas *et al*. (1995). The average EFCO from this study is 39.5 gkg^{-1} and is 1.6 times lower than the 65 gkg^{-1} by Delmas *et al*. (1995). The low emission factors for products of incomplete combustion in this study are because the majority of the annual burning in Botswana occurs in grasslands (about 91%) and to a large extent in the late dry season. Therefore, the discrepancy between the two methods is mostly attributed to the difference in emission factors and burned area. The claimed level of accuracy in the IPCC CH_4 estimate is ±40% and is attributed to uncertainties in the fuel load.

The Namibian report is based on an average fuel load of 600 gm^{-2}, combustion completeness of 0.80 and an area burned of $51.1x10^3$ km^2 (Table 4). The burned area for Namibia in this study ($46.8x10^3$ km^2) is close to the IPCC value, whereas the average fuel load (494 gm^{-2}) and average combustion completeness (0.69) are somewhat lower. The burned area is based on reports on three regions in the country. The IPCC default emission factors are used. The CO emissions are not explicitly reported but are calculated using the IPCC default emission factor for CO. The emission factors for products of

incomplete combustion are also lower in this study ($EFCH_4$ = 0.89 g kg^{-1}, EFCO = 40.4 gkg^{-1}) and are the main reason for the lower emissions in this study compared with the IPPC report. As in the case of Botswana, grassland fires account for the majority of the burning in Namibia (93%) and are mostly concentrated in the late dry season. The report acknowledges that these estimates are likely an overestimate, but they suggest that the plausible reason is the high fuel load value used rather than the emission factors. The rationale for using the high fuel load value is that it compensates for other places, which burn and are omitted from the report due to the lack of available data.

Zimbabwe used the modeling methodology by Scholes *et al*. (1996a; 1996b) to derive the burned area and biomass burned. Furthermore, emission factors from the literature were used, but no mention of the specific sources is provided. The report places the total biomass burned to 16380 Gg compared to 7500 Gg in this study. It is unclear how Zimbabwe applied the Scholes *et al* (1996a; 1996b) approach since the estimates given by Scholes *et al*. (1996a) for Zimbabwe are substantially lower (8 Gg for CH_4 and 265 Gg for CO). It is highly unlikely that these differences between IPCC and Scholes *et al*. (1996a) can be explained solely by dissimilar emission factors used in the two methods.

Regardless of modeled emissions accuracies, the above comparisons highlight the problems associated with using single universal values to quantify fire emissions and the current approach to national IPCC reporting. Fire is a dynamic process both in the space and the time domain and simplifications along the lines recommended by IPCC are inadequate to describe the nature of fire emissions. The spatially and temporally explicit modeling methodology presented here, which utilizes a suite of satellite data in concert

with fire behavior studies, can reduce uncertainties in emissions estimates and provide a means to develop emission inventories that are consistent and comparable across sectors and party nations. This approach together with the recommendations by experts for long-term revision of the inventory guidelines (IPCC, 1997b) suggests that the development of standardized spatially and temporally explicit modeling tools should be a priority for research.

6.3 Air Quality Monitoring

Air pollution is viewed as an increasingly important environmental problem in Africa which demands more attention. The Air Pollution Information Network Africa (APINA) is a southern African network of scientists, policy makers and private sector and non-governmental organizations, aiming to facilitate the development of agreements, protocols and methods to implement measures which prevent and control air pollution and its likely transboundary effects (Table 1, WWW4). The development of standardized methodologies to monitor main regional pollutants, including CO, NO_x, O_3, VOC and aerosols, and the collection of related datasets are among the regional activities of APINA. The focus is on anthropogenic emissions, including emissions from savanna fires. APINA may be viewed as a key user of the methodology developed to assess savanna fire emissions and the information provided by this study.

6.4 Fire Management Policy Development

In southern Africa a key policy issue is whether wildland fires pose a sufficiently serious problem to require some form of legislative or administrative response, and if they do, what factors govern their incidence and impacts and what are the relative costs and benefits of different options for reducing the extent and severity of the adverse

impacts (Frost, 1999). In most southern African ecosystems fire is a natural and beneficial disturbance of vegetation structure and composition and plays an important role in nutrient recycling and distribution. Problems with regards to fire in southern Africa most usually arise from unwarranted and uncontrolled burning. In most southern African countries regulations that govern the use and control of fires are in place, however they are seldom enforced (Frost 1999). Unlike in Southeast Asia (Tay, 2002), atmospheric considerations are currently not part of African fire management. Addressing all the issues that need to be taken into account to facilitate the development of informed policy recommendations is beyond the scope of this dissertation. A brief account of some of the related concerns is provided and the emissions results of this study are placed within this context.

The ecological role of fire in the maintenance of structure and function of African ecosystems is well established but certain aspects remain contentious. In general, frequent, late dry season fires have been observed to lead to changes in miombo woodland species composition and vegetation structure (Frost, 1996; Chidumayo *et al*., 1996; Mapaure and Campbell, 2002). Most of the dominant canopy species in miombo woodlands (*Julbernardia paniculata, Isoberlinia angolesis, Brachystegia spiciformis* and *Brachystegia longifolia*) are fire-tender species that decline under regular burning. Late dry-season fires occurring during the "early greening" period of the miombo woodlands, prior to spring rains, can be especially destructive (Frost, 1996). Fire may act in conjunction with disturbance by people, animals (predominantly elephants) and less obvious factors, *e.g*., porcupines and windstorms (Scholes and Walker 1993), to influence the balance between trees and grasses. In certain circumstances, frequent late dry season

fires have led to the conversion of woodlands into open tall grass savannas with scattered understorey trees and shrubs, potentially reducing the carbon storage in these areas (Mapaure and Campbell, 2002).

Early burning has been suggested as providing a practical way to protect and manage miombo woodlands (Frost, 1996). Early burning can significantly reduce the incidence of late dry season fires and favors woody plants and their recovery (Guy, 1989; Leuthold, 1996; Chidumayo *et al*., 1996; Mapaure and Campbell, 2002). At the same time, the atmospheric ramifications of early dry season-burning practices are unknown. Based on this study, early burning at the regional level emits less trace gases and particulates per unit area compared with late dry season burning. Hence, if the timing of the burning were to be shifted to earlier in the dry season, when the fuel is generally wetter, potentially, emissions from vegetation fires could be reduced. If the fuel remains dry during the whole dry season, then the timing of the burning becomes less important, from the point of reducing regional emissions budgets. Hence, from an atmospheric chemistry perspective, it appears that early burning is not undesirable.

The above should not be regarded as a recommendation for exclusion of late dry season fires. Not only would this be impractical, but late dry season burning is used as a management tool for grassland systems, and is embedded in the cultural traditions of local communities (Chidumayo *et al*., 1996). Farmers will burn the dry, unpalatable grasses to produce green grass for livestock. Late dry season intense fires might also be necessary for prevention of bush encroachment in grasslands (Bond and Archibald, 2003). Large areas in South Africa are affected by this phenomenon. Some cultures have fire ceremonies during which fires are lit in the late dry season. For example, in Malawi

late dry season burning has symbolic significance in calling the coming of the rains (Schoeffeleers, 1971). Furthermore, burning too early may induce grass growth which exhausts soil water reserves until the next rains (San José and Medina, 1975). In addition, through the integrative nature of the recirculative, predominantly anticyclonic, atmospheric gyre in southern Africa, dry deposition of aerosol material that contains biogeochemically important species (*e.g.*, nitrogen and phosphorus) can be an important nutrient source to ecosystems downwind (Garstang *et al*., 1998). The response of these ecosystems to aerosol deposition, and even more so to a changing of the timing of the burning, is not known. The formulation of sound fire management policies necessitates evaluation of the economic, socio-cultural, ecological and atmospheric benefits versus the adverse effects of different burning practices (Frost 1999).

Chapter 7: Summary

The importance of biomass burning in the tropics as a source of a variety of greenhouse gases and ozone precursors has been long recognized. However, previous emissions studies for southern Africa have largely ignored the seasonal variability of the emissions and the associated implications for emissions quantification. The research of this dissertation investigated the seasonal and spatial patterns of trace gas and particulate emissions from grassland and woodland fires in southern Africa for the year 2000. The spatially and temporally explicit modeling framework developed to incorporate and assess the seasonal dynamics of emissions, synthesized recently published satellite-driven and satellite-derived products with empirically derived parameterizations of fire emissions characteristics. This emissions model provides an improvement over previous studies because it accounts for explicit variations in emissions from vegetation fires as a function of space, time, land cover and the type of combustion.

Results of this research at the landscape scale for grassland fires provided the preliminary evidence for the significance of early dry season burning on annual emissions estimation, mainly for products of incomplete combustion. Furthermore, these results underscored a critical gap in our knowledge regarding the seasonal variations of emission factors for savanna fires and the associated parameterizations that can be used for regional emissions estimation. An important finding of this dissertation is that emission factors for trace gases and particulates exhibit significant seasonal trends, as they relate to the fuel moisture condition, and that these trends are different for grassland and woodland fires, due to differences in the fire behavior for these two land cover types. The seasonal modified combustion efficiency for grassland fires is largely controlled by grass moisture changes, resulting in up to 5 times higher emission factors for products of incomplete

combustion in the early dry season, compared with the late dry season. The seasonal modified combustion efficiency for woodland fires is controlled by the fuel composition heterogeneity, resulting in progressively lower emission factors for products of incomplete combustion as the dry grass becomes proportionally higher in the fuel mixture.

In the early stages of the research it was recognized that uncertainties in fuel moisture content would affect the regional emissions estimation. The fuel greenness is assessed in this dissertation using two independent methodologies and is applied to parameterize the combustion completeness and emission factors for grassland and woodland fires at the regional scale. One method is based on the fuel load model inputs and the other on an adjustment performed using a satellite derived NDVI. The NDVI-based method is developed because it was observed that the fuel load model under-predicted the amount of green grass relative to dead grass, when in fact persistent greenness during the 2000 dry season was evident both in satellite imagery and in the field. Furthermore, comparison of the fuel-based and NDVI-based methods allowed for an assessment of the sensitivity of the emissions results to different levels of fuel greenness. The NDVI method predicts higher levels of greenness, mostly during the early dry season, and is in better agreement with empirical measurements of fuel moisture.

The regional emissions modeling analysis conducted in this dissertation reveals that southern African emissions are largely dominated by subhumid infertile woodland fires concentrated in a band that stretches across the subcontinent between about 5^{o}S and 15^{o}S. The variable seasonal mixture of grassland and woodland fires, with distinct fire behaviors in these two land cover types, determines the net regional emissions. Seasonal

fuel moisture changes have significant implications for the emissions from woodland fires. Emission densities for all atmospheric species are lower in the early dry season than in the late dry season because less fuel gets consumed in the fires. These differences in seasonal emission densities are much larger in the NDVI-method than in the fuel load based method because of the larger effect of the increased fuel moisture on lowering the combustion completeness. In fact, the seasonal emission density differences for woodland fires are so large in the NDVI-method, that even though more area burns in the early dry season, lower quantities for all atmospheric species are emitted compared with the late dry season. On the other hand, the seasonal emission density differences for woodland fires are smaller in the fuel load method, so that because more area burns in the early dry season, higher quantities for all atmospheric species are emitted compared with the late dry season.

For grassland fires, the regional seasonal emissions dynamics are mainly controlled by the trade-off effect between lower combustion completeness and higher emission factors for products of incomplete combustion in the early dry season (wetter grass fuel) and between higher combustion completeness and lower emission factors for products of incomplete combustion at the end of the dry season (drier grass fuel). The magnitude of this trade-off effect depends on the fuel moisture condition. Emission densities for products of incomplete combustion are higher in the early dry season than in the late dry season when using the NDVI method, suggesting that early dry season burning in wetter fuels favors smoldering combustion. In the fuel load-based method, since the grass is predicted to be relatively dry throughout the dry season, emission densities for products of incomplete combustion are rather comparable between early and

late dry season. The net seasonal emissions for products of incomplete combustion depend on the seasonal timing and extent of burning and the seasonally changing emissions densities. Thus, for some products of incomplete combustion (*e.g.*, CH_4), comparable (fuel load method) or higher (NDVI method) emissions result in the early dry season, despite the fact that the majority of the burning in grasslands occurs in the late dry season. On the other hand, for other products of incomplete combustion (*e.g.*, CO) the seasonal differences in emission densities are not large enough to outweigh the higher burned area in the late dry season. Higher emissions of fully oxidized species (*e.g.*, CO_2) associated with flaming combustion occur from grassland fires at the regional scale in the late dry season compared with the early dry season.

The research in this dissertation furnishes unique information about the interactions among the key processes that determine emissions from vegetation fires in southern Africa. The need for a spatio-temporally explicit approach to estimate fuel loads, burned area, combustion completeness and emission factors, rather than representative values for broad vegetation types used by classification methodologies, is clearly demonstrated here. The significance of vegetation fires for the regional trace gas and particulate budgets remains prominent, even when other major sources are considered. A large number of atmospheric species presented in this dissertation are modeled for the first time at the regional level. The modeled estimates for 2000 are (in Tg): 537 CO_2, 23.2 CO, 0.726 CH_4, 0.661 NMHC, 2.4 particulates (< 2.5 μm), 1.0 NO_x Especially important is the high contribution of Oxygenated Volatile Organic Compounds (OVOCs) (1.8 Tg) to regional emissions (higher than CH_4+NMHC), which

indicates that these compounds need to be routinely integrated into future emissions modeling studies.

The results of this study indicate that consideration of the seasonal variability in emissions may lower the estimates of trace gas emissions and particulates. At the regional level, the fuel load-based emissions estimates are 52-61% higher than the corresponding NDVI-based emissions. These results suggest, that the wetness of the fuel significantly affects emissions but contest the hypothesis by Hoffa *et al.* (1999), that incorporation of early season burning will increase the estimates of products of incomplete combustion. The results are in agreement with some previous satellite land-based emissions studies for the region, in the sense that they predict lower emissions compared with classification methods. The disagreement of this study with more recent land-based biogeochemically driven emission studies (van der Werf *et al*., 2003; 2004) is mainly attributed to differences in fuel loads and burned area. Discrepancies between the bottom-up based approach of this research with top-down atmospheric based approaches (Arellano *et al*., 2004) still persist but may be lower than previously thought. When extrapolating the study results from southern Africa to the scale of the African continent, the contribution of African savanna fires to global emission estimates reported by Andreae and Merlet (2001) appears smaller than previously thought (about 3 times lower). However, the Andreae and Merlet (2001) estimates are also based on a classification approach and may overestimate pyrogenic emissions. In any case, it appears from this study that incorporation of the seasonal dynamics of vegetation fire emissions will affect regional emissions estimation by lowering emissions estimates even more rather than increasing them.

Potential applications of this research include the development of harmonized emission methodologies for IPCC national greenhouse gas reporting, regional air quality monitoring and examination of the atmospheric considerations of different fire management policies. In general, large differences are found between IPCC national reports and the modeled results of this study. The IPCC reports tend to significantly underestimate or overestimate the emissions compared with the modeled results. This is due to the inadequate representation of the emissions model variables used by the IPCC classification methodology compared to the spatially and temporally explicit modeling approach. A case of opposite and offsetting differences in the fuel load and burned area producing relatively similar emissions results between the IPCC estimates and this study is also found. This comparison highlights the problems associated with using single universal values to quantify fire emissions and supports recent IPCC expert panel recommendations for methodological improvements to national IPCC reporting.

The improvements in spatially-explicit regional emissions modeling have been rather incremental and have been hampered by the lack of reliable datasets. A first important step forwards towards obtaining baseline data on the extent of vegetation fires from southern Africa is the relatively recent development of three satellite-derived burned area datasets from the MODIS, SPOT-VEGETATION and ATSR-2 sensors. This study is the first to utilize three different satellite derived estimates of burned area at the regional scale. Considerable differences exist among the three burned area products with respect to the amounts and the spatial distribution of burned area. Among the central findings of this dissertation is that differences in the estimated emissions for various atmospheric species are not directly proportional to the differences in the burned area

amounts. This suggests, that simple extrapolations based on the burned area amount will introduce different levels of uncertainty for the various atmospheric species. This underscores the need for a spatially explicit, or at least land cover-based, accuracy assessment of burned area data, so that the uncertainty in the emissions model with respect to burned area may be determined. The sensitivity analysis with respect to satellite burned area inputs described in this study provides a limited verification of the model's structure and specifications. The model's predictions, regardless of burned area, are consistent with published field studies of emissions from woodland and grassland fires (Ward *et al.*, 1996) showing that burning in woodlands favors emissions of products of incomplete combustion compared with grasslands, which favors emissions of fully oxidized products.

Further research is required to improve input variables and fire emissions characterization for seasonal emissions estimation at the regional scale. The first order error analysis performed in this work highlights several of the uncertainties in the current bottom-up emissions modeling approach. A spatially explicit Monte Carlo uncertainty analysis may help define these uncertainties more rigorously. Particular attention should be given to create fuel load datasets that also contain associated uncertainty information and that can representatively capture some of the large heterogeneity in fuel amounts and fuel composition encountered in southern African savannas. Early dry season combustion completeness field measurements, especially for woodland fires, are also needed with high priority. Furthermore, a larger number of seasonal, ecosystem-specific emission factors are required to develop better predictive models of emission factors. The development of seasonal fuel chemistry databases will improve the characterization of

nitrogen, halogen and sulfur containing emission compounds. A compelling need for the prediction of combustion completeness and emission factors at the regional level is the reliable assessment of the fuel moisture content.

Remote sensing has a major role in reducing some of the uncertainties remaining in the emissions estimation process and/or providing independent routes to emissions estimates. This is particularly true with the recent availability of calibrated, atmospherically corrected, cloud-screened, geolocated data provided by the latest generation of global moderate resolution remote sensing systems. The MODIS Vegetation Index (VI) products hold promise for a more precise measure of the spatial and temporal variation in vegetation condition. Improved algorithms for determining fuel moisture content using the MODIS land surface reflectance product for visible and shortwave infrared bands also offer promise (Zarco-Tejada *et al.*, 2003). Other, currently experimental satellite based measurements of the fire radiative energy may offer an important new way of estimating the amount of fuel consumed (Kaufman *et al.*, 1998; 2003; Wooster, 2002). Satellite based techniques for direct estimation of atmospheric aerosol loading are also under development (Kaufman *et al.*, 1998; 2003). The MODIS Net Primary Production (NPP) product may be evaluated as an input to fuel load models. Through the synergestic use of the newer and improved satellite products with heritage satellite products it will be feasible to run an improved class of models to estimate the inter-annual variations in emissions. Nevertheless, all these satellite products require validation with independent data. Constraining these uncertainties will help identify the actual reasons for the still unresolved discrepancy between land-based and atmospheric-based emission estimates.

This study provides new insights into biomass burning emissions from the southern Africa region and a contribution to reducing uncertainties in current estimates. It demonstrates the complexity of the processes and how they can be resolved by the combination of new satellite data sets and spatially explicit modeling. The results have direct implications for national reporting of savanna fire emissions. It is hoped, that a standardized approach to emissions modeling will be adopted in the region, providing an improved understanding of inter and intra annual variability.

Appendix A

Chapter 3:

Table 1. Concentrations of emitted CO_2, CO, CH_4, NMHC, and PM2.5 and the proportion of total fuel consumed by the grassland (G) and woodland (W) fires.

Site	*CO_2 (ppm)*	*CO (ppm)*	*CH_4 (ppm)*	*NMHC (ppm)*	*PM2.5 (mgm^{-3})*	*FASS fuel ratio*
G1AF*[, a]	201.8	19.58	1.061	0.821	1.430	1.00
G1AS[b]	---	---	---	---	---	---
G1BF	15.8	1.89	0.103	0.120	0.200	0.86
G1BS	1.2	0.26	0.027	0.008	0.200	0.14
G2AF	376.8	30.93	1.608	1.311	2.180	0.94
G2AS	93.3	4.87	0.172	0.190	0.350	0.06
G2BF	198.1	22.33	1.216	1.041	1.620	1.00
G2BS	3.8	0.61	---	0.019	0.240	0.00
G3AF	246.5	10.55	0.393	0.350	0.770	0.99
G3AS	1.7	0.10	---	---	0.150	0.01
G3BF	233.9	12.15	0.503	0.488	0.645	0.98
G3BS	7.1	1.19	0.055	0.032	0.290	0.02
G4AF	423.7	18.94	0.761	0.569	1.040	0.99
G4AS	0.0	0.31	0.009	0.000	0.320	0.01
G4BF	840.7	24.44	0.913	0.787	1.290	1.00
G4BS	9.2	0.64	0.027	0.037	0.215	0.00
G4CF	336.1	14.07	0.519	0.423	0.770	1.00
G4CS	3.2	0.52	0.026	0.012	0.405	0.00
G5AF	413.6	13.39	0.435	0.401	0.940	0.99
G5AS	0.6	0.58	0.011	0.021	0.040	0.01
G5BF	501.4	12.73	0.382	0.381	1.185	0.99
G5BS	2.0	0.18	---	---	0.075	0.01
G6AF	10.7	1.32	0.029	0.040	---	0.80
G6AS	6.0	1.25	0.054	0.052	---	0.20

G6BF	94.1	4.70	0.150	0.140	---	0.96
G6BS	6.1	1.75	0.066	0.016	---	0.04
G6CF	49.0	2.44	0.082	0.056	---	1.00
G6CS	7.9	1.51	0.082	0.031	---	0.00
G7AF	1042.7	61.01	3.823	2.335	4.580	1.00
G7AS	19.6	2.42	0.149	0.142	0.950	0.00
G7BF	471.0	36.40	2.287	1.274	2.575	0.98
G7BS	5.8	0.79	0.045	0.026	0.580	0.02
G7CF	612.2	25.95	1.558	1.052	2.695	1.00
G7CS	3.6	0.72	0.056	0.047	0.955	0.00
W1AF	345.0	23.91	---	---	3.130	1.00
W1AS	46.6	2.55	0.118	0.090	0.080	0.00
W1BF	109.6	7.08	0.314	0.228	0.495	1.00
W1BS	13.5	0.80	0.036	0.018	0.215	0.00
W2AF	974.2	75.22	4.517	1.954	8.770	---
W2AS	77.5	9.94	0.722	0.210	0.560	---
W2BF	222.0	8.22	0.243	0.198	---	---
W2BS	46.1	3.11	0.112	0.063	---	---
W2CF	702.8	27.29	0.997	0.518	2.990	1.00
W2CS	26.9	3.57	0.145	0.058	0.195	0.00
W3AF	545.5	38.00	2.080	1.001	3.790	0.97
W3AS	24.5	2.54	0.175	0.077	0.340	0.03
W3BF	255.0	12.52	0.538	0.339	1.010	0.99
W3BS	156.0	1.67	0.084	0.024	0.145	0.01
W3CF	64.3	3.58	0.151	0.113	0.680	---
W3CS	38.9	2.86	0.140	0.083	0.295	---
W4AF	457.4	29.94	1.646	0.648	1.820	0.99
W4AS	59.6	8.59	0.564	0.185	0.320	0.01
W4BF	761.2	49.89	2.665	1.158	5.120	1.00
W4BS	92.9	8.49	0.538	0.227	0.885	0.00
W4CF	135.4	6.29	0.235	0.157	1.075	0.94
W4CS	48.7	3.87	0.191	0.133	0.480	0.06

W5AF	132.8	8.13	0.380	0.245	0.715	0.03
W5AS	289.2	17.26	0.948	0.365	1.965	0.97
W5BF	804.9	43.78	2.190	1.079	5.480	0.67
W5BS	265.3	22.99	1.405	0.516	1.730	0.33
W5CF	646.1	48.56	2.659	1.088	5.310	1.00
W5CS	58.0	7.30	0.456	0.162	0.450	0.00
W6AF	370.9	41.17	2.774	0.928	5.590	0.82
W6AI[c]	89.3	12.65	0.895	0.261	1.010	0.11
W6AS	25.7	4.18	0.282	0.099	0.895	0.07
W6BF	982.4	91.85	5.810	2.131	18.410	0.86
W6BI	185.5	25.59	1.837	0.497	1.850	0.09
W6BS	65.2	8.29	0.571	0.170	0.88	0.05
W6CF	483.1	41.78	2.522	0.921	6.765	---
W6CI	117.2	13.04	0.822	0.277	0.600	---
W6CS	46.9	6.04	0.423	0.158	0.900	---

[*] The letters A, B, and C refer to the 3 sampling clusters centered around each FASS tower that were used to calculate the average at each plot.

[a] F denotes flaming combustion.

[b] S denotes smoldering combustion.

[c] I denotes intermediate combustion.

[d] Italics denote samples that were not included in the analysis on the basis of marginal net concentrations (< 20 ppm CO_2).

Appendix B

Chapter 4:

Table 4. MODIS-based regional fire emissions (in Gg = 10^9g), southern Africa, September 2000.

*Species**	*Woodlands*	*Grasslands*	*Regional*
Carbon dioxide (CO_2)	93393	40387	133780
Carbon monoxide (CO)	5100	767	5867
Methane (CH_4)	174.8	13.3	188.1
Nonmethane hydrocarbons (NMHC)	137.9	20.5	158.4
Nitrogen oxides (as NO)	189.8	70.1	259.9
Dimethyl sulfide (CH_3SCH_3)	0.146	0.036	0.182
Methyl bromide (CH_3Br)	0.089	0.013	0.102
Methyl chloride (CH_3Cl)	4.6	1.3	5.9
Methyl iodide (CH_3I)	0.101	0.029	0.13
Methyl nitrate (CH_3ONO_2)	0.027	0.004	0.031
Ethane (C_2H_6)	12.9	1.9	14.8
Ethene (C_2H_4)	44.6	6.6	51.2
Propane (C_3H_8)	3.882	0.574	4.456
Propene (C_3H_6)	14.443	0.682	15.125
Acetylene (C_2H_2)	12.5	1.8	14.3
i-butane (*i*-C_4H_{10})	0.2321	0.0055	0.2376
n-butane (*n*-C_4H_{10})	1.249	0.185	1.434
t-2-butene (C_4H_8)	1.249	0.185	1.434
1-butene (C_4H_8)	3.005	0.299	3.304
c-2-butene (C_4H_8)	0.892	0.132	1.024
i-pentane (*i*-C_5H_{12})	0.134	0.02	0.154
n-pentane (*n*-C_5H_{12})	0.55	0.11	0.66
1, 3-butadiene (C_4H_6)	3.897	0.431	4.328
3-methyl-1-butene (C_5H_{10})	0.446	0.066	0.512
t-2-pentene (C_5H_{10})	0.2321	0.0055	0.2376
2-methyl-2-butene (C_5H_{10})	0.446	0.066	0.512
2-methyl-1-butene (C_5H_{10})	0.491	0.073	0.564
Isoprene (C_5H_8)	3.109	0.605	3.714
n-heptane (C_7H_{16})	0.937	0.139	1.076
Benzene (C_6H_6)	12.9	1.9	14.8
Toluene (C_7H_8)	9.4	1.4	10.8
Formaldehyde (HCHO)	75	14.4	89.4
Methanol (CH_3OH)	89	11.6	100.6
Acetic acid (CH_3COOH)	185.5	23.1	208.6
Formic Acid (HCOOH)	48.4	11	59.4
Ammonia (NH_3)	18.8	3.4	22.2
Hydrogen Cyanide (HCN)	33.4	10	43.4
Particulates < 2.5 μm (PM2.5)	586.9	44.4	631.3
Total particulate matter (TPM)	1077	101	1178
Organic carbon (OC)	221.6	47.3	268.9
Black Carbon (BC)	25.9	3.8	29.7
Chloride (Cl^-)	117.5	2.9	120.4

Nitrate ($NO3^-$)	16.4	3.9	20.3
Sulfate (SO_4^{2-})	18.4	1.3	19.7
Potassium (K^+)	71.4	10.6	82

Table 5. GBA-2000-based regional fire emissions (in Gg = 10^9g), southern Africa, September 2000.

*Species**	*Woodlands*	*Grasslands*	*Regional*
Carbon dioxide (CO_2)	53935	36320	90255
Carbon monoxide (CO)	2711	680	3391
Methane (CH_4)	89.2	11.6	100.8
Nonmethane hydrocarbons (NMHC)	74.8	17.8	92.6
Nitrogen oxides (as NO)	107.6	63.0	170.6
Dimethyl sulfide (CH_3SCH_3)	0.079	0.032	0.111
Methyl bromide (CH_3Br)	0.047	0.017	0.064
Methyl chloride (CH_3Cl)	2.5	1.1	3.6
Methyl iodide (CH_3I)	0.056	0.026	0.082
Methyl nitrate (CH_3ONO_2)	0.0142	0.0035	0.0177
Ethane (C_2H_6)	6.9	1.7	8.6
Ethene (C_2H_4)	23.7	5.8	29.5
Propane (C_3H_8)	2.060	0.509	2.569
Propene (C_3H_6)	7.420	0.576	7.996
Acetylene (C_2H_2)	6.6	1.6	8.2
i-butane (*i*-C_4H_{10})	0.1161	0.0042	0.1203
n-butane (*n*-C_4H_{10})	0.663	0.164	0.827
t-2-butene (C_4H_8)	0.663	0.164	0.827
1-butene (C_4H_8)	1.571	0.262	1.833
c-2-butene (C_4H_8)	0.474	0.117	0.591
i-pentane (*i*-C_5H_{12})	0.071	0.018	0.089
n-pentane (*n*-C_5H_{12})	0.297	0.098	0.395
1, 3-butadiene (C_4H_6)	2.044	0.379	2.423
3-methyl-1-butene (C_5H_{10})	0.237	0.058	0.295
t-2-pentene (C_5H_{10})	0.1161	0.0042	0.1203
2-methyl-2-butene (C_5H_{10})	0.237	0.058	0.295
2-methyl-1-butene (C_5H_{10})	0.260	0.064	0.324
Isoprene (C_5H_8)	1.673	0.539	2.212
n-heptane (C_7H_{16})	0.497	0.123	0.62
Benzene (C_6H_6)	6.9	1.7	8.6
Toluene (C_7H_8)	5.0	1.2	6.2
Formaldehyde (HCHO)	40.4	12.8	53.2
Methanol (CH_3OH)	47.0	10.3	57.3
Acetic acid (CH_3COOH)	97.8	20.4	118.2
Formic Acid (HCOOH)	26.3	9.8	36.1
Ammonia (NH_3)	10.1	3.0	13.1
Hydrogen Cyanide (HCN)	18.6	9.0	27.6
Particulates < 2.5 μm (PM2.5)	295.3	39.3	334.6
Total particulate matter (TPM)	562.0	88.5	650.5

Organic carbon (OC)	120.0	42.2	162.2
Black carbon (BC)	13.7	3.4	17.1
Chloride (Cl^-)	60.0	2.2	62.2
Nitrate ($NO3^-$)	8.9	3.5	12.4
Sulfate (SO_4^{2-})	9.6	1.1	10.7
Potassium (K^+)	37.9	9.4	47.3

Table 6. GLOBSCAR-based regional fire emissions (in Gg = 10^9g), southern Africa, September 2000.

*Species**	*Woodlands*	*Grasslands*	*Regional*
Carbon dioxide (CO_2)	24951	5368	30319
Carbon monoxide (CO)	1284	109	1393
Methane (CH_4)	42.8	2.0	44.8
Nonmethane hydrocarbons (NMHC)	35.2	3.1	38.3
Nitrogen oxides (as NO)	50.0	9.4	59.4
Dimethyl sulfide (CH_3SCH_3)	0.037	0.0049	0.0419
Methyl bromide (CH_3Br)	0.022	0.0019	0.0239
Methyl chloride (CH_3Cl)	1.184	0.170	1.354
Methyl iodide (CH_3I)	0.026	0.0040	0.03
Methyl nitrate (CH_3ONO_2)	0.0067	0.0006	0.0073
Ethane (C_2H_6)	3.255	0.271	3.526
Ethene (C_2H_4)	11.223	0.935	12.158
Propane (C_3H_8)	0.976	0.081	1.057
Propene (C_3H_6)	3.550	0.116	3.666
Acetylene (C_2H_2)	3.142	0.262	3.404
i-butane (*i*-C_4H_{10})	0.0560	0.0012	0.0572
n-butane (*n*-C_4H_{10})	0.314	0.026	0.34
t-2-butene (C_4H_8)	0.314	0.026	0.34
1-butene (C_4H_8)	0.748	0.045	0.793
c-2-butene (C_4H_8)	0.224	0.019	0.243
i-pentane (*i*-C_5H_{12})	0.0337	0.0028	0.0365
n-pentane (*n*-C_5H_{12})	0.140	0.015	0.155
1, 3-butadiene (C_4H_6)	0.972	0.063	1.035
3-methyl-1-butene (C_5H_{10})	0.112	0.0093	0.1213
t-2-pentene (C_5H_{10})	0.0560	0.0012	0.0572
2-methyl-2-butene (C_5H_{10})	0.1122	0.0093	0.1215
2-methyl-1-butene (C_5H_{10})	0.123	0.010	0.133
Isoprene (C_5H_8)	0.790	0.084	0.874
n-heptane (C_7H_{16})	0.236	0.020	0.256
Benzene (C_6H_6)	3.255	0.271	3.526
Toluene (C_7H_8)	2.357	0.196	2.553
Formaldehyde (HCHO)	19.1	2.0	21.1
Methanol (CH_3OH)	22.3	1.7	24
Acetic acid (CH_3COOH)	46.4	3.3	49.7
Formic Acid (HCOOH)	12.4	1.5	13.9
Ammonia (NH_3)	4.764	0.469	5.233
Hydrogen Cyanide (HCN)	8.7	1.4	10.1
Particulates < 2.5 μm (PM2.5)	142.2	6.3	148.5

Total particulate matter (TPM)	267.7	15.1	282.8
Organic carbon (OC)	56.5	6.5	63
Black Carbon (BC)	6.509	0.542	7.051
Chloride (Cl^-)	28.767	0.600	29.367
Nitrate ($NO3^-$)	4.194	0.529	4.723
Sulfate (SO_4^{2-})	4.560	0.200	4.76
Potassium (K^+)	18.0	1.5	19.5

Table 9. Intercomparison of the MODIS, GBA-2000 and GLOBSCAR burned area, selected trace gases and PM2.5 per country in southern Africa for September 2000

Country	*MODIS Area (km^2 x 10^2)*	*GBA-2000 Area (km^2 x 10^2)*	*GLOBSCAR Area (km^2 x 10^2)*	*MODIS CO_2 (Tg)*	*GBA-2000 CO_2 (Tg)*	*GLOBSCAR CO_2 (Tg)*	*MODIS CO (Gg)*	*GBA-2000 CO (Gg)*	*GLOBSCAR CO (Gg)*
Angola	444.9	333.1	118.9	29.824	24.707	6.461	907.11	632.74	314.33
Botswana	70.1	59.5	5.9	4.749	4.006	0.417	92.83	77.72	9.14
Burundi	2.6	0.8	0.9	0.102	0.035	0.041	4.81	1.09	1.96
Malawi	25.5	20.2	3.2	1.112	0.968	0.144	60.03	49.34	9.56
Mozambique	636.4	323.5	116.3	27.789	13.548	5.560	1517.33	742.85	266.77
Namibia	150.6	128.7	5.0	10.163	8.506	0.296	195.36	162.06	5.42
Rwanda	0.3	0.4	0.3	0.012	0.014	0.011	0.77	0.47	0.65
South Africa	263.1	198.6	107.3	13.230	10.010	5.296	389.22	294.72	169.85
Swaziland	3.3	1.9	2.4	0.173	0.098	0.132	6.85	4.03	5.63
Tanzania	128.0	125.5	31.4	5.106	5.162	1.447	324.55	237.96	82.94
Zambia	722.7	333.6	71.2	29.633	13.298	3.021	1810.36	804.11	186.05
Zimbabwe	131.5	78.4	37.1	7.623	4.474	2.574	266.12	147.40	84.06
Others	106.0	126.8	98.1	4.264	5.431	4.918	291.43	236.91	256.63

Table 9 contn'd. Intercomparison of the MODIS, GBA-2000 and GLOBSCAR burned area, selected trace gases and PM2.5 per country in southern Africa for September 2000.

Country	*MODIS CH_4 (Gg)*	*GBA-2000 CH_4 (Gg)*	*GLOBSCAR CH_4 (Gg)*	*MODIS NMHC (Gg)*	*GBA-2000 NMHC (Gg)*	*GLOBSCAR NMHC (Gg)*	*MODIS PM2.5 (Gg)*	*GBA-2000 PM2.5 (Gg)*	*GLOBSCAR PM2.5 (Gg)*
Angola	23.174	13.823	10.322	25.116	17.698	8.567	75.271	43.880	34.431
Botswana	1.590	1.319	0.170	2.385	1.992	0.252	5.423	4.507	0.540
Burundi	0.153	0.026	0.063	0.137	0.034	0.055	0.499	0.077	0.204
Malawi	2.083	1.680	0.359	1.611	1.316	0.249	7.042	5.687	1.234
Mozambique	52.474	25.759	8.693	40.723	19.919	7.319	177.131	87.018	28.882
Namibia	3.392	2.787	0.089	4.875	4.013	0.131	11.926	9.867	0.322
Rwanda	0.028	0.012	0.024	0.022	0.014	0.017	0.092	0.037	0.082
South Africa	9.508	7.248	4.426	11.195	8.431	4.864	29.885	22.914	14.057
Swaziland	0.204	0.124	0.175	0.192	0.110	0.154	0.667	0.413	0.581
Tanzania	11.892	7.761	2.906	8.712	6.693	2.291	40.363	25.578	9.693
Zambia	65.504	28.966	6.752	47.958	21.398	4.949	223.256	98.502	22.980
Zimbabwe	7.069	3.798	2.084	7.844	4.324	2.524	21.919	11.784	6.281
Others	11.019	7.458	8.746	7.625	6.701	6.958	37.821	24.323	29.231

Appendix C

Chapter 5:

Table 5. Range of emission factors for grassland fires (EF in gkg^{-1}) during the dry season using the fuel load method for GBA-2000. The ($\pm 1\sigma$) and the ratio of April EF over September EF are also shown.

Species	*April EF*	*September EF*	*Ratio*
Carbon dioxide (CO_2)	1698±60	1755±65	0.97
Nitrogen oxides (as NO)	3.25±0.16	3.10±0.17	1.05
Carbon monoxide (CO)	68.8±30.8	39.4±33.7	1.75
Methane (CH_4)	1.92±1.17	0.80±1.28	2.40
Nonmethane hydrocarbons (NMHC)	2.96±1.80	1.24±0.17	2.39
Dimethyl sulfide (CH_3SCH_3)	0.0022±0.0005	0.0017±0.0006	1.31
Methyl bromide (CH_3Br)	0.0012±0.0005	0.00068±0.00059	1.76
Methyl chloride (CH_3Cl)	0.071±0.014	0.058±0.015	1.23
Methyl iodide (CH_3I)	0.0016±0.0003	0.0013±0.0003	1.19
Methyl nitrate (CH_3ONO_2)	0.00036± 0.00016	0.00020±0.00018	1.76
Ethane (C_2H_6)	0.173±0.078	0.098±0.085	1.76
Ethene (C_2H_4)	0.596±0.269	0.339±0.294	1.76
Propane (C_3H_8)	0.052±0.023	0.030±0.026	1.76
Propene (C_3H_6)	0.168±0.121	0.053±0.132	3.19
Acetylene (C_2H_2)	0.167±0.075	0.095±0.082	1.76
i-butane (*i*-C_4H_{10})	0.0025±0.0022	0.00066±0.00248	3.79
n-butane (*n*-C_4H_{10})	0.017±0.008	0.0095±0.0082	1.76
t-2-butene (C_4H_8)	0.017±0.008	0.0095±0.0082	1.76
1-butene (C_4H_8)	0.038±0.022	0.017±0.024	2.20
c-2-butene (C_4H_8)	0.012±0.005	0.0068±0.0059	1.76
i-pentane (*i*-C_5H_{12})	0.0018±0.0008	0.0010±0.0009	1.76
n-pentane (*n*-C_5H_{12})	0.0078±0.0026	0.0053±0.0029	1.47
1, 3-butadiene (C_4H_6)	0.050±0.027	0.024±0.029	2.07
3-methyl-1-butene (C_5H_{10})	0.0060±0.0027	0.0034±0.0029	1.76
t-2-pentene (C_5H_{10})	0.0025±0.0022	0.00066±0.00248	3.79
2-methyl-2-butene (C_5H_{10})	0.0060±0.0027	0.0034±0.0029	1.76
2-methyl-1-butene (C_5H_{10})	0.0066±0.0030	0.0037±0.0032	1.76
Isoprene (C_5H_8)	0.044±0.015	0.029±0.017	1.50
n-heptane (C_7H_{16})	0.013±0.001	0.0071±0.0062	1.76
Benzene (C_6H_6)	0.173±0.078	0.098±0.085	1.76
Toluene (C_7H_8)	0.125±0.056	0.071±0.062	1.76
Formaldehyde (HCHO)	1.06±0.06	0.700±0.410	1.51
Methanol (CH_3OH)	1.16±0.57	0.617±0.626	1.89
Acetic acid (CH_3COOH)	2.41±1.22	1.24±1.33	1.94
Formic Acid (HCOOH)	0.711±0.202	0.518±0.221	1.37
Ammonia (NH_3)	0.261±0.100	0.166±0.109	1.57

Hydrogen Cyanide (HCN)	0.532±0.082	0.453±0.090	1.17
Particulates < 2.5 μm (PM2.5)	4.29±2.05	2.33±2.24	1.84
Total particulate matter (TPM)	13.4±7.9	5.9±8.6	2.27
Organic carbon (OC)	3.21±0.99	2.26±1.09	1.42
Black Carbon (BC)	0.346±0.156	0.197±0.171	1.76
Chloride (Cl^-)	1.33±1.05	0.324±1.147	4.10
Nitrate ($NO3^-$)	0.243±0.065	0.181±0.071	1.34
Sulfate (SO_4^{2-})	0.222±0.145	0.083±0.159	2.67
Potassium (K^+)	0.954±0.430	0.543±0.470	1.76

Table 6. Range of emission factors (EF in gkg^{-1}) for grassland fires during the dry season using the NDVI method for GBA-2000. The (±1σ) and the ratio of May EF over September EF are also shown.

Species	*May EF*	*September EF*	*Ratio*
Carbon dioxide (CO_2)	1636±45	1755±65	0.93
Carbon monoxide (CO)	100.7±23.1	39.3±33.3	2.56
Nitrogen oxides (as NO)	3.41±0.12	3.10±0.17	1.10
Methane (CH_4)	3.14±0.88	0.799±1.270	3.93
Nonmethane hydrocarbons (NMHC)	4.83±1.35	1.23±1.95	3.92
Dimethyl sulfide (CH_3SCH_3)	0.0028±0.0004	0.0017±0.0006	1.64
Methyl bromide (CH_3Br)	0.0018±0.0004	0.00068±0.0006	2.58
Methyl chloride (CH_3Cl)	0.086±0.011	0.058±0.015	1.48
Methyl iodide (CH_3I)	0.0019±0.0002	0.0013±0.0003	1.40
Methyl nitrate (CH_3ONO_2)	0.00053± 0.00012	0.00022± 0.00021	2.35
Ethane (C_2H_6)	0.254±0.059	0.098±0.084	2.58
Ethene (C_2H_4)	0.875±0.202	0.339±0.291	2.58
Propane (C_3H_8)	0.076±0.018	0.029±0.025	2.58
Propene (C_3H_6)	0.294±0.091	0.052±0.131	5.60
Acetylene (C_2H_2)	0.245±0.057	0.095±0.081	2.58
i-butane (*i*-C_4H_{10})	0.0049±0.0018	0.00064±0.00246	7.60
n-butane (*n*-C_4H_{10})	0.025±0.006	0.0095±0.0081	2.58
t-2-butene (C_4H_8)	0.025±0.006	0.0095±0.0081	2.58
1-butene (C_4H_8)	0.060±0.016	0.017±0.023	3.51
c-2-butene (C_4H_8)	0.018±0.004	0.00678±0.00582	2.58
i-pentane (*i*-C_5H_{12})	0.0026±0.0006	0.0010±0.0009	2.58
n-pentane (*n*-C_5H_{12})	0.011±0.020	0.0053±0.0029	1.99
1, 3-butadiene (C_4H_6)	0.078±0.020	0.024±0.029	3.25
3-methyl-1-butene (C_5H_{10})	0.0088±0.0020	0.0034±0.0029	2.58
t-2-pentene (C_5H_{10})	0.0049±0.0018	0.00064±0.00246	7.60
2-methyl-2-butene (C_5H_{10})	0.0088±0.0020	0.0034±0.0029	2.58
2-methyl-1-butene (C_5H_{10})	0.0096±0.0022	0.0037±0.0032	2.58
Isoprene (C_5H_8)	0.060±0.012	0.029±0.017	2.04
n-heptane (C_7H_{16})	0.018±0.004	0.0071±0.0061	2.58

Benzene (C_6H_6)	0.254±0.059	0.098±0.084	2.58
Toluene (C_7H_8)	0.184±0.042	0.071±0.061	2.58
Formaldehyde (HCHO)	1.45±0.282	0.699±0.406	2.07
Methanol (CH_3OH)	1.76±0.430	0.616±0.619	2.85
Acetic acid (CH_3COOH)	3.67±0.916	1.24±1.32	2.96
Formic Acid (HCOOH)	0.920±0.152	0.517±0.219	1.78
Ammonia (NH_3)	0.365±0.075	0.166±0.108	2.20
Hydrogen Cyanide (HCN)	0.618±0.062	0.453±0.089	1.36
Particulates < 2.5 μm (PM2.5)	6.41±1.54	2.32±2.22	2.76
Total particulate matter (TPM)	21.6±5.9	5.89±8.50	3.66
Organic carbon (OC)	4.24±0.75	2.25±1.08	1.88
Black Carbon (BC)	0.508±012	0.197±0.169	2.58
Chloride (Cl^-)	2.41±0.79	0.321±1.135	7.51
Nitrate ($NO3^-$)	0.310±0.049	0.181±0.070	1.71
Sulfate (SO_4^{2-})	0.373±0.109	0.083±0.157	4.49
Potassium (K^+)	1.40±0.323	0.542±0.466	2.58

Table 8. Range of emission factors for woodland fires (EF in gkg^{-1}) during the dry season using the fuel load method for GBA-2000. The (±1σ) and the ratio of June EF over September EF are also shown.

Species	*June EF*	*September EF*	*Ratio*
Carbon dioxide (CO_2)	1626±70	1674±51	0.97
Carbon monoxide (CO)	102.6±31.8	80.5±23.2	1.28
Nitrogen oxides (as NO)	3.42±0.17	3.31±0.12	1.03
Methane (CH_4)	3.74±1.66	2.58±1.21	1.45
Nonmethane hydrocarbons (NMHC)	2.68±0.63	2.25±0.46	1.19
Dimethyl sulfide (CH_3SCH_3)	0.0028±0.0006	0.0024±0.0004	1.17
Methyl bromide (CH_3Br)	0.0018±0.0006	0.0014±0.0004	1.28
Methyl chloride (CH_3Cl)	0.087±0.015	0.077±0.011	1.13
Methyl iodide (CH_3I)	0.0019±.0003	0.0017±0.0002	1.12
Methyl nitrate (CH_3ONO_2)	0.00054±0.00017	0.00042±0.0001	1.29
Ethane (C_2H_6)	0.261±0.083	0.204±0.060	1.28
Ethene (C_2H_4)	0.900±0.285	0.702±0.208	1.28
Propane (C_3H_8)	0.078±0.025	0.061±0.018	1.28
Propene (C_3H_6)	0.305±0.128	0.216±0.093	1.41
Acetylene (C_2H_2)	0.252±0.080	0.197±0.058	1.28
i-butane (*i*-C_4H_{10})	0.0051±0.0026	0.0033±0.0019	1.54
n-butane (*n*-C_4H_{10})	0.025±0.008	0.020±0.006	1.28
t-2-butene (C_4H_8)	0.025±0.008	0.020±0.006	1.28
1-butene (C_4H_8)	0.062±0.023	0.046±0.017	1.34
c-2-butene (C_4H_8)	0.018±0.006	0.014±0.004	1.28
i-pentane (*i*-C_5H_{12})	0.0027±0.0009	0.0021±0.0006	1.28
n-pentane (*n*-C_5H_{12})	0.0108±0.0028	0.0089±0.0020	1.22

1, 3-butadiene (C_4H_6)	0.080±0.029	0.060±0.021	1.33
3-methyl-1-butene (C_5H_{10})	0.0090±0.0029	0.0070±0.0021	1.28
t-2-pentene (C_5H_{10})	0.0051±0.0026	0.0033±0.0019	1.54
2-methyl-2-butene (C_5H_{10})	0.0090±0.0029	0.0070±0.0021	1.28
2-methyl-1-butene (C_5H_{10})	0.0099±0.0031	0.0077±0.0023	1.28
Isoprene (C_5H_8)	0.0613±0.0162	0.0500±0.0118	1.23
n-heptane (C_7H_{16})	0.0189±0.0060	0.0147±0.0044	1.28
Benzene (C_6H_6)	0.261±0.083	0.2044±0.0602	1.28
Toluene (C_7H_8)	0.189±0.060	0.147±0.044	1.28
Formaldehyde (HCHO)	1.48±0.40	1.21±0.289	1.23
Methanol (CH_3OH)	1.81±0.61	1.39±0.44	1.30
Acetic acid (CH_3COOH)	3.79±1.29	2.89±0.94	1.31
Formic Acid (HCOOH)	0.939±0.214	0.790±0.156	1.19
Ammonia (NH_3)	0.374±0.106	0.300±0.077	1.24
Hydrogen Cyanide (HCN)	0.625±0.087	0.564±0.064	1.11
Particulates < 2.5 μm (PM2.5)	12.8±6.2	8.5±4.53	1.51
Total particulate matter (TPM)	22.3±8.3	16.5±6.1	1.35
Organic carbon (OC)	4.33±1.1	3.60±0.77	1.20
Black Carbon (BC)	0.522±0.165	0.407±0.120	1.28
Chloride (Cl^-)	2.51±1.11	1.74±0.81	1.45
Nitrate ($NO3^-$)	0.316±0.068	0.268±0.050	1.18
Sulfate (SO_4^{2-})	0.386±0.154	0.279±0.112	1.38
Potassium (K^+)	1.44±0.46	1.12±0.33	1.28

Table 9. Range of emission factors (EF in gkg^{-1}) for woodland fires during the dry season using the NDVI method for GBA-2000. The (±1σ) and the ratio of June EF over September EF are also shown.

Species	*June EF*	*September EF*	*Ratio*
Carbon dioxide (CO_2)	1622±67	1673±51	0.97
Carbon monoxide (CO)	104.3±30.4	81.0±22.9	1.29
Nitrogen oxides (as NO)	3.43±0.16	3.31±0.12	1.04
Methane (CH_4)	3.82±1.59	2.61±1.19	1.47
Nonmethane hydrocarbons (NMHC)	2.72±0.60	2.26±0.45	1.20
Dimethyl sulfide (CH_3SCH_3)	0.0028±0.0001	0.0024±0.0004	1.17
Methyl bromide (CH_3Br)	0.0018±0.0001	0.0014±0.0004	1.30
Methyl chloride (CH_3Cl)	0.088±0.014	0.077±0.011	1.14
Methyl iodide (CH_3I)	0.0019±0.0003	0.0017±0.0002	1.12
Methyl nitrate (CH_3ONO_2)	0.00055±0.00016	0.00042±0.0001	1.30
Ethane (C_2H_6)	0.265±0.079	0.205±0.060	1.30
Ethene (C_2H_4)	0.915±0.273	0.706±0.205	1.30
Propane (C_3H_8)	0.080±0.024	0.061±0.018	1.30
Propene (C_3H_6)	0.312±0.126	0.218±0.092	1.43
Acetylene (C_2H_2)	0.256±0.076	0.198±0.057	1.30
i-butane (*i*-C_4H_{10})	0.0052±0.0025	0.0034±0.0018	1.56

n-butane (*n*-C_4H_{10})	0.026±0.008	0.020±0.006	1.30
t-2-butene (C_4H_8)	0.026±0.008	0.020±0.006	1.30
1-butene (C_4H_8)	0.063±0.022	0.047±0.016	1.36
c-2-butene (C_4H_8)	0.018±0.006	0.014±0.004	1.30
i-pentane (*i*-C_5H_{12})	0.0027±0.0008	0.0021±0.0006	1.30
n-pentane (*n*-C_5H_{12})	0.011±0.003	0.0089±0.0020	1.23
1, 3-butadiene (C_4H_6)	0.082±0.027	0.061±0.021	1.34
3-methyl-1-butene (C_5H_{10})	0.0092±0.0027	0.0071±0.0021	1.30
t-2-pentene (C_5H_{10})	0.0052±0.0024	0.0034±0.0018	1.56
2-methyl-2-butene (C_5H_{10})	0.0092±0.0027	0.0071±0.0021	1.30
2-methyl-1-butene (C_5H_{10})	0.010±0.030	0.0078±0.0023	1.30
Isoprene (C_5H_8)	0.062±0.016	0.050±0.012	1.24
n-heptane (C_7H_{16})	0.019±0.006	0.015±0.0043	1.30
Benzene (C_6H_6)	0.265±0.079	0.205±0.060	1.30
Toluene (C_7H_8)	0.192±0.057	0.148±0.043	1.30
Formaldehyde (HCHO)	1.50±0.38	1.21±0.286	1.24
Methanol (CH_3OH)	1.84±0.58	1.40±0.44	1.32
Acetic acid (CH_3COOH)	3.85±1.24	2.91±0.93	1.33
Formic Acid (HCOOH)	0.950±0.205	0.793±0.154	1.20
Ammonia (NH_3)	0.380±0.101	0.302±0.076	1.26
Hydrogen Cyanide (HCN)	0.630±0.084	0.566±0.063	1.11
Particulates < 2.5 μm (PM2.5)	13.1±5.9	8.57±4.47	1.53
Total particulate matter (TPM)	22.7±8.0	16.6±6.0	1.37
Organic carbon (OC)	4.39±1.01	3.61±0.80	1.21
Black Carbon (BC)	0.531±0.158	0.410±0.12	1.30
Chloride (Cl^-)	2.57±1.06	1.75±0.0	1.46
Nitrate ($NO3^-$)	0.320±0.065	0.270±0.049	1.19
Sulfate (SO_4^{2-})	0.394±0.147	0.281±0.111	1.40
Potassium (K^+)	1.46±0.44	1.13±0.33	1.30

Table 11. GBA-2000 regional emissions of trace gases and particulates (in Gg = 10^9g) from grassland (G) and woodland (W) fires in southern Africa in 2000, using the fuel load-based PGREEN.

Species	*Early G*	*Early W*	*Late G*	*Late W*	*Regional*
Carbon dioxide (CO_2)	55283.05	171323.87	75123.70	147375.80	449106.42
Carbon monoxide (CO)	1249.94	8772.91	1415.76	6656.70	18095.31
Nitrogen oxides (as NO)	97.62	343.05	130.36	287.42	858.45
Methane (CH_4)	25.63	291.35	24.26	205.95	547.19
Nonmethane hydrocarbons (NMHC)	39.50	240.95	37.44	189.00	506.89
Dimethyl sulfide (CH_3SCH_3)	0.0531	0.2563	0.0669	0.2035	0.5797
Methyl bromide (CH_3Br)	0.0216	0.1533	0.0244	0.1160	0.3152
Methyl chloride (CH_3Cl)	1.821	8.104	2.334	6.516	18.775
Methyl iodide (CH_3I)	0.0423	0.1796	0.0547	0.1455	0.4221

Methyl nitrate (CH_3ONO_2)	0.0065	0.0460	0.0073	0.0348	0.0946
Ethane (C_2H_6)	3.126	22.228	3.531	16.816	45.702
Ethene (C_2H_4)	10.778	76.649	12.178	57.987	157.592
Propane (C_3H_8)	0.938	6.668	1.059	5.045	13.711
Propene (C_3H_6)	1.699	24.196	1.228	17.343	44.466
Acetylene (C_2H_2)	3.018	21.462	3.410	16.236	44.126
i-butane (*i*-C_4H_{10})	0.0188	0.3809	0.0094	0.2593	0.6685
n-butane (*n*-C_4H_{10})	0.3018	2.1462	0.3410	1.6236	4.4126
t-2-butene (C_4H_8)	0.3018	2.1462	0.3410	1.6236	4.4126
1-butene (C_4H_8)	0.5472	5.1023	0.5490	3.7639	9.9624
c-2-butene (C_4H_8)	0.2156	1.5330	0.2436	1.1597	3.1518
i-pentane (*i*-C_5H_{12})	0.0323	0.2299	0.0365	0.1740	0.4728
n-pentane (*n*-C_5H_{12})	0.1686	0.9571	0.2044	0.7433	2.0734
1, 3-butadiene (C_4H_6)	0.763	6.635	0.793	4.924	13.114
3-methyl-1-butene (C_5H_{10})	0.1078	0.7665	0.1218	0.5799	1.5759
t-2-pentene (C_5H_{10})	0.0188	0.3809	0.0094	0.2593	0.6685
2-methyl-2-butene (C_5H_{10})	0.1078	0.7665	0.1218	0.5799	1.5759
2-methyl-1-butene (C_5H_{10})	0.1186	0.8431	0.1340	0.6379	1.7335
Isoprene (C_5H_8)	0.929	5.399	1.119	4.180	11.628
n-heptane (C_7H_{16})	0.2263	1.6096	0.2557	1.2177	3.3094
Benzene (C_6H_6)	3.126	22.228	3.531	16.816	45.702
Toluene (C_7H_8)	2.263	16.096	2.557	12.177	33.094
Formaldehyde (HCHO)	22.18	130.23	26.63	100.71	279.74
Methanol (CH_3OH)	19.63	152.29	21.45	114.20	307.57
Acetic acid (CH_3COOH)	39.53	316.95	42.61	236.93	636.02
Formic Acid (HCOOH)	16.38	84.64	20.33	66.56	187.91
Ammonia (NH_3)	5.259	32.555	6.219	25.014	69.047
Hydrogen Cyanide (HCN)	14.30	59.45	18.58	48.33	140.67
Particulates < 2.5 μm (PM2.5)	74.04	967.80	81.88	666.54	1790.27
Total particulate matter (TPM)	188.69	1826.29	185.52	1343.18	3543.69
Organic carbon (OC)	71.39	386.57	87.57	302.07	847.59
Black Carbon (BC)	6.251	44.456	7.063	33.633	91.403
Chloride (Cl^-)	10.53	195.97	4.98	138.64	350.11
Nitrate ($NO3^-$)	5.737	28.692	7.174	22.668	64.272
Sulfate (SO_4^{2-})	2.669	31.094	2.324	22.562	58.650
Potassium (K^+)	17.24	122.64	19.48	92.78	252.15

Table 12. GBA-2000 regional emissions of trace gases and particulates (in Gg = 10^9g) from grassland (G) and woodland (W) fires in southern Africa in 2000, using the NDVI-based PGREEN.

Species	*Early G*	*Early W*	*Late G*	*Late W*	*Regional*
Carbon dioxide (CO_2)	40774.40	62930.15	73423.30	118417.30	295545.15
Carbon monoxide (CO)	1464.86	3386.23	1488.80	5400.17	11740.06
Nitrogen oxides (as NO)	76.42	127.42	128.26	231.39	563.49
Methane (CH_4)	39.20	115.24	27.64	168.06	350.14
Nonmethane hydrocarbons (NMHC)	60.31	91.87	42.63	152.92	347.72
Dimethyl sulfide (CH_3SCH_3)	0.0492	0.0972	0.0673	0.1645	0.3782
Methyl bromide (CH_3Br)	0.0254	0.0592	0.0256	0.0941	0.2044
Methyl chloride (CH_3Cl)	1.612	3.061	2.333	5.262	12.268
Methyl iodide (CH_3I)	0.0365	0.0676	0.0545	0.1174	0.2761
Methyl nitrate (CH_3ONO_2)	0.0076	0.0178	0.0077	0.0282	0.0613
Ethane (C_2H_6)	3.680	8.589	3.718	13.645	29.632
Ethene (C_2H_4)	12.69	29.62	12.82	47.05	102.18
Propane (C_3H_8)	1.104	2.577	1.115	4.094	8.890
Propene (C_3H_6)	3.33	9.53	1.60	14.14	28.59
Acetylene (C_2H_2)	3.55	8.29	3.59	13.17	28.61
i-butane (*i*-C_4H_{10})	0.0484	0.1525	0.0136	0.2123	0.4268
n-butane (*n*-C_4H_{10})	0.355	0.829	0.359	1.317	2.861
t-2-butene (C_4H_8)	0.355	0.829	0.359	1.317	2.861
1-butene (C_4H_8)	0.777	1.989	0.609	3.060	6.436
c-2-butene (C_4H_8)	0.254	0.592	0.256	0.941	2.044
i-pentane (*i*-C_5H_{12})	0.0381	0.0889	0.0385	0.1412	0.3065
n-pentane (*n*-C_5H_{12})	0.1720	0.3663	0.2090	0.6019	1.3491
1, 3-butadiene (C_4H_6)	1.0309	2.5816	0.8653	4.0015	8.4792
3-methyl-1-butene (C_5H_{10})	0.1269	0.2962	0.1282	0.4705	1.0218
t-2-pentene (C_5H_{10})	0.0484	0.1525	0.0136	0.2123	0.4268
2-methyl-2-butene (C_5H_{10})	0.1269	0.2962	0.1282	0.4705	1.0218
2-methyl-1-butene (C_5H_{10})	0.1396	0.3258	0.1410	0.5176	1.1240
Isoprene (C_5H_8)	0.9615	2.0683	1.1474	3.3858	7.5629
n-heptane (C_7H_{16})	0.2665	0.6220	0.2692	0.9881	2.1458
Benzene (C_6H_6)	3.680	8.589	3.718	13.645	29.632
Toluene (C_7H_8)	2.665	6.220	2.692	9.881	21.458
Formaldehyde (HCHO)	23.10	49.92	27.33	81.57	181.92
Methanol (CH_3OH)	24.50	59.03	22.90	92.73	199.17
Acetic acid (CH_3COOH)	50.47	122.99	45.77	192.44	411.68
Formic Acid (HCOOH)	15.79	32.24	20.59	53.85	122.46
Ammonia (NH_3)	5.660	12.509	6.423	20.272	44.863
Hydrogen Cyanide (HCN)	12.205	22.354	18.477	38.999	92.035
Particulates < 2.5 μm (PM2.5)	90.58	386.04	86.99	545.17	1108.78
Total particulate matter (TPM)	275.29	712.76	207.67	1092.43	2288.15

Organic carbon (OC)	70.77	147.60	89.10	244.47	551.94
Black Carbon (BC)	7.360	17.178	7.435	27.291	59.264
Chloride (Cl^-)	25.68	77.49	8.33	113.13	224.63
Nitrate ($NO3^-$)	5.427	10.910	7.243	18.331	41.910
Sulfate (SO_4^{2-})	4.471	12.192	2.756	18.371	37.790
Potassium (K^+)	20.30	47.39	20.51	75.28	163.49

Table 13. MODIS emissions of trace gases and particulates (in Gg = 10^9g) from grassland (G) and woodland (W) fires in southern Africa in July and September 2000, using the fuel load-based PGREEN.

Species	*July G*	*July W*	*September G*	*September W*
Carbon dioxide (CO_2)	26432.00	150906.00	40387.30	94885.40
Carbon monoxide (CO)	559.98	7519.72	766.75	4423.61
Nitrogen oxides (as NO)	46.37	300.38	70.128	186.24
Methane (CH_4)	10.85	246.20	13.254	139.51
Nonmethane hydrocarbons (NMHC)	16.72	207.97	20.452	124.51
Dimethyl sulfide (CH_3SCH_3)	0.0247	0.2218	0.0361	0.1336
Methyl bromide (CH_3Br)	0.0096	0.1313	0.0132	0.0771
Methyl chloride (CH_3Cl)	0.8519	7.032	1.258	4.266
Methyl iodide (CH_3I)	0.0198	0.1561	0.0295	0.0951
Methyl nitrate (CH_3ONO_2)	0.0029	0.0394	0.0040	0.0231
Ethane (C_2H_6)	1.399	19.04	1.913	11.184
Ethene (C_2H_4)	4.825	65.66	6.596	38.565
Propane (C_3H_8)	0.4197	5.712	0.5738	3.355
Propene (C_3H_6)	0.6686	20.50	0.6819	11.704
Acetylene (C_2H_2)	1.351	18.38	1.847	10.798
i-butane (*i*-C_4H_{10})	0.0074	0.3196	0.0055	0.1776
n-butane (*n*-C_4H_{10})	0.1351	1.8385	0.1847	1.080
t-2-butene (C_4H_8)	0.1351	1.8385	0.1847	1.080
1-butene (C_4H_8)	0.2357	4.3483	0.2990	2.520
c-2-butene (C_4H_8)	0.0965	1.3132	0.1319	0.7713
i-pentane (*i*-C_5H_{12})	0.0145	0.1970	0.0198	0.1157
n-pentane (*n*-C_5H_{12})	0.0773	0.8244	0.1104	0.4910
1, 3-butadiene (C_4H_6)	0.3322	5.662	0.4310	3.291
3-methyl-1-butene (C_5H_{10})	0.0482	0.6566	0.0660	0.3856
t-2-pentene (C_5H_{10})	0.0074	0.3196	0.0055	0.1776
2-methyl-2-butene (C_5H_{10})	0.0482	0.6566	0.0660	0.3856
2-methyl-1-butene (C_5H_{10})	0.0531	0.7223	0.0726	0.4242
Isoprene (C_5H_8)	0.4252	4.647	0.6046	2.763
n-heptane (C_7H_{16})	0.1013	1.379	0.1385	0.8099
Benzene (C_6H_6)	1.399	19.04	1.913	11.184
Toluene (C_7H_8)	1.013	13.79	1.385	8.099
Formaldehyde (HCHO)	10.14	112.07	14.385	66.591

Methanol (CH_3OH)	8.689	130.22	11.635	76.129
Acetic acid (CH_3COOH)	17.42	270.84	23.130	158.08
Formic Acid (HCOOH)	7.575	73.10	10.966	43.82
Ammonia (NH_3)	2.391	27.98	3.362	16.57
Hydrogen Cyanide (HCN)	6.725	51.71	10.004	31.55
Particulates < 2.5 μm (PM2.5)	32.91	813.73	44.395	454.85
Total particulate matter (TPM)	80.78	1555.48	101.15	900.07
Organic carbon (OC)	32.88	333.39	47.27	199.20
Black Carbon (BC)	2.798	38.083	3.826	22.368
Chloride (Cl^-)	3.791	165.63	2.861	93.896
Nitrate ($NO3^-$)	2.660	24.803	3.869	14.906
Sulfate (SO_4^{2-})	1.103	26.412	1.275	15.174
Potassium (K^+)	7.719	105.06	10.55	61.704

Table 14. MODIS emissions of trace gases and particulates (in Gg = 10^9g) from grassland (G) and woodland (W) fires in southern Africa in July and September 2000, using the NDVI-based PGREEN.

Species	*July G*	*July W*	*September G*	*September W*
Carbon dioxide (CO_2)	19383.90	69027.60	40119.80	79310.30
Carbon monoxide (CO)	703.83	3673.14	778.65	3666.49
Nitrogen oxides (as NO)	36.39	139.41	69.80	155.40
Methane (CH_4)	18.91	124.34	13.80	115.06
Nonmethane hydrocarbons (NMHC)	29.10	99.92	21.29	103.44
Dimethyl sulfide (CH_3SCH_3)	0.0235	0.1059	0.0361	0.1111
Methyl bromide (CH_3Br)	0.0122	0.0642	0.0134	0.0639
Methyl chloride (CH_3Cl)	0.7702	3.3362	1.2576	3.550
Methyl iodide (CH_3I)	0.0174	0.0738	0.0294	0.0792
Methyl nitrate (CH_3ONO_2)	0.0037	0.0193	0.0040	0.0192
Ethane (C_2H_6)	1.768	9.315	1.943	9.268
Ethene (C_2H_4)	6.098	32.12	6.700	31.96
Propane (C_3H_8)	0.5305	2.794	0.5829	2.780
Propene (C_3H_6)	1.611	10.29	0.7422	9.661
Acetylene (C_2H_2)	1.707	8.993	1.876	8.948
i-butane (*i*-C_4H_{10})	0.0235	0.1641	0.0061	0.1460
n-butane (*n*-C_4H_{10})	0.1707	0.8993	0.1876	0.8948
t-2-butene (C_4H_8)	0.1707	0.8993	0.1876	0.8948
1-butene (C_4H_8)	0.3745	2.153	0.3087	2.085
c-2-butene (C_4H_8)	0.1220	0.642	0.1340	0.6392
i-pentane (*i*-C_5H_{12})	0.0183	0.096	0.0201	0.0959
n-pentane (*n*-C_5H_{12})	0.0824	0.398	0.1111	0.4076
1, 3-butadiene (C_4H_6)	0.4965	2.795	0.4427	2.724
3-methyl-1-butene (C_5H_{10})	0.0610	0.321	0.0670	0.3196

t-2-pentene (C_5H_{10})	0.0235	0.164	0.0061	0.1460
2-methyl-2-butene (C_5H_{10})	0.0610	0.321	0.0670	0.3196
2-methyl-1-butene (C_5H_{10})	0.0671	0.353	0.0737	0.3515
Isoprene (C_5H_8)	0.4609	2.247	0.6092	2.294
n-heptane (C_7H_{16})	0.1281	0.6745	0.1407	0.6711
Benzene (C_6H_6)	1.768	9.315	1.943	9.268
Toluene (C_7H_8)	1.281	6.745	1.407	6.711
Formaldehyde (HCHO)	11.07	54.23	14.501	55.27
Methanol (CH_3OH)	11.79	63.97	11.871	63.05
Acetic acid (CH_3COOH)	24.29	133.26	23.643	130.89
Formic Acid (HCOOH)	7.559	35.07	11.010	36.41
Ammonia (NH_3)	2.715	13.58	3.395	13.74
Hydrogen Cyanide (HCN)	5.825	24.39	9.990	26.28
Particulates < 2.5 μm (PM2.5)	43.55	415.76	45.22	374.40
Total particulate matter (TPM)	132.74	771.28	104.73	744.39
Organic carbon (OC)	33.89	160.49	47.52	165.44
Black Carbon (BC)	3.537	18.629	3.886	18.54
Chloride (Cl^-)	12.45	83.615	3.402	77.44
Nitrate ($NO3^-$)	2.596	11.874	3.881	12.39
Sulfate (SO_4^{2-})	2.160	13.179	1.345	12.54
Potassium (K^+)	9.756	51.391	10.72	51.13

Table 15. MODIS regional emissions of trace gases and particulates (in Gg = 10^9g) from grassland (G) and woodland (W) fires in southern Africa in 2000.

Species	*Early G*	*Early W*	*Late G*	*Late W*	*Regional*
Carbon dioxide (CO_2)	57601.90	170455.72	83003.18	226032.73	537093.53
Nitrogen oxides (as NO)	105.43	341.94	144.48	447.64	1039.49
Carbon monoxide (CO)	1777.85	8800.77	1620.03	11029.43	23228.08
Methane (CH_4)	44.93	293.48	28.92	358.28	725.61
Nonmethane hydrocarbons (NMHC)	69.14	241.22	44.62	306.49	661.47
Dimethyl sulfide (CH_3SCH_3)	0.0639	0.2564	0.0750	0.3274	0.7227
Methyl bromide (CH_3Br)	0.0307	0.1537	0.0279	0.1925	0.4048
Methyl chloride (CH_3Cl)	2.126	8.100	2.607	10.41	23.243
Methyl iodide (CH_3I)	0.0485	0.1794	0.0610	0.2313	0.5202
Methyl nitrate (CH_3ONO_2)	0.0093	0.0462	0.0084	0.0577	0.1216
Ethane (C_2H_6)	4.461	22.30	4.043	27.92	58.724
Ethene (C_2H_4)	15.38	76.91	13.94	96.27	202.5
Propane (C_3H_8)	1.338	6.690	1.212	8.375	17.615
Propene (C_3H_6)	3.676	24.356	1.579	29.88	59.491
Acetylene (C_2H_2)	4.305	21.528	3.904	26.95	56.687
i-butane (*i*-C_4H_{10})	0.0524	0.3845	0.0139	0.4637	0.9145
n-butane (*n*-C_4H_{10})	0.4305	2.153	0.3904	2.695	5.6689

t-2-butene (C_4H_8)	0.4305	2.153	0.3904	2.695	5.6689
1-butene (C_4H_8)	0.9031	5.127	0.6453	6.355	13.0304
c-2-butene (C_4H_8)	0.3079	1.538	0.2787	1.925	4.0496
i-pentane (*i*-C_5H_{12})	0.0462	0.2305	0.0418	0.2889	0.6074
n-pentane (*n*-C_5H_{12})	0.2168	0.9588	0.2307	1.213	2.6193
1, 3-butadiene (C_4H_6)	1.211	6.665	0.9246	8.281	17.0816
3-methyl-1-butene (C_5H_{10})	0.1538	0.7690	0.1395	0.9626	2.0249
t-2-pentene (C_5H_{10})	0.0524	0.3844	0.0139	0.4637	0.9144
2-methyl-2-butene (C_5H_{10})	0.1538	0.7690	0.1395	0.9626	2.0249
2-methyl-1-butene (C_5H_{10})	0.1693	0.8458	0.1535	1.059	2.2276
Isoprene (C_5H_8)	1.207	5.409	1.265	6.835	14.716
n-heptane (C_7H_{16})	0.3231	1.615	0.2927	2.022	4.2528
Benzene (C_6H_6)	4.461	22.30	4.043	27.92	58.724
Toluene (C_7H_8)	3.231	16.15	2.927	20.22	42.528
Formaldehyde (HCHO)	28.95	130.49	30.11	164.81	354.36
Methanol (CH_3OH)	29.29	152.88	24.73	190.71	397.61
Acetic acid (CH_3COOH)	60.01	318.24	49.28	396.50	824.03
Formic Acid (HCOOH)	20.25	84.72	22.84	107.76	235.57
Ammonia (NH_3)	7.026	32.63	7.054	41.10	87.81
Hydrogen Cyanide (HCN)	16.31	59.38	20.70	76.64	173.03
Particulates < 2.5 μm (PM2.5)	108.78	976.28	94.17	1181.79	2361.02
Total particulate matter (TPM)	318.29	1835.50	219.13	2272.72	4645.64
Organic carbon (OC)	89.99	387.10	98.61	491.03	1066.73
Black Carbon (BC)	8.922	44.61	8.087	55.84	117.459
Chloride (Cl^-)	27.74	197.40	7.540	241.05	473.73
Nitrate ($NO3^-$)	7.001	28.71	8.048	36.59	80.349
Sulfate (SO_4^{2-})	5.046	31.28	2.830	38.54	77.696
Potassium (K^+)	24.61	123.06	22.30	154.02	323.99

Table 17. Percent MODIS emissions errors, average monthly and spatially explicit total monthly modeled emissions for woodland (W) and grassland (G) fires using the fuel load (FL) and NDVI methods (NDVI).

	$e_{fuel\ load}$ (1σ)	$e_{area\ burned}$ (1σ)	$e_{combustion\ completeness}$ (1σ)	$e_{emission\ factor}$ (1σ)	e_{total} (1σ)	*Average monthly emissions* (Tg) (a)	*Spatially explicit monthly emissions* (Tg) (b)	*Ratio a/b*
July								
CO_2 G-FL	30	6.9	18.0	1.3	35.7	28	26	1.08
CO G-FL	30	6.9	18.0	3.4	35.9	0.728	0.560	1.30
CH_4 G-FL	30	6.9	18.0	77.8	85.6	0.017	0.011	1.55
CO_2 G-NDVI	30	6.9	23.5	1.4	40.8	21	19	1.11
CO G-NDVI	30	6.9	23.5	2.1	40.8	0.916	0.704	1.30
CH_4 G-NDVI	30	6.9	23.5	37.5	55.4	0.026	0.019	1.37
CO_2 W-FL	30	10.3	30.1	0.7	43.7	142	151	0.94
CO W-FL	30	10.3	30.1	0.5	43.7	8.12	7.52	1.08
CH_4 W-FL	30	10.3	30.1	9.8	44.8	0.284	0.246	1.15
CO_2 W-NDVI	30	10.3	63.6	0.7	71.9	67	69	0.97
CO W-NDVI	30	10.3	63.6	0.5	71.9	3.90	3.67	1.06
CH_4 W-NDVI	30	10.3	63.6	9.6	72.6	0.138	0.124	1.11
September								
CO_2 G-FL	30	3.8	15.1	1.3	33.8	40	40	1.00
CO G-FL	30	3.8	15.1	3.8	34.0	0.924	0.767	1.20
CH_4 G-FL	30	3.8	15.1	92.6	98.6	0.019	0.013	1.46
CO_2 G-NDVI	30	3.8	15.2	1.3	36.7	39	40	0.98
CO G-NDVI	30	3.8	15.2	3.7	34.0	0.931	0.779	1.20
CH_4 G-NDVI	30	3.8	15.2	89.7	98.6	0.020	0.014	1.43
CO_2 W-FL	30	14.5	17.8	0.7	37.8	93.0	94.9	0.98
CO W-FL	30	14.5	17.8	0.6	37.8	4.70	4.42	1.06
CH_4 W-FL	30	14.5	17.8	11.6	39.5	0.155	0.140	1.11

CO_2 W-NDVI	30	14.5	21.2	0.7	39.5	78.2	79.3	0.99
CO W-NDVI	30	14.5	21.2	0.6	39.5	3.98	3.67	1.08
CH_4 W-NDVI	30	14.5	21.2	11.5	41.1	0.132	0.115	1.15

Table 21. Intercomparison of MODIS vegetation fire emissions from southern Africa and emissions from global savanna burning, global biomass burning and global fossil fuel combustion (Tg/yr).

Species	*Southern African vegetation fires (2000) [this work]*	*Global Savanna Burning (Late 1990s) [Andreae and Merlet, 2001]*	*Global Biomass Burning (Late 1990s) [Andreae and Merlet, 2001]* [a]	*Global Fossil Fuel (1985) [Yevich and Logan, 2003]*
Biomass Burned Tg)	316	3160	8600	
Carbon dioxide (CO_2)	537	5096	13400	1943
Carbon monoxide (CO)	23.2	206	690	300-400
Methane (CH_4)	0.726	7.4	39	75-110
Nonmethane hydrocarbons (NMHC)	0.661	10.7	49	
Acetylene (C_2H_2)	0.0567	0.92	3.7	
Methanol (CH_3OH)	0.398	3.8	12.7	
Formaldehyde (HCHO)	0.354	1.1	5.5	
Formic Acid (HCOOH)	0.236	2.1	5.9	
Acetic acid (CH_3COOH)	0.824	4.2	12.6	
Nitrogen oxides (as NO)	1.04	12.2	20.7	45
Ammonia (NH_3)	0.088	3.4	10.3	
Hydrogen Cyanide (HCN)	0.173	0.09	0.90	
Methyl bromide (CH_3Br)	0.0004	0.006	0.029	
Methyl iodide (CH_3I)	0.00052	0.0016	0.014	
Methyl chloride (CH_3Cl)	0.023	0.24	0.65	
Particulates matter < 2.5 μm (PM2.5)	2.36	16.1	58.3	
Total particulate matter (TPM)	4.65	26.2	82.4	
Organic carbon (OC)	1.07	10.6	36.1	
Black Carbon (BC)	0.117	1.5	4.8	

[a] Values include emissions from savanna and grassland burning, tropical and extratropical forest burning, biofuel use, charcoal making and burning and burning of agricultural field residues.

References

Acres, B. D., A. Blair Rains, R. B. King, R. M. Lawton, A. J. B. Mitchell, and L. J. Rackham, African dambos: their distribution, characteristics and use, *Zeitschrift för Geomorphologie, Supplementband*, *52*, 63-86, 1985.

Agrawala, S., Structural and process history of the Intergovernmental Panel on Climate Change, *Climatic Change*, *39*(4), 621-642, 1998.

Allan, G., A. Johnson, S. Cridland, and N. Fitzgerald, Application of NDVI for predicting fuel curing at landscape scales in northern Australia: can remotely sensed data help schedule fire management operations?, *Int. J. Wildland Fire*, *12*(3-4), 299-308, 2003.

Andreae, M. O., The influence of tropical biomass burning on climate and the atmospheric environment, in *Biogeochemistry of Global Change: Radiatively Active Trace Gases*, edited by R. S. Oremland, pp. 113-150, Chapman and Hall, New York, 1993.

Andreae, M. O., Emissions of trace gases and aerosols from southern African savanna fires, in *Fire in the Southern African Savannas: Ecological and Environmental Perspectives*, edited by B. W. van Wilgen *et al*., pp. 161-183, Witwatersrand Univ. Press, Johannesburg, South Africa, 1997.

Andreae, M. O., and P. Merlet, Emission of trace gases and aerosols from biomass burning, *Global Biogeochem. Cy.*, *15*(4), 955-966, 2001.

Anyamba, A., C. O. Justice, C. J. Tucker, and R. Mahoney, Seasonal to interannual variability of vegetation and fires at SAFARI 2000 sites inferred from advanced very high resolution radiometer time series data, *J. Geophys. Res.*, *108*(D13), 8507, doi:10.1029/2002JD002464, 2003.

Arellano, A. F., Jr., P. S. Kasibhatla, L. Giglio, G. R. van der Werf, and J. T. Randerson, Top-down estimates of global CO sources using MOPITT measurements, *Geophys. Res. Lett.*, *31*, L01104, doi:10.1029/2003GL018609, 2004.

Barbosa, P. M., D. Stroppiana, J. -M. Grégoire, and J. M. C. Pereira, An assessment of vegetation fire in Africa (1981–1991): Burned areas, burned biomass, and atmospheric emissions, *Global Biogeochem. Cy.*, *13*, 933–950, 1999.

Bergamaschi, P., R. Hein, M. Heimann, and P. Crutzen, Inverse modeling of the global CO cycle, 1. Inversion of CO mixing ratios, *J. Geophys. Res.*, *105*(D2), 1909–1928, 2000.

Bertschi, I., R. J. Yokelson, D. E. Ward, R. E. Babbitt, R. A. Susott, J. G. Goode, and W. M. Hao, Trace gas and particle emissions from fires in large diameter and belowground biomass fuels, *J. Geophys. Res.*, *108*(D13), 8472, doi:10.1029/2002JD002100, 2003.

Bond, W. J., and G. F. Midgley, A proposed CO_2-controlled mechanism of woody plant invasion in grasslands and savannas, *Global Change Biol.*, *6*, 865-869, 2000.

Bond, W. J., and S. Archibald, Confronting complexity: Fire policy choices in South African savanna parks, *Int. J. Wildland Fire*, *12*(4), 381-389, 2003.

Bond, W. J., G. F. Midgley, and F. I Woodward, The importance of low atmospheric CO_2 and fire in promoting the spread of grasslands and savannas, *Global Change Biol.*, *9*, 973-982, 2003.

Braatz, B. V., S. Brown, A. O. Isichei, E. O. Odada, R. J. Scholes, Y. Sokona, P. Drichi, G. Gaston, R. Delmas, R. Holmes, S. Amous, R. S. Muyungi, A. De Jode, and M. Gibbs, African greenhouse gas emission inventories and mitigation options: Forestry, land-use change, and agriculture, *Environ. Monit. Assess.*, *38*, 109-126, 1995.

Brisco, B., R. J. Brown, T. J., Koehler, J. A., Sofko, G. J. and M. J. Mc Kibben, The dinurnal pattern of microwave backscattering by wheat, *Remote Sens. Environ.*, *34*, 37-47, 1990.

Brocard, D., and J. P. Lacaux, Domestic biomass combustion and associated atmospheric emissions in West Africa, *Global Biogeochem. Cy.*, *12*, 127–139, 1998.

Bucini, G., and E. F. Lambin, Fire impacts on vegetation in Central Africa: a remote-sensing-based statistical analysis, *Appl. Geogr.*, *22*, 27-48, 2002.

Burgan, R. E., R. W. Klaver, J. M. Klaver, Fuel models and fire potential from satellite and surface observations, *Int. J. Wildland Fire*, *8*(3), 159-170, 1998.

Cahoon, D. R. Jr., B. J. Stocks, J. S. Levine, W. R. Cofer III, and K. P. O'Neill, Seasonal distribution of African savanna fires, *Nature*, *359*, 812-815, 1992.

Ceccato, P., N. Gobron, S. Flasse, B. Pinty, and S. Tarantola, Designing a spectral index to estimate vegetation water content from remote sensing data: Part 1 - Theoretical approach, *Remote Sens. Environ.*, *82* (2-3), 188-197, 2002.

Chatfield, R. B., J. A. Vastano, H. B. Singh, and G. Sachse, A general model of how fire emissions and chemistry produce African/oceanic plumes (O_3, CO, PAN, smoke) in TRACE A, *J. Geophys. Res*., 101(D19), 24279-24306, 1996.

Chatfield, R. B., J. Vastano, L. Li, G. Sachse, and V. Connors, The Great African plume from biomass burning: Generalizations from a three-dimensional study of TRACE A carbon monoxide, *J. Geophys. Res.*, *103*(D21), 28,059–28,078, 1997.

Chidumayo, E. N., Species structure in Zambian miombo woodland, *J. Trop. Ecol.*, *3*, 109-118, 1987.

Chidumayo, E. N., J. Gambizi, and I. Grundy, 1996. Managing miombo woodlands, in *The Miombo in Transition: Woodlands and Welfare in Africa*, edited by B. Campbell, pp.175-194, CIFOR, Bogor, Indonesia, 1996.

Christian, H. J., R. J. Blakeslee, S. J. Goodman, D. A. Mach, M. F. Stewart, D. E. Buechler, W. J. Koshak, J. M. Hall, W. L. Boeck, K. T. Driscoll, and D. J. Bocippio, The Lightning Imaging Sensor, Proceedings of the 11th International Conference on Atmospheric Electricity, pp. 746-749, Guntersville, Alabama, June 7-11, 1999.

Cofer, W. R. III., J. S. Levine, E. L. Winstead, D. R. Cahoon, D. I. Sebacher, J. P. Pinto, and B. J. Stocks, Source compositions of trace gases released during African savanna fires, *J. Geophys. Res.*, *101*(D19), 23597-23602, 1996.

Conrad, R. and W. Seiler, Arid soils as a source of atmospheric carbon monoxide. *Geophys. Res. Lett*., *9*, 1353–1356, 1982.

Cooper, M. A. R., *Control Surveys in Civil Engineering*, Collins Professional Books, London, pp. 125-126, 1987.

Cooke, W., B. Koffi, and J. –M. Grégoire, Seasonality of vegetation fires in Africa from remote sensing data and application to a global chemistry model, *J. Geophys. Res.*, *101*(D15), 21,051–21,066, 1996.

Crutzen, P. J., and M. O. Andreae, Biomass burning in the tropics: Impact on atmospheric chemistry and biogeochemical cycles, *Science*, *250*, 1669-1678, 1990.

Crutzen P. J., and J. Lelieveld, Human impacts on atmospheric chemistry, *Annu. Rev. Earth Pl. Sc., 29*, 7-45, 2001.

Delmas, R., J. P. Lacaux, and D. Brocard, Determination of biomass burning emission factors: Methods and results, *Environ. Monit. Assess*, *38*, 181-204, 1995.

Dikshit, O., and D. P. Roy, An empirical investigation of image resampling effects upon the spectral and textural information content of a high spatial resolution multispectral image, *Photogramm. Eng. Rem. S., 62*, 1085-1092, 1996.

Duncan, B. N., R. V. Martin, A. C. Staudt, R. Yevich, and J. A. Logan, Interannual and seasonal variability of biomass burning emissions constrained by satellite observations, *J. Geophys. Res.*, *108*(D2), 4100, doi:10.1029/2002JD002378, 2003.

Dwyer E., J. M. C. Pereira , J. -M. Grégoire, and C. C. DaCamara, Characterization of the spatio-temporal patterns of global fire activity using satellite imagery for the period April 1992 to March 1993, *J. Biogeogr.*, *27*(1), 57-69, 2000.

Edwards, D. P., J. -F. Lamarque, J. -L. Attié,, Emmons, L. K.; Richter, A.; Cammas, J.-P.; Gille, J. C.; Francis, G. L.; Deeter, M. N.; Warner, J.; Ziskin, D. C.; Lyjak, L. V.; Drummond, J. R.; Burrows, J. P. Tropospheric ozone over the tropical Atlantic: A satellite perspective, *J. Geophys. Res.*, *108*(D8), 4237, doi:10.1029/2002JD002927, 2003.

Eva, H., and E. F. Lambin, Burnt area mapping in Central Africa using ATSR data, *Int. J. Remote Sens., 19*, 3473-3497, 1998.

Feral, C. J. W., H. E. Epstein, L. Otter, J. N. Aranibar, H. H. Shugart, S. A. Macko and J. Ramontsho, Carbon and nitrogen in the soil-plant system along rainfall and land-use gradients in southern Africa**,** *J. Arid Environ., 54*(2)*,* 327-343, 2003.

Fishman, J., K. Fakhruzzaman, B. Cros, and D. Nganga, Identification of widespread pollution in the southern hemisphere deduced from satellite analyses, *Science, 252*, 1693-1696, 1991.

Food and Agriculture Organization of the United Nations, Global Forest Resources Assessment 2000 (FRA 2000), Appendix 2, Terms and definitions, FAO Forestry Paper, *140*, pp. 363-370, Rome, 2001.

Frost, P. G. H., and F. I. Robertson, The ecological role of fire in savannas, in *Determinants of Ttropical Savannas*, edited by B. H. Walker, pp. 93-140, IRL Press, Oxford, 1987.

Frost, P. G. H., The ecology of miombo woodlands, in *The Miombo in Transition: Woodlands and Welfare in Africa*, edited by B. Campbell, pp. 11-58, Bogor, Indonesia, CIFOR, 1996.

Frost, P. G. H., Fire in southern African woodlands: origins, impacts, effects, and control, in *Proceedings of an FAO meeting on public policies affecting forest fires*, FAO Forestry Paper, *138*, 181-205, 1999.

Fuller, D. O., and S. D. Prince, Rainfall and foliar dynamics in tropical southern Africa: potential impacts of global climatic change on savanna vegetation, *Climatic Change*, *33*, 69-96, 1996.

Fuller, D. O., S. D. Prince, and W. L. Astle, The influence of canopy strata on remotely sensed observations of savanna-woodlands, *Int. J. Remote Sens*., *18*, 2985-3009, 1997.

Gao, B. -C., and A. F. H. Goetz, Column atmospheric water vapor and vegetation liquid water retrievals from airborne imaging spectrometer data, *J. Geophys. Res., 95*(D4), 3549-3564, 1990.

Gao, B. -C., NDWI-a normalized difference water index for remote sensing of vegetation liquid water from space, *Remote Sens. Environ.*, *58* (3), 257-266, 1996.

Garstang, M., W. N. Ellery, T. S. McCarthy, M. C. Scholes, R. J. Scholes, R. J. Swap, and P. D. Tyson, The contribution of aerosol- and water-borne nutrients to the functioning of the Okavango Delta ecosystem, Botswana, *S. Afr. J. Sci. 94*, 223-229, 1998.

Generoso, S., F. -M. Bréon, Y. Balkanski, O. Boucher, and M. Schulz, Improving the seasonal cycle and interannual variations of biomass burning aerosol sources, *Atmos. Chem. Phys.*, *3*, 1211-1222, 2003.

Giglio, L., J. D. Kendall, and C. O. Justice, Evaluation of global fire detection algorithms using simulated AVHRR infrared data, *Int. J. Remote Sens*., *20*, 1947-1985, 1999.

Giglio, L., J. D. Kendall, and C. J. Tucker, Remote sensing of fires with the TRMM VIRS, *Int. J. Remote Sens., 21*(1), 203-207, 2000.

Glantz, S. A., *Primer of Biostatistics*, 4th ed., pp. 238-241, McGraw-Hill, 1997.

Grégoire, J. -M., K. Tansey, and J. M. N. Silva, The GBA2000 initiative: Developing a global burned area database from SPOT-VEGETATION imagery, *Int. J. Remote Sens. 24*, 1369-1376, 2003.

Guenther, B., X. Xiong, V. V. Salomonson, W. L. Barnes and J. Young, On-orbit performance of the Earth Observing System Moderate Resolution Imaging Spectroradiometer; first year of data, *Remote Sens. Environ., 83*, 16-30, 2002.

Guy, P. R., The influence of elephants and fire on a Brachystegia-Julbernardia woodland in Zimbabwe, *J. Trop. Ecol.*, *5*, 215-226, 1989.

Hansen, M. C., R. S. DeFries, J. R. G. Townshend, R. Sohlberg, C. Dimiceli, and M. Carroll, Towards an operational MODIS continuous field of percent tree cover algorithm: examples using AVHRR and MODIS data**,** *Remote Sens. Environ., 83*(1-2)*,* 303-319, 2002.

Hansen, M. C., R. S. DeFries, J. R. G. Townshend, M. Carroll, C. Dimiceli and R. Sohlberg, The MODIS 500 meter global vegetation continuous field products, Second international workshop on the Analysis of Multitemporal Remote Sensing Images, Ispra, Italy, in press.

Hao, W. M., M. -H. Liu, and P. J. Crutzen, Estimates of annual and regional releases of CO_2 and other trace gases to the atmosphere from fires in the tropics, based on FAO statistics for the period 1975-1980, in *Fire in the Tropical Biota: Ecosystem Processes and Global Challenges*, vol. 84, edited by J. G. Goldammer, pp. 440-462, *Ecol. Stud.*, Springer-Verlag, New York, 1990.

Hao, W. M., and M. -H. Liu, Spatial and temporal distribution of tropical biomass burning, *Global Biogeochem. Cy.*, *8*, 495-503, 1994.

Hao, W. M., D. E. Ward, G. Olbu, and S. P. Baker, Emissions of CO_2, CO, and hydrocarbons from fires in diverse African savanna ecosystems, *J. Geophys. Res.*, *101*(D19), 23577-23584, 1996.

Hardy, C. C., and R. E. Burgan, Evaluation of NDVI for monitoring live moisture in three vegetation types of the western U.S., *Photogramm. Eng. Rem. S.*, *65*(5), 603-610, 1999.

Helas, G., and J. J. Pienaar, The influence of vegetation fires on the chemical composition of the atmosphere, *S. Afr. J. Sci., 92***,** 132-136, 1996.

Hély, C., P. R. Dowty, S. Alleaume, K. K. Caylor, S. Korontzi, R. J. Swap, H. H. Shugart, and C. O. Justice Regional fuel load for two climatically contrasting years in southern Africa, *J. Geophys. Res.*, *108*(D13), 8475, doi:10.1029/2002JD002341, 2003a.

Hély, C., K. Caylor, P. R. Dowty, R. J. Swap, H. H. Shugart, SAFARI 2000 Modeled Fuel Load in Southern Africa 1999-2000, in *SAFARI 2000 CD-ROM Series*, vol. 3, CD-ROM, edited by J. Nickeson, D. Landis, J. L. Privette, National Aeronautics and Space Administration, Goddard Space Flight Center, Greenbelt, Maryland, U.S.A. Available from Oak Ridge National Laboratory Distributed Active Archive Center, Oak Ridge, Tennessee, U.S.A. [http://www.daac.ornl.gov/], 2003b.

Heuvelink, G. B. M., P. A. Burrough, and P. A. Stein, Propogation of errors in spatial modelling in GIS, *Int. J. Geogr. Inf. Syst., 3,* 303-322, 1989.

Hicks, W. K., V. Burijson, S. Shrestha, M. Iyngararasan, S. Simukanga, A. M. Van Tienhoven, J.C.I. Kuylenstierna, V. Mathur, and Mazzucchelli S., Development of the regional policy process for air pollution in South Asia, Southern Africa and Latin America, *Water, Air, Soil Poll., 130*(2), 211-216, 2001.

Hobbs, P. V., P. Sinha, R. J. Yokelson, T. J. Christian, D. R. Blake, S. Gao, T. W. Kirchstetter, T. Novakov, and P. Pilewskie, Evolution of gases and particles from a savanna fire in South Africa, *J. Geophys. Res., 108*(D13), 8485, doi:10.1029/2002JD002352, 2003.

Hochschild, V., and M. Herold, M., Hydrological analysis of high resolution multifrequent, multipolarimetric and interferometric airborne SAR data, in *Remote Sensing and Hydrology 2000* (Proceedings of a symposium held at Santa Fe, New Mexico, USA, April 2000), pp. 349-353, IAHS Publication, *267*, 2001.

Hoffa, E. A., D. E. Ward, W. M. Hao, R. A. Susott, and R. H. Wakimoto, Seasonality of carbon emissions from biomass burning in a Zambian savanna, *J. Geophys. Res.*, *104*(D11), 13841-13853, 1999.

Holben, B. N., Characteristics of maximum-value composite images for temporal AVHRR data, *Int. J. Remote Sens., 7*, 1435-1445, 1986.

Horowitz, L. W., S. Walters, D. L. Mauzerall, L. K. Emmons, P. J. Rasch, C. Granier, X. Tie, J. -F. Lamarque, M. G. Schultz, G. S. Tyndall, J. J. Orlando, G. P. Brasseur, A global simulation of tropospheric ozone and related tracers: Description and evaluation of MOZART, version 2*, J. Geophys. Res., 108*(D24), 4784, doi:10.1029/2002JD002853, 2003.

Hurst, D. F., D. W. T. Griffith, and G. D. Cook, Trace gas emissions from biomass burning in tropical Australian savannas, *J. Geophys. Res.*, *99*, 16,441-16,456, 1994a.

Hurst, D. F., D. W. T. Griffith, J. N. Carras, D. J. Williams, and P. J. Fraser, Measurements of trace gases emitted by Australian savanna fires during the 1990 dry season, *J. Atmos. Chem*., *18*, 33-56, 1994b.

Intergovernmental Panel on Climate Change (IPCC), Revised 1996 IPCC Guidelines for National Greenhouse Gas Inventories Workbook, vol. 2, pp. 4.23-4.28, 1997a.

Intergovernmental Panel on Climate Change (IPCC), Expert group meeting on biomass burning and land-use change and forestry, Rockhampton, Australia, 15-18 September, 1997b.

Jacobson M. Z., Strong radiative heating due to the mixing state of black carbon in atmospheric aerosols, *Nature, 409*(6821), 695-697, 2001.

Justice, C. O, and P. H. Y. Hiernaux, Monitoring the grasslands of the Sahel using NOAA AVHRR data-Niger 1983, *Int. J. Remote Sens., 7*(11), 1475-1479, 1986.

Justice, C. O., J. P. Malingreau, and A. Setzer, Satellite remote sensing of fires: potential and limitation, in *Fire in the Environment: Its Ecological, Climatic and Atmospheric Chemical Importance*, edited by P. Crutzen and J. Goldammer, pp. 77-88, John Wiley and Sons, Chichester, 1993.

Justice, C. O., J. D. Kendall, P. R. Dowty, and R. J. Scholes, Satellite remote sensing of fires during the SAFARI campaign using NOAA advanced very high resolution radiometer data, *J. Geophys. Res*., *101*(D19), 23,851-23,864, 1996.

Justice, C. O., and S. Korontzi, A review of the status of satellite fire monitoring and the requirements for global environmental change research, in *Global and Regional Wildland Fire Monitoring from Space: Planning a Coordinated International Effort*, edited by F. J. Ahern, J. G. Goldammer, and C. O. Justice, pp. 1-18, The Hague, SPB Academic Publishing, 2001.

Justice, C. O., L. Giglio, S. Korontzi, J. Owens, J. T. Morisette, D. P. Roy, J. Descloitres, S. Alleaume, F. Petitcolin, and Y. Kaufman, The MODIS fire products, *Remote Sens. Environ.*, *83*(1-2), 244-262, 2002a.

Justice, C. O., J. R. G. Townshend, E. F. Vermote, E. Masuoka, R. E. Wolfe, N. Saleous, D. P. Roy, and J. T. Morisette, An overview of MODIS Land data processing and product status, *Remote Sens. Environ.*, *83*(1-2), 3-15, 2002b.

Kaufman, Y. J., and T. Nakajima, 1993, Effect of Amazon smoke on cloud microphysics and albedo-analysis from satellite imagery, *J. Appl. Meteorol*., *32*(4), 731-744, 1993.

Kaufman, Y. J., and Fraser, R. S., The effect of smoke particles on clouds and climate forcing, *Science*, *277*, 1636-1638, 1997.

Kaufman, Y. J., C. O. Justice, L. P. Flynn, J. D. Kendall, E. M. Prins, L. Giglio, D. E. Ward, W. P. Menzel, and A. W. Setzer, Potential global fire monitoring from EOS-MODIS, *J. Geophys. Res.*, *103*, 32,215-32,238, 1998.

Kaufman, Y. J., C. Ichoku, L. Giglio, S. Korontzi, D. A. Chu, W. M. Hao, R. -R. Li, and C. O. Justice, Fires and smoke observed from the Earth Observing System MODIS

instrument: products, validation, and operational use, *Int. J. Remote Sens.*, *24*, 1765-1781, 2003.

Kogan, F. N., Global drought watch from space, *B. Am. Meteorol. Soc.*, *78*, 621-636, 1997.

Kuhlbusch, T. A. J., M. O. Andreae, H. Cachier, J. G. Goldammer, J. -P. Lacaux, R. Shea, and P. J. Crutzen, Black carbon formation by savanna fires: Measurements and implications for the global carbon cycle, *J. Geophys. Res.*, *101*(D19), 23,651-23,666, 1996.

Lacaux, J., R. A. Delmas, B. Cros, B. Lefeivre, and M. O. Andreae, Influence of biomass burning on precipitation chemistry in the equatorial forests of Africa, in *Global Biomass Burning*: *Atmospheric, Climatic and Biospheric Implications*, edited by J. S. Levine, pp. 167–173, MIT Press, Cambridge, Mass., 1991.

Lacaux, J. P., R. Delmas, C. Jambert, and T. A. J. Kuhlbusch, NO_x emissions from African savanna fires, *J. Geophys. Res.*, *101*(D19), 23,585-23,596, 1996.

Langenfelds, R. L., R. J. Francey, B. C. Pak, L. P. Steele, J. Lloyd, C. M. Trudinger, and C. E. Allison, Interannual growth rate variations of atmospheric CO_2 and its $\delta^{13}C$, H_2, CH_4, and CO between 1992 and 1999 linked to biomass burning, *Global Biogeochem. Cy.*, *16* (3), 1048, doi:10.1029/2001GB001466, 2002.

Leuthold, W., Recovery of woody vegetation in Tsavo Nations Park, Kenya, *Afr. J. Ecol.*, *34*, 106-117, 1996.

Levine, J. S., W. R. Cofer III, D. R. Cahoon Jr., E. L. Winstead, D. I. Sebacher, M. S. Scholes, D. A. B. Parsons, and R. J. Scholes, Biomass burning, biogenic soil emissions, and the global nitrogen budget, in *Biomass Burning and Global Change*, vol. 1, edited by J. S. Levine, pp. 370-380, MIT Press, Cambridge, Mass., 1996.

Li, Q. B., D. J. Jacob, I. Bey, R. M. Yantosca, Y. J. Zhao, Y. Kondo, and J. Notholt, Atmospheric hydrogen cyanide (HCN): Biomass burning source, ocean sink?, *Geophys. Res. Lett*., *27*, 357-360, 2000.

Lindesay, J. A., M. O. Andreae, J. G. Goldammer, G. Harris, H. J. Annegarn, M. Garstang, R. J. Scholes, and B. W. van Wilgen, International Geosphere-Biosphere Programme/International Global Atmospheric Chemistry SAFARI-92 field experiment: background and overview, *J. Geophys. Res.*, *101*(D19), 23521-23530, 1996.

Liousse, C., J. Penner, C. Chuang, J. Walton, H. Eddleman, and H. Cachier , A global three-dimensional model study of carbonaceous aerosols, *J. Geophys. Res.*, *101*(D14), 19,411–19,432, 1996.

Lobert, J. M., D. H. Scharffe, W. M. Hao, and P. J. Crutzen, Importance of biomass burning in the atmospheric budgets of nitrogen-containing gases, *Nature*, *346*(6284), 552-554, 1990.

Lobert, J. M., and J. Warnatz, Emissions from the combustion process in vegetation, in *Fire in the Environment: The Ecological, Atmospheric and Climatic Importance of*

Vegetation Fires, edited by P. J. Crutzen and J. G. Goldammer, pp. 15-37, John Wiley and Sons, Chichester, 1993.

Lobert, J. M., W. C. Keene, J. A. Logan, and R. Yevich, Global chlorine emissions from biomass burning: Reactive chlorine emissions inventory, *J. Geophys. Res*., *104*, 8373-8389, 1999.

Los, S. O., Calibration adjustment of the AVHRR Normalized Difference Vegetation Index without recourse to the component channel data, *Int. J. Remote Sens*., *14*, 1907-1917, 1993.

Ludwig, J., L. T. Marufu, B. Hiber, M. O. Andreae, and G. Helas, Domestic combustion of biomass fuels in developing countries: A major source of atmospheric pollutants, *J. Atm. Chem.*, *44*, 23-37, 2003.

Mapaure, I. N., and B. M. Campbell, Changes in miombo woodland cover in and around Sengwa Wildlife Research Area, Zimbabwe, in relation to elephants and fire, *Afr. J. Ecol.*, *40*(3), 212-219, 2002.

Mason, S. A., R. J. Field, R. J. Yokelson, M. A. Kochivar, M. R. Tinsley, D. E. Ward, and W. M. Hao, Complex effects arising in smoke plume simulations due to inclusion of direct emissions of oxygenated organic species from biomass combustion, *J. Geophys. Res*., *106*, 12,527 –12,539, 2001.

McKenzie, L. M., D. E. Ward, and W. M. Hao, Chlorine and bromine in the biomass of tropical and temperate ecosystems, in *Biomass Burning and Global Change*, vol. 1, edited by J. S. Levine, pp. 240-248, MIT Press, Cambridge, Mass., 1996.

Menaut, J. C., L. Abbadie, F. Lavenu, P. Loudjani, and A. Podaire, Biomass burning in West African savannas, in *Global Biomass Burning: Atmospheric*, *Climatic and Biospheric Implications*, edited by J. S. Levine, pp. 133-142, MIT Press, Cambridge, Mass., 1991.

Morisette, J. T., J. L. Privette, and C. O. Justice, A framework for the validation of MODIS land products, *Remote Sens. Environ.*, *83*(1-2), 77-96, 2002.

New, M. G., M. Hulme, and P. D. Jones, Representing twentieth century space-time climate variability. Part I: Development of a 1961-1990 mean monthly terrestrial climatology, *J. Climate*, *12*, 829-856, 1999.

Notholt, J., Z. Kuang, C. P. Rinsland, G. C. Toon, M. Rex, N. Jones, T. Albrecht, H. Deckelmann, J. Krieg, C. Weinzierl, H. Bingemer, R. Weller, and O. Schrems, Enhanced upper tropical tropospheric COS: Impact on the stratospheric aerosol layer, *Science*, *300*, 307-310, 2003.

Otter, L., and M. C. Scholes, Methane sources and sinks in a periodically flooded South African savanna, *Global Biogeochem. Cy.*, *14*(1), 97-112, 2000.

Otter, L., L. Marufu, and M. C. Scholes, Biogenic, biomass and biofuel sources of trace gases in southern Africa, *South Afr. J Sc.*, *97*(3-4), 131-138, 2001.

Otter, L., A. Guenther, C. Wiedinmyer, G. Fleming, P. Harley, and J. Greenberg, Spatial and temporal variations in biogenic volatile organic compound emissions for Africa south of the equator, *J. Geophys. Res.*, *108*(D13), 8505, doi:10.1029/2002JD002609, 2003.

Page, S. E., F. Siegert, J. O. Rieley, H. -D. V. Boehm, A. Jaya, and S. Limin, The amount of carbon released from peat and forest fires in Indonesia during 1997, *Nature*, *420*(6911), 61-65, 2002.

Paltridge, G. W., and J. Barber, Monitoring grassland dryness and fire potential in Australia with NOAA/AVHRR data, *Remote Sens. Environ.*, *25*(3), 381-394, 1988.

Parsons, D. A. B., M. C. Scholes, R. J. Scholes, and J. S. Levine, Biogenic NO emissions from savanna soils as a function of fire regime, soil type, soil nitrogen, and water status, *J. Geophys. Res*., *101*(D19), 23,683-23,688, 1996.

Piccolini, I., Development and validation of an adaptive algorithm for burn scar detection using ERS/ATSR-2 data, *Ph.d. Thesis*, Univ. La Sapienza, Rome, Italy, 1998.

Pinzón, J. E., M. E. Brown, and C. J. Tucker, Satellite time series correction of orbital drift artifacts using empirical mode decomposition, in *EMD and its Applications*, edited by N. E. Huang and S. S. P. Shen, World Scientific, Singapore, in press.

Price, C. G., J. E. Penner, and M. J. Prather, NO_X from lightning, Part I: Global distribution based on lightning physics, *J. Geophys. Res., 102*, 5929-5941, 1997.

Radke, L. F., J. L. Stith, D. A. Hegg, and P. V. Hobbs, Airborne studies of particles and gases from forest fires, *J. Air Pollut. Control Assoc*., *28*, 30– 34, 1978.

Robinson, J. M., Fire from space: global fire evaluation using infrared remote sensing, *Int. J. Remote Sens*., *12*(1), 3-24, 1991.

Rosenfeld, D., TRMM observed first direct evidence of smoke from forest fires inhibiting rainfall**,** *Geophys. Res. Lett*., *26*(20), 3105-3108, 1999.

Roy, D. P., P. Lewis, and C. O. Justice, Burned area mapping using multi-temporal moderate spatial resolution data-a bi-directional reflectance model-based expectation approach, *Remote Sens. Environ.*, *83*, 263-286, 2002a.

Roy, D. P., J. Borak, S. Devadiga, R. Wolfe, M. Zheng, and J. Descloitres, The MODIS land product quality assessment approach, *Remote Sens. Environ.*, *83*, 62-76, 2002b.

Roy, D. P., SAFARI 2000 July and September MODIS 500 m Burned Area Products for Southern Africa, in *SAFARI 2000 CD-ROM Series*, vol. 3, CD-ROM, edited by J. Nickeson, D. Landis, J. L. Privette, National Aeronautics and Space Administration, Goddard Space Flight Center, Greenbelt, Maryland, U.S.A. Available from Oak Ridge National Laboratory Distributed Active Archive Center, Oak Ridge, Tennessee, U.S.A. [http://www.daac.ornl.gov/], 2003a.

Roy, D. P., J. Yufang, C. O. Justice, L. Giglio, and P. E. Lewis, Multi-year southern Africa MODIS burned area product generation and validation, Fall AGU Meeting, San Francisco, December 8-12, 2003, Presented in Session "Validation and Application of Land Surface Products From the MODIS Sensor", *Eos Trans. AGU, 84*(46), Abstract B22E-02, 2003b.

Roy, D. P., and T. Landmann, Characterizing the surface heterogeneity of fire effects using multi-temporal reflective wavelength data, *Int. J. Remote Sens*., in press.

Roy, D. P., P. G. H. Frost, C. O. Justice, T. Landmann, J. L. Le Roux, K. Gumbo, S. Makungwa, K. Dunham, R. Du Toit, K. Mhwandagara, A.Zacarias, B. Tacheba, O. P. Dube, J.M.C. Pereira, P. Mushove, J.T.Morisette, S. K. Santhana Vannan, and D. Davies, The Southern Africa Fire Network (SAFNet) regional burned area product validation protocol, *Int. J. Remote Sens*., in press.

Russell-Smith, J., P. G. Ryan, and R. Durieu, A LANDSAT MSS-derived fire history of Kakadu National Park, Monsoonal Northern Australia, 1980-94: Seasonal extent, frequency and patchiness, *J. Appl. Ecol.*, *34*(3), 748-766, 1997.

Saarnak, C. F., *Trace Gas Emissions from Savanna Fires in West Africa*, Institute of Geography, University of Copenhagen, Ph.D. Thesis, 1999.

San José, J. J., and E. Medina. Effect of fire on organic matter production and water balance in a tropical savanna, in *Tropical ecological systems: Trends in terrestrial and aquatic Research*, edited by F. B. Golley and E. Medina, Springer-Verlag, New York, 1975.

Schimel, D., and D. Baker, Carbon cycle:The wildfire factor, *Nature, 420*, 29-30, 2002.

Scholes, R. J., and B. H. Walker, *An African Savanna: Synthesis of the Nylsvley study*, Cambridge Studies in Applied Ecology and Resource Management, Cambridge University Press, 1993.

Scholes, M. C., and M. O. Andreae, Biogenic and pyrogenic emissions from Africa and their impact on global atmosphere, *Ambio*, *29*, 23-29, 2000.

Scholes, R. J., and D. O. Hall, The carbon budget of tropical savannas, woodlands and grasslands. in *Global Change Effects on Coniferous Forests and Grasslands*, edited by A. I. Breymeyer, D. O. Hall *et al*., pp. 69-100, John Wiley and Sons, New York, 1996.

Scholes, R. J., D. E. Ward, and C. O. Justice, Emissions of trace gases and aerosol particles due to vegetation burning in southern hemisphere Africa, *J. Geophys. Res., 101*(D19), 23,677-23,682, 1996a.

Scholes, R. J., J. Kendall, and C. O. Justice, The quantity of biomass burned in southern Africa, *J. Geophys. Res., 101*(D19), 23,667-23,676, 1996b.

Scholes, R. J., and M. R. van der Merwe, Greenhouse gas emissions from South, *S. Afr. J. Sci.*, *92*, 220-222, 1996.

Scholes, R.J. and M. C. Scholes, Natural and human-related sources of ozone-forming trace gases in southern Africa, *S. Afr. J. Sci.*, *94*, 422-425, 1998.

Scholes, R. J., P. R. Dowty, K. Caylor, D. A. B. Parsons, P. G. H. Frost, and H. H. Shugart, Trends in savanna structure and composition along an aridity gradient in the Kalahari, *J. Veget. Sci.*, *13*, 419-428, 2002.

Scholes, M. C., and M. O. Andreae, Biogenic and pyrogenic emissions from Africa and their impact on global atmosphere, *Ambio*, *29*, 23-29, 2000.

Schoffeleers, M., The religious significance of bush fires in Malawi, *Cahiers des Religions Africaines*, *10*, 271-287, 1971.

Schultz, M. G., On the use of ATSR fire count data to estimate the seasonal and interannual variability of vegetation fire emissions, *Atmos. Chem. Phys.*, *2*, 387-395, 2002.

Seiler, W., and P. J. Crutzen, Estimates of gross and net fluxes of carbon between the biosphere and the atmosphere from biomass burning, *Climatic Change*, *2*(3), 207-247, 1980.

Shade, G. W., and P. J. Crutzen, CO emissions from degrading plant matter (II). Estimate of a global source strength, *Tellus*, *51*, 889-908, 1999.

Shea, R. W., B. W. Shea, J. B. Kauffman, D. E. Ward, C. I. Haskins, and M. C. Scholes, Fuel biomass and combustion factors associated with fires in savanna ecosystems of South Africa and Zambia, *J. Geophys. Res.*, *101*(D19), 23551-23568, 1996.

Sherwood, S., A microphysical connection among biomass burning, cumulus clouds, and stratospheric moisture, *Science*, *295*, 1272-1275, 2002.

Silva, J. M. N., J. M. C. Pereira, A. I. Cabral, A. Sá, M. J. P. Vasconcelos, B. Mota, and J.-M. Grégoire, The area burned in southern Africa during the 2000 dry season, *J. Geophys. Res.*, *108*(D13), 8498, doi:10.1029/2002JD002320, 2003.

Simon, M., S. Plummer, F. Fierens, J. J. Hoelzmann, and O. Arino, Burnt area detection at global scale using ATSR-2: the GLOBSCAR products and their qualification, *J. Geophys. Res.*, in press.

Singh, H., Y. Chen, A. Staudt, D. Jacob, D. Blake, B. Heikes, and J. Snow, Evidence from the Pacific troposphere for large global sources of oxygenated organic compounds, *Nature*, *410*, 1078-1081, 2001.

Sinha, P., P. V. Hobbs, R. J. Yokelson, I. T. Bertschi, D. R. Blake, I. J. Simpson, S. Gao, T. W. Kirchstetter, and T. Novakov, Emissions of trace gases and particles from biomass burning in southern Africa, *J. Geophys. Res., 108*(D13), 8487, doi:10.1029/2002JD002325, 2003.

Stocks, B. J., B. W. van Wilgen, W. S. W. Trollope, D. J. McRae, J. A. Mason, F. Weirich, and A. L. F. Potgieter, Fuels and fire behavior dynamics on large-scale savanna fires in Kruger National Park, South Africa, *J. Geophys. Res*., *101*(D19), 23,541-23,550, 1996.

Stroppiana, D., S. Pinnock, J. M. C. Pereira, and J. -M. Grégoire, Radiometric analysis of SPOT-VEGETATION images for burnt area detection in northern Australia, *Remote Sens. Environ.*, *82*, 21-37, 2002.

Swap, R. J., H. J. Annegarn, J. T. Suttles, J. Haywood, M. C. Helmlinger, C. Hély, P. V. Hobbs, B. N. Holben, J. Ji, M. D. King, T. Landmann, W. Maenhaut, L. Otter, B. Pak, S. J. Piketh, S. Platnick, J. Privette, D. P. Roy, A. M. Thompson, D. E. Ward, and R. J. Yokelson, The Southern African Regional Science Initiative (SAFARI 2000): overview of the dry season field campaign, *S. Afr. J. Sci.*, *98*(3-4), 125-130, 2002.

Swap, R. J., H. J. Annegarn, J. T. Suttles, M. D. King, S. Platnick, J. L. Privette, and R. J. Scholes, Africa burning: A thematic analysis of the Southern African Regional Science Initiative (SAFARI 2000), *J. Geophys. Res.*, *108*(D13), 8465, doi:10.1029/2003JD003747, 2003.

Tansey, K., E. Binaghi, L. Boschetti, P.A. Brivio, A. Cabral, D. Ershov, S. Flasse, R. Fraser, I. Gallo, D. Graetz, J. -M. Grégoire, M. Maggi, P. Peduzzi, J. M. Pereira, A. Sá, J. Silva, A. Sousa, D. Stroppiana, and M. J. P. Vasconcelos, Implementation of regional burnt area algorithms for the GBA2000 initiative. European Commission Joint Research Centre, EUR 20532 EN, pp. 159, 2002.

Tay, S., Fires, haze and acid rain: The social and political framework on air pollution in ASEAN and Asia, in *Challenges of a Changing Earth*, edited by W. Steffen, J. Jäger, D. J. Carson and C. Bradshaw, pp. 49-55, The IGBP Series, Springer-Verlag, Berlin, 2002.

Thompson, A. M., R. D. Diab, G. E. Bodeker, M. Zunckel, G. J. R. Coetzee, C. B. Archer, D. P. McNamara, K E. Picketing, J. Combrink, J. Fishman, and D. Nganga, Ozone over southern Africa during SAFARI-92/TRACE A, *J. Geophys. Res., 101*(19), 23,793-23,807, 1996.

Thompson, A. M., J. C. Witte, R. D. Hudson, H. Guo, J. R. Herman, and M. Fujiwara, Tropical tropospheric ozone and biomass burning, *Science*, *291*, 2128-2132, 2001.

Trollope, W. S. W., L. A. Trollope, A. L. F. Potgieter, and N. Zambatis, SAFARI-92 characterization of biomass and fire behavior in the small experiment

burns in the Kruger National Park, *J. Geophys. Res.*, *101*(D19), 23,531-23,540, 1996.

Trollope, W. S. W., and L. A. Trollope, Fire behaviour a key factor in the fire ecology of African grasslands and savannas, in *Forest Fire Research and Wildland Fire Safety*, edited by X. Viegas, pp. 1-15, Millpress, Rotterdam, 2002.

Tucker, C. J., Red and photographic infrared linear combinations for monitoring vegetation, *Int. J. Remote Sens*., *8*, 127-150, 1979.

Tucker, C. J., W. W. Newcomb, and H. E. Dregne, AVHRR data sets for determination of desert spatial extent, *Int. J. Remote Sens*., *17*, 3547-3565, 1994.

Van der Werf, G. R., J. T. Randerson, G. J. Collatz, and L. Giglio, Carbon emissions from fires in tropical and subtropical ecosystems, *Global Change Biol.*, *9*(4), 547-562, 2003.

Van der Werf, G. R., J. T. Randerson, G. J. Collatz, L. Giglio, P. S. Kasibhatla, A. F. Arellano Jr., S. C. Olsen, and E. S. Kasischke, Continental-Scale partitioning of fire emissions during the 1997 to 2001 El Niño/La Niña period, *Science*, *303*, 73-76, 2004.

Van Wilgen, B. W., and R. J. Scholes, The vegetation and fire regimes of southern hemisphere Africa, in *Fire in the Southern African Savannas: Ecological and Environmental Perspectives*, edited by B. W. van Wilgen *et al*., pp. 27-46, Witwatersrand Univ. Press, Johannesburg, South Africa, 1997.

Ward, D. E, R. A. Susott, J. B. Kauffman, R. E. Babbitt, D. L. Cummings, B. Dias, B. N. Holben, Y. J. Kaufman, R. A. Rasmussen, and A. W. Setzer, Smoke and fire characteristics for cerrado and deforestation burns in Brazil: BASE-B experiment, *J. Geophys. Res., 97*(D13), 14,601-14,619, 1992.

Ward, D. E., and L. F. Radke, Emissions measurement from vegetation fires: A comparative evaluation of methods and results, in *The ecological, atmospheric, and climatic importance of vegetation fires*, edited by P. J. Crutzen and J. G. Goldammer, pp. 53-76, John Wiley and Sons, 1993.

Ward, D. E., W. M. Hao, R. A. Susott, R. E. Babbitt, R. W. Shea, J. B. Kauffman, and C. O. Justice, Effect of fuel composition on combustion efficiency and emission factors for African savanna ecosystems, *J. Geophys. Res.*, *101*(D19), 23569-23576, 1996.

Wennberg, P. O., T. F. Hanisco, L. Jaeglé, D. J. Jacob, E. J. Hintsa, E. J. Lanzendorf, J. G. Anderson, R. -S. Gao, E. R. Keim, S. G. Donnelly, L. A. Negro, D. W. Del Fahey, S. A. McKeen, R. J. Salawitch, C. R. Webster, R. D. May, R. L. Herman, M. H. Proffitt, J. J. Margitan, E. L. Atlas, S. M. Schauffler, F. Flocke, C. T. McElroy, and T. P. Bui, Hydrogen radicals, nitrogen radicals, and the production of O_3 in the upper troposphere, *Science*, *279*, 49-53, 1998.

Williams, R. J., A. M. Gill, and P. H. R. Moore, Seasonal changes in fire behaviour in a tropical savanna in northern Australia, *Int. J. Wildland Fire*, *8*(4), 227-239, 1998.

Wolfe, R., M. Nishihama, A. Fleig, J. Kuyper, D. P. Roy, J. Storey, and F. Patt, Achieving sub-pixel geolocation accuracy in support of MODIS land science, *Remote Sens. Environ.*, *83*, 31-49, 2002.

Wooster, M. J., Small-scale experimental testing of fire radiative energy for quantifying mass combusted in natural vegetation fires, *Geophys. Res. Lett.*, *29*(21), 2027-2034, 2002.

Yevich, R., and J. A. Logan, An assessment of biofuel use and burning of agricultural waste in the developing world, *Global Biogeochem. Cy.*, *17*(4), 1095, doi:10.1029/2002GB001952, 2003.

Yokelson, R. J., D. W. T. Griffith, and D. E. Ward, Open-path Fourier transform infrared studies of large-scale laboratory biomass fires, *J. Geophys. Res., 101*(D15), 21,067-21,080, 1996.

Yokelson, R. J., I. T. Bertschi, T. J. Christian, P. V. Hobbs, D. E. Ward, and W. M. Hao, Trace gas measurements in nascent, aged, and cloud-processed smoke from African savanna fires by airborne Fourier transform infrared spectroscopy (AFTIR), *J. Geophys. Res.*, *108*(D13), 8478, doi:10.1029/2002JD002322, 2003.

Zarco-Tejada, P. J., C. A. Rueda, and S. L. Ustin, Water content estimation in vegetation with MODIS reflectance data and model inversion methods, *Remote Sens. Environ.*, *85*(1), 109-124, 2003.

Zepp, R. G., W. L. Miller, R. A. Burke, D. A. B. Parsons, and M. C. Scholes, Effects of moisture and burning on soil-atmosphere exchange of trace carbon gases in a

southern African savanna, *J. Geophys. Res*., *101*(D19), 23,699-23,706, 1996.